# Coexistence of Vehicular Communication Technologies and Wi-Fi in the 5 and 6 GHz bands

by

Gaurang Ramesh Naik

Dissertation submitted to the Faculty of the
Virginia Polytechnic Institute and State University
in partial fulfillment of the requirements for the degree of

Doctor of Philosophy
in
Electrical Engineering

Jung-Min (Jerry) Park, Chair
Y. Thomas Hou
Jeffrey Reed
Pratap Tokekar
Ali Butt

October 21, 2020
Arlington, Virginia

Keywords: Vehicular communications, Wi-Fi, Wireless Local Area Networks, Dynamic Spectrum Sharing

# Coexistence of Vehicular Communication Technologies and Wi-Fi in the 5 and 6 GHz bands

Gaurang Ramesh Naik

ABSTRACT

The unlicensed wireless spectrum offers exciting opportunities for developing innovative wireless applications. This has been true ever since the 2.4 GHz band and parts of the 5 GHz bands were first opened for unlicensed access worldwide. In recent years, the 5 GHz unlicensed bands have been one of the most coveted for launching new wireless services and applications due to their relatively superior propagation characteristics and the abundance of spectrum therein. However, the appetite for unlicensed spectrum seems to remain unsatiated; the demand for additional unlicensed bands has been never-ending. To meet this demand, regulators in the US and Europe have been considering unlicensed operations in the 5.9 GHz bands and in large parts of the 6 GHz bands.

In the last two years alone, the Federal Communications Commission in the US has added more than 1.2 GHz of spectrum in the pool of unlicensed bands. Wi-Fi networks are likely to be the biggest beneficiaries of this spectrum. Such abundance of spectrum would allow massive improvements in the peak throughput and potentially allow a considerable reduction of latency, thereby enabling support for emerging wireless applications such as augmented and virtual reality, and mobile gaming using Wi-Fi over unlicensed bands. However, access to these bands comes with its challenges. Across the globe, a wide range of *incumbent* wireless technologies operate in the 5 GHz and 6 GHz bands. This includes weather and military radars, and vehicular communication systems in the 5 GHz bands, and fixed-service systems, satellite systems, and television pick-up stations in the 6 GHz bands. Furthermore, due to the development of several cellular-based unlicensed technologies (such as Licensed Assisted Access and New Radio Unlicensed, NR-U), the competition for channel access among unlicensed devices has also been increasing. Thus, coexistence across wireless technologies in the 5 GHz and 6 GHz bands has emerged as an extremely challenging and interesting research problem.

In this dissertation, we first take a comprehensive look at the various coexistence scenarios that emerge in the 5 GHz and 6 GHz bands as a consequence of new regulatory decisions. These scenarios include coexistence between Wi-Fi and incumbent users (both in the 5 GHz and 6 GHz bands), coexistence of Wi-Fi and vehicular communication systems, coexistence across different vehicular communication technologies, and coexistence across different unlicensed systems. Since a vast majority of these technologies are fundamentally different from each other and serve diverse use-cases each coexistence problem is unique. Insights derived from an in-depth study of one coexistence problem do not help much when the coexisting technologies change. Thus, we study each scenario separately and in detail. In this process, we highlight the need for the design of novel coexistence mechanisms in several cases and outline potential research directions.

Next, we shift our attention to coexistence between Wi-Fi and vehicular communication technologies designed to operate in the 5.9 GHz intelligent transportation systems (ITS) bands. Until the development of Cellular V2X (C-V2X), dedicated short range communications (DSRC) was the only major wireless technology that was designed for communication in high-speed and potentially dense vehicular settings. Since DSRC uses the IEEE 802.11p standard for its physical (PHY) and medium access control (MAC) layers, the manner in which DSRC and Wi-Fi devices try to gain access to the channel is fundamentally similar. Consequently, we show that spectrum sharing between these two technologies in the 5.9 GHz bands can be easily achieved by simple modifications to the Wi-Fi MAC layer.

Since the design of C-V2X in 2017, however, the vehicular communication landscape has been fast evolving. Because DSRC systems were not widely deployed, automakers and regulators had an opportunity to look at the two technologies, consider their benefits and drawbacks and take a fresh look at the spectrum sharing scenario. Since Wi-Fi can now potentially share the spectrum with C-V2X at least in certain regions, we take an in-depth look at various Wi-Fi and C-V2X configurations and study whether C-V2X and Wi-Fi can harmoniously coexist with each other. We determine that because C-V2X is built atop cellular LTE, Wi-Fi and C-V2X systems are fundamentally incompatible with each other. If C-V2X and Wi-Fi devices are to share the spectrum, considerable modifications to the Wi-Fi MAC protocol would be required.

Another equally interesting scenario arises in the 6 GHz bands, where 5G NR-U and Wi-Fi devices are likely to operate on a secondary shared basis. Since the 6 GHz bands were only recently considered for unlicensed access, these bands are free from Wi-Fi and NR-U devices. As a result, the *greenfield* 6 GHz bands provide a unique and rare opportunity to freshly evaluate the coexistence between Wi-Fi and cellular-based unlicensed wireless technologies. We study this coexistence problem by developing a stochastic geometry-based analytical model. We see that by disabling the listen before talk based legacy contention mechanism—which has been used by Wi-Fi devices ever since their conception—the performance of both Wi-Fi and NR-U systems can improve. This has important implications in the 6 GHz bands, where such legacy transmissions can indeed be disabled because Wi-Fi devices, for the first time since the design of IEEE 802.11a, can operate in the 6 GHz bands without any backward compatibility issues.

In the course of studying the aforementioned coexistence problems, we identified several gaps in the literature on the performance analysis of C-V2X and IEEE 802.11ax—the upcoming Wi-Fi standard. We address three such gaps in this dissertation.

First, we study the performance of C-V2X sidelink mode 4, which is the communication mode in C-V2X that allows direct vehicular communications (i.e., without assistance from the cellular infrastructure). Using our in-house standards-compliant network simulator-3 (ns-3) simulator, we perform simulations to evaluate the performance of C-V2X sidelink mode 4 in highway environments. In doing so, we identify that packet re-transmissions, which is a feature introduced in C-V2X to provide frequency and time diversity, thereby improving the

system performance, can have the opposite effect if the vehicular density increases. In fact, packet re-transmissions are beneficial for C-V2X system performance only at low vehicular densities. Thus, if vehicles are statically configured to always use/disable re-transmissions, the maximum potential of this feature is not realized. Therefore, we propose a simple and effective, distributed re-transmission control mechanism named Channel Congestion Based Re-transmission Control ($C^2RC$), which leverages the locally available channel sensing results to allow vehicles to autonomously decide when to switch on re-transmissions and when to switch them off.

Second, we present a detailed analysis of the performance of Multi User Orthogonal Frequency Division Multiple Access (MU OFDMA)—a feature newly introduced in IEEE 802.11ax—in a wide range of deployment scenarios. We consider the performance of 802.11ax networks when the network comprises of only 802.11ax as well as a combination of 802.11ax and legacy stations. The latter is a practical scenario, especially during the initial phases of 802.11ax deployments. Simulation results, obtained from our ns-3 based simulator, give encouraging signs for 802.11ax performance in many real-world scenarios. That being said, there are some scenarios where naive usage of MU OFDMA by an 802.11ax-capable Wi-Fi AP can be detrimental to the overall system performance. Our results indicate that careful consideration of network dynamics is critical in exploiting the best performance, especially in a heterogeneous Wi-Fi network.

Finally, we perform a comprehensive simulation study to characterize the performance of Multi Link Aggregation (MLA) in IEEE 802.11be. MLA is a novel feature that is likely to be introduced in next-generation Wi-Fi (i.e., Wi-Fi 7) devices and is aimed at reducing the worst-case latency experienced by Wi-Fi devices in dense traffic environments. We study the impact of different traffic densities on the 90 percentile latency of Wi-Fi packets and identify that the addition of a single link is sufficient to substantially bring down the 90 percentile latency in many practical scenarios. Furthermore, we show that while the addition of subsequent links is beneficial, the largest latency gain in most scenarios is experienced when the second link (i.e., one additional) link is added. Finally, we show that even in extremely dense traffic conditions, if a sufficient number of links are available at the MLA-capable transmitter and receiver, MLA can help Wi-Fi devices to meet the latency requirements of most real-time applications.

# Coexistence of Vehicular Communication Technologies and Wi-Fi in the 5 and 6 GHz bands

Gaurang Ramesh Naik

GENERAL AUDIENCE ABSTRACT

Wireless networks have become ubiquitous in our lives today. Whether it is cellular connectivity on our mobile phones or access to Wi-Fi hotspots on laptops, tablets, and smartphones, never before has wireless communication been as integral to our lives as it is today.

In many wireless communication systems, wireless devices operate by sending signals to and receiving signals from a central entity that connects to the wired Internet infrastructure. In the case of cellular networks, this entity is the cell tower deployed by the operators (such as AT&T, Verizon, etc. in the US), while the Wi-Fi router deployed in homes and offices plays this role in Wi-Fi networks. There is also another class of wireless systems, where wireless devices communicate with each other without requiring to communicate with any central entity. An example of such a *distributed* communication system—which is fast gaining popularity—is vehicular communication networks.

End-user devices (e.g. cellphone, laptop, tablet, or a vehicle) can communicate with each other or the central entity only if they are both tuned to the same frequency channel. This channel can lie anywhere within the radio frequency spectrum, but some frequency channels (the collection of channels is referred to as frequency bands) are more favorable——in terms of how far the signal sent over these channels can reach——than others. Another dimension to these frequency bands is the licensing mechanism. Not all frequency bands are free to use. In fact, most frequency bands in the US and other parts of the world are licensed by the regional regulatory agencies. The most well-known example of this licensing framework is the cellular network. Cellular operators spend large amounts of money (to the tune of billions of dollars) to gain the privileges of exclusively operating in a given frequency band. No other operator or wireless device is then allowed to operate in this band. Without any external interfering wireless device, cellular operators can guarantee a certain quality of service that is provided to its customers. Thus, the benefits of using licensed frequency bands are obvious but these bands and their associated benefits come at a high price.

An alternative to licensed frequency bands are the unlicensed ones. As the name suggests, unlicensed frequency bands are those where any two or more wireless devices can communicate with each other (subject to certain rules) without having to pay any licensing fees. Unsurprisingly, because there is no limit to who or how many devices can communicate over these bands, wireless devices in these bands frequently experience external interference, which manifests to the end-user in terms of interruption of service. The best example of a wireless technology that uses unlicensed bands is Wi-Fi. One of the greatest advantages of Wi-Fi networks is that anyone can purchase a Wi-Fi router and deploy it within their homes or offices——flexibility not afforded by licensed bands. However, this very flexibility and ease-of-use can sometimes contribute negatively to Wi-Fi performance. Arguably, we have all faced scenarios where the performance of Wi-Fi is poor. This is most likely to happen in

scenarios where there are hundreds (or even thousands) of neighboring Wi-Fi devices, such as at stadiums, railway stations, concerts, etc. Based on our discussions above, it is clear as to why Wi-Fi performance suffers in such scenarios. Thus, although unlicensed bands are lucrative in terms of low-cost, and ease of use, there is no guarantee on how good a voice/video call or a video streaming session conducted over Wi-Fi will be.

The above problem is well-known and well-researched. Regulators, researchers, and service providers actively seek solutions to offer better performance over unlicensed bands. An obvious solution is to make more unlicensed bands available; if all neighboring Wi-Fi users communicate with their respective routers on different channels, everyone could communicate interference-free. The problem, however, is that frequency bands are limited. Even more limited are those bands that support wireless communications over larger distances. Another solution is to improve the wireless technology——if a Wi-Fi device can more efficiently utilize the channel, its performance is likely to improve. This fact has driven the constant evolution of all wireless technologies. However, there are fundamental limits to how much a frequency channel can be exploited. Therefore, in recent years, stakeholders have turned to *spectrum sharing*. Even though a wireless network may possess an exclusive license to operate on a given frequency band, its users do not use the band everywhere and at all times. Then why not allow unlicensed wireless devices to operate in this band at such places and times? This is precisely the premise of spectrum sharing.

In this dissertation, we look at the problem of coexistence between wireless technologies in the 5 GHz and 6 GHz bands. These two bands are extremely lucrative in terms of their relatively favorable propagation characteristics (i.e., their communication range) and the abundance of spectrum therein. Consequently, these bands have garnered considerable attention in recent years with the objective of opening these bands up for unlicensed services. However, the 5 GHz and 6 GHz bands are home to several licensed systems, and the performance of these systems cannot be compromised if unlicensed operations are allowed. Significant activity has taken place since 2013 concerning new technologies being developed, new spectrum sharing scenarios being proposed, and new rules being adopted in these two bands. We begin the dissertation by taking a comprehensive look at these issues, describing the various coexistence scenarios, surveying the existing literature, describing the major challenges, and providing directions for potential research.

Next, we look at three coexistence problems in detail: (i) coexistence of dedicated short range communications (DSRC) and Wi-Fi, (ii) coexistence of cellular V2X (C-V2X) and Wi-Fi, and (iii) coexistence of 5G New Radio Unlicensed (5G NR-U) and Wi-Fi. The former two scenarios involve the coexistence of Wi-Fi with a vehicular communication technology (DSRC or C-V2X). These scenarios arose due to considerations in the US and Europe to allow Wi-Fi operations (on an unlicensed *secondary* basis) in the spectrum that was originally reserved for vehicular communications. Our work shows that because DSRC and Wi-Fi are built on top of fundamentally similar protocols, they are, to an extent, compatible with each other, and coexistence between these two technologies can be achieved by relatively simple modifications to the Wi-Fi protocol. However, C-V2X, owing to its inheritance from the

cellular LTE, is not compatible with Wi-Fi. Consequently, significant research is required if the two technologies are to share the spectrum.

On the other hand, in the coexistence of 5G NR-U and Wi-Fi, we focus on the operations of these two technologies in the 6 GHz bands. NR-U is a technology that is built atop the 5G cellular system, but is designed to operate in the unlicensed bands (in contrast to *traditional* cellular systems which only operate in licensed bands). Although these two technologies can coexist in the 5 GHz and 6 GHz bands, we restrict our attention in this dissertation to the 6 GHz bands. This is because the 6 GHz bands are unique in that the entire range of the 6 GHz bands were opened up for unlicensed access all at once recently, and no Wi-Fi or NR-U devices currently operate in these bands. As a result, we can learn from the mistakes made in the 5 GHz bands, where a vast majority of today's Wi-Fi networks operate. Our work shows that, indeed, we can take decisive steps—such as disabling certain Wi-Fi functions—in the 6 GHz bands, which can facilitate better coexistence in the 6 GHz bands.

Finally, in the course of identifying and tackling the various coexistence scenarios in the 5 GHz and 6 GHz bands, we identify some open issues in the performance of new wireless technologies designed to operate in these bands. Specifically, we highlight the need to better understand and characterize the performance of Multi User Orthogonal Frequency Division Multiple Access (MU OFDMA), a feature common in cellular networks but newly introduced to Wi-Fi, in the upcoming Wi-Fi 6 generation of devices. We propose and evaluate an analytical model for the same. We also characterize the performance of Multi Link Aggregation—which a novel feature likely to be introduced in future Wi-Fi 7 devices—that is aimed at reducing the worst-case delay experienced by Wi-Fi devices in dense traffic conditions. Additionally, we identify an issue in the performance of the distributed operational mode of C-V2X. We show that *packet re-transmissions*, which is a feature aimed at improving the performance of C-V2X, can have a counter-productive effect and degrade the C-V2X performance in certain environments. We address this issue by proposing a simple, yet effective, re-transmission control mechanism.

# Dedication

*To my family*

# Acknowledgments

It is difficult to acknowledge every person that has touched my life over these past five years and has guided, motivated, and assisted me through my journey at Virginia Tech. I am grateful to every single person that has helped me make this journey the most enriching experience in my life so far.

First and foremost, I would like to express my sincere gratitude to Dr. Jerry Park, who has guided me week after week throughout my stay here. A significant part of my character as a researcher— how I identify problems, approach them, and make attempts to solving them— has been influenced by him. His constant support and guidance helped me stay focused and kept me motivated. Dr. Park's constructive criticisms, as difficult as they were to tackle at the time, have helped me become a better researcher. His dedication, hard work, and critical thinking have been an inspiration to me, and my journey at Virginia Tech would have been incomplete had it not been for him as my advisor.

I owe a debt of gratitude to Virginia Tech (VT), the institution, as well as all the wonderful people who make this institution a nurturing place for its students. To begin with, I am extremely grateful to all members of my Ph.D. advisory committee, Dr. Tom Hou, Dr. Jeffrey Reed, Dr. Ali Butt, and Dr. Pratap Tokekar, who have guided me, motivated me, and have been kind enough to help me every time I reached out to them. Secondly, I want to thank Roxanne for being the kindest and the most supportive graduate advisor one can hope for. I sincerely regret that most of our conversations were over e-mail and we did not have more in-person interactions. And yet, thanks to your support, I have always felt that I could reach out to you with the silliest of my questions. I was fortunate enough to have worked with a very supportive professor—Dr. William Plymale as his Graduate Teaching Assistant. Thanks to him, I got the opportunity to interact with some extremely talented seniors in the ECE department. I am also thankful to all the professors at VT who made my student life a great learning experience. In particular, I would like to thank Dr. Scotland Leman for his wonderful class on Bayesian Statistics, Dr. Chandan Reddy for his amazing lectures on Deep Learning, and his support during my project, Dr. Michael Buehrer for making wireless communications more interesting than I believed it could be, and Dr. Vuk Marojevic for his guidance during and after I was his student.

My experience in these last 5+ years has been beautifully shaped by some of the most unique, intelligent, and sincere people I have met. I consider myself extremely fortunate to have met them. Aakash, you have been my greatest source of support and enthusiasm during these past few years. Throughout this time, we enjoyed our successes and laughed through our failures together. And although our research areas are poles apart, the passion you have for your work has motivated me to give my best in my research. Revati, in you, I found the little sister I always wished I had. The more I have known you, the more have I grown to adore

you. Shubham, you have been the closest person I have known to a brother. You have been with me through some of the most difficult times. And yes, we shall go on that much-awaited Midwest trip someday! Pratham, you are one of the most brilliant and genuine persons I have come across. Conversations with you have always lifted my spirits. Also, you are, by far, the best cook I have known. Geeta, you have been one of the most reliable friends I have ever had. I know I can always count on you! Tanmaya, you are an extremely fun and smart person to be around. I have learned so much from our conversations, often when I did not even wish to learn them! Mahsa, I will miss you and our conversations. And yes, you're the best! Himanshu and Rajeev, you two have been, and will always be, great sources of emotional support to me.

Jinshan, you and I have had a large part of this journey together. I have always admired (and to an extent envied) your brilliance. I got to learn a lot from you during the first couple of years that we worked together. Taiwo, I am going to miss and cherish all the long conversations we have had over these years—not only the technical ones but also about our experiences growing up, the similarities between our cultures, and so many other topics. I am grateful to the two of you for making our lab fun and an intellectual place. Sudeep and Viresh, you have been great friends and mentors to me. Sudeep, you have helped me on innumerable occasions both during the times we worked together and more recently with our phone conversations. Viresh, talking to you is *always* a very pleasant experience. Right from the first time we spoke, you have had a very calming and positive influence on me. I am extremely grateful to both of you for all the guidance and motivation you have given me. Biplav, it was a great experience working alongside you. I admire your dedication and hope you have a great experience moving forward. Ali, I have enjoyed our long conversations in the lab. Your curiosity to know things has pushed me to expand my thinking, for which I am extremely thankful to you. Tolga, although I did not get to work and speak with you much, largely due to the current remote working environment, I have come to know you as a very dedicated person. I wish you the best in your research and life.

Riddhi, Siddhant, Mariam, Maisam, and Rewa, I have had so many wonderful interactions with you. Thanks to all of you, this long stay away from home has been exciting and remains bearable. Saket, Krati, and Anusha, thank you for making my life in Blacksburg one of the most memorable phases in life. Kedar and Hatte, thank you for making my shorter stays in Blacksburg extremely fun and ones to remember. Leila, Boyu, and Anway thank you for making the fourth floor a more pleasant place. Pradeep, I have you to thank for many reasons – from being a great friend, making our long stays in the lab interesting and intellectual, to my stay in San Diego. Priyanka, thank you for being such a wonderful friend and believing in me all these years. Sudesh, Venkhat, Kumar, PJ, Anirudh, Zutshi, and Sanket, thank you for being such great friends even though we haven't always been able to keep in touch.

Ashok and Victor, I was lucky to have the two of you as my first ever mentors at a formal workplace. Thanks to you, I got to experience my biggest dream —working at Bell Labs—in the most unique and memorable way possible. Abhishek and Sameer, thank you for being amazing mentors to me during my internship at Qualcomm. I have been very fortunate to

see you work with such passion, integrity, and dedication.

Writing the dissertation during a global pandemic, I cannot help but realize how fortunate I have been through this entire period. I am, like so many of us are, eternally grateful to all the healthcare and essential workers who have fought tirelessly against this virus and helped maintain the fabric of our society. As the world, both around me and distant continues to suffer through the effects of this pandemic, I sincerely hope we all stay safe and emerge out of this stronger.

Now, to the most important people in my life. Suraj, Vignesh, Laxmi, Murali *mhantu*, Pushpa *mhave*, Gowri *pacchi*, thank you for being invaluable sources of love and inspiration. Pawan and Vasudeo, thank you for being the bundles of joy that you are! *Ajja*, I miss you! Manju *mhantu*, thank you for those small electronics projects during my childhood. You have been an inspiration. Alok and Ankush, although we haven't been able to keep in touch, I am grateful to you for all the memorable times.

Divya, I cannot thank you enough for all the love, support, and care that you have given me. You have been my pillar of strength during my weakest moments and added to my cheer when I have had successes. You have seen me at my worst, and yet, have been by my side like a rock. You are the best architect I know, and your passion, dedication, and sincerity in your work have been a benchmark that I try to meet in my work.

And finally, *Ammu*, I cannot possibly express what I owe to you in any number of pages. Thank you for everything! *Anna*, you are my role model. I have always aspired to be like you, and I hope that someday I can be half the person you are. Although I shall never be able to quantify your importance in my life, I know this — you have taught me the true meaning of hard work, perseverance, and humility. Whatever little I have been fortunate enough to achieve in my life, it is because of the two of you.

# Contents

# List of Figures

# List of Tables

# List of Abbreviations

3GPP 3rd Generation Partnership Project

ACK Acknowledgement

AP Access Point

BSM Basic Safety Message

BSR Buffer Safety Report

BSS Basic Service Set

C-V2X Cellular V2X

CAC Channel Availability Check

CBR Channel Busy Ratio

CCA Clear Channel Assessment

CCH Control Channel

COT Channel Occupancy Time

CSA Channel Switch Announcement

CSAT Carrier Sense Adaptive Transmission

CSMA/CA Carrier Sense Multiple Access with Collision Avoidance

CSR Candidate single sub-frame resource

CTS Clear To Send

CW Contention Window

DAM Detect and Mitigate

DAV Detect and Vacate

DCA Dynamic Channel Access

DCF Distributed Coordination Function

DCM Dual Carrier Modulation

DENM Decentralized Environmental Notification Messages

DFS Dynamic Frequency Selection

DIFS DCF Inter-frame Spacing

DMRS Demodulation Reference Signal

DOT Department of Transportation

DSC Dynamic Sensitivity Control

DSRC Dedicated Short Range Communications

EDCA Enhanced Distributed Channel Access

eMBMS Enhanced Multimedia Broadcast Multicast

EPC Evolved Packet Core

ETSI European Telecommunications Standards Institute

FBE Frame Based Equipment

FCC Federal Communications Commission

FDD Frequency Division Duplexing

FDM Frequency Division Multiplexing

HARQ Hybrid Automatic Repeat Request

HD Half Duplex

HE High Efficiency

IEEE Institute for Electrical and Electronics Engineers

IFS Inter-frame Spacing

IP Internet Protocol

ITS Intelligent Transportation Systems

LAA License Assisted Access

LBE Load Based Equipment

LBT Listen Before Talk

LSA Licensed Shared Access

LTE Long Term Evolution

LTE-U Long Term Evolution Unlicensed

LWA LTA-WLAN Aggregation

MAC Medium Access Control

MCS Modulation and Coding Scheme

MIMO Multiple Input Multiple Output

MU Multi User

NLOS Non Line of Sight

NPRM Notice of Proposed Rulemaking

NR New Radio

NR-U New Radio Unlicensed

OFDM Orthogonal Frequency Division Multiplexing

OFDMA Orthogonal Frequency Division Multiple Access

PDCP Packet Data Convergence Protocol

PDR Packet Delivery Ratio

PER Packet Error Rate

PHY Physical (layer)

PIFS Point Coordination Function IFS

PSCCH Physical Sidelink Control Channel

PSFCH Physical Sidelink Feedback Channel

PSSCH Physical Sidelink Shared Channel

QoS Quality of Service

RAT Radio Access Technology

RB Resource Block

RLC Radio Link Control

RRC Radio Resource Control

RRM Radio Resource Management

RSRP Reference Signal Received Power

RTA Real-Time Application

RTS Request To Send

RU Resource Unit

SC-FDMA Single Carrier Frequency Division Multiple Access

SCA Static Channel Access

SCH Shared Channel

SCI Sidelink Control Information

SDL Supplemental Downlink

SIR Signal-to-Interference Ratio

SNR Signal-to-Noise Ratio

SPS Semi-Persistent Scheduling

STA Station

TCP Transmission Control Protocol

TDD Time Division Duplexing

TDM Time Division Multiplexing

TF Trigger Frame

TXOP Transmission Opportunity

U-NII Unlicensed National Information Infrastructure

UDP User Datagram Protocol

UE User Equipment

V2I Vehicle-to-Infrastructure

V2N Vehicle-to-Network

V2P Vehicle-to-Pedestrian

V2V Vehicle-to-Vehicle

V2X Vehicle-to-Everything

WAVE Wireless Access in Vehicular Environments

WLAN Wireless Local Area Network

# Chapter 1

# Introduction

Wireless devices have become tightly integrated with our day-to-day lives. It is estimated that an average household in the US has as many as 11 connected devices [4]. While it was once common to think of smartphones, laptops, and tablets as primary devices connecting to the Internet using wireless access, today, a broad range of devices require (or at least benefit from) wireless connectivity. These devices include televisions, speakers, thermostats, lighting, etc. [4]. A vast majority of these in-home devices connect to the Internet using Wi-Fi. However, connectivity in home environments represents only a fraction of total Wi-Fi devices. It is estimated that in 2018 there were as many as 169 million Wi-Fi hotspots worldwide. This number is estimated to increase four-fold to 628 million by the year 2023 [5]. The popularity of Wi-Fi and its importance in our lives today can be estimated by the fact that there are 9.5 billion Wi-Fi devices in use today [2]. At the same time, we have witnessed an explosive growth in the demand for mobile data traffic sent over cellular networks. It is estimated that by the year 2025, this data will amount to 164 exabytes per month (1 exabyte = $10^9$ gigabytes!) [6]. Despite this demand, however, the underlying resource that enables wireless communications—the wireless spectrum—remains limited.

In the ever-increasing demand for wireless connectivity, stakeholders have turned to unlicensed portions of the wireless spectrum. Until a decade ago, Wi-Fi was the *de-facto* technology that delivered wireless access in low-mobility environments. In the last decade, however, with the design of several new unlicensed technologies, this has changed. Since 2010, at least five new unlicensed technologies have been developed (we describe these technologies in Chapter 2). While this increased number of options is appealing to the users and service providers, from a technical standpoint a large number of wireless devices across different technologies creates complex coexistence issues. No other bands exemplify this better than the 5 GHz and 6 GHz bands.

## 1.1 Wireless Local Area Networks

Wireless local area networks (WLANs) support last-mile Internet connectivity, i.e., WLAN technologies enable end-user devices (such as laptops, smartphones, tablets, etc.) to connect to the Internet infrastructure through a wireless *gateway* device. The most well-known and widely-used WLAN technology is Wi-Fi, where the gateway device is referred to as the Wi-Fi

Access Point (AP) and end-user devices are referred to as stations (STAs).

Wi-Fi devices are developed as per the IEEE 802.11 specifications for their physical (PHY) and medium access control (MAC) layers. The first 802.11 specifications— labeled IEEE 802.11b—were released more than two decades ago in 1999. IEEE 802.11b devices could communicate at a peak PHY rate of 11 Mbps [7]. Since then, Wi-Fi specifications have continuously evolved over the years; today's Wi-Fi—based on IEEE 802.11ac specifications—boasts a peak PHY rate of over 6.9 Gbps [8]. The recently standardized IEEE 802.11ax specifications will allow Wi-Fi devices to communicate at a peak rate of over 9.6 Gbps [9].

To achieve the aforementioned improvements in the peak PHY rates, the IEEE 802.11 Task Group has constantly worked on PHY layer enhancements, ranging from the introduction of Orthogonal Frequency Division Multiplexing (OFDM) in IEEE 802.11a/g, multi-antenna techniques in 802.11n, increased modulation orders across all specifications, continuous support for increased bandwidth, and an increased number of spatial streams in 802.11ac and 802.11ax [9]. At the same time, to ensure that improvements made at the PHY layer translate to improved end-user performance, the MAC layer of Wi-Fi has also undergone significant enhancements. This includes the introduction of frame aggregation and enhanced distributed coordination access (EDCA) in 802.11n [8], and orthogonal frequency division multiple access (OFDMA) in 802.11ax [9].

Wi-Fi devices operate on a secondary basis in unlicensed spectrum. Today, the most widely used unlicensed bands are the 2.4 GHz and 5 GHz bands [10]. Since Wi-Fi devices use these bands on a shared and non-exclusive basis, Wi-Fi specifications have been developed in a manner that Wi-Fi devices can coexist harmoniously with other unlicensed devices such as Bluetooth and ZigBee in the 2.4 GHz bands, and unlicensed flavors of LTE in the 5 GHz bands [10].

In addition to Wi-Fi, several unlicensed WLAN technologies primarily inherited from the cellular Long Term Evolution (LTE) and New Radio (NR) technology have been developed in recent years. These technologies—License Assisted Access (LAA) [11], LTE Unlicensed (LTE-U) [12], and NR Unlicensed (NR-U) [13]—are designed to mainly operate in the 5 GHz bands. Additionally, NR-U will also operate in the 6 GHz bands in regions where these bands are available for unlicensed access [13].

## 1.2 Vehicular Communications

Today's vehicles are equipped with a plethora of sensors. These sensors enable several applications that are primarily targeted at driver convenience and passenger and driver safety. For example, the lane departure warning system [14] leverages the cameras mounted in the vehicle to observe lane markings and provides an alert to the driver (and in some cases, even takes corrective actions) if the vehicle is veering out of its lane. Another example is the blind-spot monitoring system [15], which facilitates safe lane-changing maneuvers by

using the on-board radar and/or cameras to detect the presence of another vehicle in the *blind spot* of a vehicle. This sensor-based approach to safety is the basis of many autonomous vehicle models [16].

The benefits of in-vehicle sensors notwithstanding, the perception range of most sensors—including cameras, radars, and Lidar—is limited to line-of-sight (LOS) visibility. The LOS constraint limits the scope of safety applications enabled by these sensors. Today's vehicles cannot *see* beyond corners. Potential crashes and deaths and injuries resulting from this inability can be avoided if a vehicle's perception range can be increased to beyond other vehicles, curves, and buildings. This is the primary motivation for vehicular communications.

The communication paradigm of vehicles communicating with near-by entities is often referred to as vehicle-to-everything (V2X) communications [17]. V2X encompasses a vehicle's ability to communicate with nearby vehicles (V2V), road-side infrastructure (V2I), vulnerable road-side users such as cyclists and pedestrians (V2P), and the network (V2N). When employed in vehicles, V2X-capability will serve as an additional sensor with an increased perception range to observe non-line-of-sight (NLOS) obstacles.

V2X communications have the potential to significantly bring down the number of vehicle crashes, thereby reducing the number of associated fatalities [18, 19]. However, the benefits of V2X communications are not limited to safety applications alone. V2X-capable vehicles can assist in better traffic management leading to greener vehicles and lower fuel costs [17]. Such vehicular safety and non-safety applications constitute a critical element of Intelligent Transportation Systems (ITS).

### 1.2.1 V2X Communication Applications & Messages

Day-1 safety applications refer to applications that were envisioned during the conception of vehicular communications and are likely to become operational as soon as V2X-equipped vehicles hit the roads. Broadly speaking, day-1 safety applications are enabled by two types of messages. The first kind referred to as basic safety messages (BSMs) (referred to as Cooperative Awareness Message, or CAM, in Europe), requires each vehicle to broadcast information such as its velocity, heading direction, position, etc. on a regular basis. When these messages are received and processed by neighboring vehicles, these vehicles become aware of each others' presence. A majority of such day-1 applications require the transmission of BSMs at regular intervals on the order of 100 milliseconds [20, 21].

The second kind of message, referred to as event-driven messages (also known as Decentralized Environmental Notification Message, or DENM, in Europe), enable use cases that require timely and reliable delivery of messages when specific events occur. For example, if a vehicle comes to a sudden halt on a busy highway, a broadcast message indicating this emergency braking event can help in avoiding pile-ups on the highways. Although such event-driven messages are likely to be generated much less often (order of a few seconds or

more) in comparison to BSMs, the successful delivery of such messages is extremely critical.

Regardless of the type of the safety application enabling message—BSM or event-driven message—it can be inferred that vehicular safety applications impose two critical requirements on the underlying communication technology – (i) low latency, and (ii) high reliability.

In addition to day-1 safety applications, there is a growing impetus for the development of advanced vehicular applications, which not only increase the safety of drivers and passengers, but also aim at increasing traffic efficiency, cutting down pollution levels, and improve the driving experience. Furthermore, provisioning support for basic safety applications alone is unlikely to meet the requirements of self-driving autonomous cars. For example, while existing applications such as left turn assist and emergency electronic brake lights [22] are beneficial for vehicle safety, autonomous vehicles will require vehicles to be capable of transmitting messages indicative of maneuver changes, trajectory alignments, platoon formations, sensor data exchange, etc. [23]. Besides, even for human-driven vehicles, processing of data received from sensors of surrounding vehicles—for example, where one vehicle shares its live camera feed with a vehicle behind it—is expected to increase the safety benefits well beyond what can be achieved by basic safety applications.

Requirements of some advanced vehicular applications have been studied by the 3rd Generation Partnership Project (3GPP) in [23]. These applications fall under four broad categories: (i) vehicle platooning, (ii) advanced driving, (iii) extended sensors, and (iv) remote driving. The Quality of Service (QoS) requirements of these applications are summarized in Table 1.1.

Table 1.1: QoS requirements of advanced V2X applications

| **Use Case Group** | **Max. Latency (msec)** | **Payload Size (Bytes)** | **Reliability (%)** | **Data Rate (Mbps)** | **Min. Range (meters)** |
|---|---|---|---|---|---|
| Vehicle Platooning | 10 - 500 | 50 - 6000 | 90 - 99.99 | 50 - 65 | 80 - 350 |
| Advanced Driving | 3 - 100 | 300 - 12000 | 90 - 99.999 | 10 - 50 | 360 - 500 |
| Extended Sensors | 3 - 100 | 1600 | 90 - 99.999 | 10 - 1000 | 50 - 1000 |
| Remote Driving | 5 | - | 99.999 | UL: 25 DL: 1 | - |

As shown in Table 1.1, the latency and reliability requirements of these advanced V2X applications are much more stringent than those of basic safety applications. Furthermore, these advanced applications are characterized by the use of large and variable-sized packets and rely on messages that are transmitted aperiodically. This is in stark contrast to the applications that are based on the transmission of basic safety messages, which are transmitted periodically (typically once every 100 msec).

### 1.2.2 Spectrum for V2X Applications and its Underutilization

The spectrum reserved for V2X applications is globally in the 5.9 GHz band. In the US and most parts of Europe, this band is the 5.85–5.925 GHz band. However, recent efforts to allow unlicensed operations in the 5.9 GHz band on a secondary basis (as discussed shortly) are likely to result in the restructuring of this band in many regions of the world [24].

Despite undeniable arguments in favor of V2X communications, apart from a few pilot trials [25], vehicles enabled with communication devices are extremely few in number[1]. In 1999, the US Federal Communications Commission (FCC) assigned 75 MHz of spectrum in the 5.9 GHz band for the exclusive use of V2X applications. However, to date, there are no widespread deployments of vehicles that communicate using this frequency band. This slow adoption of V2X-capable vehicles can be largely attributed to the fact that V2X safety applications have very stringent communication requirements in potentially dense traffic environments. This is exacerbated by highly mobile wireless environments that pose unprecedented challenges in designing reliable communication mechanisms.

Citing the aforementioned underutilization of the 5.9 GHz band, regulators in the US and Europe began considering unlicensed operations in this band. We discuss the implications of this spectrum sharing in detail later in this dissertation. It is interesting to note, however, that on the one hand, the existing 75 MHz of spectrum available in the 5.9 GHz band may be insufficient to support the advanced vehicular applications envisioned for the future, while on the other hand, because this spectrum is currently underutilized, Wi-Fi and other unlicensed technologies may soon begin to operate in and share the band with vehicular technologies.

### 1.2.3 V2X Technologies

Until the release of 3GPP Release 14 specifications in 2017, the *de-facto* V2X technology was Dedicated Short Range Communications (DSRC) [20]. Relying on IEEE 802.11p specifications, DSRC borrowed large parts of its PHY and MAC layers from Wi-Fi. Consequently, DSRC systems enjoyed all benefits of Wi-Fi: a simple and efficient MAC protocol, the ability to operate in distributed environments, and no reliance on any external infrastructure. At the same time, DSRC also inherited Wi-Fi's problems, primarily its poor scalability.

DSRC systems have been extensively tested, especially through several large-scale testbeds. Nevertheless, because commercial vehicles were not equipped with DSRC modules, there was scope to develop, test, and deploy alternate technologies if they proved to sufficiently address the needs and requirements of V2X communications. This motivated the development of Cellular V2X (C-V2X) in 3GPP Release 14 specifications [26, 27, 28]. C-V2X is built atop LTE and borrows large parts of LTE PHY and MAC layers. However, since a fundamental

[1]Vehicles with cellular capabilities are available in the market. However, such cellular modules are primarily used for infotainment applications, with limited support for safety applications.

element of cellular networks is the base station (eNodeB in LTE), significant efforts went into developing mechanisms for distributed C-V2X operations. The communication mode of C-V2X that allows vehicles to communicate in a distributed fashion is referred to as sidelink mode 4.

The debate among which of the two technologies is superior in terms of better scalability, larger communication range, and superior performance is ongoing. There are merits to both technologies. DSRC is well-tested and is known to provide support for day-1 safety applications [29]. On the other hand, C-V2X performance is superior to DSRC in many practical scenarios [30]. The ultimate choice between the two technology will depend on many factors, including but not limited to automaker preferences, future integration paths, cost, and regulatory decisions. Nevertheless, both technologies may be adopted within a geographical region. Further, it is also possible that some geographical regions adopt C-V2X while other regions adopt DSRC.

## 1.3 Coexistence of Heterogeneous Technologies

Wi-Fi systems are designed to coexist. This is true not only across different wireless technologies (such as coexistence between Wi-Fi and Bluetooth/ZigBee) but also across different Wi-Fi generations (e.g., coexistence between IEEE 802.11a-based Wi-Fi and 802.11ac-based Wi-Fi). Furthermore, Wi-Fi devices, in many cases, also coexist with incumbent users of the band in which they operate. An example of this is Wi-Fi operations in the 5.47–5.725 GHz band, where Wi-Fi devices must coexist with radar systems—the primary users of the band [10]. With the addition of each new technology for sharing in a given band, however, the coexistence scenario becomes more complicated, and the implications of the coexistence can be grave on Wi-Fi or the other technology if proper care is not taken.

In the past few years, the number of technologies with which Wi-Fi devices must coexist has increased substantially. With the growing demand for mobile high-speed Internet access, designers of cellular technology turned to unlicensed spectrum. Thus were born technologies like LTE-U and LAA, which, thanks to their cellular inheritance, were not inherently compatible with Wi-Fi. Because unaltered operations of LTE could significantly hamper Wi-Fi performance [12, 31], which were deployed in the millions across the 5 GHz bands, significant research went into designing simple, effective, and robust coexistence mechanisms between LTE-U/LAA and Wi-Fi [32]. With the design of NR-U in 3GPP Release 16 specifications [33], this coexistence scenario remains challenging and interesting.

While other technologies have been entering bands in which Wi-Fi devices currently operate, Wi-Fi stakeholders have been seeking additional bands in which the next generation of Wi-Fi devices can operate. Responding to this demand, FCC and other regulators have taken decisive steps to open up parts of the 5.9 GHz band and the 6 GHz bands [2, 24, 34]. With the fresh entry of unlicensed technologies into these bands, coexistence mechanisms,

protocols, and parameters, which have been long frozen in the 2.4 GHz and 5 GHz bands can be re-visited, and the efficiency of technologies when they coexist can be improved. This is especially true for the 6 GHz bands, where an extremely large amount of spectrum is available and where Wi-Fi and NR-U devices are likely to be the two major unlicensed technologies operating for the first time.

At the same time, additional unlicensed bands bring with them a new and diverse set of incumbent users with which unlicensed technologies must coexist. While insights drawn from all past coexistence scenarios can influence regulatory decision-making in these new bands, new and improved mechanisms are often desired. Furthermore, the diversity of incumbent technologies in the 5.9 GHz and 6 GHz bands implies that coexistence solutions developed for one scenario often do not translate well in another scenario. Thus, the availability of additional unlicensed bands creates a diverse set of coexistence scenarios and opens up several unaddressed research problems.

## 1.4 Contributions

In this dissertation, we tackle several issues related to the coexistence of heterogeneous technologies in the 5 GHz and 6 GHz bands. Our main contributions are briefly highlighted below.

**Survey of coexistence issues in the 5 GHz and 6 GHz bands:** In Chapter 3, we provide a comprehensive survey of coexistence issues in the 5 GHz and 6 GHz bands. The coexistence scenarios studied include: (i) coexistence of radars and Wi-Fi in the 5 GHz bands, (ii) coexistence of 6 GHz incumbents and Wi-Fi, (iii) coexistence of DSRC and Wi-Fi, (iv) coexistence of C-V2X and Wi-Fi, (v) coexistence across V2X technologies (i.e., DSRC and C-V2X), (vi) coexistence across heterogeneous Wi-Fi generations, and (vii) coexistence of unlicensed cellular technologies (e.g., LTE-U, LAA, and NR-U) and Wi-Fi. These scenarios include coexistence problems that already exist today (such as the radar–Wi-Fi coexistence problem in the 5 GHz bands), ones that were likely to arise due to regulatory decisions (such as co-channel coexistence of DSRC/C-V2X and Wi-Fi), and those problems that might occur in the future (such as coexistence between DSRC and C-V2X). Because each coexistence scenario has unique characteristics, we look at these coexistence scenarios on a case-by-case basis. We provide an overview of related literature, highlight the major challenges moving forward, and identify the most significant research challenges for each coexistence scenario.

**Study of coexistence between DSRC and Wi-Fi:** In Chapter 4, we investigate the DSRC–Wi-Fi coexistence problem in detail. Even though spectrum sharing between DSRC and Wi-Fi can benefit users of Wi-Fi networks, it must be ascertained that such secondary usage of the 5.9 GHz band by Wi-Fi devices does not lead to deterioration of the DSRC system performance. Therefore, in Chapter 4, we leverage proposed mechanisms from existing literature to study whether Wi-Fi induced interference can be mitigated at DSRC receivers

when the two technologies operate and coexist in a shared channel. We observe that because DSRC and Wi-Fi are fundamentally similar in their MAC layers, relatively simple modifications at Wi-Fi devices can protect DSRC devices sufficiently. We verify these conclusions through extensive simulations and an experimental testbed.

Having established that simple modifications to the Wi-Fi protocol can protect DSRC system performance from interference, the question that remains to be answered is that—*is the 5.9 GHz band useful from the Wi-Fi performance viewpoint?* In our testbed experiments, we observe that as a consequence of the aforementioned modifications, the performance of Wi-Fi can significantly deteriorate. To strike a balance between DSRC system performance protection and Wi-Fi performance, we propose and evaluate a Real-time Channelization Algorithm, which can be deployed at Wi-Fi APs. This algorithm ensures that Wi-Fi devices can leverage the 5.9 GHz band when channels are available while maintaining an interference-free environment for DSRC devices.

**Study of coexistence between C-V2X and Wi-Fi:** Because C-V2X was developed only in 2017 while the FCC began considerations to open up the 5.9 GHz band for unlicensed access in 2013, all existing studies that look at the V2X–Wi-Fi spectrum sharing problem consider DSRC as the default V2X technology. However, with the rising popularity of and support for C-V2X, a scenario where C-V2X would be chosen as the preferred V2X technology is plausible. Consequently, in Chapter 5, we investigate whether Wi-Fi can harmoniously coexist with C-V2X users in the 5.9 GHz band. We investigate whether mechanisms that were originally designed to facilitate DSRC–Wi-Fi coexistence can sufficiently protect C-V2X performance. Unsurprisingly, we observe that these coexistence mechanisms either do not adequately protect the performance of C-V2X or completely suppress Wi-Fi transmissions, thereby rendering the band unusable for Wi-Fi devices. Thus, we conclude that if C-V2X and Wi-Fi devices are to share the 5.9 GHz band, novel coexistence mechanisms that leverage the characteristics of the C-V2X MAC layer must be designed.

Co-channel coexistence between C-V2X and Wi-Fi, although desirable, is not the only mechanism by which Wi-Fi and C-V2X devices can use the 5.9 GHz band. The *re-channelization* proposal for Wi-Fi operations in this band proposes to re-farm the 5.9 GHz band, exclusively allocating the top 30 MHz for vehicular safety applications while allowing unlicensed Wi-Fi operations in the bottom 45 MHz of the 5.9 GHz band. Since this proposal places C-V2X and Wi-Fi devices in channels that are close to each other in the frequency domain, we investigate the impact of adjacent channel Wi-Fi interference on C-V2X performance. We learn that (i) the farther Wi-Fi devices are in the frequency domain from the C-V2X operational channel the better it is for C-V2X performance, and (ii) for a given C-V2X and Wi-Fi channel configuration, wider bandwidth Wi-Fi channels cause considerably higher interference at the C-V2X receivers than narrower Wi-Fi channels.

**Study of coexistence between 5G NR-U and Wi-Fi in the 6 GHz bands:** As noted previously, the 6 GHz bands present a unique opportunity to take a fresh look at the coexistence of Wi-Fi and other unlicensed technologies. Ideally, all aspects of coexistence

can be re-engineered. This includes the listen-before-talk protocol used by Wi-Fi and other unlicensed technologies and their respective parameters. However, given that the first two technologies that are likely to operate in the 6 GHz bands—IEEE 802.11ax and 5G NR-U—have already been standardized, a complete overhaul of the MAC protocol may not be feasible. Nevertheless, in Chapter 6, we seek to identify whether simple, standards-compliant mechanisms can facilitate better coexistence between these two technologies.

We develop a stochastic geometry-based model to derive an expression for the probability of successful transmissions when Wi-Fi and NR-U devices coexist. We observe that by simply restricting Wi-Fi uplink transmissions to the Multi User (MU) OFDMA mode, which will be used for the first time in Wi-Fi in IEEE 802.11ax based devices, we can obtain significant improvements in the performance of not only NR-U devices but also uplink Wi-Fi. All that is required to realize this improvement is to disable the *legacy* listen-before-talk mechanism used by Wi-Fi devices. Although such a proposal is unthinkable in the 5 GHz bands, where millions of Wi-Fi devices already operate and use this legacy contention mechanism, it is indeed possible in the 6 GHz bands, where there are no current Wi-Fi devices in use.

**Performance evaluation of C-V2X sidelink mode 4:** The 3GPP Release 14 specifications defined sidelink modes 3 and 4 for direct vehicular communications. In sidelink mode 3, vehicles equipped with C-V2X modules are assumed to be under cellular coverage. In such scenarios, radio resource management is handled by the eNodeB. However, because cellular coverage cannot always be relied upon, especially in rural areas, C-V2X equipped vehicles must be able to communicate without any assistance from the cellular infrastructure. This is the sidelink mode 4 in C-V2X. It is widely known that the PHY layer performance of C-V2X is superior to DSRC. However, whether this improved PHY performance translates to superior application-level performance depends largely on the efficiency of the MAC layer. Thus, in Chapter 7, we use our in-house C-V2X sidelink simulator to analyze the performance of C-V2X sidelink mode 4 in highway environments.

One of the features introduced in C-V2X sidelink modes 3 and 4 is packet re-transmissions, which, if enabled, allows vehicles to transmit each packet twice to improve the reliability of transmissions. Indeed, from the PHY layer perspective, packet re-transmissions are beneficial because they introduce time and frequency diversity; packets sent over different frequency resources and at different times are likely to suffer through different levels of channel impairments. Consequently, the probability that both packets are lost diminishes, and the system performance increases. However, such re-transmissions come at the cost of increased overhead. This cost is borne by the MAC layer, which is responsible for arbitrating channel access across vehicles. In Chapter 7, we show that the performance of C-V2X indeed deteriorates if packet re-transmissions are enabled without due consideration of channel congestion. Motivated by this, we propose, design and evaluate a re-transmission control mechanism using which C-V2X enabled vehicles can maximize their performance in lightly-loaded environments, while not suffering through the negative effects of re-transmissions in heavily-loaded environments.

**Performance evaluation of IEEE 802.11ax MU OFDMA:** One of the most important objectives of IEEE 802.11ax is to improve the perceived experience of the end-user. This implies that in addition to increasing the peak PHY throughput—which has been one of the primary objectives in previous Wi-Fi amendments—metrics like the per-user throughput and latency must also be improved upon. A critical feature that is expected to help IEEE 802.11ax achieve this objective is MU OFDMA. In all previous 802.11 specifications, Wi-Fi devices are allowed to *contend* for the channel, and if a device wins access to the channel, it transmits on the entire channel. While this simple protocol works well for small network sizes (i.e., when the number of devices contending for channel access is small), the performance quickly deteriorates as the network size increases. MU OFDMA, on the other hand, divides the channel into orthogonal frequency resource units, and the Wi-Fi AP assigns these resource units to individual STAs based on their traffic demands. This approach is likely to significantly boost the efficiency of the Wi-Fi MAC layer in IEEE 802.11ax.

The benefits of MU OFDMA notwithstanding, there are several challenges to MU OFDMA operations in IEEE 802.11ax devices, especially when they coexist with legacy Wi-Fi devices. For example, how often does the AP *trigger* this MU OFDMA mode when both legacy and 802.11ax devices operate in the network? Furthermore, how do STAs transmitting in the uplink notify the AP that they have pending packets? These are some of the issues we look at in Chapter 8. We build atop a seminal Markov Chain model to characterize the performance of Uplink OFDMA-based Random Access (UORA)—a mechanism designed in 802.11ax to allow STAs to randomly access the resource units. We then develop a mathematical model to compute the normalized MAC layer throughput of 802.11ax in a stand-alone 802.11ax network as well as when the 802.11ax AP has 802.11ax and legacy Wi-Fi STAs associated with it. Furthermore, we propose and evaluate a resource allocation algorithm that is optimal in terms of the achieved aggregated throughput.

**Performance evaluation of Multi Link Aggregation in IEEE 802.11be:** One of the critical objectives of next-generation Wi-Fi—Wi-Fi 7—is to facilitate better support for real-time applications such as augmented reality (AR) and virtual reality (VR) over wireless networks. Today, although Wi-Fi networks can support AR, VR and other real-time applications in sparse to modest deployment scenarios, their ability to support such applications worsens as the density of traffic increases. The biggest contributor to this worsening performance is the worst-case end-to-end latency. Many studies on the technical requirements of real-time applications suggest that if the end-to-end latency experienced by packets exceeds 10 msec, the performance of the real-time application suffers. To address this, work is actively underway within the IEEE 802.11be Task Group to develop novel features that reduce the worst-case latency experienced by Wi-Fi devices.

In Chapter 9, we investigate the impact of Multi Link Aggregation (MLA)—a new feature likely to be introduced in IEEE 802.11be—on the worst-case Wi-Fi latency. We study the performance of MLA-capable Wi-Fi devices under various traffic conditions. In doing so, we highlight that even if a single additional link is made available to future Wi-Fi devices, the resulting reduction in the worst-case end-to-end latency is substantial. In many scenar-

ios, we see an order of magnitude latency reduction (i.e., from seconds to milliseconds, or milliseconds to microseconds). Furthermore, even in the densest of scenarios, as long as a sufficient number of links are provisioned at the Wi-Fi transmitter and receiver, MLA can help such devices to meet the 10 msec latency requirement, which is demanded by most real-time applications.

## 1.5 List of Publications

The work done in this dissertation has led to the publication of the following papers.

### Journals

1. **G. Naik**, J. Park, J. Ashdown, W. Lehr, "Next Generation Wi-Fi and 5G NR-U in the 6 GHz Bands: Opportunities & Challenges", *IEEE Access*, Vol. 8, Issue 1, pages 153027-153056, 2020.

2. **G. Naik**, B. Choudhury, J. Park, "IEEE 802.11bd & 5G NR V2X: Evolution of Radio Access Technologies for V2X Communications", *IEEE Access*, Vol. 7, Issue 1, pages 70169-70184, 2019.

3. **G. Naik**, J. Liu, J. Park, "Coexistence of Wireless Technologies in the 5 GHz Bands: A Survey of Existing Solutions and a Roadmap for Future Research", *IEEE Comm. Surveys & Tutorials*, Vol. 20, Issue 3, 2018, pages 1777-1798, Third Quarter, 2018.

### Conference Proceedings

1. **G. Naik**, D. Ogbe, J.Park, "Can Wi-Fi 7 support Real-Time Applications? On the Impact of Multi Link Aggregation on Latency," under review.

2. **G. Naik**, J. Park, "Coexistence of Wi-Fi 6E and 5G NR-U: Can We Do Better in the 6 GHz Bands?," under review.

3. **G. Naik**, J. Park, J. Ashdown, "C$^2$RC: Channel Congestion-based Re-transmission Control for 3GPP-based V2X Technologies," in *Proc. IEEE WCNC*, Virtual conference, 2020.

4. **G. Naik**, J. Park, "Impact of Wi-Fi Transmissions on C-V2X Performance", in *Proc. IEEE DySPAN*, Newark, NJ, USA, November, 2019.

5. S. Bhattarai, **G. Naik**, J. Park, "Uplink resource allocation in IEEE 802.11ax", in *Proc. IEEE ICC*, Shanghai, China, May 2019.

6. **G. Naik**, S. Bhattarai, J. Park, "Performance Analysis of Uplink Multi-User OFDMA in IEEE 802.11ax", in *Proc. IEEE ICC*, Kansas City, USA, May, 2018.

7. J. Liu, **G. Naik**, J. Park, "Coexistence of DSRC and Wi-Fi: Impact on the performance of vehicular safety applications", in *Proc. IEEE ICC*, Paris, France, May 2017.

8. **G. Naik**, J. Liu, J. Park, "Coexistence of Dedicated Short Range Communications (DSRC) and Wi-Fi: Implications to Wi-Fi performance", in *Proc. IEEE INFOCOM*, Atlanta, GA, USA, May, 2017.

# Chapter 2

# Technical Background

## 2.1 Status of the 5 GHz & 6 GHz Bands

### 2.1.1 The Unlicensed 5 GHz Bands

The FCC in the US first opened up the 5.725-5.85 GHz band (along with the 2.4-2.4835 GHz band) for unlicensed access in 1985 [35]. The success of wireless technologies that operate in these bands, and other unlicensed bands, has been unprecedented. There are a large number of wireless radio access technologies (RATs) that operate in various parts of the unlicensed 5 GHz bands. Arguably the most popular RAT among them is the 802.11-based Wi-Fi. The success of the unlicensed bands can be best understood from the number of deployed Wi-Fi devices: there are an estimated 9.5 billion Wi-Fi devices in use today [35], a large number of which operate in the unlicensed 5 GHz bands.

The success of unlicensed bands can be, at least in part, attributed to the exorbitant cost of operating in licensed spectrum. While cellular operators must participate in lengthy auctions and expend large sums of money to operate in licensed spectrum, unlicensed Wi-Fi devices are readily available off-the-shelf and can be easily deployed at homes and office networks with little or no expert knowledge [36]. Another factor that plays a key role in the success of unlicensed 5 GHz bands in particular[1] is the large amount of bandwidth available therein. Globally, there is up to 500 MHz of spectrum in the 5 GHz bands available for unlicensed applications. Compare this to the nation-wide average spectrum available per wireless carrier in the US—Sprint Wireless, the entity that holds access to the largest amount of licensed spectrum in the US, owns only about 200 MHz (on average) across all licensed bands [37].

In addition to unlicensed portions of the 5 GHz bands, unlicensed RATs (such as the IEEE 802.11ad and IEEE 802.11ay) also operate in unlicensed portions of millimeter-wave (mmWave) frequencies. These bands indeed have a larger amount of bandwidth available. However, the use of these mmWave bands comes with a large number of challenges such as high propagation losses, sensitivity to blockage, etc. [38]. Thus, the 5 GHz unlicensed bands have emerged as one of the most coveted bands for launching new wireless applications and services not only because of the abundance of spectrum therein but also due to their

[1]The 2.4 GHz band, referred to as the Industry, Scientific and Medical (ISM) band, has only about 80 MHz of spectrum available worldwide.

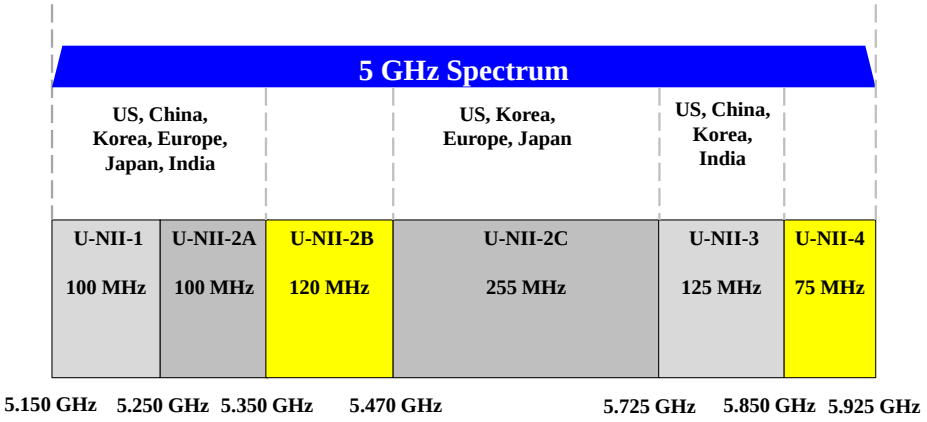


Figure 2.1: Unlicensed spectrum and regulations in the 5 GHz band. Regions marked yellow are U-NII bands proposed to open up for use by unlicensed devices in US.

relatively favorable propagation characteristics [39].

Different countries have their own requirements for unlicensed operations in the 5 GHz bands [32]. In the US, the unlicensed 5 GHz bands are referred to as the Unlicensed National Information Infrastructure (U-NII) bands. The $5.15 - 5.35$ GHz band is available in the US, China, Korea, Europe, Japan, and India. $5.47 - 5.725$ GHz is open for unlicensed access in the US, Korea, Europe, and Japan. In addition, the $5.725 - 5.85$ GHz is available in the US, China, Korea, and India. Fig. 2.1 summarizes the spectrum regulations in these regions.

Throughout the 5 GHz bands, channels used by unlicensed devices are in increments of 20 MHz bandwidths. Unlike the 2.4 GHz band, all 20 MHz channels in the 5 GHz bands are non-overlapping. Each channel is uniquely identified by its channel number, which is related to the center frequency of the channel as given by Eq. (2.1).

$$f_c(g)\ (\text{MHz}) = 5000 + 5 \times g, \tag{2.1}$$

where $g$ is the channel number and $f_c(g)$ is the center frequency of that channel.

In the US, the allocation of the U-NII-2B and U-NII-4 bands for unlicensed operations was considered by the FCC in 2013 [40]. The primary reason for this consideration was that by allowing unlicensed devices to operate in these two bands the amount of available spectrum for unlicensed access would have increased by up to 70%, thereby increasing the number of 80 MHz channels by 125% (from 4 to 9) [41]. After considerable debate, however, it was decided to not allow unlicensed operations in the U-NII-2B band and reserve the band for its incumbent users [42]. On the other hand, the creation of the U-NII-4 band—traditionally a band reserved for V2X communications—invited a considerable amount of debate between

proponents of the Wi-Fi and automotive industry. After significant debate and deliberations, portions of the U-NII-4 band were recently allocated to Wi-Fi services in the US [24]. We discuss the 5.9 GHz band next.

### 2.1.2 The 5.9 GHz ITS Band

#### 2.1.2.1 Initial Proposals

In 1999, the FCC in the US allocated 75 MHz of spectrum in the 5.9 GHz band for vehicular communications [20]. This band spans the 5.85–5.925 GHz range. Following suit, in 2008, the European Communications Commission (ECC) allocated three 10 MHz channels for similar applications and included four 10 MHz channels for future deployment in Europe [43].

While the fundamental nature of systems that are designed to use the 5.9 GHz bands remain similar worldwide, there are several differences in the terminologies adopted, regulations, and channel-specific use-cases in the two regions. In general, ITS systems in Europe, Japan, and the US are not compatible. Until recently, all of the channels were reserved in the US and (wherever applicable in) Europe for ITS applications. However, the V2X communication landscape throughout the world has been a rapidly evolving one. This includes the spectrum allocated for ITS applications worldwide. As noted in Sec. 2.1.1, regulators in the US and Europe started considerations to allow unlicensed operations in the 5.9 GHz band. We discuss the more recent developments related to the 5.9 GHz band shortly. However, in what follows, we first outline the initial plans for this band in the US and Europe.

The 75 MHz of spectrum in the ITS band is traditionally divided into seven 10 MHz channels. Keeping with the channel numbering convention used in the 5 GHz bands (given by Eq. (2.1)), these channels are numbered 172 (centered at 5.86 GHz) through 184 (centered at 5.92 GHz). These channels for the US are shown in Fig. 2.2.

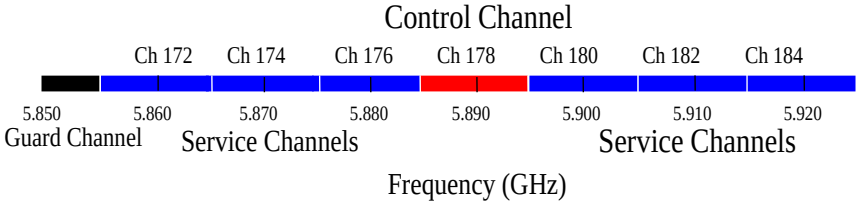


Figure 2.2: DSRC spectrum map in the US

In the US, the ITS band channels were divided into six service channels (SCHs) and one control channel (CCH)—channel 178. Additionally, there was a provision to combine channels 174 and 176 (to form channel 175) and channels 180 and 182 (to form channel 181). Further, channels 172 and 184 were designated for public safety applications involving the safety of

life and property. Together, these SCHs and the CCH were to be used to communicate safety-critical messages[2] such as the BSM and event-driven messages.

The ETSI standard EN 302 571 defines ITS spectrum regulations in Europe [44]. Under the specifications provided in [44], channels in the 5.855–5.875 GHz range in Europe were allocated for use by non-safety related applications (in contrast to the US where channel 172 in Fig. 2.2 was intended solely for safety applications), channels in the 5.875–5.905 GHz range to be used for safety applications and control, while channels in the 5.905–5.925 GHz range were reserved for future ITS applications. The authors in [20] and [43] provide a comprehensive overview of ITS spectrum-related issues in the US and Europe, respectively.

#### 2.1.2.2 Considerations for Unlicensed Access

Two decades have passed since the 5.9 GHz band was allocated in the US for ITS applications and more than a decade has passed in Europe. The adoption of DSRC—the first RAT designed exclusively for V2X applications—was very slow [45], and although DSRC-based systems were extensively tested through several test-beds [25], simulation studies [46], and analytical models [47], the ITS band remained underutilized throughout the world. Citing this underutilization, and coupled with the ever-increasing demand for unlicensed spectrum, the FCC in 2013 issued an NPRM for potentially opening up the 5.9 GHz band for unlicensed access in the US [40]. As noted in Sec. 2.1.1, this band is referred to as the U-NII-4 band in the US.

The above-mentioned proposals motivated industry, regulatory, and academic researchers to investigate coexistence mechanisms between DSRC and Wi-Fi in the 5.9 GHz ITS band. We discuss these coexistence mechanisms in detail in Sec. 3.3. Eventually, two coexistence mechanisms for DSRC and Wi-Fi coexistence were finalized in Europe [48], while the FCC in the US proposed to move forward with the *re-channelization* proposal in the US [49]. This proposal involves re-farming the ITS band, essentially ruling out the channel-specific use-cases discussed in Sec. 2.1.2.1.

#### 2.1.2.3 Current Status

Amidst the ongoing debate on whether DSRC systems could function in an uncompromised manner in environments where potential Wi-Fi interference existed, the 3GPP developed C-V2X—an LTE-based RAT that offered V2X capabilities—in its Release 14 in 2017 [30]. It is argued that within a given geographical region, DSRC and C-V2X cannot effectively coexist with each other [50]. Thus, automakers and regulators had to make a decision not only on whether unlicensed operations in the 5.9 GHz band could be allowed but also on which of the two RATs to opt for.

[2]The Service Channels can also be used to provide non-safety services like congestion control, mobile Internet access, etc.

In the US, the FCC sought answers to several questions related to DSRC, C-V2X, and unlicensed Wi-Fi (or Wi-Fi like) operations in the ITS band. Following answers to these questions from all stakeholders, the FCC issued an NPRM in November 2019 [24], which allocated the bottom 45 MHz of the ITS band (i.e., 5.85–5.895 GHz) for unlicensed Wi-Fi operations, while the upper 30 MHz (i.e., 5.895–5.925 GHz band) was reserved for V2X safety applications. Furthermore, following a request from the 5G Automotive Association (5GAA) to the FCC [51], the FCC NPRM proposed to allocate channels 182 and 184 for C-V2X operations in the US. The NPRM further sought comments on the future use of channel 180.

In Europe, on the other hand, the European Commission issued a delegated act in March 2019 to adopt ITS systems based on IEEE 802.11p throughout Europe [45]. However, in July 2019, twenty-one of the twenty-eight European Union countries voted against, and rejected this proposal [52], thereby keeping the DSRC-versus-C-V2X debate ongoing in Europe.

### 2.1.3 The Unlicensed 6 GHz Bands

A natural extension to the 5 GHz bands is the adjacent 6 GHz bands. These bands offer a similar communication range as the 5 GHz bands but have a large amount of bandwidth therein, which can potentially be used for not only supporting the growing needs of current wireless applications but also promoting the growth of the emerging ones. Motivated by this, the FCC in the US and the European Commission (EC) in Europe initiated studies to determine the feasibility of unlicensed operations in the 6 GHz bands. Specifically, the EC mandated a feasibility study of unlicensed operations in the 5.925-6.425 GHz band in Europe [34]. At the same time, the FCC 6 GHz Notice of Proposed Rulemaking (NPRM) [35] sought comments on opening up the 5.925-7.125 GHz band for unlicensed access in the US. In the US, this band will be divided into four sub-bands: U-NII-5 (5.925–6.425 GHz), U-NII-6 (6.425–6.525 GHz), U-NII-7 (6.525–6.875 GHz), and U-NII-8 (6.875–7.125 GHz). Spectrum sharing rules for the U-NII-5 through U-NII-8 bands in the US were recently finalized by the FCC in the 6 GHz Report & Order (R&O) [2].

The additional spectrum that the 6 GHz bands will unlock (500 MHz in Europe and 1.2 GHz in the US) will significantly increase the amount of unlicensed spectrum available in these regions. For example, the 6 GHz bands will more than double the current amount of unlicensed spectrum in the US. Unlicensed channels in the 6 GHz bands in the US are shown in Fig. 2.3. In Fig. 2.3, the channels in the U-NII-5 band correspond to those available for unlicensed access in Europe.

The number of 6 GHz channels available in the US and Europe is shown in Table 2.1. The relationship between the center frequency of a channel and the corresponding channel number in the 6 GHz band, as adopted by the IEEE 802.11ax specifications [53] and the European Communications Committee (ECC) Report 302 [54] is given by Eq. (2.2).

$$f_c(g)\ (\text{MHz}) = 5940 + (g \times 5) \quad \text{MHz}, \tag{2.2}$$

where $g$ is the channel number and $f_c(g)$ is the center frequency of that channel. The 20 MHz channels shown in Fig. 2.3 are given by channel numbers $1, 5, 9 \cdots$, while the 40 MHz channels are given by channel numbers $3, 11, 19, \cdots$. Channel numbers for 80, 160 and 320 MHz channels are shown in Fig. 2.3.

| **Bandwidth** | **United States** | **Europe** |
|---|---|---|
| 20 MHz | 59 | 24 |
| 40 MHz | 29 | 12 |
| 80 MHz | 14 | 6 |
| 160 MHz | 7 | 3 |
| 320 MHz | 3 | 1 |

Table 2.1: Number of 6 GHz channels in the US and Europe.

The 6 GHz bands are deemed critical in supporting emerging bandwidth-intensive and latency-sensitive applications such as wireless augmented reality (AR), virtual reality (VR), and mobile gaming applications [55]. The availability of large amounts of bandwidth in the 6 GHz bands could make it possible to deliver extremely high throughput (rivaling those offered by the mmWave bands but without their associated challenges), coupled with tight latency and reliability requirements. This has prompted industry stakeholders to expedite their efforts on research and development of new mechanisms that leverage the abundant spectrum available in the 6 GHz bands. For example, in the development of IEEE 802.11be [56]—the successor to the upcoming IEEE 802.11ax [57] standard—one of the critical goals is to effectively utilize the 6 GHz bands. Furthermore, the availability of the first set of Wi-Fi devices capable of operating in the 6 GHz bands, which will be based on IEEE 802.11ax, has already been announced [58, 59]. These devices will be referred to as Wi-Fi 6E devices.

Unlicensed users operating in the 6 GHz bands must coexist with the incumbent users of the band. We discuss the coexistence-related regulations mandated by the FCC in the US and those being considered in Europe in Sec. 3.2. In what follows, we provide a summary of these coexistence rules in the US. While these coexistence rules have been finalized in the US, coexistence mechanisms in Europe are likely to be finalized soon. Furthermore, because the nature of the incumbent users operating in the 6 GHz bands in the US and Europe are largely similar (see Sec. 2.2.1.2), coexistence mechanisms adopted in Europe are likely to be similar to those finalized in the US [13].

In the US, the FCC mandates the use of an Automatic Frequency Coordination (AFC) system in the U-NII-5 and U-NII-7 bands, whereby unlicensed devices must first contact the AFC system database and acquire a list of permissible frequencies. For the U-NII-6 and U-NII-8 bands, unlicensed devices shall be allowed to operate only in indoor settings at low transmission powers, thereby relying on building entry losses to mitigate interference at

incumbent receivers [2]. Table 2.2 contains the summary of 6 GHz specific operations, as permitted by the FCC, in the US.

| | U-NII-5 | | U-NII-6 | | U-NII-7 | | U-NII-8 | |
|---|---|---|---|---|---|---|---|---|
| **Frequency range** | 5.925–6.425 GHz | | 6.425–6.525 GHz | | 6.525–6.875 GHz | | 6.875–7.125 GHz | |
| **Channels** | **20 MHz** | 24 | **20 MHz** | 4 | **20 MHz** | 18 | **20 MHz** | 11 |
| | **40 MHz** | 12 | **40 MHz** | 1 | **40 MHz** | 9 | **40 MHz** | 5 |
| | **80 MHz** | 6 | **80 MHz** | 0 | **80 MHz** | 4 | **80 MHz** | 2 |
| | **160 MHz** | 3 | **160 MHz** | 0 | **160 MHz** | 2 | **160 MHz** | 1 |
| **Constraints** | Indoor operations permitted. Outdoor operations permitted *only if* device is outside exclusion zones. | | Indoor operations permitted. Outdoor operations *not* permitted. | | Indoor operations permitted. Outdoor operations permitted *only if* device is outside exclusion zones. | | Indoor operations permitted. Outdoor operations *not* permitted. | |
| **Outdoor** | Devices must connect to the AFC system database. Max power: 36dBm (AP)/ 30dBm (client) | | N/A | | Devices must connect to the AFC system database. Max power: 36dBm (AP)/ 30dBm (client) | | N/A | |
| **Indoor** | - Devices *cannot* be weather resistant.<br>- Devices *cannot* be equipped with external antennas.<br>- Devices *cannot* be operated on battery power.<br>- Max power: 30dBm (AP)/ 24dBm (client) | | | | | | | |

Table 2.2: Summary of 6 GHz operations in the US.

## 2.2 Wireless Technologies in the 5 GHz & 6 GHz Bands

The 5 GHz and 6 GHz bands are home to a variety of wireless technologies. These technologies enable a rich and diverse set of wireless applications. These range from WLANs that enable high-speed Internet connectivity, a range of radar systems, vehicular communication technologies, mobile and nomadic television pickup stations that broadcast (or relay) television content in real-time from special event locations, ultra-wideband (UWB) systems that support several low-cost applications, fixed service systems that enable backhaul connectivity for mobile networks, etc. While some of these technologies are incumbents, i.e., possess exclusive rights to operate in their designated spectrum, others (such as Wi-Fi and UWB

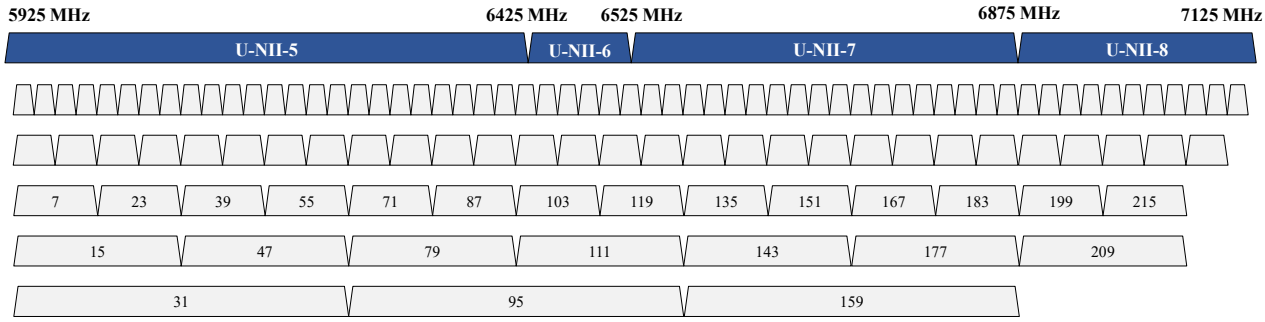


Figure 2.3: The 6 GHz channels for unlicensed access in the US.

systems) operate on a secondary basis, and can operate on a channel only when the incumbent user (if any) of the channel is not in operation. In what follows, we briefly describe the major wireless technologies that operate in different portions of the 5 GHz and 6 GHz bands.

### 2.2.1 Incumbent Technologies

#### 2.2.1.1 Radars in the 5 GHz Bands

Radar systems operate in various portions of 5 GHz bands worldwide. For example, in the US, radars operate in $5.25-5.725$ GHz bands [60]. In UK and Europe, radars operate across the band from $5.25-5.85$ GHz [41, 61]. While the nature and applications of these radars vary from band-to-band and from one country to another, these radars are generally used for applications that include defense (such as tactical and weapon radars), and ground-based and airborne weather radars. Radars are used for civilian (such as meteorological radars), military/defense applications as well as radio navigation applications (such as those used by the National Aeronautical and Space Agency in the US). A comprehensive summary of radars operating in the 5 GHz bands in the US is presented in [60].

Unlicensed devices operate on a secondary basis in the $5.25-5.35$ GHz and $5.47-5.725$ GHz bands in most parts of the world based on ITU regulations [62]. Radars operating in these bands mostly include civilian radars. As far as these bands are concerned, weather radars operating in the $5.6-5.65$ GHz band have been the primary victims of interference from unlicensed Wi-Fi users. Many of the radar systems operating in the 5 GHz bands are used for mission and safety-critical applications. The sharing of spectrum with unlicensed or other licensed devices may be highly undesirable from the point of view of such radar operating agencies.

#### 2.2.1.2 Incumbent Users of the 6 GHz Bands

The 6 GHz bands are home to several non-federal incumbent users in the US [35]. Among these, the most prominent ones are the fixed point-to-point services [63]. These services are used for providing highly-reliable backhaul links to critical services such as police and fire vehicles, electric grids, coordination of train movements, etc. A majority of these fixed point-to-point services are licensed to operate in the U-NII-5 and U-NII-7 bands [35]. Safety-related fixed service links in these two bands have a reliability requirement of 99.9999%, while most other links have a reliability requirement of 99.999% [64]. Such point-to-point microwave links are also used for providing backhaul to cellular mobile networks, e.g., links between the eNodeB/gNodeB of an LTE/5G network and its core network. Services provided using the U-NII-5 and U-NII-7 bands are such that the locations of incumbent users can be known beforehand and do not change frequently. Furthermore, new incumbent users in these bands are added infrequently [2].

The U-NII-6 and U-NII-8 bands, on the other hand, are licensed to users whose locations cannot be determined accurately at all times. These users include local television transmission services and cable television relay services [35]. The former services are used by television pickup stations to stream content from special events or remote locations (e.g., electronic newsgathering services) to central locations such as the television studio. The latter services operate similarly in that fixed/mobile transmitting stations send audio and video data back to the receiving stations. Incumbent users in these bands are *nomadic* in that the locations of transmitters and receivers can change frequently based on the location of special events such as sporting events and concerts. Consequently, licenses are granted to these users to operate in vast areas and throughout the frequency bands for maximum flexibility.

In addition to the aforementioned incumbent users, fixed satellite services are also offered using various portions of the 6 GHz bands. For example, the U-NII-5 band supports earth-to-space fixed satellite services that cater to applications like content distribution for radio and television broadcasters. However, since receivers of these applications (i.e., satellites) are located far from potential unlicensed interferers, individual unlicensed devices are likely to cause no interference at satellite receivers.

The U-NII-6 band also enables applications that use UWB systems. These systems operate under FCC's Part 15 rules for unlicensed operations. They include real-time locating systems, which are used for tool tracking and worker safety in industrial environments, ball and player tracking in National Football League matches [65], airport baggage handling systems, and robotic applications [66]. UWB systems are characterized by extremely low transmit powers (less than -41.3 dBm/MHz [2]) spread out over large bandwidths, which makes these systems extremely susceptible to external interference.

In Europe, the 5.925-6.425 GHz band—which has the same frequency range as the U-NII-5 band in the US—is under consideration for unlicensed use by radio local area networks, including Wi-Fi. The incumbent users of this band include fixed services and fixed satellite

(earth-to-space) services [54]. This band also supports long-distance point-to-point links that are used to backhaul mobile broadband networks similar to that in the US [34]. Some countries in Europe also use parts of this band for railroad train control, referred to as the communication-based train control (CBTC)[3] [34]. Additionally, like in the US, this band supports unlicensed users that use UWB systems. Because UWB systems are unlicensed users, they operate on a non-interference and non-protected basis. Note that with a few exceptions, the nature of the incumbent users in Europe is the same as those in the US.

### 2.2.2 IEEE 802.11 (Wi-Fi) Family of Standards

Wi-Fi is arguably the most popular unlicensed wireless technology. It is estimated that by 2021 there will be 200 million public Wi-Fi hotspots in the US alone [67]! The popularity of Wi-Fi stems from the ease of its access in terms of cost and deployment—it takes little to no experience to deploy a Wi-Fi AP, which is readily available for as low as $10 in most parts of the world. Furthermore, the constant evolution of Wi-Fi specifications has ensured that Wi-Fi devices remain competitive in provisioning emerging wireless applications. Consider, for example, the peak PHY layer throughput. While the peak Wi-Fi PHY rate achievable in the early 2000s was 54 Mbps, this number has increased to 9.6 Gbps with the now available 802.11ax devices [68]. In addition to PHY layer enhancements, the MAC layer of Wi-Fi has also steadily evolved, with promising changes introduced in the IEEE 802.11ax specifications. In this sub-section, we briefly introduce the prominent Wi-Fi characteristics, features, and mechanisms.

#### 2.2.2.1 Legacy Wi-Fi

In the context of WLANs, the term legacy Wi-Fi is typically used to refer to Wi-Fi devices that predate the current/latest Wi-Fi generation. Throughout this dissertation, we use the term *legacy Wi-Fi networks* to describe Wi-Fi networks based on standards that predate IEEE 802.11ax. These legacy standards include IEEE 802.11a, IEEE 802.11b, IEEE 802.11g, IEEE 802.11n, and IEEE 802.11ac.

**Physical Layer**

Wi-Fi devices use OFDM at the PHY layer. The default bandwidth of a Wi-Fi channel is 20 MHz, which is composed of 64 orthogonal sub-carriers in legacy Wi-Fi devices. Thus, the OFDM sub-carrier spacing in Wi-Fi is 312.5 kHz. Starting from IEEE 802.11n, Wi-Fi specifications allow transmissions in wider (than 20 MHz) channels. While 802.11n allows up to 40 MHz wide channels, 802.11ac permits the use of up to 160 MHz channels.

The IEEE 802.11n specifications permitted the use of multiple antennas at the transmitter

[3] CBTC systems use the 5.915–5.935 GHz band in France, 5.925–5.975 GHz band in Denmark, and 5.905–5.925 GHz band in Spain [54].

and receiver for the first time, thereby enabling the use of Multiple Input Multiple Output (MIMO) in Wi-Fi systems. MIMO was a key enabler to high data rates in 802.11n. Using multiple antennas at the transmitter and receiver, MIMO can be used to achieve higher reliability (via spatial diversity) or higher data rates (via spatial multiplexing). In 802.11n, using $2 \times 2$ MIMO, transmitters can theoretically achieve up to twice the maximum data rate of legacy devices. In the 802.11ac, the maximum number of antennas at the transmitter and receiver was increased to eight.

In addition to multiple antenna techniques, Wi-Fi devices have benefitted from a gradual increase in the maximum allowable modulation order. While the IEEE 802.11n standard provisioned support for modulation schemes up to 64-QAM with a coding rate of 5/6, the IEEE 802.11ac specifications introduced 256 QAM, with a maximum coding rate of 5/6.

### The CSMA/CA protocol

Legacy Wi-Fi devices use the IEEE 802.11 Distributed Coordination Function (DCF) or the EDCA protocol as the basic channel access mechanism[4]. The DCF and EDCA protocols are shown in Fig. 2.4. The channel access protocol used in Wi-Fi is broadly referred to as Carrier Sense Multiple Access with Collision Avoidance (CSMA/CA). CSMA/CA belongs to a class of MAC protocols where every transmitting device must sense the channel (i.e., *listen*) before it initiates a transmission (i.e., *talks*). Naturally, this class of MAC protocols is often referred to as the Listen Before Talk (LBT) protocols.

Pending transmission, each Wi-Fi device performs the Clear Channel Assessment (CCA) mechanism to sense the channel for a duration referred to as Inter-frame Spacing (IFS)[5]. If idle, the device enters an exponential backoff procedure [69] in order to avoid simultaneous transmissions with other nodes, thus avoiding packet collisions. If the channel becomes busy during this backoff procedure, the devices freeze their backoff mechanism and resume when the channel becomes idle once again.

The exponential backoff procedure in Wi-Fi requires that the Wi-Fi devices maintain and update four channel access parameters in DCF and four channel access parameters per traffic category in EDCA. These four parameters are the Backoff counter (BO), Contention Window (CW), the minimum value of the CW (CWmin), and the maximum value of the CW (CWmax). When the transmitting device first enters the exponential backoff phase, it picks a random integer uniformly in the range [0,CW-1]. This integer is assigned to the BO. For each idle *slot*, the duration of which is 9 $\mu$sec, the BO value is decremented by one. If the BO value reaches zero, the device transmits. If a packet transmission succeeds, i.e., the receiver acknowledges the receipt of the packet by transmitting an acknowledgment (ACK)

[4]In addition to DCF, the 802.11 specifications also define Point Coordination Function (PCF), wherein the Wi-Fi AP *polls* Wi-Fi stations and coordinates their transmissions. However, because of the overhead introduced due to this polling mechanism, PCF is rarely used in practice.

[5]The value of IFS depends on the frame type at the transmitter queue. The deferral of channel access for IFS serves prioritization of different traffic types (traffic classes with smaller IFS values have a higher priority in accessing the channel).

frame, the CW value is reset to CWmin. However, if the transmitting Wi-Fi device does not receive an ACK within a specified duration (the ACK timeout), the packet is assumed to be lost due to collision(s) and the CW is doubled[6]. Once the CW value reaches CWmax, the CW doubling ceases and the CW value is maintained at CWmax until either the packet transmission succeeds or the packet is dropped after a maximum retry limit. Once a device gains access to the channel, it continues to transmit on the channel without stopping or contention for a duration referred to as the transmission opportunity (TXOP). The value of this parameter is different for different traffic classes.

Channel sensing in Wi-Fi comprises of two different elements, (i) physical carrier sensing, and (ii) virtual carrier sensing. Physical carrier sensing involves the mechanism of physically sensing the energy available on the channel and comparing this energy against a predetermined detection threshold. If the energy level is above this detection threshold, the channel is declared *Busy*. Otherwise, the channel is considered *Idle*. Depending on whether the signal on-the-air being sensed is transmitted by another Wi-Fi device or not, physical carrier sensing can be of two types—(a) preamble detection, and (b) energy detection. The former sensing mechanism, as the name indicates, is used to detect the preamble sequence of neighboring Wi-Fi devices. The threshold energy value for preamble detection is $-82$ dBm/20 MHz. The latter scheme, i.e., energy detection, is used for the detection of non-Wi-Fi signals on-the-air. The energy detection threshold used in Wi-Fi is $-62$ dBm/20 MHz.

Virtual carrier sensing in Wi-Fi can only be used in conjunction with preamble detection. Since the preamble of the Wi-Fi signal is detected as a part of the preamble detection mechanism, it's contents can be decoded and utilized. One such field is the duration of the current transmission. Once the duration of the current transmission is decoded, the sensing Wi-Fi sets the parameter Network Allocation Vector (NAV) to this duration value and ceases sensing for the remainder of the NAV duration. This allows power-constrained Wi-Fi devices to enter the sleep state, thereby saving energy.

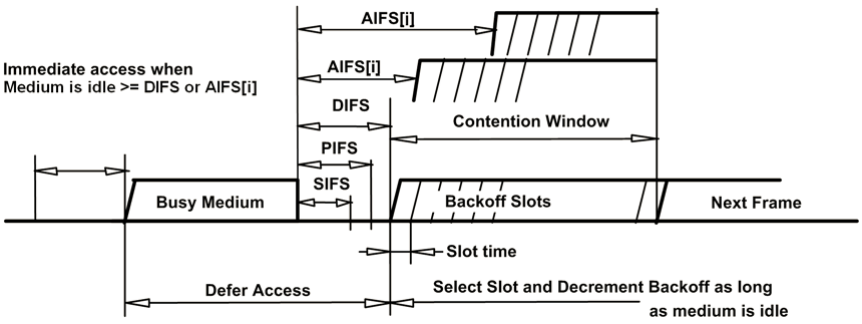


Figure 2.4: IEEE 802.11 DCF basic access

[6]Note that packet collision(s) need not always be the cause for packet losses. Packet losses can also occur due to other wireless channel impediments. However, since the transmitter has no way of knowing the cause of the packet loss, it is always assumed that the packet loss is due to collision(s).

Despite the elegance of the MAC protocol used in DCF and EDCA, every frame transmitted by an 802.11 device has a significant amount of overhead. This overhead includes radio level headers, MAC frame fields, IFS, the backoff slots, and acknowledgment of transmitted frames. In high data rate transmissions, these overheads are comparable to the time taken to transmit the payload frame itself, thereby reducing the *goodput* of Wi-Fi transmissions. To amortize this overhead and to increase the goodput, starting from 802.11n, Wi-Fi allows for aggregation of multiple frames to form a larger frame.

### Channel Bonding

The granularity of channel bandwidth in Wi-Fi is 20 MHz. IEEE 802.11n supported provisions to "bond" two adjacent 20 MHz channels and form a 40 MHz channel. One of the two 20 MHz channels—referred to as the primary channel—is used to transmit Wi-Fi control information, while the other 20 MHz channel is referred to as the secondary channel and is solely used for data transmissions.

Different channel sensing mechanisms are followed for the primary and secondary channels. The primary channel is where the binary exponential mechanism described above is used. Thus, the primary channel is sensed for the duration of (AIFS/DIFS[7] + backoff). The secondary channel, on the other hand, is sensed only for a duration of PIFS[8] preceding the end of the primary channel backoff, as shown in Fig. 2.5. If the secondary channel is idle for this PIFS duration, data transmission proceeds on the bonded (primary + secondary) channels.

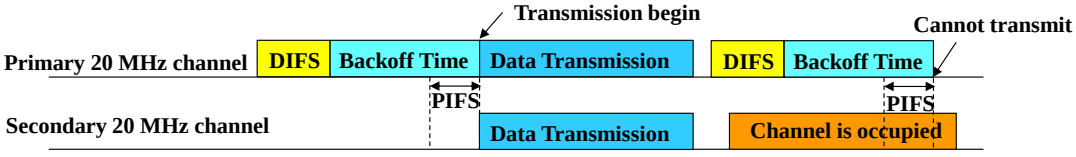


Figure 2.5: IEEE 802.11n carrier sensing for primary and secondary channels.

In addition to 20 MHz and 40 MHz channels, the IEEE 802.11ac specifications also support 80 and 160 MHz channels: two adjacent 20 MHz channels can be bonded to form a 40 MHz channel, two adjacent 40 MHz channels can form an 80 MHz channel and two adjacent or non-adjacent 80 MHz channels can form a 160 MHz channel [70]. For bonded channels, one 20 MHz channel is selected as the primary channel, while the remaining channels constitute the secondary channels. The channel sensing mechanism is similar to that used in 802.11n. The secondary channels are sensed only for a duration of PIFS immediately preceding the end of the primary channel backoff. The response of the 802.11ac transmitter at this stage

[7]AIFS – Arbitration Inter-frame Spacing, and DIFS – DCF Inter-frame Spacing
[8]PIFS – Point Coordination Function Inter-frame Spacing

can be classified into two types: (i) static channel access (SCA), or (ii) dynamic channel access (DCA). In SCA, if any of the secondary channel(s) is occupied, the transmitter ceases its transmission on all channels and restarts the backoff process. In DCA, the 802.11ac transmitter transmits on the primary channel (as long as the primary channel is idle) and available secondary channel(s). SCA and DCA mechanisms are illustrated in Fig. 2.6.

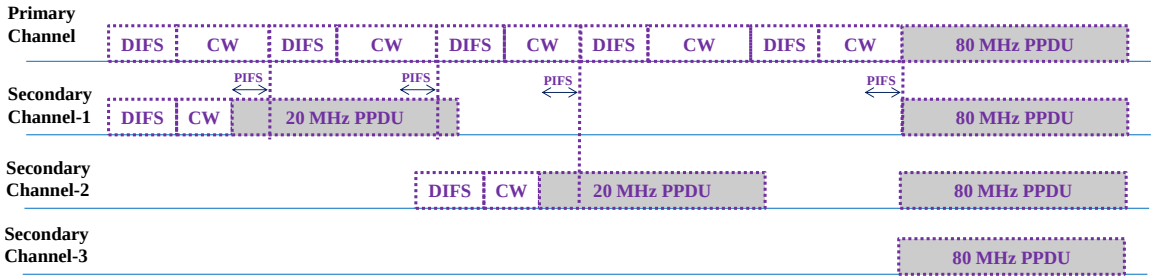


**(a) Static 80 MHz bandwidth channel access**

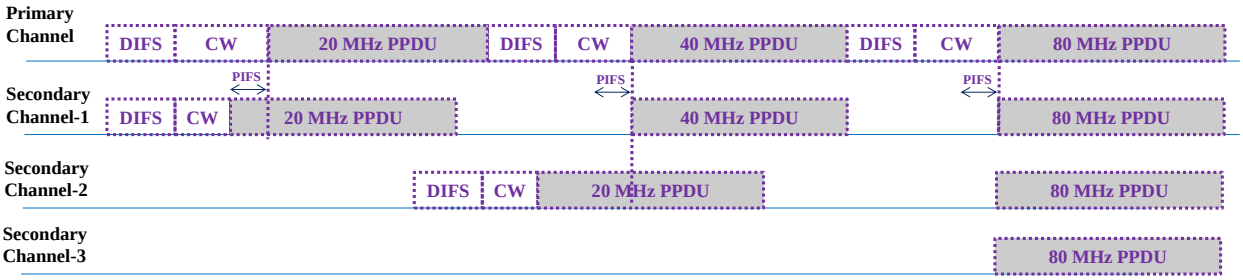


**(b) Dynamic 80 MHz bandwidth channel access**

Figure 2.6: Channel access mechanism for primary and secondary channels in 802.11ac

#### 2.2.2.2 Wi-Fi 6: IEEE 802.11ax

Wi-Fi 6 refers to the set of Wi-Fi devices that are certified as per the IEEE 802.11ax specifications [57]. In contrast to the previous generation of Wi-Fi standards, where the focus was primarily on increasing the offered throughput, Wi-Fi 6 introduces a range of features that are expected to enhance the perceived experience of Wi-Fi users. The focus in designing Wi-Fi 6 features was on creating improvements to support extremely dense environments such as corporate offices, outdoor hotspots, dense residential apartments, and stadiums. These features include the use of MU OFDMA for channel access, spatial re-use, target wake time for improved power efficiency, and the use of higher-order modulation and coding schemes (MCS) such as 1024 Quadrature Amplitude Modulation (QAM) for increased throughput [71]. The most prominent Wi-Fi 6 features are summarized below.

- OFDMA: The 802.11ax standard uses OFDMA to multiplex more users in the same

channel bandwidth. It divides the existing 802.11 channels (20, 40, 80, and 160 MHz wide) into smaller sub-channels with a predefined number of subcarriers. The smallest sub-channel is referred to as a Resource Unit (RU), with a minimum size of 26 subcarriers.

- MU OFDMA: 802.11ax will not only inherit MU downlink transmission features from 802.11ac but also support MU uplink transmissions. To coordinate uplink MU-MIMO or MU OFDMA transmissions, the AP sends a trigger frame (TF) that contains the number of spatial streams and the OFDMA allocations (frequency and RU sizes) of each user, to its associated STAs. TF also contains power control information, so that individual users can adjust their transmit powers.
- MU-MIMO: Borrowing from the 802.11ac standard, 802.11ax devices will use beamforming techniques to direct packets simultaneously to spatially divided users. The AP may initiate simultaneous uplink transmissions from multiple STAs using a TF. The AP may also initiate uplink MU transmissions to receive beamforming feedback information from all participating STAs.

#### 2.2.2.3 Wi-Fi 7: IEEE 802.11be

Even as Wi-Fi 6 certified devices continue to be rolled out, work on the specifications of its successor—IEEE 802.11be Extremely High Throughput (EHT)—has already begun [56, 72]. The first draft standard of IEEE 802.11be is expected to be completed by May 2021 [73]. Target applications of IEEE 802.11be include Wi-Fi-based AR and VR, real-time gaming, and industrial automation, which are often characterized by high throughput coupled with extremely high reliability and low latency requirements [74, 75]. The Task Group (TG) be, i.e., TGbe, responsible for the standardization of PHY and MAC layer features that will eventually constitute IEEE 802.11be, was formed in May 2019. In contrast to IEEE 802.11ax, which was initially designed to operate in unlicensed portions of the sub-6 GHz bands, IEEE 802.11be considers the use of unlicensed bands, wherever available, in the 1 GHz to 7.125 GHz range [76].

IEEE 802.11be will support all features introduced in 802.11ax. Additionally, 802.11be is likely to introduce new features that contribute toward meeting the high throughput, high reliability, and low latency objectives set forth by the TGbe [77]. Some of these features include multiple AP coordination [78, 79], MIMO enhancements including provisioning support for up to 16 spatial streams [80], potential support for 4096 QAM [81] and Hybrid Automatic Repeat Request (HARQ) [82], providing support for 240 MHz and 320 MHz channelization[9] [83], and multi-link aggregation (MLA) [84].

MLA will allow 802.11be devices that can operate in different bands (such as 2.4 GHz, 5 GHz, and 6 GHz) to use these bands concurrently. Using MLA, IEEE 802.11be stations

[9]IEEE 802.11ax and IEEE 802.11ac allow maximum channel bandwidth of 160 MHz.

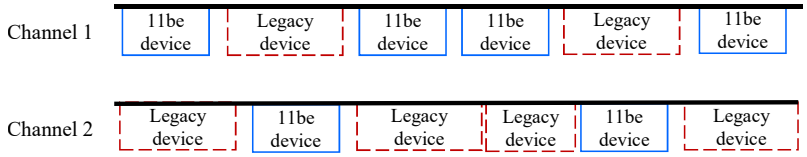


(a) Asynchronous MLA. 802.11be device contends on both channels independently.

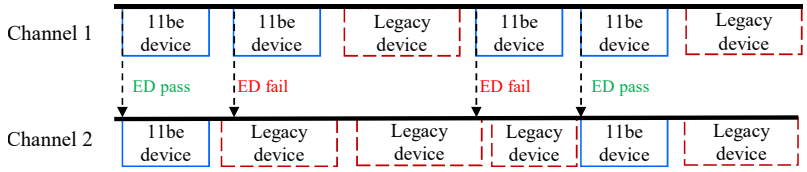


(b) Synchronous single-primary MLA. 802.11be device contends only on channel 1.

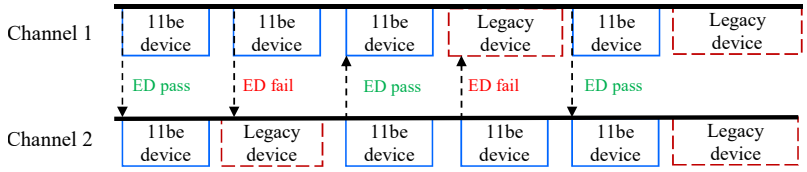


(c) Synchronous multi-primary MLA. 802.11be device contends on both channel 1 & channel 2.

Figure 2.7: Multi Link Aggregation Schemes in IEEE 802.11be.

(STAs) and AP can send/receive MAC service data units belonging to the same flow on multiple bands (e.g., 2.4 GHz and 5 GHz, or 5 GHz and 6 GHz) or channels (two channels in the 6 GHz band) simultaneously [85]. At present, there are three MLA schemes under consideration [86]. The choice of the MLA scheme depends on the implementation complexity and the frequency separation between aggregated channels. These schemes are illustrated in Fig. 2.7 for aggregation of two links, although the same principles can be used for aggregation of more than two links.

Independent/asynchronous MLA is used when the two aggregated links are sufficiently far apart in frequency resulting in no or negligible inter-link cross-talk (e.g., aggregation of 2.4 GHz and 5 GHz bands, or aggregation of 2.4 GHz and 6 GHz bands). The MLA-capable AP/STA contends for channel access on both channels and transmits the packet on the contention-winning channel. Fig. 2.7a demonstrates the operation of asynchronous MLA for two links. The name independent/asynchronous signifies that contention on the two operating channels is independent of each other. Thus, transmissions on the two channels need not be synchronized.

Synchronous/simultaneous MLA, on the other hand, is further of two types depending on whether the MLA-capable AP/STA contends on only one link (referred to as the primary) or on both links. The former scheme is referred to as synchronous/simultaneous *single*-primary MLA, while the latter is referred to as synchronous/simultaneous *multi*-primary MLA. In

both schemes, right before the MLA-capable AP/STA wins access to the primary channel[10] (i.e., when the back-off counter strikes zero), energy detection (ED) check is performed on the other channel for a duration referred to as the PIFS. PIFS stands for Point Coordination Function Interframe spacing. This other link is referred to as the secondary link for synchronous/simultaneous single primary MLA. If the ED check passes, i.e., if the energy observed on the other link is less than the ED threshold, the two channels are aggregated, and the MLA device transmits on both links. This ensures that the two channels if aggregated, are always synchronized. Fig. 2.7b and Fig. 2.7c demonstrate the operation of synchronous single-primary MLA and multi-primary MLA, respectively. Note that the synchronous single primary MLA bears similarities with the channel bonding feature used in 802.11n and 802.11ac [10].

Synchronous/simultaneous MLA is suitable for aggregation of links when the frequency separation between the aggregated links is small. For example, when a channel in the U-NII-5 band is aggregated with another in the U-NII-6 band, there can be significant leakage across the radio frontends. Such inter-link cross-talk can hamper the reception of signals on one link when the other link is in the transmit state. Synchronous MLA schemes maximize the likelihood of all links simultaneously being in the transmit state. However, there can still arise scenarios where only a subset of links is in the transmit state.

### 2.2.3 Unlicensed Cellular Technologies

Traditional cellular radio access networks (RANs) comprise of centralized coordinators, typically referred to as Base Stations, which communicate with mobile terminals. In LTE and NR terminologies, the central coordinator is referred to as the eNodeB and gNodeB, respectively. On the other hand, the mobile terminals are referred to as User Equipments (UEs) in both LTE and NR. Until recently, commercial cellular networks operated in licensed portions of the wireless spectrum, whereby cellular operators purchase rights for the exclusive use of their designated frequency bands, often at exorbitantly high costs [36].

While the demand for high-speed broadband and multimedia access from mobile users has dramatically increased, licensed portions of the spectrum that are suitable for supporting such applications remain limited. This prompted the cellular industry to investigate whether unlicensed spectrum—available in large amounts at the time in the 5 GHz bands—were suitable for supplementing licensed cellular operations [87]. This move resulted in an explosion of research and development activities within the industry and academia, giving birth to several approaches that facilitated the entry of cellular technologies in the unlicensed bands.

One of the primary focus in the design of all unlicensed cellular technologies has been ensuring fairness with Wi-Fi devices, which are deployed in the millions throughout the 5 GHz

[10]Note that in synchronous/simultaneous multi-primary MLA, each of the two channels is a primary channel.

bands [2]. Fairness concerns arise from the fundamental differences in the channel access mechanisms used by cellular RATs and Wi-Fi. On one hand, cellular RATs use a centralized scheduling mechanism, wherein the Base Station assigns time and frequency resources to the mobile terminals. On the other hand, Wi-Fi uses a distributed channel access protocol whereby each Wi-Fi STA autonomously decides when to transmit over the channel.

Unsurprisingly, unaltered versions of LTE caused significant degradation of Wi-Fi performance when the two RATs coexisted [12, 31]. This made it clear that further research was required on how cellular technologies could harmoniously coexist with Wi-Fi if they were to operate in the unlicensed spectrum. At first, four major candidate technologies emerged – (i) LTE-U, (ii) LTE-WLAN Aggregation (LWA), (iii) MulteFire, and (iv) LAA. LAA has since matured to give way to its successor—NR-U—the fifth major cellular-based RAT to operate in unlicensed spectrum.

Cellular RATs that operate in the unlicensed spectrum can be classified in one of two categories, (i) *license-anchored* systems, and (ii) *non license-anchored* systems. In license-anchored unlicensed LTE systems (e.g. LTE-U, LAA), the primary carrier, referred to as the anchor, uses licensed portions of the spectrum. The guaranteed availability of the licensed anchor implies that it can be used for transmitting control information and QoS sensitive data where reliability is of primary concern. The secondary carriers, wherever available, can then operate in the 5 GHz unlicensed spectrum, thereby maximizing the network capacity. In unlicensed LTE systems that do not use licensed-anchor (e.g. MulteFire), on the other hand, control and data traffic are transmitted in the unlicensed spectrum. NR-U, being the latest *flavor* of cellular-based unlicensed RATs, supports both, license-anchored and non-license-anchored modes.

#### 2.2.3.1 LTE Unlicensed

LTE-U is a cellular-based RAT that is built atop cellular LTE with minimal modifications. Developed by an industry group—the LTE-U Forum—LTE-U is designed such that the unlicensed bands carry the downlink traffic. Uplink traffic and control signaling is done over the licensed anchor. Thus, LTE-U is said to operate in a supplemental downlink-only (SDL) mode.

LTE-U was designed so that LTE could make a quick inroad into unlicensed bands. Because the specifications of LTE-U relied on features that were already available in LTE specifications, LTE-U devices could quickly be launched into markets where LBT in unlicensed spectrum was not a mandatory requirement.

To coexist with existing Wi-Fi devices in the 5 GHz band and other LTE-U eNBs, LTE-U provides a three-step coexistence mechanism [88, 89]. This coexistence mechanism operates as illustrated in Fig. 2.8.

*Step 1) Channel selection:* The LTE-U eNB scans the unlicensed portions of the spectrum in

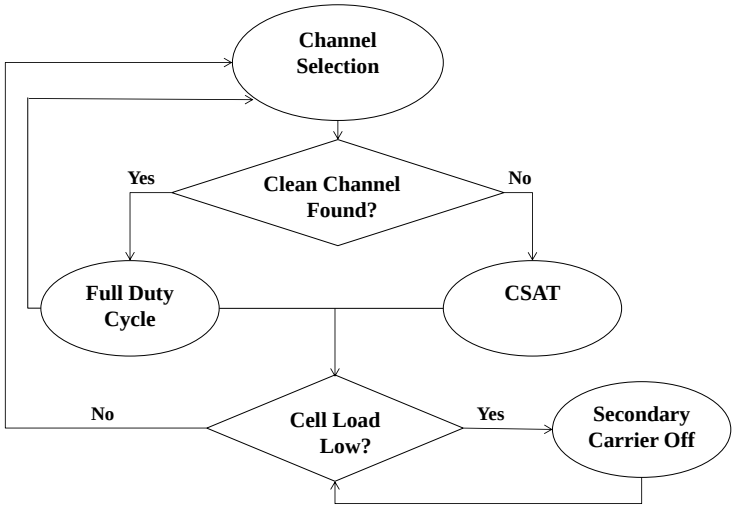


Figure 2.8: LTE-U algorithm flow chart

order to determine if a "clean" channel is available for SDL transmissions. A clean channel refers to a channel that is not used by any Wi-Fi or LTE-U systems in the vicinity of the LTE-U eNB performing the scan. Channel measurements and determination of a clean channel are to be performed at the initial power-up stage, as well as periodically during the SDL operation stage. If a clean channel is determined during the power-up stage, the LTE-U eNBs communicate with the UEs using frequencies in that channel. During subsequent measurements, if interference is experienced on the previously clean channel, and a new clean channel is available, the SDL transmissions shall be switched to the new channel.

*Step 2) Duty-cycling:* In the high-density deployment of Wi-Fi and LTE-U small cells, it is likely that no clean channel is found during the scan process. In such circumstances, LTE-U uses a mechanism named Carrier Sense Adaptive Transmission (CSAT) to coexist with Wi-Fi and/or other LTE-U eNBs in a given channel. The CSAT mechanism is based on duty-cycling — the LTE-U eNB ceases all its transmissions for $x$ $m$sec, followed by a burst of continuous LTE transmissions for $y$ $m$sec. This process repeats periodically with the period ranging from $20 - 100$ $m$sec as shown in Fig. 2.9. The durations $x$ and $y$, i.e. the *on*-time and *off*-time in the CSAT procedure can be dynamically adapted based on the channel utilization.

*Step 3) Opportunistic secondary cell switch-off:* Since the anchor carrier in the licensed band is always available, the SDL carrier in the unlicensed band can be used on an opportunistic basis [88]. If traffic demands from the LTE-U UEs can be met using only the primary carrier, the LTE-U system can turn off the secondary carrier to ease the load on the secondary channels.

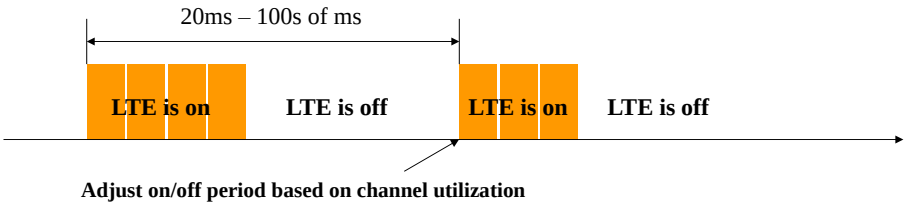


Figure 2.9: CSAT process

#### 2.2.3.2 LTE-WLAN Aggregation

The development and deployment of LTE-U or LAA based unlicensed LTE systems would require significant investment in terms of additional hardware (LTE-U/LAA enabled eNBs and UEs) and processing capabilities (detection of signals from Wi-Fi and other unlicensed devices). In contrast, LWA emerged as an unlicensed LTE alternative to LTE-U and LAA that leverages the existing LTE and Wi-Fi infrastructures.

LWA was standardized by 3GPP Release 13 in March 2016. In contrast to LTE-U and LAA, LWA transmits LTE data on unlicensed bands using the Wi-Fi protocol. This is achieved by splitting the LTE payload at the higher layers into two classes — one transmitted over licensed spectrum bands using the LTE radio, while the other class of traffic transmitted over unlicensed spectrum using the Wi-Fi radio. Thus, a fraction of the total LTE traffic is tunneled over the Wi-Fi interface. The basic idea behind LWA is to use Wi-Fi APs to augment the LTE RAN by tunneling LTE data in the 802.11 MAC frame such that despite carrying LTE payload, Wi-Fi devices in the network can "see" this data as Wi-Fi traffic. As a result, problems arising due to differences in the channel access mechanisms of LTE and Wi-Fi can be alleviated.

The architecture of an LWA system is shown in Fig. 2.10, and consists of an LWA eNB, LWA-aware Wi-Fi AP, and LWA UE. The LWA eNB performs splitting of packet data convergence protocol (PDCP)[11] packets at the PDCP layer, and transmits some of these packets over the LTE air interface, while the remaining are transmitted through the Wi-Fi AP after encapsulating them in Wi-Fi frames. These packets can then be reassembled at the PDCP layer of the LWA UE. It must be noted that LWA also leverages the fact that almost all LTE enabled UEs are equipped with Wi-Fi capabilities.

The LWA aware Wi-Fi APs are connected to LWA eNBs and can report channel information to the LWA eNB, which can use the channel and traffic information to determine whether the Wi-Fi air interface must be used or not. This architecture also enables the functioning

[11]PDCP is a set of protocols (layer) that lies between the Internet Protocol (IP) and radio link control (RLC) layers in the data plane, and radio resource control (RRC) and RLC layers in the control plane. PDCP is responsible for functions such as header compression for IP packets, data integrity protection and ciphering.

of the LWA aware Wi-Fi AP to function as a standalone Wi-Fi AP when the LTE network load is low [1].

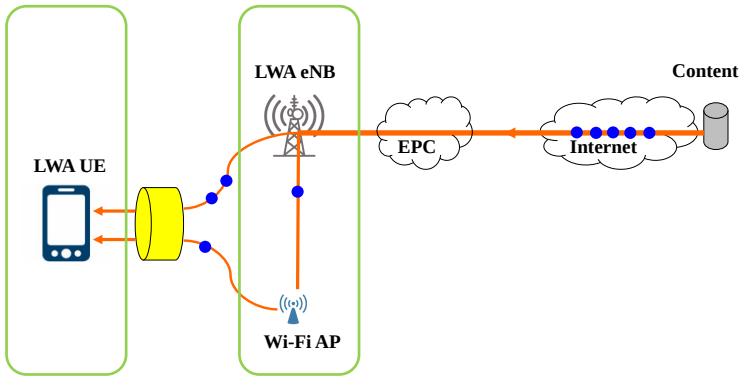


Figure 2.10: LWA conceptional architecture [1]

A significant advantage of the LWA system over LTE-U and LAA systems is that it can be enabled using software upgrades at the eNBs, UEs and Wi-Fi APs, thus leveraging existing LTE and Wi-Fi infrastructures. Moreover, Wi-Fi traffic can benefit from the services provided by the mobile operator's evolved packet core (EPC). These services include authentication, billing, deep packet inspection, etc.

#### 2.2.3.3 MulteFire

MulteFire emerged as a standalone version of unlicensed LTE which solely operates in the unlicensed spectrum. As a result, MulteFire systems do not require an "anchor" in the licensed spectrum. MulteFire is designed to bring the best of both, LTE and Wi-Fi, worlds by incorporating features from LTE such as user mobility, seamless handovers, integration with LTE operators, and from Wi-Fi like neutral host options – i.e., the ability to serve subscribers from different operators.

In December 2015, the MulteFire Alliance announced the formation of an international association open to new members for the development of MulteFire. The MulteFire Alliance released its MulteFire specification Release 1.0.1 [90] based on 3GPP Release 13 and Release 14 advancements, including downlink and uplink in the unlicensed spectrum bands.

MulteFire is primarily designed for entities that have limited or no access to licensed spectrum bands while giving these entities the benefits of LTE technology [91, 92]. Moreover, MulteFire can also be used by mobile service providers that already have access to licensed spectrum in order to augment their network capabilities. Thus, MulteFire is capable of operating either independently as a private network (much like Wi-Fi APs) or work alongside existing mobile networks. There are three types of architectures envisioned for MulteFire operations [93].

- Standalone operations as a private self-contained network.
- A self-contained network working closely with mobile networks.
- A network with a RAN interconnection through an interface with the mobile network.

Moreover, a MulteFire network can support one or all of the three architectures simultaneously.

The MulteFire channel access procedure borrows largely from the 3GPP LAA and enhanced LAA (eLAA, an evolution of LAA with boosted downlink performance) procedures. The procedure used by MulteFire devices to share the spectrum with other unlicensed devices (operating over Wi-Fi or LAA air interfaces) is much like the Wi-Fi CSMA procedure with four access classes and similar contention parameters [92]. The overall procedure is summarized below.

1) Using CCA, MulteFire selects a channel for its operations dynamically, avoiding overlapping transmissions with unlicensed devices such as other MulteFire, LAA, and Wi-Fi.
2) If no clear channel can be found, an LBT mechanism is used to contend for the spectrum.
3) MulteFire also supports channel aggregation to improve system capacity.

The MulteFire technology uses the LAA and eLAA in downlink and uplink respectively. This makes MulteFire suitable for operations in any band (including bands other than 5 GHz) and regulatory regimes that require over-the-air contention and coexistence with heterogeneous technologies. For example, MulteFire is a high-performance option for General Authorized Access in the 3.5 GHz band in US [93].

MulteFire is a promising technology with characteristics derived from Wi-Fi as well as LTE. However, being a relatively new technology with no devices available, the performance of MulteFire remains unknown. As the channel access procedure in MulteFire is much similar to that of Wi-Fi, MulteFire can be expected to be a friendly neighbor to Wi-Fi systems, while being prone to performance degradation in the presence of LAA or LTE-U systems.

#### 2.2.3.4 License Assisted Access

In countries across Europe and Japan, regulations mandate the use of sensing mechanisms before transmissions from unlicensed devices. While LTE-U uses sensing mechanisms to detect a clean channel during the power-up stage, and periodically during its operations, each transmission from an LTE-U node does not precede a channel sensing procedure. This makes LTE-U unsuitable for markets where the regulations mandate LBT capability.

LAA is an unlicensed cellular RAT that is designed for operations where LBT capability is desired. ETSI provides two options for LBT schemes: Frame-Based Equipment (FBE) and Load-Based Equipment (LBE) [1, 94].

- *FBE-based LBT.* In the FBE-based LBT, transceivers operate using fixed timing and with a fixed frame period. At the end of each idle frame, FBE performs CCA on an operating channel. If the channel is idle, the transceiver transmits data immediately at the beginning of the next frame. If, however, the channel is busy, CCA is performed in the next frame period.
- *LBE-based LBT.* In the LBE-based LBT, a transmitter performs CCA every time it has data to transmit in its queue. If the channel is idle during this sensing period, data is transmitted immediately over the channel. If the channel is determined to be busy, a back-off counter is initialized, and the transmitter attempts to transmit the frame when the back-off counter decrements to 0.

In addition to FBE and LBE versions of LBT, based on regional regulations and/or the type of traffic transmitted by the LAA device, there are four categories of LBT. Devices using category 1 LBT transmit immediately after a period of 16 $\mu$s once the channel becomes idle. This is typically used for ACK packets sent by the receiver upon successful reception of a packet. Category 2 LBT also involves the transmission of a packet following a fixed time interval. However, this interval is 25 $\mu$s in the case of category 2 LBT. On the other hand, devices using category 3 and 4 LBT transmit their packets after a fixed time interval (16 $\mu$s) followed by a random number of time slots (each of duration 9 $\mu$s), where this random number is picked between 0 and CW-1, CW being the parameter Contention Window. What differentiates category 3 and 4 LBT is that the CW size remains fixed in the former while it varies in the latter. Note that LBE with category 4 LBT closely resembles the CSMA/CA MAC protocol used in Wi-Fi, as discussed in Sec. 2.2.2.

#### 2.2.3.5 New Radio Unlicensed

NR-U is an unlicensed RAT that was recently developed by the 3GPP as one of its Release 16 work items [95]. NR-U is a successor to LAA and subsequent releases. Thus, in the design of NR-U PHY and MAC layer procedures, is considered as the starting point [96, 97]. For example, the channel access mechanism used in LAA is adopted as the baseline for NR-U operations in the 5 GHz bands. This also implies that in areas where the absence of Wi-Fi networks cannot be guaranteed, NR-U devices will operate (and hence, perform sensing) in bandwidths that are integer multiples of 20 MHz. Nevertheless, the 3GPP Technical Report 38.889 [96] identifies the need to customize channel access protocols according to the operating band and/or regional regulations.

NR-U derives its PHY layer from 5G NR [97, 98] and, thus, can benefit from leveraging PHY layer enhancements made in 5G NR. These include the use of flexible numerologies and mini-

slot scheduling, among others. The use of mini-slot scheduling in NR-U is especially beneficial because sending packets in mini-slots minimizes the use of reservation signals such as those used in LAA to reserve the channel during shared channel access [99]. Reservation signals were required in LAA because unlicensed transmissions from LAA devices are required to be synchronized with sub-frame boundaries of the anchored licensed carrier—a constraint that came from LAA's inheritance of licensed cellular operations. This meant that LAA devices could start transmitting data and control symbols only at the beginning of the sub-frame boundary. However, LAA devices can gain access to the channel at any given instant, depending on when the channel becomes idle. Thus, reservation signals were transmitted in the time duration between gaining access to the channel and the start of the sub-frame boundary.

A critical difference between NR-U and previous 3GPP-based unlicensed RATs is that NR-U does not require a licensed primary carrier for its operation [95, 100], which was mandatory in LAA [10]. In this scenario, the NR-U network is connected to 5G Core Network [95]. The ability of NR-U to operate without a licensed primary carrier is significant because this enables NR-U networks to be deployed by any parties similar to Wi-Fi AP deployments.

The harmonious coexistence of NR-U with other unlicensed RATs necessitates the design of a MAC protocol that is efficient, yet fair toward other RATs. The channel access mechanism in NR-U will be based on LBT [33], much like the LBT protocol used in previous 3GPP-defined unlicensed technologies [101].

### 2.2.4 Dedicated Short Range Communications

#### 2.2.4.1 IEEE 802.11p

DSRC is a communications technology specifically designed to support ITS applications [102, 103]. Specifically, DSRC modules can be installed on vehicles to enable V2V communications, thereby enabling various vehicular safety applications [104].

The PHY and MAC layer protocols for DSRC have been defined in the 802.11p amendment of the IEEE 802.11 standards. This amendment is referred to as Wireless Access in Vehicular Environments (WAVE) [105]. The DSRC standard is an extension of IEEE 802.11a, designed for vehicles traveling at high speeds. Most of the changes made in the amendment are at the MAC layer, while changes at the PHY layer are minimal [106].

DSRC-enabled vehicles periodically exchange two types of safety-critical messages: event-driven messages and BSMs. Event-driven messages are broadcasted by a DSRC node when the vehicle encounters a potentially unsafe situation, such as an emergency brake or an imminent collision due to vehicle pile-up. On the other hand, BSMs convey the senders' position, speed, acceleration, direction, etc. [107]. BSMs provide information that can be processed at the higher layers to enable applications such as blind-spot detection, intersection

assist, etc. that require vehicles to be aware of their surroundings. DSRC can also be used for non-safety applications such as downloading digital maps, automatic toll collection, etc. While these services are offered only on the SCHs, the SCHs can also be used to transmit safety application packets [108]. Thus, the successful delivery of packets transmitted by DSRC nodes on all channels is of critical importance.

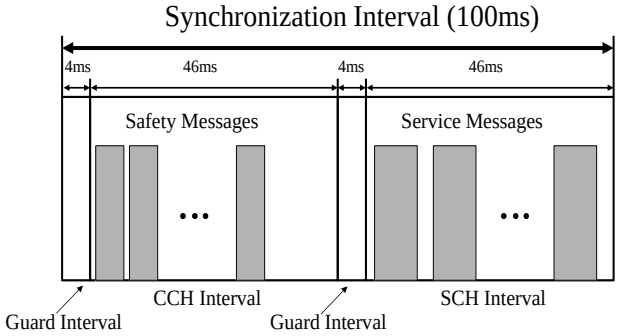


Figure 2.11: The multi-channel MAC scheme used by DSRC

While the basic channel access mechanism used in 802.11p is similar to that used in other 802.11 standards, 802.11p has some distinguishing features. To minimize the setup latency, 802.11p eliminates the association mechanism used in conventional Wi-Fi systems and instead defines "communication outside the context of a Basic Service Set (BSS)" MAC. According to this MAC protocol, a transmitter broadcasts each packet to all other nodes in the network. Furthermore, to prevent the network from being flooded with ACKs, 802.11p receivers do not send an ACK to the transmitter. Thus, there is no feedback mechanism at the transmitter.

If a particular node fails to gain access to the channel within the inter-broadcast interval, the packet is discarded at the transmitter. This is mainly due to the delay-sensitive nature of vehicular networks; the information contained in such a packet is out of date, and a new packet containing updated information should be generated in the next inter-broadcast interval. This is referred to as *packet expiration* at the transmitter. Another notable difference in 802.11p networks is that unlike traditional 802.11 networks, 802.11p nodes do not use the request-to-send (RTS)/ clear-to-send (CTS) handshake mechanism to reduce the number of collisions due to the hidden node problem, as the exchange of RTS/CTS packets can lead to large overhead in transmissions.

#### 2.2.4.2 IEEE 802.11bd: The Evolution of IEEE 802.11p

**Objectives**

During the development of IEEE 802.11p, the focus was to develop a vehicular communica-

tion standard that assisted in (i) vehicular safety, (ii) better traffic management, and (iii) other applications that add value, such as parking and vehicular diagnostics. The requirements set for 802.11p were to support:

- relative velocities up to 200 km/hr,
- response times of around 100 msec, and
- communication range of up to 1000 m.

Since the design of 802.11p, 802.11a—the baseline IEEE standard used in 802.11p—has given way to its successors i.e., 802.11n and 802.11ac, while 802.11ax is in its final stages of standardization. Considering that 802.11p was developed nearly two decades ago, advanced PHY and MAC techniques introduced in 802.11n/ac/ax can be leveraged to enhance 802.11p. With this objective, the IEEE 802.11 Next Generation V2X Study Group was formed in March 2018. After an initial feasibility study, the IEEE 802.11bd Task Group was created in January 2019. The primary design objectives of 802.11bd include supporting the following [109]:

- at least one mode that achieves twice the MAC throughput of 802.11p with relative velocities up to 500 km/hr;
- at least one mode that achieves twice the communication range of 802.11p;
- at least one form of vehicle positioning in affiliation with V2X communications.

Additionally, 802.11bd must support the following [109]:

- Interoperability: 802.11p devices must be able to decode (at least one mode of) transmissions from 802.11bd devices, and vice-versa.
- Coexistence: 802.11bd must be able to detect 802.11p transmissions and defer channel access, and vice-versa.
- Backward compatibility: At least one mode of 802.11bd must be interoperable with 802.11p.
- Fairness: In co-channel scenarios, 802.11bd and 802.11p must get equal channel access opportunities.

### Novel Features and Mechanisms

A comprehensive overview of features and mechanisms that are likely to be a part of 802.11bd, and the challenges likely to be encountered in the implementation of these mechanisms is presented in [50]. In what follows, we briefly summarize the prominent 802.11bd features.

- Midambles: To improve the resilience of 802.11bd-based devices in rapidly fluctuating channels, 802.11bd proposes to use *midambles*, which are similar in form and function to the preamble except for their location within the frame. The preamble, which is at the beginning of the frame, is used for initial channel estimation. However, for fast-varying channels, the initial estimate may quickly become obsolete. As shown in Fig. 2.12, midambles, which will be introduced in between the OFDM data symbols with appropriate frequency, will serve in channel tracking so that an accurate channel estimate is obtained for all data symbols.

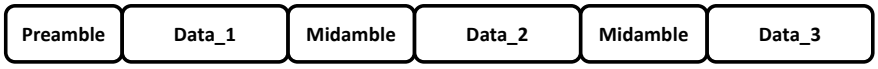


Figure 2.12: Insertion of midambles for improved channel estimation.

- Re-transmissions: A mechanism to increase the reliability is to have one or more re-transmissions of a packet. Using the frame structure shown in Fig. 2.13, reliability gains can be achieved for both 802.11p and 802.11bd devices. The TGbd proposes an adaptive re-transmission scheme, where decisions to re-transmit a frame and the number of re-transmissions is based on the congestion level [110].


Figure 2.13: Frame format used for re-transmissions in 802.11bd.

- Dual Carrier Modulation: DCM is a technique introduced in 802.11ax. DCM includes transmitting the same symbols twice over sufficiently far-apart sub-carriers such that frequency diversity is achieved [111]. Because each symbol transmission is repeated over two different sub-carriers, the modulation order must be doubled (e.g. from BPSK to QPSK, or QPSK to 16-QAM) to maintain the throughput. Despite the increase in modulation order, DCM can help improve the block-error-rate (BLER) performance.

- mmWave Frequencies: mmWave frequency bands (i.e., 60 GHz and above) have enormous potential in catering to use-cases that require communication over small distances, but with very high throughput (e.g., video streaming, downloading high-resolution 3D maps, etc). mmWave bands are particularly lucrative due to the abundance of spectrum therein, allowing very high throughputs even at lower order MCS [112]. The basis for the design of mmWave 802.11bd can be existing 802.11 standards like 802.11ad, or its enhancement 802.11ay, which already operate in the mmWave bands [113]. However, one drawback of this frequency band is that its utility is limited to use-cases that do not require a large communication range.

- Multi-channel operations: The working assumption in 802.11p has been that each vehicle is equipped with a single ITS-band radio [114]. To facilitate the use of multiple

channels in the ITS band, the IEEE 1609.4 [114] standard defines multi-channel operations (MCO) for 802.11p through time-division multiplexing, whereby a 100 msec interval is divided into two slots (default 50 msec each). The 802.11p radio switches between two channels in these two slots, with a 4 msec guard interval reserved at the beginning of each slot.

#### Comparison with IEEE 802.11p

Table 2.3 summarizes the key differences between features/mechanisms of 802.11p and 802.11bd.

Table 2.3: Comparison of 802.11p and 802.11bd

| **Feature** | **802.11p** | **802.11bd** |
|---|---|---|
| Radio bands of operation | 5.9 GHz | 5.9 GHz & 60 GHz |
| Channel coding | BCC | LDPC |
| Re-transmissions | None | Congestion dependent |
| Countermeasures against Doppler shift | None | Midambles |
| Sub-carrier spacing | 156.25 kHz | 312.5 kHz, 156.25 kHz, 78.125 kHz |
| Supported relative speeds | 252 kmph | 500 kmph |
| Spatial Streams | One | Multiple |

### 2.2.5 Cellular V2X

C-V2X refers to the RAT that is designed atop 3GPP-based cellular technologies for enabling V2X communications. The first C-V2X technology was designed by the 3GPP in its Release 14 in 2017 and is based on cellular LTE. Proponents of C-V2X argue that C-V2X users can benefit from leveraging the existing cellular infrastructure. However, since the availability of the cellular infrastructure cannot always be relied upon, C-V2X defines transmission modes that enable direct V2V communications using the sidelink channel[12] over the *PC5 interface*.

#### 2.2.5.1 C-V2X based on LTE

#### The Physical Layer

Much like LTE, in C-V2X, resources are shared in time and frequency. The time-frequency resource structure of C-V2X is similar to traditional LTE as shown in Fig. 2.14. Time is

[12]The LTE sidelink channel was introduced in 3GPP Release 12 for public safety (device-to-device or D2D) applications. D2D was designed for energy-efficient communications with support for only a few tens of users at a time and is, hence, inefficient for V2X.

divided into 10 msec long frames, which are further divided into ten 1 msec long subframes. Each subframe comprises of 14 OFDM symbols. On the other hand, in the frequency domain, each sub-carrier is 15 kHz wide. The smallest granularity of a resource in C-V2X (and in LTE) is one resource block (RB), which is made up of 15 sub-carriers in the frequency domain (180 kHz) and 14 OFDM symbols in the time domain (1 subframe, or 1 msec).

In addition to data symbols, resources in LTE also carry control information and reference signals. The demodulation reference signal (DMRS) is used by the vehicles to estimate the channel between two users. DMRS is typically inserted in two of the 14 OFDM symbols, which works well in traditional LTE. C-V2X, however, is designed for high-mobility environments, with relative speeds up to 500 km/hr. For such channels with small coherence times, 4 DMRS symbols are inserted in each C-V2X subframe.

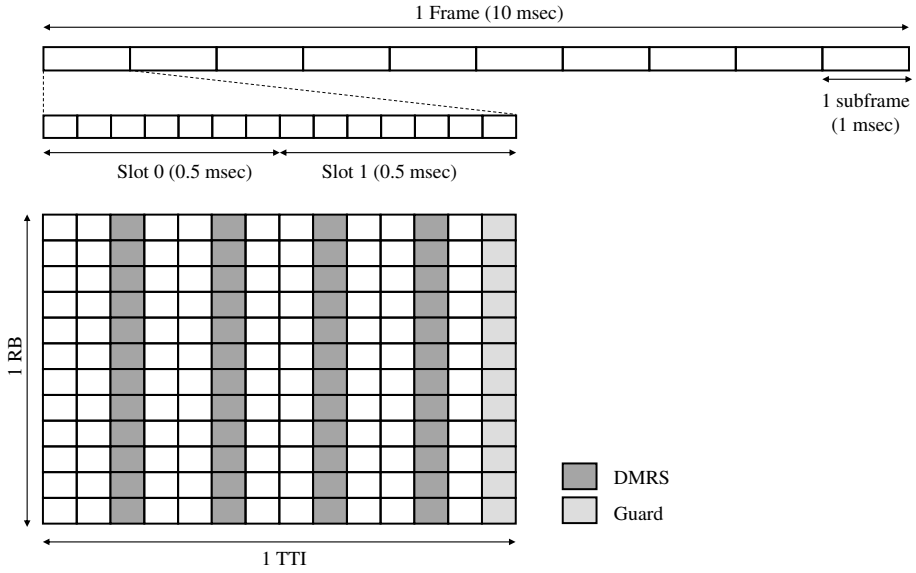


Figure 2.14: C-V2X PHY layer structure

### V2X using LTE-Uu Air Interface

*LTE-Uu* is the traditional air interface between an eNodeB and a UE. In some scenarios (for example, an announcement of an approaching emergency vehicle) large coverage areas (order of kilometers) may be desired. Using the LTE-Uu interface, a vehicular UE can transmit a packet to the eNodeB in the uplink. Based on the desired coverage, the same or a different eNodeB can transmit this packet to a far away UE either using unicast downlink or enhanced Multimedia Broadcast Multicast Service (eMBMS) [115].

LTE-Uu enhancements for V2X are generally at the higher (network and above) layers and/or system architecture level. C-V2X mainly considers eMBMS for the downlink (as opposed to unicast). This eMBMS architecture is further optimized by bringing eMBMS related entities closer to the eNodeB. This is beneficial for V2X applications because – for most transmitters in C-V2X, intended receivers are located nearby and are likely to be served by

the same eNodeB. To further enhance the end-to-end latency, for packets with low latency budgets, two new Quality Control Indicator (QCI) have been defined for V2X messages [115] – one for UE uplink transmissions, while another for eNodeB's eMBMS transmissions.

Additionally, to reduce the scheduling overhead associated with V2X uplink transmissions, the eNodeB can use semi-persistent scheduling (SPS). Using SPS, the eNodeB assigns resources not only for the very next transmission but also for a number of subsequent transmissions. SPS is beneficial because the majority of the network traffic in V2X is from BSM transmissions that are periodic and have similar packet sizes.

### V2X using PC5 Air Interface

Designers of C-V2X considered the sidelink channel introduced in Release 12 as the baseline for C-V2X performance. Thereafter, enhancements were made to make the sidelink channel more suitable for dense and high-speed environments. In comparison to the LTE-Uu interface, the sidelink interface – PC5 – presents the following unique challenges.

- *In-band Emissions:* If the strength of the received signal from different transmitters at a receiver is considerably different, the stronger signal can *leak* out to the resources reserved for weaker signals. This phenomenon is referred to as in-band emissions (IBE) [116]. Traditional cellular networks use uplink power control so that signals received from different transmitters have roughly the same power. However, such a solution is not possible in C-V2X, since there is no single intended receiver in general.
- *Half Duplex:* UEs using C-V2X are assumed to support only half-duplex (HD) transmissions. This implies that when a UE transmits on certain frequency resource(s) in a given subframe, it cannot receive packets *on any other frequency resource*. Consequently, two UEs transmitting in the same subframe cannot *hear* each other.

IBE can potentially be reduced in C-V2X using *geo-zoning* [116]. This entails division of resources either in time, frequency, or both into *resource pools*. Resource pools are then reserved according to geographical locations. For example, consider an intersection scenario shown in Fig. 2.15a, where the potential leakage of UE C's transmission on to resources used by UE A at UE B can be reduced by dividing resources used by east-west and north-south traveling vehicles into two pools.

The HD problem is mitigated in C-V2X using retransmissions. In addition to adding reliability, UEs that transmit within the same subframe (and cannot decode each other's packets) retransmit in randomized subframes, thereby being able to *hear* each other during retransmissions.

### eNodeB assisted Resource Control

The sidelink transmission mode 3 is defined for scenarios where eNodeB coverage is available. At the eNodeB, the computation of resources to be assigned to individual UEs is performed by a new architectural entity called V2X control function [115].

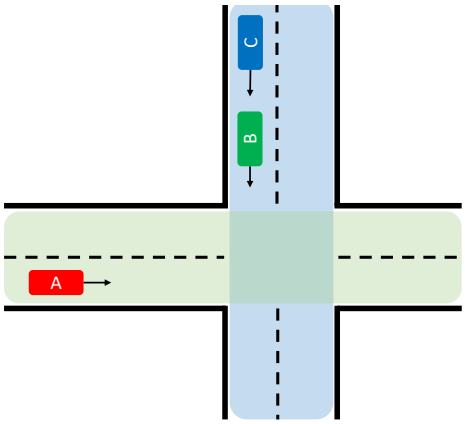


(a) Vehicles approaching an intersection

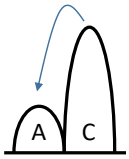


(b) Without geo-zoning


(c) With geo-zoning

Figure 2.15: An illustrative example of the In-band emissions problem

A transmitted packet on the PC5 interface comprises of the data component and sidelink control information (SCI). To achieve minimal latency, SCI and data are transmitted in the same subframe, which is different from Release 12 where SCI and data are multiplexed in time in different sub-frames. The physical channel used to transmit the SCI is called the Physical Sidelink Control Channel (PSCCH), while the Physical Sidelink Shared Channel (PSSCH) carries the data component. In C-V2X, a sub-channel is defined as a group of contiguous RBs. SCI occupies two RBs, while the remaining RBs in a sub-channel is used to accommodate data. To facilitate different data sizes, the number of RBs constituting a sub-channel can be variable.

Sidelink mode 3 uses the following notable mechanisms.

- SPS: Similar to scheduling over the LTE-Uu interface, eNodeB supports SPS for sidelink transmission mode 3.
- UE-report based scheduling: UEs can report their observations on their radio environments to assist the eNodeB in sidelink resource allocation.
- Cross-carrier scheduling: If an operator has two carriers at its disposal, the eNodeB can schedule resources on the operator's licensed carrier where the operator controls all resources. PC5 transmissions can occur in the ITS band, where UEs subscribed to different operators can share the spectrum.

**Autonomous Resource Control**

If UEs are outside the coverage area of the operator's eNodeB, or if the eNodeB cannot assign resources to the UEs for some reason, UEs use sidelink transmission mode 4. In this mode, UEs reserve resources autonomously using the distributed *resource reservation algorithm* [26].

We assume that the (re)selection process is triggered at UE A. The resource reservation algorithm proceeds as follows,

**Step 1:** UE A identifies a set of candidate single-subframe resources (CSRs) within a time period referred to as the *selection window*. Let us call this set $S_A$. CSRs are contiguous sub-channels within the same subframe inside which the sidelink packet (SCI + data) can fit.

**Step 2:** Next, the congestion level on each CSR in $S_A$ is estimated using sensing results for the previous 1000 subframes – a duration referred to as *sensing window*.

**Step 3:** On decoding SCIs received in the sensing window if UE A finds that a certain CSR in $S_A$ is reserved by another UE *and* if the reference signal reserved power (RSRP) of that UE's latest packet is above a certain threshold, then the CSR is excluded from $S_A$.

**Step 4:** All reservations are periodic with a fixed period $\mathrm{P_{step}}$. UE A, therefore, excludes all CSRs from $S_A$ that might have been reserved when UE A was transmitting.

**Step 5:** If the number of CSRs remaining in $S_A$ is less than $M$, Steps 3 and 4 are repeated. Here $M$ is 20% of the number of all CSRs within the selection window.

**Step 6:** UE A ranks CSRs remaining in $S_A$ based on their received energy, and moves $M$ of these CSRs to a new set $S_B$. Now, UE A picks one of the CSRs in $S_B$ at random and transmits the sidelink packet (say in subframe $d$).

**Step 7:** If UE A is configured to transmit each packet twice, it retransmits in one of the CSRs of $S_B$ that is within $\pm 15$ subframes from $d$.

The algorithm operation for a three-vehicle scenario is illustrated in Fig. 2.16. UE A first selects $[T_1, T_2]$ as the selection window as per the packet latency budget. We assume that each CSR is one sub-channel long. CSRs within $[T_1, T_2]$ constitute $S_A$. UE A processes all SCIs received within the sensing window and decodes SCI from UEs B and C. It is found that the RSRP of UE B's packet is below the threshold, while that of UE C is above the threshold. Hence, the CSR indicated by UE C's SCI is excluded from $S_A$. Assuming $\mathrm{P_{step}} = 100$, UE A excludes all CSRs in subframe $z$ from $S_A$, since it was transmitting in subframe $(z-100)$, and consequently could not receive any packets. Next, UE A ranks all CSRs in $S_A$ and selects $M$ of these CSRs with the lowest energy to form the set $S_B$. Finally, UE A picks a CSR from $S_B$ at random and transmits (subframe $d$ in Fig. 2.16). If configured, retransmission is done in a CSR (subframe $e$ in Fig. 2.16) randomly chosen from subframes $[d-15, d+15]$ excluding subframe $d$.

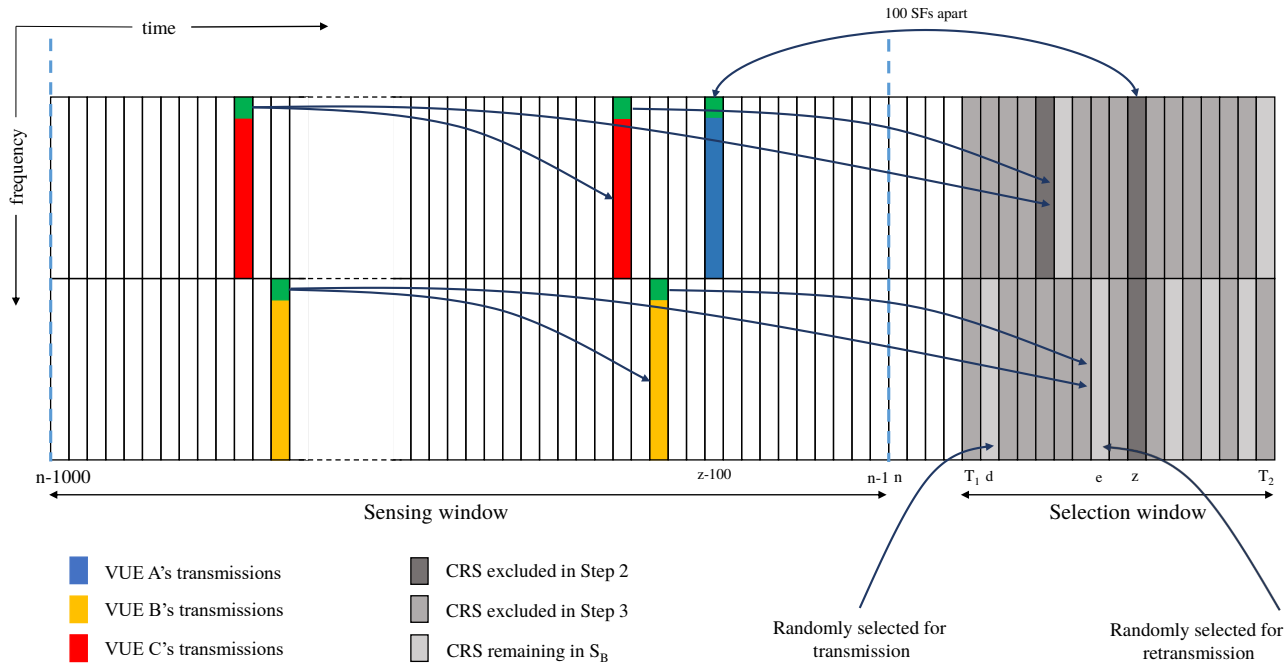


Figure 2.16: An illustrative example of the mode 4 Resource Reservation Algorithm

#### 2.2.5.2 NR V2X: C-V2X based on 5G New Radio

**Objectives**

The NR V2X Study Item [117] indicates that the design objective of NR V2X is *not* to replace C-V2X, but to supplement C-V2X in supporting those use cases that cannot be supported by C-V2X. Because C-V2X is already standardized and commercial deployments are underway [118], C-V2X and NR V2X might likely coexist in the same geographical region, where newer vehicles will have both C-V2X and NR V2X capabilities. Under such circumstances, use cases that can be supported reliably by using C-V2X can use C-V2X procedures, while the remaining use cases can use NR V2X procedures [117]. However, to ensure that NR V2X can provide unified support for all V2X applications in the future, NR V2X must be capable of supporting not only advanced V2X applications but also basic safety applications that are supported by present-day C-V2X.

NR V2X is being designed to support V2X applications that have varying degrees of latency, reliability, and throughput requirements. While some of these use cases require the transmission of periodic traffic, a large number of NR V2X use cases are based on the reliable delivery of aperiodic messages. Furthermore, while some use cases require broadcast transmissions, others such as vehicle platooning are efficiently supported by the transmission of messages only to a specific sub-set of vehicles (UEs). In some cases, in fact, 3GPP sees benefits in transmitting packets to only a single vehicle (UE) [23]. To support such use cases, two

new communication types, viz., unicast, and groupcast, will be introduced in NR V2X. Like IEEE 802.11bd, NR V2X also considers the use of mmWave bands for V2X applications, particularly for applications that require a short range and high to very high throughputs.

The NR V2X Study Item outlines its following objectives.

- *Enhanced sidelink design:* Re-design sidelink procedures to support advanced V2X applications.
- *Uu interface enhancements:* Identify enhancements to the NR Uu interface to support advanced V2X applications.
- *Uu interface based sidelink allocation/configuration:* Identify enhancements for configuration/allocation of sidelink resources using the NR Uu interface.
- *RAT/Interface selection:* Study mechanisms to identify the best interface (among LTE sidelink, NR sidelink, LTE Uu and NR Uu) for given V2X message transmission.
- *QoS Management:* Study solutions that meet the QoS requirements of different radio interfaces.
- *Coexistence:* Feasibility study and technical solutions for the coexistence of C-V2X and NR V2X within a single device, also referred to as *in-device coexistence*.

**Terminology**

- NR V2X Sidelink Modes: Like C-V2X, NR V2X defines two sidelink modes. The *NR V2X sidelink mode 1* defines mechanisms that allow direct vehicular communications within gNodeB coverage. In this mode, the gNodeB allocates resources to the UEs. The *NR V2X sidelink mode 2*, on the other hand, supports direct vehicular communications in the out-of-coverage scenario. For direct comparison with 802.11bd, in the remainder of this section, we keep our discussions restricted to NR V2X sidelink mode 2.
- Unicast, Groupcast, and Broadcast: In NR V2X unicast transmissions, the transmitting UE has a *single* receiver UE associated with it. On the other hand, the groupcast mode is used when the transmitting UE wishes to communicate with more than one, but only a specific subset of UEs in its vicinity. Finally, broadcast transmissions enable a UE to communicate with all UEs within its transmission range. These communication types are illustrated in Fig. 2.17. Note that C-V2X only provisions support for broadcast transmissions. A single UE can have multiple communication types active simultaneously. For example, a platoon leader UE can communicate with its platoon member UEs using the groupcast mode, while using the broadcast mode to transmit other periodic messages to UEs that are not part of the platoon as shown in Fig. 2.17. When a packet arrives at a transmitting UE, it is assumed that the higher layers notify

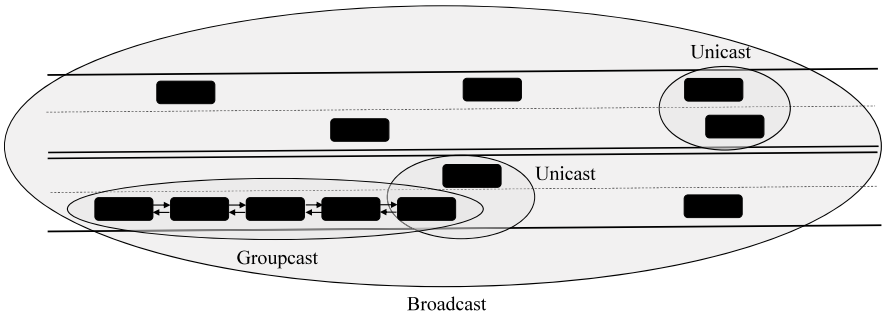


Figure 2.17: Communication types in NR V2X.

whether the packet must be sent in unicast, groupcast, or broadcast mode [119]. Note that these transmission modes were also defined in LTE D2D communications [120]. However, the identification of packets as unicast, groupcast, and broadcast is performed at Layer-2. Thus, the PHY layer of the UE must always decode the packet and send it to the higher layer. To reduce the decoding burden of all received packets, NR V2X will define these transmission modes at the PHY layer. Thus, if a packet belongs to a unicast or groupcast mode, then non-participant UEs need not decode the entire packet.

### Novel Features and Mechanisms

NR V2X will define features and mechanisms that are derived from NR (defined in 3GPP Release 15). In most cases, the baseline solution for design is taken to be what is defined in NR, followed by V2X specific enhancements [117]. In this subsection, we list the key enhancements that are undergoing design in NR V2X.

- Flexible numerologies: Support for flexible numerologies is a key feature introduced in 3GPP Release 15. As opposed to a fixed sub-carrier spacing used in LTE, NR supports different sub-carrier spacings, which are multiples of the LTE sub-carrier spacing, i.e., 15 kHz. Sub-carrier spacing of 15, 30 and 60 kHz will be supported for sub-6 GHz NR V2X (i.e., Frequency Range 1, FR1), while 60 and 120 kHz will be supported for frequency bands above 6 GHz (i.e., FR2) [119]. The use of higher sub-carrier spacings facilitates latency reduction. Assuming each UE requires one slot for its transmission, the transmission time of a UE decreases as the sub-carrier spacing increases. Note that the term "slot" and "sub-frame" hold different meanings in NR V2X. NR defines the duration corresponding to 14 OFDM symbols as one slot, while a sub-frame has a fixed duration of 1 msec. Furthermore, due to smaller slot durations at higher sub-carrier spacings, variations within the slot will be smaller, thereby needing fewer DMRS symbols per slot for channel estimation.

- Slot, mini-slot, and multi-slot scheduling: In LTE and C-V2X, the transmission time is tightly coupled to the sub-frame duration, i.e., all UEs always transmit for a duration

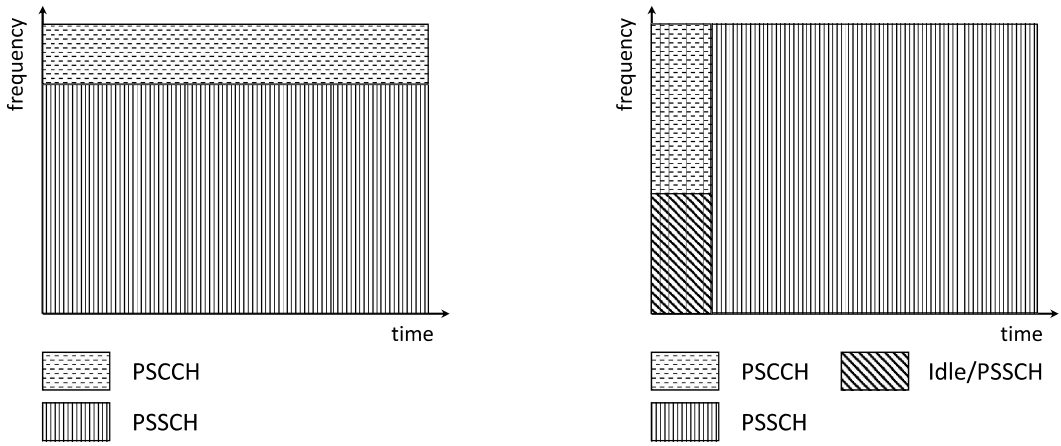


(a) Multiplexing in C-V2X (b) Multiplexing in NR V2X

Figure 2.18: Multiplexing of PSCCH and PSSCH in C-V2X and NR V2X.

of 1 sub-frame (1 msec). However, if a UE has only a small amount of data to send, which can be accommodated in less than 14 OFDM symbols, allocating the entire slot for its transmission is resource inefficient. Second, whenever a packet arrives at a UE for transmission, the UE has to wait until the beginning of the next slot to begin transmitting. Such slot-based scheduling is supported by default in NR V2X. However, NR V2X will also support *mini-slot* scheduling, where UEs that have latency-critical messages to send can start their transmissions at any of the 14 OFDM symbols and can occupy any number of OFDM symbols within the slot. Furthermore, slot-aggregation, i.e., combining two or more slots to form a *multi-slot*, will also be supported in NR V2X to cater to use-cases that require the exchange of large-sized packets.

- Multiplexing of PSCCH and PSSCH: In C-V2X, PSCCH and PSSCH are multiplexed in frequency (see Fig. 2.18a). The drawback of this approach is that a receiver must buffer the message for the entire sub-frame and can decode the message only at the end of the sub-frame. This may prove to be inefficient in NR V2X due to the tight latency constraints of certain messages. To address this problem, PSCCH and PSSCH will be multiplexed in time in NR V2X, i.e., the PSCCH will be transmitted first, followed by the transmission of PSSCH. This is illustrated in Fig. 2.18b, where the use of resources marked as "Idle/PSSCH" is still under consideration and can be left idle or used for the transmission of PSSCH [119].

- Sidelink feedback channel: For unicast and groupcast communications, reliability can be improved if the source UE can re-transmit the packet if the reception fails at UE(s) during the initial transmission. Although C-V2X provides support for re-transmissions, these re-transmissions are blind, i.e., the source UE, if configured, re-transmits without knowing if the initial transmission has been received by surrounding UEs. Such blind re-transmissions are resource inefficient if the initial transmission is success-

ful. Blind re-transmissions are also ineffective if more than two transmissions are required for a given reliability requirement. Furthermore, if the source UE has access to the channel state information at its destination UE, this can be leveraged to adapt transmission parameters such as the MCS. To facilitate these two enhancements, i.e., enabling feedback-based re-transmissions and channel state information acquisition, NR V2X will introduce a new feedback channel—Physical Sidelink Feedback Channel (PSFCH) [121]. The selection of resources to use for PSFCH is still under study. However, to reduce the complexity associated with resource selection, preliminary studies in 3GPP recommend that the transmitter UE must notify the receiver UE about which resource to use for transmission on PSFCH [122].

- Additional sidelink sub-modes: Unlike in C-V2X sidelink mode 4, where there were no sub-modes, 3GPP began with evaluating four sub-modes of NR V2X sidelink mode 2 [123]. These sub-modes are as follows (i) Mode 2 (a): Each UE autonomously selects its resources. This mode is similar to C-V2X sidelink mode 4, (ii) Mode 2 (b): UEs assist other UEs in performing resource selection. The assisting UE can be the receiver UE, which can potentially notify the transmitting UE of its preferred resources using the PSFCH, (iii) Mode 2 (c): In this sub-mode, UEs use pre-configured sidelink grants to transmit their messages. This sub-mode will be facilitated through the design of two-dimensional time-frequency patterns such as those described in [124], and (iv) Mode 2 (d): UEs select resources for other UEs. This sub-mode can be seen as an extension of sub-mode 2 (b).

### Comparison with C-V2X

Table 2.4 summarizes the key differences between features/mechanisms of C-V2X and NR V2X.

Table 2.4: Comparison of C-V2X and NR V2X

| **Feature** | **C-V2X** | **NR V2X** |
|---|---|---|
| Comm. types | Broadcast | Broadcast, Groupcast, Unicast |
| MCS | QPSK, 16-QAM | QPSK, 16-QAM, 64-QAM |
| Waveform | SC-FDMA | OFDM |
| Re-transmissions | Blind | HARQ |
| PHY channels | PSCCH, PSSCH | PSCCH, PSSCH, PSFCH |
| Control & data multiplexing | FDM | TDM |
| DMRS | Four/sub-frame | Flexible |
| Sub-carrier spacing | 15 kHz | sub-6 GHz: 15, 30, 60 kHz<br>mmWave: 60, 120 kHz |
| Scheduling interval | one sub-frame | slot, mini-slot or multi-slot |
| Sidelink modes | Modes 3 & 4 | Modes 1 & 2 |
| Sidelink sub-modes | N/A | Modes 2(a), 2(d) |

# Chapter 3

# An Overview of Coexistence Issues in the 5 GHz and 6 GHz Bands

The diverse set of wireless technologies operating in the 5 GHz and 6 GHz bands, and the frequency bands in which they operate, create several scenarios where two or more RATs operate in partially or completely overlapping frequency bands. Since these wireless technologies are often incompatible with each other, i.e., their PHY and the MAC layers are not necessarily designed to harmoniously coexist with each other, tailor-made solutions are required for coexistence between any two (or more) distinct RATs when they operate in overlapping frequency bands.

In this chapter, we provide a comprehensive survey of several such coexistence scenarios. These scenarios include coexistence between secondary users of the band and the band's incumbent users (e.g., coexistence between Wi-Fi and radars, or coexistence between Wi-Fi and ITS systems), and coexistence amongst unlicensed secondary users (e.g., coexistence between Wi-Fi and unlicensed cellular technologies).

## 3.1 Coexistence of Radar and Wi-Fi

The first step toward allowing unlicensed devices to operate in the $5.150 - 5.350$ GHz and $5.470 - 5.725$ GHz bands was taken at the World Radiocommunication Conference, 2003 (WRC-03) [62]. As per the WRC-03 regulations, unlicensed devices could operate in these frequency bands so long as they do not interfere with the incumbent users of the spectrum – radars. Thus, radars are the primary users of the band, and Wi-Fi devices can operate in the shared spectrum if no radar activity is reported.

In this section, we look at coexistence issues with radars that arise due to Wi-Fi operations in the 5 GHz bands. We divide the discussions into two parts — (i) coexistence issues in the U-NII-2A and U-NII-2C bands, where Wi-Fi devices continue to coexist with radars, and (ii) coexistence issues in the U-NII-2B band, where the 2013 FCC NPRM proposed to allow unlicensed Wi-Fi operations [40].

### 3.1.1 Coexistence issues in the U-NII-2A and U-NII-2C bands

Wi-Fi devices operating in the U-NII-2A and U-NII-2C bands must use the Dynamic Frequency Selection (DFS) mechanism[1] to detect the presence of operating radars and avoid co-channel operations. The sensing technique in DFS involves signal detection at the Wi-Fi transmitter based on the knowledge of radar parameters, such as pulse width, pulse repetition rate, number of pulses per burst, etc.

The DFS mechanism is implemented at the Wi-Fi AP. Associated STAs have to rely on the AP to avoid causing any interference to radar systems. Before selecting a channel for operations, a Wi-Fi AP must perform a Channel Availability Check (CAC) whereby the AP must check for the presence of radar signals for a predetermined interval[2]. If a channel has ongoing radar activity (i.e., the sensed radar energy is greater than $-62$ dBm), the AP continues to scan for other idle channels in the band. If none of the channels are idle, the AP enters a "sleep mode", or moves to channels where DFS is not required (such as the U-NII-1 or U-NII-3 bands). If an idle channel is available, the Wi-Fi AP and STAs can continue their transmissions on such a channel. The AP must periodically perform CAC for radar activity in between transmissions. If radar activity is detected, the AP and its associated STAs must cease channel usage within 10 seconds. During these 10 seconds, the AP can send normal data traffic to the STAs for a maximum duration of 200 $m$sec. The AP can also transmit control information to its associated STAs to facilitate moving to an idle channel. The channel must then be declared busy for 30 minutes.

Before WLAN products operating in the 5 GHz bands can be introduced in the market, the product manufacturers are required to test the devices for compliance certifications from the regulatory agencies (such as FCC in the US and ETSI in Europe). For WLAN devices operating in the U-NII-2A and U-NII-2C bands, these compliance tests usually involve checking the ability of the deployed DFS algorithm to detect characteristic radar signals, specified in terms of radar pulse width and pulse repetition factors. In the case of the $5.47 - 5.725$ GHz band, where weather radars are prone to interference from Wi-Fi transmissions, it is sometimes possible to provide a pre-decided set of waveforms for testing. However, with newer radar systems being developed, providing an exhaustive set of waveforms is infeasible, and maybe impossible in scenarios where the radars are developed for defense purposes.

The DFS algorithm has continued to evolve ever since the ITU regulations in 2003. Several experimental studies have been conducted to determine the efficacy of DFS in detecting radar activity and the ability of the Wi-Fi devices to move to a different channel when radar activity is detected. Experiments performed by Joe et al. [125] show that Wi-Fi APs are

[1] The exact frequencies that require the use of DFS is regulation specific. For example, Ofcom in the UK mandates the use of DFS from $5.47 - 5.85$ GHz, while FCC in the US requires DFS in the $5.47 - 5.725$ GHz bands [61].

[2] The exact interval is decided by country-specific regulations. For example, regulations in the US require the AP to scan the channel for 60 seconds, while the Canadian regulations specify an interval of 10 minutes – a duration that overlaps with the scan cycle time of most weather radars operating in 5.6 GHz.

capable of detecting the activity of weather radars operating in the 5.6 GHz band in a highly mobile environment like inside an aircraft. However, at low enough distances ($< 25$ km) the WLAN presence can be seen at the weather radars. In [126], the authors show that the detection threshold of $-62$ dBm is sufficient to detect weather radar activity on most occasions. However, this detection capability depends to a large extent on the direction of the radar signals. If the AP is unable to detect the radar activity before the radar beam directly aims at the Wi-Fi network, the radar system is blinded by Wi-Fi transmissions. Moreover, radar systems with larger bandwidths are more susceptible to Wi-Fi interference.

Tercero et al. [127] present a mathematical model to analyze the interference caused by aggregate Wi-Fi users to weather radars operating in the 5.6 GHz band. The authors consider the basic DFS mechanism at the Wi-Fi AP and show that in dense urban scenarios where the density of Wi-Fi users is greater than 10 WLANs per square kilometer, radar systems experience aggregated interference larger than their interference threshold.

Several approaches have been adopted to mitigate Wi-Fi interference at radar receivers. For example, the authors in [128] propose a channel allocation scheme that takes into consideration meteorological radar operations and show that by using existing Wi-Fi mechanisms such as the RTS/CTS handshake, Wi-Fi devices can minimize interference at radar systems. Signal processing based interference cancellation strategies have also been proposed in the literature. Take [129] for example. The authors argue that Wi-Fi transmission characteristics can be leveraged at radar systems to detect and cancel interfering signals. Moreover, since Wi-Fi standards are universal, the authors claim that techniques based on identifying Wi-Fi characteristics can be used to solve such interference problems universally. The authors test their scheme on time-series waveforms obtained from Brazil, India, and Estonia to validate their claims. Similar work has been presented in [130]. In [131], the author proposes the use of computer vision-based techniques for removal of interference signals at radar receivers that can potentially filter out transmissions from Wi-Fi like emitters.

Technologies to enhance the DFS mechanisms have also been proposed in the literature. Tercero et al. [132] exploit the temporal nature of radar systems to increase the transmission opportunities for Wi-Fi devices. The authors quantitatively estimate the number of Wi-Fi users that can operate as secondary users in radar occupied bands. Furthermore, they show that using their scheme, a Wi-Fi user operating as close as 4 km from the radar can transmit up to 99.45% of the time without interfering with the radar receiver.

Despite the proposal and adoption of the aforementioned interference-mitigation techniques, incidences of interference caused to radar systems (particularly to the weather radars operating in $5.60 - 5.65$ GHz) by Wi-Fi operations have been reported in US [133, 134], Canada [135], across Europe [136, 137, 138] and other regions [139]. The primary reasons for such Wi-Fi-induced interference are summarized below.

- DFS mechanism can be deliberately turned off by the operator or even by the users. Detection and enforcement of these rogue WLAN devices is difficult even with the

presence of azimuth data at the radars. In the past, several cases of interference to the weather radars have been reported in the US and Europe due to deliberate disabling of the DFS mechanism in WLAN devices [134, 136].

- DFS does not address the *hidden node* problem. The DFS mechanism is used only at the AP to detect the presence of radar systems. However, there is a possibility that the radar signal is not detectable at the AP, but associated STAs may cause interference at the radar receivers [128].
- Unlicensed devices operating on an adjacent channel can cause harmful interference to radar systems. In the ideal scenario, once a DFS device detects a radar signal, it must move to a channel that is separated far enough in frequency to eliminate adjacent channel interference. However, interference investigations lead by the National Telecommunications and Information Administration in the US have determined that some devices have not been moving far enough away in frequency, and as a result, their out-of-channel emissions were causing interference to weather radars [60].

### 3.1.2 Coexistence issues in the U-NII-2B band

Coexistence between radars and Wi-Fi in the U-NII-2A and U-NII-2A bands has been a problem worldwide. In what follows, we discuss issues of coexistence between Wi-Fi and radar systems if Wi-Fi devices are to operate in the U-NII-2B band. It must be noted that Wi-Fi devices do not currently operate in the U-NII-2B band worldwide. Although the FCC NPRM in 2013 did consider to allow operations in the U-NII-2B band, it was decided that coexistence between Wi-Fi and radars in this band would pose great technical challenges. The primary reason for such considerations in the first place was that allowing unlicensed devices to operate in the $5.35 - 5.47$ GHz band in addition to the $5.85 - 5.925$ GHz band would result in up to 70% increase in the available spectrum, and an increase the number of 80 MHz channels by 125% (from 4 to 9) [41].

Notwithstanding the advantages of allowing Wi-Fi operations in the U-NII-2B band, the coexistence of Wi-Fi and radars in this band faced several challenges. These challenges are summarized below.

- Unlike other 5 GHz bands, the U-NII-2B band is used for many military and safety-critical applications. Adequate protection for these systems from WLAN-induced interference is extremely important. In the DFS certification test, a set of waveforms is defined, but it does not necessarily include waveforms from all radar systems. There are a large number of radar systems operating in the U-NII-2B band, which are not present in the U-NII-2A and U-NII-2C bands.
- In the U-NII-2A and U-NII-2C bands, radar parameters such as pulse width, pulse repetition interval, and the number of pulses per burst are well-known [60]. On the

other hand, a large and diverse set of radar systems operate in the U-NII-2B band. The pulse widths, pulse repetition frequency, and other characteristics vary significantly from system to system. Even for a single radar, the pulse width can change with time. In addition, some radar systems in this band operate in low power modes or are designed to avoid detection to meet their mission requirements. These radar systems are challenging for the WLAN devices to correctly detect.

- Signal processing techniques are typically employed at radars to minimize the impact of interference caused by other radars. However, these techniques are only effective for low duty cycle emitters. WLAN devices typically use very high duty cycles (for instance, with frame aggregation techniques the duty cycle can go as high as 80% [60]). This makes it difficult for radar systems to mitigate WLAN interference using signal processing techniques that are useful in the case of low duty-cycle (single-pulse) filters at the radars.

- The existing DFS mechanisms were developed specifically to protect radar systems in which the transmitter and receiver are co-located. Airborne systems employ ground and airborne transmitters and receivers located at different locations. Full duplex systems with the uplink and downlink on different frequencies can introduce hidden node problems for WLAN APs that rely on sensing.

- The use of signal detection-based DFS techniques used in other 5 GHz bands may be unsuitable for use in the U-NII-2B band. Detection techniques based on the use of geo-location databases used in TV White Space (TVWS) [140, 141, 142, 143] were generally considered to be more suitable for spectrum sharing in the U-NII-2B band [60]. Although database based techniques can be useful in scenarios where the radar transmitter and receiver are collocated, radar systems with non-collocated transmitters and receivers may not be adequately protected from Wi-Fi transmissions.

- Moreover, several database management, and authorization related issues while drafting regulations for the TV band devices (e.g., construction of databases, sharing data between databases, how to determine available channels, securing the information, etc. [140]) had to be addressed if geo-location databases were to be created to protect critical radar systems.

- Furthermore, this necessitates the protection of incumbent information in case of radar systems that are of critical importance for national security. Such studies have been carried out in the context of radar systems operating in other spectrum bands [144, 145].

### 3.1.3 Open Research Problems

We list the following open research problems concerning the coexistence of Wi-Fi and radar systems in the U-NII-2A and U-NII-2C bands.

- Technologies and techniques for detecting, identifying, and adjudicating rogue devices are needed. Here, rogue devices refer to devices that have disabled the DFS functionality or intentionally operate in the presence of incumbent systems. In addition, these enforcement approaches need to be automated and cost-effective to be considered commercially viable.
- Solutions to combat the hidden node problem in the $5.25 - 5.35$ GHz and $5.47 - 5.725$ GHz bands (due to DFS implementation only at the AP) need to be developed.
- PHY layer techniques that enable underlay cognitive radio networks, such as transmit beamforming [146, 147] that can null the secondary user waveforms at the radar systems can be an interesting subject of investigation.

## 3.2 Coexistence of 6 GHz Incumbents and Unlicensed RATs

### 3.2.1 Coexistence in the US

#### 3.2.1.1 U-NII-5 and U-NII-7 bands

The FCC 6 GHz R&O [2] allows standard power APs[3] (23 dBm/MHz) to operate in the U-NII-5 and U-NII-7 bands under the constraints that the APs must not operate within the *exclusion zone* of incumbent receivers. The exclusion zone for incumbent receivers is computed as the region around the receiver where unlicensed operations can result in interference-to-noise-power ratio, I/N = -6 dB, or greater [2]. Exclusion zones for incumbent receivers operating in U-NII-5 and U-NII-7 bands will be computed by a centrally-implemented AFC system. These computations will take into account the antenna pattern of the incumbent receiver, antenna heights of the incumbent and unlicensed users, the Effective Isotropic Radiated Power (EIRP) of the unlicensed devices, and appropriate propagation models.

To mitigate adjacent channel interference resulting from unlicensed transmitters at a given incumbent receiver, the AFC database will compute not only the co-channel (i.e., the channel

[3]Here, the term AP, as used in the FCC NPRM and R&O, refers to the entity that coordinates transmissions in the network. For example, in Wi-Fi networks, this is the Wi-Fi AP. On the other hand, for LAA or NR-U networks, this the eNB or gNB, respectively.

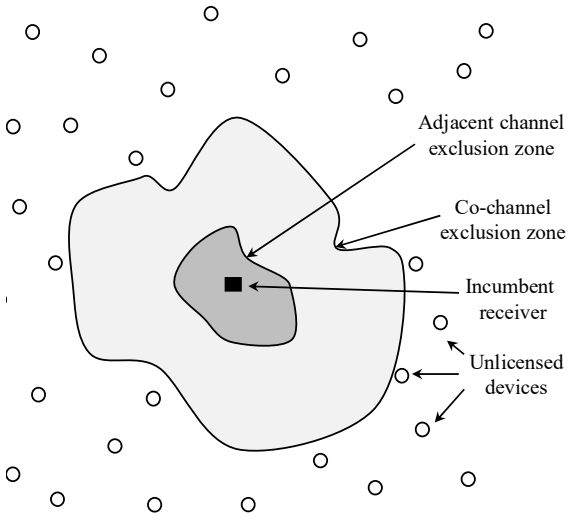


Figure 3.1: Co-channel and adjacent channel exclusion zones.

on which the incumbent receiver operates) exclusion zone but also the adjacent-channel exclusion zone. The concept of co-channel and adjacent channel exclusion zones is illustrated in Fig. 3.1. Suppose the incumbent user operates on channel $c$. Unlicensed devices are then prohibited from operating on channel $c$ (or channels that overlap partially with channel $c$) inside the co-channel exclusion zone. Further, unlicensed devices are prohibited from operating on any channel that is immediately adjacent to channel $c$ within the adjacent channel exclusion zone. Note that because wireless devices radiate less power into adjacent channels than in the intended channel, the exclusion zone for adjacent channels is smaller than the co-channel exclusion zones.

A standard power unlicensed AP, before beginning operations in the U-NII-5 and U-NII-7 bands, must contact the AFC system database and obtain a list of permissible frequencies for operations. To facilitate the computation of this list, the AP must provide its location and antenna height. This requirement necessitates either the possession of geo-location capabilities (such as Global Positioning System, GPS) at APs operating in the U-NII-5 and U-NII-7 bands or access to an external geo-location source. In addition to its location, the AP must report the uncertainty in its location (i.e., accuracy in meters) to the AFC system. Further, if the AP's geo-location is obtained through an external source, it must report its distance from this external source as a part of its location uncertainty. Because incumbent users in these bands are static and new users become operational infrequently, the FCC R&O requires unlicensed APs to query the database and obtain a list of permissible frequencies once every 24 hours.

The AFC system database will provide a set of transmission powers that the standard power AP can select. For each transmission power in this set, a corresponding list of permissible frequencies will be provided. The FCC R&O states that the AFC system must compute, at

a minimum, the list of frequencies for transmission power in increments of 3 dB from 21 dBm to 36 dBm [2]. The unlicensed AP can then operate on one of these permitted frequencies. Unlicensed clients (STAs for Wi-Fi and UEs for NR-U) can operate in the 6 GHz bands only when associated with an AP. Note that both indoor and outdoor operations of standard power APs are permitted as long as the AFC system database indicates that the given frequency is available at the AP's location.

In addition to standard power APs, the FCC R&O allows low-power APs (5 dBm/MHz) and clients (-1 dBm/MHz) to operate throughout the 6 GHz bands without contacting the AFC system as long as these devices are confined to indoor environments [2]. This implies that as long as such APs are indoors and operate within the permissible power levels, they can operate inside the exclusion zones of incumbent receivers. To ensure that such APs—referred to as Low Power Indoor (LPI) APs—operate only in indoor settings, the FCC has placed the following three constraints: (i) LPI APs *cannot* be weather resistant, (ii) LPI APs must be equipped with integrated antennas and the capability of connecting such APs with external antennas is prohibited, and (iii) LPI APs cannot operate on battery power.

The FCC Further Notice of Proposed Rulemaking (FNPRM) [2] additionally seeks comments on allowing unlicensed devices operating at extremely low powers throughout the 6 GHz bands. These devices—referred to as very low power (VLP) devices—can operate within the exclusion zones of incumbent users and in both indoor and outdoor environments. Such VLP devices are critical in enabling personal area network applications such as wireless AR and VR through wearable devices and in-car connectivity [148]. Although the power spectral density (PSD) for VLP devices is yet to be determined, the FCC FNPRM proposes allowing VLP devices radiating under 4–14 dBm EIRP to operate in all four 6 GHz sub-bands. Note that due to building entry losses, the median value of which is 20.25 dB [2], LPI devices are permitted to operate within the exclusion zones of incumbent users. The choice of EIRP for VLP devices (4–14 dBm) is motivated by the fact that VLP devices radiating in outdoor environments and within the exclusion zones of incumbent receivers must at least compensate for the building entry losses faced by signals from LPI devices.

Table 3.1 shows the different categories of unlicensed devices permitted to operate in the 6 GHz bands in the US [2]. Note that for standard power devices, considering the PSD limits per MHz of spectrum, the maximum EIRP is achieved for 20 MHz channels (23 dBm/MHz + 10 $\times$ $\log_{10}$ (20) = 36 dBm). This implies that if the bandwidth is increased beyond 20 MHz (say to 40 MHz), the power per sub-carrier is reduced by the corresponding factor (halved for 40 MHz). For LPI and VLP devices, the maximum EIRP is achieved for 320 MHz (5 dBm/MHz + 10 $\times$ $\log_{10}$ (320) = 30 dBm) and 160 MHz (-8 dBm/MHz + 10 $\times$ $\log_{10}$ (160) = 14 dBm), respectively. Further, note that the EIRP limit for clients is 6 dB is lower than those for the corresponding APs. This is due to the following two reasons: (i) Restricting the transmission power of client devices reduces their transmission range. This ensures that client devices will operate close to their respective APs. This is especially important in the U-NII-5 and U-NII-7 bands, where the permissible frequencies of operation are closely tied to the location of devices. (ii) Client devices are typically battery-operated and hence,

| **Bands** | **Device class** | **Maximum EIRP** | **Maximum EIRP PSD** |
|---|---|---|---|
| U-NII-5/U-NII-7 | Standard power AP | 36 dBm | 23 dBm/MHz |
| | Clients connected to standard power AP | 30 dBm | 17 dBm/MHz |
| U-NII-5 through U-NII-8 | LPI AP | 30 dBm | 5 dBm/MHz |
| | Clients connected to LPI AP | 24 dBm | -1 dBm/MHz |
| U-NII-5 through U-NII-8 | VLP devices* | 4 to 14 dBm | -18 to -8 dBm/MHz |

Table 3.1: Unlicensed devices allowed to operate in the 6 GHz bands in the US. * indicates device classes considered in the FCC FNPRM [2]. Note that throughout the 6 GHz bands, deployment of unlicensed devices in moving vehicles, trains and unmanned aerial vehicles is prohibited.

power-limited. This reduces the incentive of client devices to transmit at higher power levels.

While AFC-like database systems have previously been used for enabling coexistence between incumbent and unlicensed devices [149], studies on the impact of Wi-Fi devices on the performance of fixed services operating in the 6 GHz bands have so far been inconclusive. The Fixed Wireless Communications Coalition estimates that if Wi-Fi devices are permitted to operate within the incumbent users' exclusion zone, fixed service links can fail with 1.6% probability. At the same time, bit errors can occur with 7.1% probability [64]. The coalition further argues that because fixed service links have very stringent reliability requirements, studies on the impact of unlicensed devices on incumbent services must perform worst-case interference analysis. For example, instead of assuming *typical* terrain and clutter conditions, simulation studies must use free space path loss models to compute the interference power at incumbent receivers [150, 151]. Additionally, incumbent operators have argued for mandatory AFC system requirements for not only standard power devices (as indicated in the R&O) but also LPI devices [64, 151, 152].

Notwithstanding the above arguments, several studies from proponents of unlicensed services have dismissed incumbent users' concerns [153, 154, 155, 156, 157, 158]. Specifically, reference [156] notes that for standard power unlicensed services to interfere with incumbent users, a series of unlikely events must co-occur, thereby indicating that the probability of harmful interference from unlicensed users is extremely small. Results from bench-top testing performed in reference [157] indicate that when the interference protection criterion is fixed to I/N=-6 dB, the presence of Wi-Fi devices does not impact the performance at fixed service receivers. Furthermore, using simulation studies reference [158] shows that harmful interference resulting from LPI devices at fixed service links is extremely unlikely. Studies performed in [159] for LPI devices located in high rises of New York City and Washington DC yield similar conclusions. Before the FCC R&O was released, results from these studies were taken into consideration. Since the FCC R&O allows for standard power APs to op-

erate in the U-NII-5 and U-NII-7 bands and LPI devices to operate throughout the 6 GHz bands, it can be inferred that the FCC concludes that studies from proponents of unlicensed services are more practical and representative of real-world coexistence environments.

#### 3.2.1.2 U-NII-6 and U-NII-8 bands

As noted in Sec. 2.2.1.2, incumbent users of the U-NII-6 and U-NII-8 bands are such that their exact locations are hard to determine at a given time. This renders an AFC-like database system inefficient in protecting such incumbent users from interference resulting from unlicensed operations. Consequently, in these bands, the FCC R&O allows only LPI operations and seeks comments in its FNPRM on whether VLP devices can be permitted in outdoor environments. The constraints set by the FCC for ensuring that unlicensed devices operating in the U-NII-6 and U-NII-8 bands are restricted to indoor environments are the same as those outlined in Sec. 3.2.1.1.

By restricting unlicensed devices in indoor environments, it is expected that the additional propagation losses, e.g., building entry loss, which is typically on the order of 20 dB [2], will considerably reduce the strength of unlicensed interference at incumbent receivers. Nevertheless, just like in the U-NII-5 and U-NII-7 bands, proponents of unlicensed services have faced resistance in the U-NII-6 and U-NII-8 bands from its incumbent and existing users. For example, using simulation studies reference [160] shows that roughly two-thirds of television pick-up cameras in indoor environments and half of the cameras in outdoor settings can suffer from harmful interference in the presence of unlicensed users. Further, reference [161] analyzes Wi-Fi-induced interference to electronic newsgathering systems. The analysis, which is performed for three representative locations, shows that the interference increases with an increase in the Wi-Fi duty cycle and antenna height of the newsgathering stations.

Similarly, existing users of these bands that rely on UWB have expressed concerns regarding unlicensed device-induced harmful interference, thereby significantly compromising their performance [65]. Although UWB system users are not entitled to protection from external sources of interference, if new unlicensed operations in the U-NII-6 and U-NII-8 bands deteriorate their system performance, the resulting impact on applications that are already deployed will be significant.

In comparison to the U-NII-5/7 bands, studies defending unlicensed operations in the U-NII-6/8 bands are fewer in number. Monte Carlo simulation studies reported in [162] have shown that restriction of Wi-Fi devices to indoor environments is effective in mitigating interference to Broadcast Auxiliary Services operating in the U-NII-6 and U-NII-8 bands. On the other hand, simulations results reported in [163] acknowledge that unlicensed devices can indeed negatively affect the performance of nomadic incumbent users operating in these bands. However, the fraction of incumbent users that suffer from complete link failure and bit errors are reported to be as low as 0.2% and 1.1%, respectively.

### 3.2.2 Coexistence in Europe

Studies on coexistence between Wi-Fi-like unlicensed users and the existing users of the 5.925–6.425 GHz bands (including adjacent bands) in Europe are reported in the ECC Report 302 [54]. These current users include fixed services, fixed satellite services, ITS services, CBTC, radio astronomy, and UWB systems. Results from minimum coupling loss and Monte Carlo analyses carried out in the report conclude that unlicensed devices, as long as they operate indoors (EIRP 23–24 dBm), present a minimal risk of causing interference at fixed service receivers. Thus, the study concluded that spectrum sharing between unlicensed RATs and fixed services is feasible.

Further, assuming unlicensed devices' deployment models for the year 2025, the aggregate interference from unlicensed devices at satellite receivers in space was estimated. Considering these future unlicensed deployments, the study concludes that as long as *no more than 5%* of unlicensed devices operate outdoors, fixed satellite services and unlicensed devices can feasibly share the spectrum[4]. In terms of coexistence with incumbent systems operating in adjacent (i.e., ITS) or partially overlapping bands (i.e., CBTC), the report concludes that unlicensed devices can share the spectrum with added constraints. These constraints include tighter spectral masks and restricted operations in the lowermost 6 GHz channels (i.e., channels 1, 3, 7, etc.).

Based on the findings presented in [54], the European Conference of Postal and Telecommunication (CEPT) approved the CEPT report 73 [3]. The recommendations made by this report—submitted in response to the ECC mandate [34]—for unlicensed operations in the 6 GHz bands are shown in Table 3.2. Observe that because the nature of existing users operating in the 6 GHz bands in Europe and the US is similar, the proposed permitted device classes, constraints, and solutions for coexistence between the unlicensed RATs and incumbents are also similar. It must be noted that studies conducted in the ECC Report 302 [54] evaluate the technical conditions on unlicensed device operations in the 6 GHz bands. These studies will serve as guidelines for the final technical rules, which are likely to be finalized soon [34]. Furthermore, although current studies do not focus on mitigation strategies, if found feasible, outdoor unlicensed operations could be permitted in the future under a geo-location database system constraint (like the AFC system in the US).

### 3.2.3 Open Research Challenges

The introduction of new unlicensed RATs in a band introduces several challenges in achieving coexistence between the band's incumbent users and unlicensed devices. The 6 GHz bands

[4]Note that in the US, the FCC does not take the aggregate interference resulting from outdoor unlicensed devices into consideration. The two primary reasons for this, as stated in the FCC R&O [2], are: (i) unlicensed devices have little incentive to radiate upward (in the direction of the satellites), and (ii) computation of aggregate power at the incumbent satellite receivers will complicate the AFC system design.

| Device class | Constraint | Maximum unlicensed EIRP | |
|---|---|---|---|
| | | **Coexisting Incumbent** | **Permitted EIRP** |
| LPI | Indoor | Fixed services | 23–24 dBm |
| | | Fixed satellite services | 23–24 dBm |
| | | CBTC | 21.5 dBm/20 MHz (in-band) and -29.5 dBm/5 MHz (out-of-band) |
| | | ITS | -69 to -36 dBm/MHz (out-of-band) |
| VLP | Indoor and outdoor | Under consideration | |
| Standard power | To be considered (AFC-like database) | To be considered, approximately 30 dBm | |

Table 3.2: Unlicensed device classes feasible in the 6 GHz bands in Europe [3]. For LPI operations, the maximum EIRP is evaluated on a case-by-case basis for each incumbent system. The final rules will likely be the intersection of all criteria.

are no exception to this. Several incumbent users have highlighted the need for Wi-Fi and NR-U devices to exercise more caution during their operation in these bands. This is critical because once the proliferation of unlicensed devices takes place in the 6 GHz bands, much like in the 5 GHz bands, it becomes extremely difficult to identify and enforce restrictions on potentially rogue unlicensed devices that are already deployed. However, a novel characteristic of the 6 GHz bands, and the unlicensed devices operating in these bands, is that currently, no such unlicensed devices are operating in these bands. The 6 GHz bands, therefore, offer a *clean slate*, where novel coexistence mechanisms can be tested and deployed. The following aspects of coexistence between incumbent and unlicensed devices must be investigated.

#### 3.2.3.1 Efficiency of the AFC System

In the US, incumbent users in the U-NII-5 and U-NII-7 bands will be protected by using the concept of exclusion zones. Unlicensed devices operating in these bands must connect to the AFC system database to determine if their location is within the exclusion zone of any incumbent receiver. If an unlicensed device is found to be within the exclusion zone of an incumbent receiver, it can operate on all frequencies other than the operating frequency of the incumbent receiver. Such database-driven coexistence mechanisms are shown to be effective in other frequency bands [164]. Furthermore, proponents of unlicensed services have claimed that unlicensed devices operating in the U-NII-5/7 bands are highly unlikely

to interfere with incumbents operating in these bands. Even though these claims are backed by preliminary simulation studies and experimental results, considering the stringent outage constraints placed on incumbent services, these coexistence scenarios must be investigated with rigorous analytical models and experimental studies.

At the same time, the AFC system must not be too conservative in allowing unlicensed access in the U-NII-5 and U-NII-7 bands. The boundary of a conventional exclusion zone is determined based on an estimate of the union of all likely interference scenarios, and this results in an overly conservative boundary that often leads to low spectrum utilization efficiency. To address this shortcoming, authors in [165] have proposed the concept of Dynamic Incumbent Protection Zones (DIPZ). Unlike conventional exclusion zones, a DIPZ is a dynamic spatial separation region surrounding an incumbent receiver whose boundary is dynamic in terms of geolocation, time, and frequency. Such schemes have the potential to increase spectrum utilization efficiency while protecting incumbent users. More research is needed to determine whether such schemes can be adopted in the 6 GHz bands to improve spectrum utilization efficiency.

#### 3.2.3.2 Interference characterization of VLP and LPI devices

In comparison to incumbent receivers operating in the U-NII-5/7 bands, the nomadic incumbent users in the U-NII-6/8 bands can be more vulnerable to interference from unlicensed devices. This is because receivers of such nomadic incumbent systems are more likely to come close to unlicensed devices. To tackle this issue, the FCC R&O restricts unlicensed operations in the U-NII-6/8 bands to indoor-only LPI devices, thereby relying on lower transmit powers and building entry losses to mitigate interference at incumbent receivers. Although the FCC believes such measures are sufficient to protect the incumbent users in these bands, several incumbent users have raised concerns regarding interference from LPI devices (see Sec. 3.2.1.2). Similar issues can be expected if VLP devices are permitted to operate in the U-NII-6/8 bands, as indicated in the FCC FNPRM. To ensure that the performance of incumbent systems remains uncompromised, it is necessary to characterize the interference resulting from VLP and LPI devices at incumbent receivers, especially before unlicensed LPI and VLP devices proliferate in these bands.

Interference characterization of LPI and VLP devices can be performed by considering the typical operating characteristics of unlicensed and incumbent systems. This includes factors such as the link budget of incumbent systems, operating environments (such as indoor/outdoor stadiums, public parks, concert halls, etc.), locations of incumbent receivers, and unlicensed transmitters, transmit power of unlicensed devices, appropriate propagation models, etc. For example, given that a special event occurs inside an indoor stadium, the locations of incumbent and unlicensed devices can be modeled as two independent 2-D point processes [166]. Using an appropriate propagation model, such as the WINNER model [167], the impact of VLP and LPI devices can be analyzed as the fraction of time during which the

unlicensed interference power at an arbitrary incumbent receiver exceeds the link budget of the system.

#### 3.2.3.3 Mechanisms for detection of incumbent users in the U-NII-6 and U-NII-8 bands

Without a method for detecting incumbents and/or coordinating channel access, access by unlicensed devices needs to be strictly limited. For instance, the FCC FNPRM proposes to limit the transmission power of unlicensed devices operating outdoors (such as the case with VLP devices) while the FCC R&O only allows indoor operations (such as the case with LPI devices). However, such restrictions may significantly limit the utility of the U-NII-6/8 bands to unlicensed users.

An efficient way to ensure that incumbent users remain interference-free while unlicensed devices have the maximum operational flexibility is to define incumbent user detection mechanisms for unlicensed devices. If any incumbent user activity is detected in the vicinity of the monitoring unlicensed device, it must cease its operations on that channel and move to other frequencies. This is similar in spirit to the DFS mechanism deployed at Wi-Fi devices operating in the U-NII-2C band (see Sec. 3.1.1). However, the DFS mechanism is known to be conservative beyond necessity and makes Wi-Fi operations infeasible in channels where radar systems operate. Thus, alternate mechanisms that are more efficient at utilizing the spectrum must be defined in the 6 GHz bands. Such a dynamic frequency coordination mechanism can leverage the signal characteristics of incumbent users and detect their on-air presence.

To define such a dynamic frequency coordination mechanism, the following specific aspects must be studied — (i) what characteristics of the incumbent signal can be used for reliable detection? (ii) to alleviate the hidden node problem, what threshold energy level must the unlicensed devices use for detecting the presence of incumbent users? (iii) what should the initial sensing time be for which unlicensed devices *listen* without transmitting on the channel?, (iv) if the incumbent activity is not detected, how often must unlicensed devices perform the detection routine? (v) once incumbent user activity is detected, what is the maximum time for which unlicensed devices can operate on the channel without degrading the incumbent system performance? and (vi) how soon can unlicensed devices resume operating on the channel if the incumbent activity is detected?

#### 3.2.3.4 Enforcement of rogue unlicensed devices

Despite the use of interference mitigation schemes like DFS, weather radar operators in the 5 GHz bands have reported harmful interference from Wi-Fi operations [134, 135, 138]. Once deployed, the enforcement of such rogue Wi-Fi transmitters is known to be an extremely difficult problem [10]. Similar problems can occur in the 6 GHz bands. Standard

power APs operating in the U-NII-5 and U-NII-7 bands are required to provide their FCC identifier during their registration with the AFC system database [2]. The enforcement of such standard power APs, therefore, is likely to be straightforward. However, recall that LPI unlicensed devices are permitted to operate inside the exclusion zones of incumbent receivers in the U-NII-5 and U-NII-7 bands as long as they operate indoors. If building entry losses are small, such devices can interfere with incumbent users. Further, as proposed in the FCC FNPRM [2], if VLP devices are permitted to operate in the 6 GHz bands, incumbent receivers (especially those in the U-NII-6 and U-NII-8 bands) can be susceptible to interference from nearby VLP devices.

To ensure that the performance of incumbent users is not compromised, enforcement of sharing rules at potentially rogue unlicensed devices must be proactively addressed in these bands. Spectrum sharing enforcement involves the following three stages, (i) identification of interfering device, (ii) localization of the interfering device, and (iii) imposing punitive actions. The state-of-the-art literature on these stages of enforcement (such as [168, 169, 170, 171, 172, 173, 174, 175, 176, 177, 178, 179, 180]) must be investigated for their suitability for the 6 GHz bands. If these mechanisms are deemed inappropriate, novel mechanisms that consider the specific characteristics of incumbent and unlicensed users of the 6 GHz bands must be developed.

## 3.3 Coexistence of DSRC and Wi-Fi

Following the FCC NPRM in 2013 [40], a large number of studies focused on if and how co-channel coexistence between DSRC and Wi-Fi systems can be enabled. At first look, since the 802.11p amendment is derived from 802.11a, and since both systems use an LBT-based approach for accessing the channel, it might seem like this coexistence scenario is similar to coexistence between Wi-Fi devices (and in particular, coexistence across heterogeneous Wi-Fi devices). However, on closer inspection, there are several key differences between the coexistence of heterogeneous Wi-Fi devices and the coexistence between DSRC and Wi-Fi.

Firstly, 802.11p uses 10 MHz wide channels. Present-day Wi-Fi transmitters have no support for preamble detection of 10 MHz wide signals, and 802.11p cannot decode 20 MHz preambles. Thus, if 802.11p and 802.11ac transmitters were to operate in the same spectrum, both transmitters would detect each others' presence only using energy detection. The detection thresholds using energy detection being much higher (approx. 20 dB) than preamble detection [181], the sensing range of both transmitters will be much smaller as compared to that in traditional coexistence scenarios, resulting in collisions at both, Wi-Fi and DSRC receivers.

Secondly, 802.11p is the primary user of the spectrum. Thus, if a packet is available for transmission at both, DSRC and Wi-Fi devices, the 802.11p transmitter must be able to gain access to the channel before the Wi-Fi transmitter. The reverse situation, i.e. a Wi-Fi

transmitter has a higher priority over DSRC transmitter, is referred to as a priority reversal problem. To adhere to the regulations, it is clear that the priority reversal problem must be avoided in a coexisting network.

### 3.3.1 Status of Existing Research

In August 2013, the IEEE 802.11 Regulatory Standing Committee created a subcommittee called the *DSRC Coexistence Tiger Team* to explore possible band sharing techniques that will enable the coexistence of DSRC and 802.11ac, and also help inform the regulatory process. In March 2015, Tiger Team published their final report [182] that summarizes the issues surrounding the proposed band sharing ideas discussed in the group. Two proposals are summarized in [182]:

- *Sharing using existing DSRC channelization and CCA in* 10 *MHz channels.* Details of this technique are presented in [183]. This proposal is a hybrid solution of the traditional CCA and DFS mechanisms. The proposal assumes that all unlicensed devices must embed hardware that can detect 10 MHz wide 802.11p preambles. If an unlicensed device needs to operate in any of the DSRC channels, the device must sense all seven 10 MHz DSRC channels. If a single 10 MHz 802.11p preamble is detected by the Wi-Fi transmitter, the frequency band from $5825 - 5925$ MHz must be declared busy for at least 10 seconds. During this busy period, the DSRC channels will continue to be monitored, and any new DSRC packet detection will extend the busy state for another ten seconds from the time of detection.
- *Sharing using modified DSRC channelization and CCA in* 20 *MHz channels.* Details of this proposal are presented in [49]. The basic idea of this proposal is that the upper three 10 MHz channels can be reserved for DSRC safety applications, where the unlicensed devices must not be allowed to share the channels with DSRC nodes. The lower 45 MHz spectrum, on the other hand, can be shared with unlicensed devices. Furthermore, DSRC channelization in the lower 45 MHz spectrum must be changed to 20 MHz instead of the currently used 10 MHz, which would alleviate the constraints of detecting 10 MHz signals at the Wi-Fi transmitters. However, some members of the Tiger Team argue that compressing 7 channels of critical traffic into 2 or 3 may result in excess packet loss and latency, thus degrading vehicular safety application performance [184].

In Europe, on the other hand, following recommendations from the Wi-Fi industry, two coexistence mechanisms, viz. Detect and Mitigate (DAM) and Detect and Vacate (DAV), have been standardized by the ETSI [48]. The two proposals offer a varying degree of flexibility to Wi-Fi devices operating in the ITS band depending on the required interference mitigation at the DSRC devices. Both proposals, i.e., DAM and DAV, require Wi-Fi transmitters to

sense 10 MHz DSRC preambles as valid Wi-Fi frames. We discuss DAM and DAV in further detail in Chapter 5.

Wang et al. [185] model the coexisting DSRC and Wi-Fi systems as a Poisson point process and characterize DSRC and Wi-Fi performance in different spectrum sharing conditions. The authors also evaluate the performance resulting from the two proposals described above ([49, 183]), and report that while the first proposal ([183]) protects DSRC systems, the second proposal ([49]) exclusively favors Wi-Fi's system performance.

In recent years, several papers analyzing issues of coexistence between DSRC and 802.11ac devices have been published [106, 186, 187]. These papers explore ideas other than those described in the aforementioned Tiger Team proposals and often leverage the similarities in the MAC protocols of Wi-Fi and DSRC. For example, Lansford et al. [106] qualitatively argue that an increase in the value of Wi-Fi parameters (such as IFS) can ensure higher channel access priority to 802.11p nodes as compared to Wi-Fi nodes. We verify that this qualitative assessment is indeed true in Chapter 3.3 (and is reported in [188]).

With the help of experiments, Park et al. [187] show that increasing the Arbitration Inter Frame Spacing (AIFS) value of 802.11ac transmitters can indeed help in mitigating the above priority reversal problem. In particular, the authors show that by increasing the AIFS value of Wi-Fi to 17, the impact of Wi-Fi transmissions on the DSRC system performance can become negligible. However, we see in Chapter 4 (and as reported in [189]) that because the authors in [187] use IEEE 802.11a compliant devices for studying the coexistence performance, frame aggregation (which was introduced to Wi-Fi in IEEE 802.11n) is neglected. As a result, the real impact of Wi-Fi devices on DSRC system performance is worse, and that AIFS values on the order of 100 must be used by Wi-Fi devices to adequately protect the performance of DSRC systems.

### 3.3.2 Open Research Problems

It must be noted that with the new FCC NPRM on the 5.9 GHz ITS band [24], co-channel coexistence between Wi-Fi and DSRC is no a concern in the US. However, the technology of choice for V2X communications in Europe and other regions of the world remains uncertain (as noted in Sec. 2.1.2). Consequently, several research problems can still arise between DSRC and Wi-Fi systems, if DSRC is adopted as the V2X RAT and Wi-Fi devices are allowed to coexist with DSRC systems. We list some of these challenges below.

- Some of the proposed coexistence solutions, such as the sense and vacate mechanism in the US [183] and the DAV mechanism in Europe [48], may starve the Wi-Fi users operating in the shared spectrum. For instance, in dense urban scenarios, a large number of vehicles enabled with DSRC modules may render the shared channel of little use for Wi-Fi devices if they were to vacate the channel for 10 seconds every time a DSRC node is detected. Granted, the primary objective in any coexistence scenario

is to protect the operational integrity of the primary users of the spectrum. However, an equally important objective in allowing coexistence between two wireless systems in the first place is to allow for meaningful use of the spectrum by secondary/unlicensed devices. Thus, in order to enable any meaningful coexistence between DSRC and Wi-Fi systems, if such a scenario is to arise in the future, more suitable coexistence mechanisms are desirable.

- Conservative coexistence mechanisms can provide adequate protection to DSRC users but may limit spectrum access opportunities to the Wi-Fi users. The impact of spectrum sharing (between DSRC and Wi-Fi) on the performance of Wi-Fi systems needs to be studied thoroughly to understand the usability of the shared spectrum by Wi-Fi systems.
- If coexistence mechanisms based on leveraging the similarities between DSRC and Wi-Fi MAC protocols are to be adopted, change of suitable parameters in the current Wi-Fi standards (such as the Wi-Fi IFS, as suggested in [106, 187]) can be further explored. Such mechanisms can potentially enable harmonious coexistence between DSRC and Wi-Fi, without the necessity of using conservative backoff mechanisms at Wi-Fi transmitters.

## 3.4 Coexistence of C-V2X and Wi-Fi

In contrast to DSRC–Wi-Fi coexistence, the coexistence between C-V2X and Wi-Fi has not been well investigated. This subject has only been touched upon in [10]. It must be noted that mechanisms developed for DSRC and Wi-Fi coexistence cannot be re-used for C-V2X and Wi-Fi coexistence because C-V2X uses a considerably different MAC protocol from Wi-Fi. If C-V2X is used to provision V2X applications, solutions for secondary Wi-Fi operations need to be re-designed with the MAC protocol of C-V2X taken into consideration. Ideally, coexistence mechanisms must be agnostic to the choice of V2X technology. However, considering the differences in MAC protocols of DSRC and C-V2X, a unified coexistence mechanism may be improbable. Nevertheless, mechanisms must be at least forward compatible, i.e., any coexistence mechanism developed for C-V2X–Wi-Fi coexistence must also be compatible with NR V2X–Wi-Fi coexistence.

## 3.5 Coexistence between V2X Technologies

### 3.5.1 Coexistence between IEEE 802.11p and IEEE 802.11bd

802.11bd considers scenarios where coexistence between 802.11p and 802.11bd devices is desired. In scenarios where 802.11p and 802.11bd devices operate nearby, 802.11bd must

support two types of operations: (i) backward compatibility, and (ii) coexistence. Coexistence, as defined by the TGbd, differs from backward compatibility in that the former does not require 802.11p devices to decode 802.11bd frames, but only to detect 802.11bd transmissions as valid 802.11 frames and defer channel access.

Coexistence between 802.11p and 802.11bd devices is desirable when the transmitted messages correspond to 802.11bd-specific use cases. Consequently, 802.11p devices need not decode such messages. The TGbd proposes to achieve coexistence by manipulating the frame headers. For example, the frame format shown in Fig. 3.2 can be used by 802.11bd devices to transmit a particular frame intended only for other 802.11bd (and not 802.11p) devices. Legacy devices receiving this frame will identify the channel as *Busy* and defer channel access after decoding the legacy fields, i.e., Legacy Short Training Field (L-STF), Legacy Long Training Field (L-LTF), and Legacy Signal (SIG) fields.


Figure 3.2: Frame format for 802.11p–802.11bd coexistence.

### 3.5.2 Coexistence between C-V2X and NR V2X

Vehicles equipped with C-V2X are expected to hit the roads soon [118]. Considering that vehicles typically have a life-span of one or more decades [190], NR V2X is likely to have to coexist with C-V2X. However, NR V2X is not backward compatible with C-V2X [117]. This incompatibility stems from, among other factors, the use of multiple numerologies in NR V2X. A C-V2X device operating at 15 kHz sub-carrier spacing, cannot decode messages transmitted using the 30 or 60 kHz spacing. Newer vehicles will, thus, be equipped with modules of both technologies, i.e., C-V2X and NR V2X, making it imperative to design effective coexistence mechanisms [117].

For C-V2X and NR V2X coexistence, the NR V2X study item [117] considers only the "not co-channel" scenario, i.e., a scenario where C-V2X and NR V2X operate in different channels. Two approaches can be used for such non-co-channel coexistence [191]: i) frequency division multiplexing (FDM), or ii) time division multiplexing (TDM). Note that the term TDM is somewhat misleading in this context because not only are C-V2X and NR V2X resources orthogonal in time, but they are also orthogonal in frequency.

*FDM approach for coexistence:* In this approach, transmissions on two RATs can overlap in time. This approach is advantageous because there is no need for tight time synchronization between the C-V2X and NR V2X modules. However, despite the use of two different radios (one for C-V2X and another for NR V2X), if the assigned channels are adjacent or are not sufficiently far apart, leakage due to out-of-band emissions from one radio terminal will impair the reception at the other radio terminal. Furthermore, if the two RATs operate in the same band (e.g. 5.9 GHz ITS band), the total power radiated by the vehicle may be

restricted by regulatory limits and may have to be split across the two RATs, affecting the QoS requirements of V2X applications. Adjustment of the transmit power across the two RATs can take the packet priorities into consideration [192]. For example, if the NR V2X packet has a higher priority, then the transmit power of C-V2X can be lowered such that the total radiated power is within regulatory limits.

*TDM approach for coexistence:* In this approach, transmissions on the two RATs occur in different channels *and* at different time instants. The advantage of this approach is that the maximum permissible transmission power can be used by both technologies because only one interface transmits at any given time. Furthermore, there is no leakage across channels. However, the TDM approach is disadvantageous for latency-critical use-cases as the NR V2X interface may be *off* while a latency-sensitive packet is generated at the vehicle. Additionally, the TDM approach puts severe restrictions on time synchronization between C-V2X and NR V2X [193]. Further, if the TDM approach is used when the C-V2X and NR V2X channels are adjacent, due to the half-duplex problem when one RAT transmits (say NR V2X), the other RAT (C-V2X) will be unable to perform sensing for that duration, which will affect the performance of its (C-V2X) sensing-based resource reservation algorithm.

### 3.5.3 Coexistence between DSRC and 3GPP-based V2X Technologies

With DSRC and C-V2X as the two major developed RATs, and their corresponding evolutions—IEEE 802.11bd and NR V2X—underway, regional regulators and automakers have different choices to provision V2X communications in vehicles. While some automakers have committed to the use of DSRC in their vehicles [194], others prefer C-V2X [118]. C-V2X and DSRC are not compatible with each other. Thus, if some vehicles use DSRC and others use C-V2X, these vehicles will be unable to communicate with each other—a scenario where the true potential of V2X communications cannot be attained. To address this, some proposals such as [195] suggest that, at least within a given geographical region, regulatory agencies must permit only one V2X technology (either DSRC or C-V2X) to operate in a vehicle[5].

## 3.6 Coexistence between Heterogeneous Wi-Fi Technologies

WLAN deployments have become heterogeneous due to devices operating with different bandwidth configurations (ranging from 5 MHz to 160 MHz) and employing different PHY and MAC layer techniques. Early Wi-Fi devices (802.11b) were deployed in the 2.4 GHz band. The scarcity of spectrum in the 2.4 GHz band has led to the development of Wi-Fi

[5]This does not preclude simultaneous use of DSRC/802.11bd or C-V2X/NR V2X.

devices operating in the 5 GHz bands and now also in the 6 GHz bands. Today, the 802.11a, 802.11n, and 802.11ac devices operate in the $5.25 - 5.35$ GHz and $5.47 - 5.75$ GHz bands, while 802.11ax devices are likely to be adopted in mainstream wireless devices soon.

As we in this section, several coexistence problems arise because of dissimilarities in the bandwidth configurations used by Wi-Fi devices. Note that the current channelization in the 5 GHz band is based on 20 MHz channel widths with non-overlapping channels (unlike 2.4 GHz). However, with devices operating on different channel widths, a partial overlap between different devices becomes inevitable, particularly in dense deployment scenarios. Furthermore, although IEEE 802.11ax devices will be the first set of Wi-Fi devices that will be allowed to operate in the 6 GHz bands, in the future, these problems are likely to occur in the 6 GHz bands, too.

In this section, we discuss coexistence issues arising between different classes of Wi-Fi devices in the 5 GHz bands. We identify three key coexistence issues in inter Wi-Fi coexistence, which are described next.

### 3.6.1 Coexistence between DCF and EDCA devices

IEEE 802.11a devices use DCF as the channel access mechanism, while 802.11n and 802.11ac devices use the EDCA mechanism for channel access. The fundamental difference between DCF and EDCA is that while APs deploying DCF treat traffic to and from all clients with the same priority, EDCA divides traffic into four ACs — Background (BK), Best Effort (BE), Video (VI), and Voice (VO) — and prioritizes traffic from these classes differently. This differentiation is carried out by using different values of the contention window and AIFS for each class. The AIFS and contention window of DCF devices and different classes of EDCA are shown in Table 3.3. Naturally, stations using smaller values of AIFS have a higher priority than those using larger values of AIFS.

Table 3.3: Channel access parameters for DCF and EDCA

| **Access Category** | **CWmin** | **CWmax** | **AIFSN** |
|---|---|---|---|
| DCF | 15 | 1023 | 2 |
| Background (BK) | 15 | 1023 | 7 |
| Best Effort (BE) | 15 | 1023 | 7 |
| Video (VI) | 7 | 15 | 2 |
| Voice (VO) | 3 | 7 | 2 |

Since DCF devices (802.11a) and EDCA devices (802.11n/ac) operate in the same frequency band, fairness issues arise. From Table 3.3, it is clear that in a heterogeneous network comprising of DCF devices and different EDCA service classes, VI and VO traffic will have the highest priority, while DCF, BK, and BE traffic have similar priorities. Since the CWmin and CWmax values for VI and VO traffic classes are small, the presence of a large number

of DCF (or even EDCA) devices can lead to poor QoS due to excessive collisions [196]. The coexistence of DCF and EDCA devices has been extensively studied in the literature. The coexistence between EDCA and DCF devices has been a well-investigated research problem. Although several solutions have been proposed to mitigate the impact of legacy devices on the newer generations of Wi-Fi devices, the inherent nature of the CSMA protocol continues to pose problems for coexistence. With the development of the 802.11ax standard that aims to improve per user Wi-Fi performance in extremely dense deployment scenarios, the study of the above coexistence problems can provide insights in the context of 802.11ax - legacy coexistence. We discuss coexistence between legacy Wi-Fi and 802.11ax devices in Sec. 3.6.3.

### 3.6.2 Coexistence between 20 MHz and 40/80/160 MHz devices

The IEEE 802.11a protocol provided support for only 20 MHz wide channels. The IEEE 802.11n standard [181] introduced the use of 40 MHz wide channels among several other features to increase the maximum PHY layer throughput from 54 Mbps in 802.11a to as high as 600 Mbps (with 40 MHz channel width, a short guard interval (SGI) and 4 spatial streams). The IEEE 802.11ac standard further increased the PHY layer data rate to a maximum of 2.34 Gbps (using 160 MHz, SGI, and 8 spatial streams)[6]. While the 802.11 family of standards have advanced to make use of sophisticated PHY and MAC layer techniques, the newer standards have continued to support backward compatibility to all existing 802.11 devices. Backward compatibility is considered essential for all Wi-Fi standards primarily due to the proliferation of legacy devices in home and enterprise networks.

Today, Wi-Fi devices are capable of using wide-bandwidth channels (40, 80, 160 MHz) to transmit packets. The objective of using wide bandwidth channels is to increase the achievable throughput. However, the presence of heterogeneous Wi-Fi devices in the same geographical area pose network management challenges. Deek et al. [198] have shown that naive channel assignments at 802.11n Wi-Fi APs in the presence of older devices can lead to a substantial reduction in performance. Intelligent channel assignment (for both 20 and 40 MHz APs) are essential for efficient utilization of the spectrum. The authors show the impact of transmissions from 20 MHz Wi-Fi devices on adjacent channel interference for 40 MHz systems. As the channel bandwidth of the Wi-Fi link increases, the same transmit power is spread across a larger bandwidth, which results in a decrease of 3 dB in power per subcarrier for a bandwidth increase by a factor of 2. This translates to a low Signal to Noise Ratio (SNR) at the intended receiver, resulting in the lowering of the PHY layer data rate. As a result, if a 20 MHz Wi-Fi device is located in the vicinity of a Wi-Fi receiver operating at 40 MHz, and the 20 MHz and 40 MHz channels are adjacent (in frequency), the out of band leakage from the 20 MHz transmitter leads to additional interference at the 40 MHz

[6] Although the 802.11n standard allows operation in the 2.4 GHz as well as the 5 GHz band, using 40 MHz channels in the 2.4 GHz band becomes infeasible due to the limited availability of spectrum and the presence of other unlicensed technologies, such as Bluetooth, ZigBee, microwave ovens, etc. [197]. Considering this, the 802.11ac standard allows operations only in the 5 GHz band.

receiver, and in the worst case can reduce the throughput of 802.11n system down to 50%. A similar phenomenon is expected for 80 MHz Wi-Fi systems.

It is also worthwhile to analyze the impact of a new AP on an existing network that uses wide-bandwidth channels. This problem has been studied in the context of 802.11ac networks. Zeng et al. [199] experimentally evaluate the performance of a Wi-Fi system using 80 MHz channels in the presence of 802.11a and 802.11n devices. The authors conclude that the impact on 802.11ac's performance depends on the sub-channel in which these older devices operate. If 802.11ac and older systems share the same primary channel, then the performance of both systems drops proportionally, as is expected in a CSMA based network. However, if the 802.11a/n device's primary channel[7] overlaps with any secondary channel of an 802.11ac system using an 80 MHz channel, then the 802.11ac link throughput drops drastically (even to 0 if the 802.11a signal is strong enough at the 802.11ac receiver). This drastic drop can be attributed to the different channel access mechanisms for primary and secondary channels in 802.11ac as described in Sec. 2.2.2. In this context, Zeng et al. [199] evaluate the performance of an 802.11ac transmitter operating in the SCA mode. It is clear that if any 802.11a device operates on one (or more) of the secondary channels of the 80 MHz wide channel, the probability that the entire 80 MHz channel is available diminishes, particularly in dense deployment scenarios. Moreover, every time the secondary channel is sensed busy, the Wi-Fi backoff mechanism is repeated before trying to transmit the packet again. This leads to severe degradation of 802.11ac's performance. This coexistence issue has also been studied in [200, 201], where similar findings are reported.

Another possible reason for the significant degradation in 802.11ac's performance when coexisting with older Wi-Fi systems is the asymmetry between the coexisting Wi-Fi systems in terms of the ability to decode preambles. When 802.11a systems operate in the secondary channel of 802.11ac, the 802.11ac transmitter can decode the preambles of the 802.11a systems (preamble detection: sensing sensitivity $-72$ dBm); however, the 802.11a systems cannot decode 802.11ac preambles since these preambles are transmitted only over the primary channel (energy detection: sensing sensitivity $-62$ dBm). This asymmetry puts 802.11ac systems at a disadvantage compared to 802.11a systems with respect to channel access opportunities. This issue can partially be alleviated by using the DCA mechanism for secondary channel access as described by Park in [200], where the author shows that DCA can outperform SCA by up to 85% in terms of network throughput.

Extensions to the DCA mechanism have also been proposed. Kim et al. [202] propose a virtual primary channel reservation extension to standard DCA that can achieve up to 10% higher throughput than standard DCA. Furthermore, although DCA improves 802.11ac performance as compared to SCA, some secondary channels could be left unutilized. For example, in Fig. 2.6, if the 802.11ac transmitter uses DCA, and senses the secondary channel-

[7]The notion of a primary channel exists only for 802.11n and 802.11ac systems using 40 MHz and 80 MHz channels. The only bandwidth configuration available at an 802.11a transmitter is 20 MHz. Thus, the primary channel and 20 MHz operating channel hold the same meaning for 802.11a devices.

2 busy, it transmits over 40 MHz bonded channel (primary + secondary channel-1). In 802.11ac, there is no provision to bond non-contiguous channels. Thus, even if secondary channel-3 is idle, it is left unutilized. This is because the current 802.11ac standard only allows bonding 40, 80, and 160 MHz channels. Thus, if secondary channel-3 is sensed busy, the 802.11ac transmitter transmits over 40 MHz bonded channel (primary + secondary channel-1) even though secondary channel-2 is idle and there are three contiguous idle channels. Stelter et al. [203] recommend that to maximize 802.11ac performance in the presence of 802.11a devices, transmitters should be allowed to bond 60 MHz channels (contiguous as well as non-contiguous) in addition to the existing 40 and 80 MHz bonding. The authors propose a receiver design towards this objective and using simulations, show that the resulting network throughput gain can be as high as 25%. It must be noted that with preamble puncturing being introduced in IEEE 802.11ax, this is indeed possible for Wi-Fi 6 devices.

The aforementioned studies analyzed 802.11ac performance when 802.11a devices operate in the secondary channels. However, even when the operating channel of 802.11a devices overlaps with the primary channel of 802.11ac, the 802.11ac system's performance drops. This phenomenon is due to two factors. First, since 802.11a devices communicate over narrower bandwidth, the transmission typically occurs at lower PHY layer data rates. As a result, when 802.11a devices gain access to the channel, they occupy the channel for a longer interval of time [204]. Second, while the 802.11a devices communicate over the primary channel, none of the secondary channels can be used by the 802.11ac transmitters since all Wi-Fi clients in the BSS expect to receive beacon signals and other control messages which are transmitted by the AP only in the primary channel. Fang et al. [205] propose a solution to address this issue, by adopting an approach wherein if the 802.11ac primary channel is occupied by an 802.11a device, the clients within the basic service set relay their transmissions to the AP over secondary channels. The authors show that using their proposed scheme, the overall network throughput can increase by up to 38%.

### 3.6.3 Coexistence between 802.11ax and legacy 802.11

IEEE 802.11ax is the latest 802.11 standard that is ratified. While previous 802.11 amendments have increased the PHY throughput using advanced techniques, the MAC layer protocols used have been fairly similar. Inefficiencies at the MAC layer form a major bottleneck in translating the high PHY throughput into high throughput at the application layer in real-world scenarios, particularly when Wi-Fi deployment is dense. The *IEEE Task Group ax* (TGax) was formed in 2014 to increase the MAC efficiency of densely deployed 802.11ax STAs with overlapping BSS in the presence and absence of legacy 802.11 STAs [206].

802.11ax introduces several modifications to the 802.11 MAC layer protocol, including the use of MU OFDMA in both the uplink and downlink, TF, Dynamic Sensitivity Control (DSC), etc. as noted in Sec. 2.2.2, to improve the MAC layer efficiency. The success of 802.11ax, to a large extent, will depend on the efficacy of such mechanisms in the presence

of legacy 802.11 devices, as well as the impact of 802.11ax devices on legacy devices and vice versa.

The DSC mechanism enables 802.11ax APs and STAs to adapt their carrier sensing threshold based on traffic conditions as opposed to fixed thresholds used until 802.11ac. The use of DSC has been shown to improve the performance of 802.11ax devices as well as aggregate system performance when the network consists of only 802.11ax devices [207, 208, 209]. However, in the presence of legacy devices, the impact of DSC on 802.11ax and legacy devices remains unclear. For example, using simulations, Son et al. [210] show that the impact of devices using DSC on the performance of legacy devices is not negligible, and in some cases, the legacy throughput may go down by as much as $70 - 80\%$. This finding is supported by Wang et al. [211], who attribute the drop in the legacy devices' performance to the unfairness caused by Transmit Opportunity (TXOP) rules set by the 802.11 standard[8]. Wang et al. propose an 802.11ah based solution to mitigate this fairness issue. On the contrary, Wikstrom et al. [212] show that in some situations, legacy throughput can improve by up to 10%. Thus, it is clear that the impact of the use of DSC in 802.11ax on legacy systems is highly use-case dependent. Moreover, the findings presented in [210, 211, 212] are exclusively simulation-driven, and thus are not entirely convincing. More comprehensive studies that include analytical evaluation and testbed experiments are needed to gain a better understanding of how the DSC mechanism impacts legacy devices.

The use of MU OFDMA in the uplink of 802.11ax is envisioned to enable multi-user transmissions by dividing the entire channel into multiple sub-channels (i.e., a contiguous or non-contiguous group of subcarriers), and assigning these sub-channels to different STAs. The performance analysis of MU OFDMA in 802.11ax has been carried out in [213, 214]. However, these papers consider an 802.11ax only network, and the performance of a heterogeneous network comprising of legacy and 802.11ax devices remains unclear at the moment. Furthermore, the use of MU OFDMA in uplink by STAs is likely to complicate the channel state assessment procedure. As described by Hedayat et al. in [215], an STA participating in uplink MU OFDMA could transmit less or no energy in some of the sub-channels of the channel used by the AP. As a result, a legacy STA present in its vicinity may determine that these sub-channels are idle, and start transmitting data frames, resulting in collisions at the 802.11ax AP. This can potentially degrade the performance of 802.11ax as well as legacy devices. This situation is referred to as the creation of *artificial hidden nodes* in 802.11ax [215].

### 3.6.4 Open Research Problems

Current Wi-Fi standards do not explicitly address the inter Wi-Fi coexistence problems. As a result, reactive mechanisms have been proposed in the literature to achieve coexistence

[8]This was introduced in IEEE 802.11e as a part of EDCA, and enabled transmitters with high-QoS traffic to continue channel access for a time duration up to TXOP.

between newer and legacy Wi-Fi systems. We argue that in the upcoming Wi-Fi standards, proactive steps can be taken to facilitate harmonious coexistence between current and future Wi-Fi standards. The following prominent research problems have been identified.

- It is well known that providing support to legacy devices results in the degradation of 802.11ax's overall performance. While the initial working documents on IEEE 802.11ax mention the need to provide backward compatibility and support to legacy devices, there are limited discussions on how the coexistence between 802.11ax and legacy Wi-Fi systems may impact 802.11ax's performance. This complex issue needs to be studied qualitatively as well as quantitatively.
- The use of trigger frames in scheduling multi-user transmissions is expected to have an impact on the performance of legacy systems, especially because whenever the MU OFDMA mode is in progress, legacy systems will have to cease their contention process. However, there have been no studies on this important problem. This problem needs to be better understood.
- The impact of using DSC on legacy performance and other 802.11ax systems needs to be investigated.
- In order to mitigate the artificial hidden nodes problem, Hedayat et al. [215] propose that the AP must assign sub-channels to different STAs in a manner such that each 20 MHz sub-channel has a minimum number of subcarriers so that any legacy device operating in the neighborhood can detect that all sub-channels are busy. The design of such a subcarrier division mechanism in a heterogeneous Wi-Fi network warrants further studies.

## 3.7 Coexistence between Unlicensed Cellular Technologies and Wi-Fi

### 3.7.1 Coexistence of LTE-U and Wi-Fi

There have been some controversies regarding the effectiveness of LTE-U in achieving harmonious coexistence with Wi-Fi devices. For example, in June 2015, Google argued against the usage of LTE-U in its White Paper [216]. There were several arguments made against using LTE-U in the unlicensed spectrum. For instance, as described in the CSAT procedure details, LTE-U devices start their transmissions at the beginning of every cycle without sensing the channel for other unlicensed devices' transmissions. Consequently, the beginning of every LTE-U transmission can potentially interrupt an ongoing Wi-Fi transmission. As a result, Wi-Fi frames during this interval are susceptible to erroneous reception. Moreover, such errors are likely to occur at the beginning of each CSAT cycle, thus resulting in the

lowering of the MCS used by the transmitting Wi-Fi devices. This can lead to a drastic reduction in Wi-Fi system performance.

Additionally, results of experimental investigations in [216] show that LTE-U is not equipped with an effective coexistence technique to handle scenarios in which LTE-U and Wi-Fi devices sense each other at moderate (below −62 dBm) signal levels. In August 2015, the Wi-Fi Alliance and National Cable & Telecommunications Association (NCTA) also raised opposition to the approval of LTE-U systems in the unlicensed bands without adequate testing, citing concerns that LTE-U operations could degrade the performance of existing Wi-Fi systems by 50% to 100% depending on network scenario [217].

In a rebuttal to these claims, Qualcomm [218] stated that results obtained from its field tests show that LTE-U coexists harmoniously with Wi-Fi regardless of whether LTE-U operates above or below Wi-Fi's energy detection level, with Wi-Fi DL data rate remaining the same in the presence as well as the absence of LTE-U transmissions. Qualcomm attributed this discrepancy in the results to the pessimistic and impractical technical assumptions made by the other studies [216, 219]. Moreover, tests conducted by Qualcomm used a realistic setup, including actual LTE-U equipment as opposed to signal generators used in Google's study.

### 3.7.2 Coexistence of LAA and Wi-Fi

Analysis and performance enhancement of LAA systems has received a lot of attention in the literature. An extensive survey of LAA and Wi-Fi coexistence has been carried out in [32]. Interested readers can refer to [32] and the references therein for more details on LAA Wi-Fi coexistence and corresponding deployment scenarios. In what follows, we discuss two primary directions of research followed in most papers on LAA Wi-Fi coexistence.

#### 3.7.2.1 Control of LAA backoff procedure

To achieve fair coexistence between LAA and Wi-Fi devices, one of the most critical issues is to determine how quickly an LAA device starts transmitting after sensing the channel idle. The transmissions could be immediate as in FBE-based LBT or based on a backoff mechanism as defined in LBE-based LBT. The design of an appropriate channel access mechanism is crucial towards LAA and Wi-Fi performance in this coexistence scenario.

In [220], Chen et al. propose a Markov Chain based model to characterize the performance of LAA as well as Wi-Fi devices and determine the downlink throughput for each set of devices. Moreover, the proposed model shows the effectiveness of using the LBT mechanism in terms of the impact of LAA transmissions on Wi-Fi performance. Downlink throughput for both, LTE and Wi-Fi systems, can be theoretically calculated in different coexistence scenarios (LAA and LAA, or LAA and Wi-Fi). Intra-system interference in LAA-LAA and LAA-WiFi as well as LAA-WiFi hidden terminal problems are analyzed by Lien et al. in [221]. Lien et

al. [221] also propose dynamic switching between scheduling-based access and random access scheme as an outcome of their model.

Three different Wi-Fi and LTE deployment scenarios, namely indoor, outdoor, and indoor/outdoor mixed scenarios are tested by Jeon et al. in [222]. It is observed that if WLAN BSSs are located indoors, the impact of LAA transmissions on WLAN performance is not severe. However, the performance of Wi-Fi devices suffers from non-negligible degradation in other cases. Besides the above-mentioned works, enhancements to the basic LAA mechanism have been proposed [223, 224, 225, 226, 227, 228, 229, 230]. An important objective of these works is to ensure fair coexistence in terms of Wi-Fi performance in the presence of LAA.

#### 3.7.2.2 Control of LAA sensing mechanism

Along with a careful design of the LAA back-off mechanism, the appropriate setting of the CCA threshold is also critical to LAA as well as Wi-Fi performance. Chai et al. [231] point out that there exists a subtle, yet critical, problem that arises due to the asymmetric channel access mechanisms employed by Wi-Fi and LTE technologies with the potential to degrade the performance of LAA as well as Wi-Fi users, with more impact on Wi-Fi's performance. Both, Wi-Fi and LTE transmitters, can use energy detection to detect signals stronger than $-62$ dBm. However, Wi-Fi devices can also perform preamble detection, which enables Wi-Fi transmitters to detect signals from other Wi-Fi transmitters that are larger than $-82$ dBm in signal strength. The performance of LAA, as well as Wi-Fi systems, is, thus, unclear when the signal strength at both devices is within the $[-82, -62]$ dBm range. Experimental results in [216, 231] show that when the strength of the LAA signal at the Wi-Fi transmitter and Wi-Fi signal at the LAA transmitter is in the $[-82, -62]$ dBm range, simultaneous packet transmissions can result in collisions in numerous situations since LTE and Wi-Fi cannot detect each other, resulting in a drop in throughput of LAA and Wi-Fi systems by up to 15% and 37% respectively.

To mitigate the above problem, a naive solution would be to lower the energy detection CCA threshold. However, this would lead to under-utilization of the channel due to the well known exposed-node problem. The authors in [231] argue that it is critical for LAA systems to homogenize its channel access mechanism with that of the incumbent Wi-Fi system by incorporating the latter's preamble detection and notification capabilities (such as the use of Wi-Fi CTS frame to reserve channel access for LAA transmissions). For more discussions on the setting of the CCA threshold in LAA transmitters, readers can refer [222, 232].

## 3.7.3 Coexistence of NR-U and Wi-Fi

### 3.7.3.1 Channel Access Protocol

Coexistence between IEEE 802.11ac and LAA in the 5 GHz bands has been extensively studied at the time of LAA standardization [10, 32]. Since IEEE 802.11ax/802.11be and NR-U are successors to IEEE 802.11ac and LAA, respectively, insights drawn from the 5 GHz coexistence studies can be leveraged to orchestrate efficient coexistence between Wi-Fi and NR-U (and potentially other future RATs), particularly in the greenfield 6 GHz spectrum. In what follows, we discuss the coexistence issues between Wi-Fi and NR-U in the 6 GHz bands.

The design of LAA emphasized ensuring that the introduction of an LAA network in the vicinity of existing Wi-Fi networks must not affect them any worse than another Wi-Fi network [101]. The most convenient manner in which this objective could be achieved was to design the MAC protocol of LAA similar to that of Wi-Fi. With this in consideration, LBT—which is fundamentally identical to CSMA/CA used by IEEE 802.11 devices—was chosen as the underlying MAC protocol for LAA. As the greenfield 6 GHz bands provide an opportunity to investigate and design coexistence mechanisms from the ground up, coexistence between unlicensed RATs in the 6 GHz bands need not consider the CSMA/CA-like LBT mechanisms as the baseline. Although such *modified* LBT-based mechanisms have been proposed in the literature (e.g., [233]), at the time of writing this paper the LBT mechanism used in Wi-Fi and LAA continues to be the baseline for 6 GHz operations. In what follows, we describe key considerations that will govern the performance of all unlicensed RATs operating and coexisting in the 6 GHz bands.

#### LBE v/s FBE

For more than two decades, Wi-Fi—the predominant WLAN technology—has used the Load Based Equipment (LBE) variant of LBT, which allows transmitters to contend for the medium as soon as the channel becomes idle. However, there exists another option of LBT—Frame Based Equipment (FBE), which is argued to yield superior performance—that allows unlicensed devices to contend for the channel beginning only at synchronized frame boundaries [234]. FBE is especially beneficial for NR-U networks because the frame intervals can be defined to be the same as the NR licensed carrier's slot boundaries. However, the NR-U work item [95] states that NR-U systems can use FBE LBT only in environments where the absence of Wi-Fi networks is guaranteed.

Fig. 3.3 shows the conceptual differences between LBE and FBE LBT as described in [235]. As shown in Fig. 3.3a, LBE LBT devices can contend for the channel as soon as the previous transmission ends and the channel becomes idle. However, Fig. 3.3b shows that FBE LBT devices must wait until the next frame interval for contention (and hence, transmission) even if a given transmission does not last until the end of a frame boundary. This implies that FBE LBT devices achieve maximum MAC efficiency when the transmissions last until the

end of each frame boundary. However, this may not necessarily be the case, depending on the size of the payload at the transmitter queue. Furthermore, it is important to note that while transmission duration in LBE LBT is limited only by regional regulations, it is the frame interval that limits the transmission duration in FBE LBT, i.e., each transmission must cease by the end of the current frame boundary.

FBE operations for the 5 GHz bands in Europe are defined by ETSI regulations in [236]. Although Fig. 3.3b shows that the contention occurs at the beginning of every frame interval, ETSI regulations specify an alternate version of FBE, where the contending devices perform fixed-duration CCA (category 1 or 2 LBT) towards the end of each frame interval [237, 238]. In this case, transmitting devices must restrict their maximum channel occupancy time (to 95% of the frame interval as per [236]) so that the end of each frame is idle. The duration of the frame interval can be between 1 and 10 msec. However, once declared, ETSI regulations permit the frame interval to be changed at most every 200 msec [236]. Lack of randomization in this version of FBE LBT, where all contending devices perform fixed-duration CCA at the end of each frame interval, makes it susceptible to persistent collisions and is suitable only if interference coordination schemes are used [238].

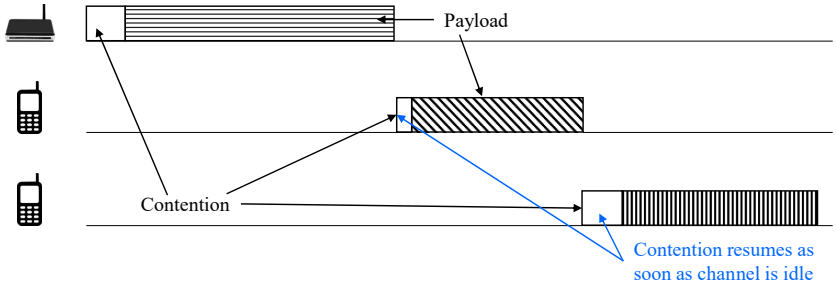


(a) Load Based Equipment. Devices contend for the channel as soon as the channel becomes idle.

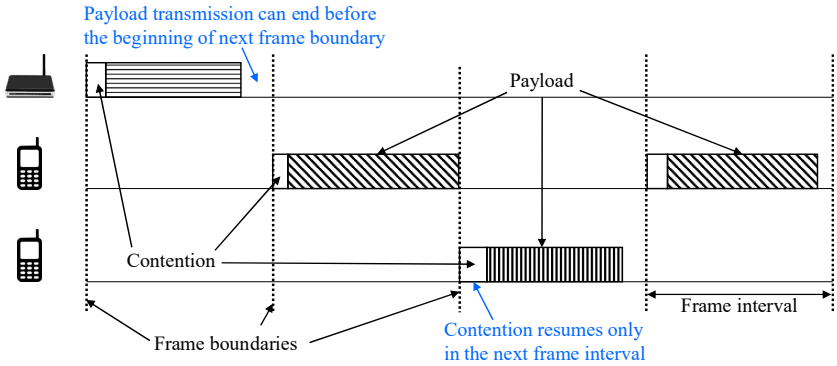


(b) Frame Based Equipment. Devices contend for the channel only at the beginning of a new frame.

Figure 3.3: LBE and FBE flavors of LBT.

It is well known that if LBE and FBE LBT devices coexist and operate on the same channel, FBE devices get a smaller share of the channel. This is because FBE devices must wait until

the next frame boundary, while LBE devices can gain access to the channel immediately after an ongoing transmission ends [238]. Thus, to ensure that LAA devices are not starved of channel access in the presence of Wi-Fi users, 3GPP adopted the LBE flavor of LBT in LAA. The NR-U work item, on the other hand, contains explicit provisions to define mechanisms for channel access protocols for FBE LBT, at least in environments where the absence of Wi-Fi networks can be guaranteed [95, 97]. It has been proposed that FBE operations in NR-U must be restricted to gNB-initiated channel occupancy time. This would imply that NR-U UEs cannot initiate uplink transmissions using FBE LBT and can transmit in the uplink only when the corresponding gNB wins access to the medium [239, 240].

Despite the challenges associated with FBE LBT, it is argued that synchronized access in FBE can yield better performance in comparison to LBE LBT systems [238]. If all unlicensed devices in the 6 GHz bands were to operate using FBE LBT, the spectral efficiency of unlicensed RATs could be increased. With this in consideration, reference [235] proposes to use FBE LBT across all unlicensed RATs for synchronized access in the 6 GHz bands. Based on the deployment scenario, it is shown that FBE LBT can improve the user-perceived throughput by 10-50%. FBE LBT yields performance gains due to the reduction of the hidden nodes problem [241]. Since all potential transmitters sense the channel at the same time, i.e., at the beginning of the synchronized frame intervals, the fraction of time during which collisions can occur is reduced and is limited to the start of each frame interval. Furthermore, when transmissions on the channel are synchronized, coordinated interference mitigation and suppression schemes can be leveraged so that multiple devices belonging to the same operator can transmit simultaneously, thereby increasing the spectral efficiency [242]. A critical factor against the use of FBE LBT, however, is that FBE systems require a global clock to have consistent frame boundaries across all unlicensed devices. Thus, even though FBE LBT is promising in terms of improved system performance, it is necessary to weigh this improvement against the added system requirement.

### Contention Parameters

LBE LBT and CSMA/CA, both require a device (with pending packets to transmit) to sense the channel and contend for it before initiating its transmission. If the channel is occupied, i.e., if there is an ongoing transmission, the contending device must wait until the channel is idle. Once the channel is idle, devices enter the well known *exponential back-off* phase, whereby the CSMA/CA or LBE LBT protocol is used (by Wi-Fi and NR-U devices, respectively) to contend for the channel. Interested readers can refer to references [10, 69] for more details on the exponential back-off protocol.

Values of CSMA/CA or LBE LBT contention parameters vary according to the priority of the packet at the contending device. These parameters include the minimum and maximum values of the Contention Window (CWmin and CWmax, respectively) and the fixed interval for which the channel must be sensed following an ongoing transmission (IFS for Wi-Fi and the defer time ($T_d$) for NR-U). The priority of transmissions is determined by the QoS requirements of the application that generates the packet. QoS requirements are specified in

terms of the worst-case latency and reliability requirements. A high priority packet has low worst-case latency and high-reliability requirements. Thus, for packets with higher priority, the wait time after the channel becomes idle (i.e., IFS or $T_d$) and the CWmin and CWmax values are smaller than those for low priority packets. Wi-Fi and NR-U, both classify packets into four access categories. In Wi-Fi, these categories are referred to as voice (VO), video (VI), best-effort (BE), and background (BK), in decreasing order of priority.

The contention parameters for the four access categories in Wi-Fi and NR-U are shown in Table 3.4. It must be noted from Table 3.4 that the wait times (i.e., IFS and $T_d$) and CW values for NR-U and Wi-Fi packets that belong to a given access category are the same. This ensures that Wi-Fi and NR-U devices are fair to each other in the probability of accessing the channel.

| **Access Category** | | **Wait Time ($\mu$s)** | | **CWmin** | | **CWmax** | | **TXOP (msec)** | |
|---|---|---|---|---|---|---|---|---|---|
| **Wi-Fi** | **NR-U** | **Wi-Fi (IFS)** | **NR-U ($T_d$)** | **Wi-Fi** | **NR-U** | **Wi-Fi** | **NR-U** | **Wi-Fi** | **NR-U** |
| VO | 1 | 25 | 25 | 4 | 4 | 8 | 8 | 2.080 | 2 |
| VI | 2 | 25 | 25 | 8 | 8 | 16 | 16 | 4.096 | 3 |
| BE | 3 | 43 | 43 | 16 | 16 | 1024 | 1024 | 2.528 | 8 or 10 |
| BK | 4 | 79 | 79 | 16 | 16 | 1024 | 1024 | 2.528 | 8 or 10 |

Table 3.4: Contention Parameters for Wi-Fi and NR-U.

### Transmission Duration

Contention parameters outlined in the previous subsection control the probability by which contending devices gain access to the channel. Ensuring that this probability is the same for Wi-Fi and NR-U devices, however, does not guarantee fair coexistence between NR-U and Wi-Fi in the shared spectrum. Once Wi-Fi or NR-U devices gain access to the channel, they can transmit uninterrupted (i.e., without contention) for a duration referred to as the TXOP. This parameter, again, varies with the access category of packets. Observe from the TXOP values of the different access categories of Wi-Fi and NR-U in Table 3.4 that NR-U devices can transmit unhindered for a longer duration than Wi-Fi devices. This gives NR-U devices an undue advantage in terms of the average observed throughput.

It has been previously argued that Wi-Fi and LAA devices must use the same TXOP values for any given access category to ensure air-time fairness. For example, reference [243] shows that when both LAA and Wi-Fi devices coexist, Wi-Fi devices get a smaller share of the channel due to differences in TXOP used by LAA and Wi-Fi devices. Simulation results in [244] show that a TXOP duration of 6 msec can achieve fair coexistence between Wi-Fi and NR-U devices. The TXOP values for different access categories to be used in the 6 GHz bands are likely to be standardized by ETSI BRAN. However, it is critical that regardless of the chosen TXOP values, for a given access category, they must be the same for Wi-Fi and NR-U devices to ensure fair coexistence.

#### 3.7.3.2 Detection of Wi-Fi and NR-U signals

**Energy Detection v/s Preamble Detection**

A key consideration that will govern the efficacy of coexistence between NR-U and Wi-Fi devices in the 6 GHz bands is the choice of the mechanism by which Wi-Fi 6 and NR-U devices will detect each other as well as the corresponding detection threshold. Two possible mechanisms exist for the detection of wireless signals on the air—(i) energy detection, i.e., ED, and (ii) preamble detection (PD). In ED, devices measure the energy locally and determine channel availability. If the measured energy is greater than a predetermined ED threshold, the channel is declared busy. Otherwise, the channel is considered idle and devices can begin to contend for the channel. PD, on the other hand, requires that devices must transmit and detect a known preamble signal. Upon reception of this preamble, its energy is compared against the PD threshold. The channel is declared busy if the energy is greater than the PD threshold and idle otherwise.

In the 2.4 GHz and 5 GHz bands, Wi-Fi devices use PD to detect other Wi-Fi signals. To ensure backward compatibility toward all Wi-Fi generations, IEEE 802.11n/ac/ax devices transmit (and decode) the IEEE 802.11a preamble. On the other hand, ED is used to determine the occupancy of the channel by non-Wi-Fi devices (such as ZigBee in the 2.4 GHz band and LAA in the 5 GHz bands). Since LAA was designed at a time when Wi-Fi devices were widely deployed, its designers had two options—(i) adopt the IEEE 802.11a preamble, i.e., transmit this preamble at the beginning of each LAA frame and decode the IEEE 802.11a preamble to infer channel availability, or (ii) use energy detection to detect both LAA and non-LAA signals. Eventually, 3GPP decided to use the latter approach. However, the NR-U work item [95] considers extending the detection mechanism beyond ED to include detection of IEEE 802.11a/ax preamble or existing NR signals.

At present, there is no consensus on the choice between ED and PD as the detection mechanism for coexistence between Wi-Fi and NR-U devices in the 6 GHz bands. While some contributions prefer ED [245, 246, 247, 248], others such as [249, 250, 251, 252] prefer PD. Based on the discussions presented in these contributions, there are several arguments in favor of both mechanisms.

ED is simple to implement in NR-U and Wi-Fi devices. Additionally, it is argued that ED is technology-neutral in that NR-U (and possible future RATs) need not possess the ability to transmit and decode an arbitrary preamble signal [248]. PD across different coexisting RATs, on the other hand, necessitates an agreement on which preamble to use. References [250, 251, 252] have argued that the IEEE 802.11a preamble, which is used by all Wi-Fi devices in the 5 GHz bands, is suitable for enabling fair coexistence between NR-U and Wi-Fi devices. This implies that NR-U devices must be equipped with capabilities to transmit and decode 802.11a preambles, while no modifications will be required at 802.11ax devices. It is claimed in [252] that since typical mobile devices are likely to have access to both NR-U and Wi-Fi modules, 802.11a preambles can be decoded in real-time using the collocated Wi-Fi module.

| Mechanism | Pros | Cons |
|---|---|---|
| Energy Detection | - Simple, low-cost implementation<br>- Technology Neutral<br>- ED with high threshold can yield improvements through spatial reuse | - No power saving feature<br>- Not suitable for low thresholds<br>- ED with high threshold can worsen the hidden node problem |
| Preamble Detection | - Reliable at low detection threshold<br>- Power saving through virtual carrier sensing<br>- New, efficient common preamble can be defined | - More complex implementation than ED<br>- Specification of a common preamble will be time-consuming<br>- Low threshold in PD exacerbates the exposed node problem |
| Hybrid (ED + PD) | - Greater flexibility | - Complex implementation<br>- Performance in dense scenarios is questionable |

Table 3.5: A comparison of Energy Detection and Preamble Detection for coexistence between unlicensed RATs.

Reference [253], on the other hand, argues for a fresh design of a common preamble that can be transmitted and decoded by both NR-U and Wi-Fi devices. The principal merit of this choice is that the 802.11a preamble contains several fields that are unnecessary from the point of view of NR-U and Wi-Fi coexistence. Therefore, a common preamble that contains only the minimum information required to enable coexistence is desirable for maximizing spectral efficiency.

The advantage of PD lies in the fact that upon decoding the preamble, the duration of the transmission can be inferred. This mechanism, referred to as virtual carrier sensing in Wi-Fi [69], is important in power saving [252]. Thereafter, the sensing device can enter the sleep mode for the remainder of transmission duration and resume contention for the channel once the channel is known to be idle. Such power saving mechanisms are not possible with ED-based coexistence, where sensing devices must continuously monitor the channel for any activity. In addition to power saving, it is argued in [252] that for detection thresholds lower than -72 dBm, energy detection is often unreliable, while preamble detection can reliably be used for threshold values up to -82 dBm.

An alternative to fixed use of ED or PD is to use a hybrid solution, whereby devices use both ED and PD for channel access. This approach is similar to how Wi-Fi currently operates in the 5 GHz bands—detect Wi-Fi signals at -82 dBm and non-Wi-Fi signals at -62 dBm. Such schemes have also been proposed for LAA devices operating in the 5 GHz bands [254]. In the 6 GHz bands, this would extend as follows: Wi-Fi and NR-U devices sense inter-RAT transmissions using ED, which is technology-neutral. However, intra-RAT transmissions can be detected using technology-specific preambles, i.e., PD. The benefit of this approach is that individual RATs can optimize their performance by adapting spatial reuse through dynamic adaptation of the PD threshold. This spatial reuse technique is widely considered in IEEE

802.11ax [53]. However, contributions against this proposal, such as [248], have argued that the sole benefit of using this hybrid detection approach, i.e., flexibility to individual RATs and resulting performance gains, is questionable in dense deployment scenarios.

The merits and demerits of ED, PD, and a hybrid approach are outlined in Table 3.5.

**Choice of the Detection Threshold**

The detection threshold used by Wi-Fi and NR-U devices to detect and defer to each other is one of the most contentious topics being debated at the IEEE Coexistence SC and ETSI BRAN meetings [255]. Wi-Fi devices in the 2.4 GHz and 5 GHz bands use different detection thresholds to detect other Wi-Fi and non-Wi-Fi signals. The former threshold is set to -82 dBm, while the latter is -62 dBm. During LAA design, there was considerable debate over the choice of detection threshold used by LAA devices to detect Wi-Fi signals. This was a contentious issue because of two reasons, (i) at the time of LAA design Wi-Fi devices were already ubiquitous in home and enterprise wireless networks with millions of users worldwide; on the other hand, LAA was a new technology that could potentially negatively affect the performance of existing Wi-Fi users, and (ii) it was not possible to change the detection thresholds across the millions of already deployed Wi-Fi APs and STAs so that LAA and Wi-Fi could detect each other using the same threshold. Eventually, it was decided that LAA devices would use a fixed energy detection threshold (-72 dBm) to detect both LAA and non-LAA signals [245].

The argument used while adopting the -72 dBm threshold for LAA devices in the 5 GHz bands is no longer valid in the greenfield 6 GHz bands. Furthermore, the first two technologies to operate in these bands on an unlicensed basis, i.e., IEEE 802.11ax and NR-U, are still undergoing (albeit final stages of) design. Thus, the detection threshold for the 6 GHz bands can be decided after thoroughly studying its impact on the performance of Wi-Fi and NR-U networks, especially taking into consideration the nature of applications to be supported by these RATs.

Detection mechanisms and thresholds used in the 5 GHz bands are known to be unfair toward one technology or the other (based on the network topology). However, some contributions argue Wi-Fi and NR-U operations in the 6 GHz bands must adopt the *status quo* in terms of these mechanisms/thresholds from the 5 GHz sharing rules [256]. Nevertheless, a vast majority of contributions to the IEEE Coexistence SC and ETSI BRAN have argued for a technology-neutral and common threshold to be used in the 6 GHz bands [244, 245, 247, 257]. Despite this, however, there is no consensus on the choice of an appropriate detection threshold. Reference [244], for example, argues that a common ED threshold of -82 dBm improves the performance of both Wi-Fi and 3GPP-based networks. However, a different common threshold (-62 dBm) is shown to be more effective for both NR-U and Wi-Fi performance in [246], while references [248, 252, 257] argue for the use of -72 dBm.

In addition to the aforementioned references that advocate fixed thresholds, some contributions have argued for adjustable threshold values so that interference can be mitigated

in real-world deployment scenarios [251]. Reference [252] proposes a hybrid solution where a common detection threshold is used across different RATs (i.e., for NR-U's detection of Wi-Fi signals and vice-versa). Each RAT can then use adaptive thresholds for intra-RAT detection (e.g., detection of Wi-Fi signals at a Wi-Fi transmitter) to maximize their respective performance using spatial reuse. In this approach, a lower threshold (e.g., -82 dBm) could be used to detect intra-RAT transmissions, while a higher threshold (e.g., -62/-72 dBm) can be used for detecting inter-RAT (i.e., Wi-Fi detection at NR-U transmitters and vice-versa) transmissions.

The references mentioned above present their arguments with an underlying assumption that NR-U and Wi-Fi devices both use LBT-based channel access protocols. However, Wi-Fi 6 devices can also use MU OFDMA for scheduled uplink and downlink transmissions. In this case, although the AP must first sense and contend for the channel for transmitting the scheduling Trigger Frame, uplink transmitter STAs do not need to contend for the channel. Furthermore, the presence of more than one active transmitter at a time (as is the case in uplink MU OFDMA transmissions) reduces the probability of transmitting devices being hidden to sensing devices. Thus, the implications of a particular detection threshold on the performance of Wi-Fi 6 and NR-U in such coexistence scenarios could be different in comparison to single user Wi-Fi transmissions as noted in [258].

### 3.7.4 Open Research Problems

Coexistence between unlicensed technologies is an open problem in the 5 GHz as well as 6 GHz bands. On one hand, in the 5 GHz bands, these cellular-based technologies are constrained by the MAC protocol of Wi-Fi. On the other hand, however, the greenfield 6 GHz bands provide an opportunity to design coexistence mechanisms that are optimized from the point of view of not only Wi-Fi devices but also the cellular-based unlicensed technologies. Thus, in what follows, we outline the research challenges with a focus on coexistence between unlicensed cellular technologies (particularly NR-U) and Wi-Fi in the 6 GHz bands.

#### 3.7.4.1 Analysis and Optimization of Channel Access Parameters

Traditionally, Wi-Fi networks have been unable to satisfy the QoS requirements of high reliability and latency-sensitive applications. This inability stems in part from the unlicensed (and hence, non-guaranteed) nature of the wireless spectrum on which Wi-Fi networks operate. However, the fundamental cause of this problem is the tail (i.e., worst-case) access latency encountered due to Wi-Fi's CSMA/CA-based channel access procedure [259, 260]. With the likely introduction of MLA in IEEE 802.11be and the availability of a large number of *links* in the 6 GHz bands to contend on, the tail latency in IEEE 802.11be is likely to be substantially lowered. A significant research problem, therefore, is to quantitatively assess

the latency gains of MLA in IEEE 802.11be over traditional single-link Wi-Fi networks. There is rich literature on the latency and throughput analysis of IEEE 802.11 networks (e.g., [259, 260, 261, 262, 263, 264], and the references therein). A vast majority of these works rely on one-dimensional or multi-dimensional Markov Chain models of the Wi-Fi MAC protocol. Naturally, such models can be extended to study the behavior of MLA in different traffic conditions. Such studies can provide an accurate assessment of whether future Wi-Fi devices (with features like MLA) can reliably enable the emerging QoS-sensitive applications in the 6 GHz bands.

An additional research problem that will likely gain traction in the upcoming years is the optimization of the channel access parameters used by the LBT-based MAC protocols in NR-U and Wi-Fi. At the time of writing this paper, the contention parameters outlined in Table 3.4 are likely to be reused in the 6 GHz bands. Here, the problem arises in the coexistence of the emerging QoS-sensitive applications (such as AR/VR) with the existing ones (such as voice and video traffic). Whether the emerging class of wireless applications can be supported reliably using traffic classes that were originally designed for voice and video traffic remains to be seen. If the channel access parameters for these existing traffic classes are deemed insufficient in supporting such applications, like several other aspects in the 6 GHz bands, channel access parameters can be optimized without encountering backward compatibility hurdles. If this were to be true, the Markov Chain-based analytical models (as noted above [259, 260, 261, 262, 263, 264]) can be used in the optimization of 6 GHz bands-specific channel access parameters.

#### 3.7.4.2 Detection Mechanism and Threshold for NR-U and Wi-Fi Coexistence in the 6 GHz Bands

Perhaps the most significant parameter influencing the coexistence performance of NR-U and Wi-Fi is the detection threshold used by Wi-Fi and NR-U devices to detect and back-off to each other. While this subject has been widely discussed (as discussed in Sec. 3.7.3.2), there is no consensus on the choice of an appropriate value for the detection threshold. The chosen detection threshold not only has a direct impact on the performance of the two RATs when they coexist but also has implications on which mechanism (i.e., energy detection or preamble detection) is eventually chosen by NR-U and Wi-Fi devices to detect each other. For example, if the detection threshold selected is too low (such as -82 dBm), the only suitable mechanism by which Wi-Fi and NR-U devices can detect each other is preamble detection. On the other hand, if the chosen detection threshold is higher (such as -72 dBm or -62 dBm), energy detection can be reliably used for NR-U and Wi-Fi signal detection.

If preamble detection is used as the detection mechanism in the 6 GHz bands, an additional problem emerges—a suitable common preamble must be chosen for the 6 GHz bands. The criteria for the design of such a preamble are: (i) The preamble must (ideally) convey information on the duration of the following packet. This, as discussed in Sec. 3.7.3.2, can

increase the energy efficiency of devices by enabling devices to *sleep* for the remainder of the packet duration once the duration is decoded; (ii) The accuracy of detection of the preamble must be high across both technologies, i.e., NR-U and Wi-Fi; (iii) The complexity of detection of the preamble at Wi-Fi and NR-U devices, given their dissimilar and non-compatible PHY layers, must be low; (iv) The preamble must be spectrally efficient, i.e., it must consume the minimum possible amount of resources while carrying the minimum necessary information for enabling efficient coexistence. This implies that technology-specific information, such as those present in the IEEE 802.11 preamble, must be kept at a minimum while designing a new common preamble. (v) In an ideal scenario, the preamble must be forward-looking, i.e., the aforementioned factors must also hold for a potentially new RAT that may operate in the 6 GHz bands in the future.

To determine a suitable detection threshold that enables fair and efficient coexistence between NR-U and Wi-Fi, the impact of the chosen threshold on the system-wide performance of the two RATs must be studied. In doing so, it must be noted that small-scale experimental studies can often lead to misleading conclusions [101]. Thus, the coexistence of NR-U and Wi-Fi must be studied using rigorous and extensive analytical models, simulation platforms, and large-scale experiments. The foundation for such studies has already been laid out during the study of LAA–Wi-Fi coexistence in the 5 GHz bands [101, 265, 266]. Such analytical models, supplemented by experimental and simulation results, must be extended to study the 6 GHz coexistence problem.

#### 3.7.4.3 Impact of MU OFDMA on NR-U and Wi-Fi Coexistence

A key distinguishing factor between the LAA–Wi-Fi and the NR-U–Wi-Fi coexistence scenarios is that during the former study, 802.11ac was the default Wi-Fi standard under consideration. Today, on the other hand, Wi-Fi 6 is the new and upcoming Wi-Fi standard, which introduces MU OFDMA for increased MAC layer efficiency. The use of MU OFDMA in Wi-Fi 6, especially in the uplink, introduces several similarities in the operations of Wi-Fi and NR-U. For example, for downlink transmissions, the NR-U gNB and the Wi-Fi 6 AP contend for channel access and transmit packets to the designated UEs/STAs on specific RBs/RUs. On the other hand, for uplink transmissions, the NR-U gNB/Wi-Fi 6 AP will first contend for the channel and schedule a certain number of RBs/RUs to specific UEs/STAs. OFDMA-based downlink transmissions in Wi-Fi are similar to CSMA/CA-based single user transmissions in that the Wi-Fi AP contends for the channel and occupies the entire channel bandwidth. However, in the case of uplink OFDMA transmissions, there is likely to be more than one active transmitter transmitting simultaneously on orthogonal frequency resources. As a result, for a given detection threshold, the probability that at least one of the uplink Wi-Fi transmitters is within the sensing range of NR-U devices increases, and the probability of Wi-Fi devices being hidden to NR-U devices diminishes. Furthermore, transmit power control, which was optionally used in legacy Wi-Fi systems is introduced as a mandatory feature for uplink MU OFDMA transmissions in Wi-Fi 6. As a result, the

use of MU OFDMA in Wi-Fi, especially for uplink transmissions, is likely to have different implications on the choice of the optimal detection threshold.

From the above discussions, it is clear that the impact of MU OFDMA on NR-U–Wi-Fi coexistence is another critical subject worthy of investigation. Intuitively, it is expected that the reduced hidden node probability due to a greater number of simultaneously active transmitters will improve the system performance of both Wi-Fi and NR-U. This intuition must be verified using rigorous models, and simulation, and experimental studies. Again, the analytical models developed for LAA–Wi-Fi coexistence can serve as the starting point for NR-U–Wi-Fi coexistence. For example, reference [266] studies the coexistence performance of LAA and 802.11ax for both single user and MU OFDMA transmissions. Such models can be extended to study the 6 GHz coexistence problem. Furthermore, if MU OFDMA is found to be more suitable in promoting fair and efficient coexistence in the 6 GHz bands, the 6 GHz bands provide a unique opportunity where single user transmissions can indeed be disabled (since there are no legacy Wi-Fi operations in these bands).

# Chapter 4

# Coexistence of Dedicated Short Range Communications and Wi-Fi

## 4.1 Introduction

The FCC's band sharing NPRM in 2013 [40] proposed to create a spectrum sharing scenario between DSRC and Wi-Fi in which the two access technologies would coexist harmoniously with a minimal negative impact on each other (under ideal circumstances). In this case, DSRC would be the incumbent system and Wi-Fi would be the secondary system. The main objective of this plan was to assign more spectrum to Wi-Fi users in order to accommodate additional wide-bandwidth channels, and in turn, to enhance support for high data-rate applications.

In August 2013, the IEEE 802.11 Regulatory Standing Committee created a subcommittee called the *DSRC Coexistence Tiger Team* to explore possible band sharing techniques that would enable harmonious coexistence of DSRC and Wi-Fi, and also help inform the regulatory process. In March 2015, the Tiger Team published their final report [182] that summarizes the issues surrounding the proposed band sharing ideas discussed in the group. Two key proposals are described in the report. In the first proposal, it is suggested that spectrum sharing is enabled by using the existing DSRC channelization and CCA in 10 MHz-wide channels [183]. This requires all Wi-Fi (and other unlicensed, if any) devices to be equipped with a new component to detect 802.11p preambles. This approach is similar to the Dynamic Frequency Selection (DFS) mechanism, and it requires that once a Wi-Fi device detects a DSRC preamble, the frequency band from $5850 - 5925$ MHz must be declared busy for 10 seconds. The second proposal, on the other hand, requires modifying the DSRC channelization scheme [49]. The proposal suggests limiting the safety-critical applications to operate only in the upper DSRC channels, which are not shared with Wi-Fi, while the non-safety applications operate in the lower channels, which are shared with Wi-Fi. However, the report stressed the need for further analysis, simulations, and field testing to determine an appropriate coexistence approach.

In this chapter, we present the findings from our in-depth study on the coexistence of DSRC and Wi-Fi. We study both, the impact of Wi-Fi on DSRC system performance as well the impact of DSRC on Wi-Fi system performance. According to our analysis, the rudimentary DFS-like technique discussed in the Tiger Team's report is an unnecessarily heavy-handed

approach that will result in unacceptably poor Wi-Fi performance when there is more than a modest density of DSRC nodes. In [106], Lansford et al. suggest potentially more effective and elegant approaches that warrant further study. Motivated by the discussions in [106], we propose coexistence techniques that rely on adjusting the IFS value of Wi-Fi. Unless stated otherwise, we use the terms 802.11ac and Wi-Fi, and 802.11p and DSRC interchangeably.

The main contributions of this work are listed below.

- To the best of our knowledge, the findings presented in this chapter represent results from one of the first systematic studies on the coexistence of DSRC and 802.11ac. Although the challenges of this spectrum sharing scenario were discussed in a few prior works (e.g., [60, 106, 187]), they provided only high-level discussions without concrete technical solutions based on rigorous analysis or simulations.

- We propose an analytical model that enables us to quantify the impact of Wi-Fi transmissions on DSRC's performance. Moreover, the proposed model provides valuable insights on how two key Wi-Fi parameters—IFS and sensing range—influence the performance of DSRC.

- We have validated the proposed analytical model by comparing the results derived from it with results obtained from extensive *network simulator-3* (ns-3) simulations. In our simulation model, we have implemented the *message expiration* feature, which is critical for obtaining high-fidelity simulation results. This feature enables us to simulate safety messages that have a limited lifetime, which means that they are dropped from the MAC layer queue when the expiration time is reached.

- We further validate the inferences derived from our simulation study using test-bed experiments. Based on our experimental findings, we show that under the current 802.11ac standard, not all of the Wi-Fi channelizations (i.e., channel and bandwidth combinations) in the U-NII-4 band—particularly the high bandwidth options (i.e., 40 and 80 MHz channels)—can be used by 802.11ac devices without causing significant interference to DSRC nodes.

- Under these channelization constraints, we propose a Real-time Channelization Algorithm (RCA) to maximize the throughput of Wi-Fi APs operating in the shared spectrum.

- We evaluate the effectiveness of the proposed RCA using a prototype implementation on commodity hardware. We also use simulations to validate our RCA in at-scale networks.

## 4.2 Related Work

In terms of optimizing Wi-Fi performance, dynamic channel bandwidth adaptation for Wi-Fi APs has been previously studied. In [197], Chandra et. al. suggest a dynamic adaptation of Wi-Fi channel bandwidth to maximize the throughput of a single AP-client pair. The IEEE 802.11n standard introduced channel bonding that enables the use of wider (40 MHz) channels. However, the use of wider channels does not necessarily provide performance gains. Deek et. al. [198] and Arslan et. al. [267] show that naïve channel allocation and bandwidth selection schemes in heterogeneous 802.11 networks can lead to severe performance degradation. These studies consider 802.11 devices operating in enterprise networks and do not consider changing the channelization in response to varying traffic conditions.

In recent years, studies have characterized the performance of 802.11ac links in the presence of legacy 802.11 systems (802.11 a/b/g/n). In [199], Zeng et. al. investigate the performance of 80 MHz wide 802.11ac links in the presence of 20 MHz legacy 802.11 systems operating in the secondary channels of 802.11ac. The authors show that in such a coexistence scenario, the performance of the 802.11ac system suffers severe degradation. Similar results have been reported in [200].

As the above studies indicate, the characterization of 802.11ac (or 802.11n) performance in the presence of legacy 802.11 systems has attracted significant attention from the research community. In contrast, spectrum sharing between 802.11p and 802.11ac has not garnered much attention yet. Relevant literature of DSRC and Wi-Fi coexistence has been discussed in Sec. 3.3. In this chapter, we build on top of basic ideas proposed in [106, 187] and develop mechanisms for coexistence between DSRC and Wi-Fi such that a sufficient degree of protection can be provided to DSRC devices, while also working toward throughput maximization of Wi-Fi devices.

## 4.3 Channelization of the U-NII-4 Band

The channelization in the U-NII-4 band is shown in Fig. 4.1. The unlicensed use of the $5.850 - 5.925$ GHz band, as considered by the FCC in [40], would have enabled an additional five 20 MHz, two 40 MHz, and one each of 80 MHz and 160 MHz channels.

## 4.4 System Model for Analysis of DSRC – Wi-Fi Coexistence

In our analysis, we consider a randomly chosen pair of DSRC nodes—one is a transmitter ($W$) and the other one is a receiver ($V$), and the two are separated by a distance of $x$.

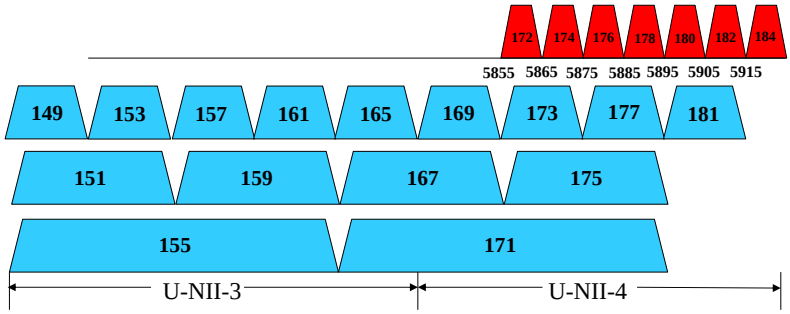


Figure 4.1: Channelization of the U-NII-4 band.

The two nodes are in each other's transmission and sensing range. The main motivation for constructing the analytical model, which is described in the next section, is to calculate the probability that $V$ can successfully receive a BSM packet from $W$ within each inter-broadcast interval in the presence of 802.11ac interference.

The 802.11ac as well as 802.11p use the IEEE 802.11 DCF protocol. Each node in the network contends for channel access using the CSMA/CA protocol. When a node has a packet to transmit, it senses the corresponding channel for an interval called the IFS. In 802.11p, various types of IFS are used. In our analysis, we consider *PIFS, which is used to give priority access to beacons.*

The analytical model, which will be described in the next section, makes the following two assumptions. First, during each inter-broadcast interval, we assume that the DSRC nodes do not move during an inter-broadcast interval, and move to their next positions instantaneously at the start of the next inter-broadcast interval. This is a reasonable assumption considering that the change in a vehicle's position is minimal during an inter-broadcast interval. Secondly, we model the road segment as a line with zero width. According to [268], this assumption is reasonable when the transmission range of DSRC nodes is significantly larger than the width of the road.

Denote the average vehicle density as $\lambda$ vehicles per kilometer. We assume that vehicles are placed on the road according to a Poisson distribution with density $\lambda$ [268, 269]. This implies that, for any road segment of length $l$, the probability that there are $i$ vehicles in that segment of the road is

$$P(\text{i vehicles in length l}) = \frac{(\lambda l)^i e^{-\lambda l}}{i!}.$$

The DSRC system parameters are defined as follows. All vehicles in the network have the same transmission and sensing range of $R$. BSM packets are broadcast periodically within every inter-broadcast interval, denoted by $T_c$. We define $T_1$ as the time required to transmit a DSRC packet and its headers.

Our model considers a single 802.11ac transmitter that has an infinite number of packets to transmit, and is *constantly* attempting to access the medium. *This assumption will maximize the influence of 802.11ac nodes on DSRC performance.* Note that in practice, a Wi-Fi transmitter contends with other Wi-Fi transmitters, and hence multiple Wi-Fi transmitters (as compared to a single transmitter that constantly attempts to access spectrum) would have less impact. We denote the IFS of 802.11ac as $\text{IFS}_2$ and use $T_2$ to denote the time required for an 802.11ac node to transmit a packet and its headers.

An 802.11ac node can transmit at a maximum power of 30 dBm, while a DSRC node can transmit at a maximum power of approximately 20 dBm in the CCH. Since 802.11ac has higher permissible transmit power than DSRC, 802.11ac's sensing sensitivity threshold (the minimum Signal to Noise Ratio (SNR) required to successfully decode the signal) is higher than that of DSRC. This difference in sensing sensitivity can lead to scenarios where Wi-Fi transmissions can interfere with DSRC node's ability to receive DSRC frames. Such interference is contrary to the rules under which unlicensed systems share the spectrum with licensed users. To adequately protect DSRC nodes, the sensing sensitivity of 802.11ac needs to be adjusted such that its sensing range is at least as large as its transmission range. Hence, in our model, we assume that the sensing range ($R_s$) of 802.11ac is larger than its transmission range ($R_t$), i.e., $R_s \geq R_t$.

The 802.11ac transmitter is assumed to be located at the side of the road. The vertical distance between the 802.11ac transmitter and the road is $d$. Since we are interested in the transmission and sensing range of 802.11ac along the road, we denote $S = \sqrt{R_s^2 - d^2}$ and $S_t = \sqrt{R_t^2 - d^2}$ as the transmission and sensing distance projected along the road. The locations of the DSRC and 802.11ac nodes are shown in Fig. 4.2.

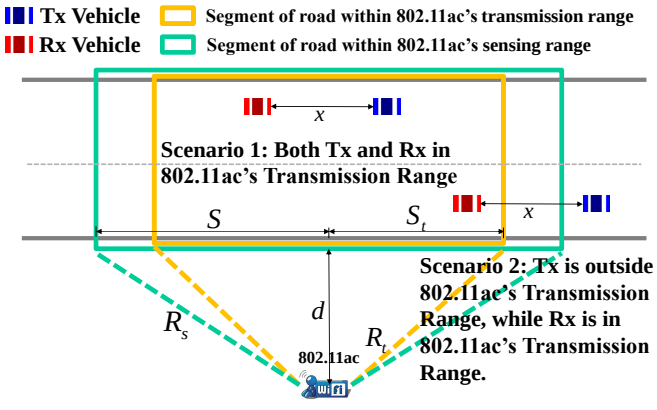


Figure 4.2: Locations of the DSRC nodes and the 802.11ac node.

## 4.5 Performance Analysis of DSRC in the presence of Wi-Fi

In this section, we analyze the performance of a DSRC network in the presence of 802.11ac transmissions using an analytical model. Our model ignores the PHY-layer factors that impact the DSRC network's performance (such as channel fading, shadowing, etc.) to limit the complexity of the model and ensure the feasibility of the analysis.

Most DSRC safety applications such as cooperative forward collision warning, lane change warning, etc., require the transmission of BSMs. In our model, we consider a DSRC broadcast network where each DSRC node is continuously broadcasting BSMs at a regular interval of 100 msec to all DSRC nodes within its transmission range.

When a packet sent by $W$ fails to reach its destination, $V$, this can be attributed to one of the following reasons:

- *Packet expiration.* We denote the probability that a packet is successfully transmitted within an inter-broadcast interval as $P_{\text{tran}} = 1 - \text{PEP}$, where PEP stands for the Packet Expiration Probability.
- *Concurrent transmission.* We assume that packets will collide at a receiver if two or more DSRC nodes in the receiver's sensing range begin transmitting in the same time slot. Given that a DSRC transmitter has successfully transmitted a BSM, let $P_c$ denote the probability that a concurrent transmission will *not* occur.
- *Hidden nodes.* Given that a DSRC transmitter has successfully transmitted a BSM, let $P_H$ denote the probability that the BSM packet will *not* collide with another packet from a hidden node.

Thus, Packet Delivery Ratio (PDR) can be expressed as

$$\text{PDR} = P_{\text{tran}} P_c P_H. \tag{4.1}$$

As shown in Fig. 4.2, 802.11ac's transmissions can impact the DSRC nodes in one of two possible scenarios:

I: $W$ is located inside the road segment that is within the 802.11ac transmitter's transmission range. So $W$ is not hidden to the 802.11ac transmitter. However, the presence of the 802.11ac transmitter increase the PEP.

II: $W$ is located outside the road segment that is within the sensing range of the 802.11ac transmitter, while $V$ is located inside it. In this scenario, 802.11ac transmissions may not have an impact on the PEP. However, $W$ is hidden to the 802.11ac transmitter.

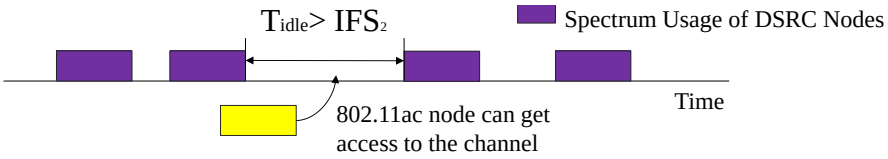


Figure 4.3: A Wi-Fi node gaining access to the channel.

Before we describe how to compute the values of $P_{\text{tran}}$, $P_c$, and $P_H$, let us first study a scenario in which a Wi-Fi transmitter gains access to the channel before all DSRC nodes finish transmitting their BSMs; such a scenario is illustrated in Fig. 4.3. If the time interval between adjacent packets from two different DSRC nodes (say $\text{T}_{\text{idle}}$) exceeds $\text{IFS}_2$, an 802.11ac node will regard the channel as idle, and start transmitting its packets. During 802.11ac node's transmission, all DSRC nodes within the 802.11ac node's transmission range will cease their backoff counter. In general, an 802.11ac transmitter can transmit $k$ packets in between DSRC transmissions if $k \cdot \text{IFS}_2 \leq \text{T}_{\text{idle}} < (k+1) \cdot \text{IFS}_2$.

Suppose $k = \lfloor \frac{\text{IFS}_2 - \text{PIFS}}{\sigma} \rfloor$, where $\sigma$ is the length of one 802.11p time slot. The parameter $k$ can be interpreted as the "virtual back-off counter" of 802.11ac. In other words, the duration of time that the 802.11ac transmitter must sense the channel before it can begin transmitting is $\text{PIFS} + k\sigma$.

The distribution of back-off counter values of DSRC nodes in the network follows ordered statistics. However, obtaining closed-form expressions for discrete ordered statistics is computationally very expensive, and requires solving integrals with a large number of variables. Hence, we use a Monte Carlo sampling method (Algorithm 1) to sample $P_{\text{tran}}$ and $P_c$.

We first consider the case when $R > R_s$. Recall that $R$ denotes the transmission range of a DSRC transmitter. We first sample DSRC nodes within 802.11ac's sensing range from a Poisson distribution with the mean value of $2\lambda R$ and let $X_1$ denote the number of such nodes. We then sample DSRC nodes which are outside 802.11ac's sensing range while still within $W$'s transmission range and let $X_2$ denote the number of such nodes. Thus, the total number of DSRC nodes in $W$'s transmission range is $N = X_1 + X_2$. This is extended to the case when $R < R_s$. We sample $X_1$ DSRC nodes that are within $W$'s transmission range and then sample $X_2$ DSRC nodes that are inside 802.11ac's transmission range, but outside $W$'s transmission range.

Each DSRC node chooses a random back-off counter uniformly distributed in [0, CW-1]. We sample $N$ back-off counter values of DSRC nodes, and store these back-off counter values in matrix $\mathbf{B} = [B^{(1)}, \cdots, B^{(N)}]$, where $B^{(i)}$ is the back-off counter of the $i$th DSRC node. Let $\mathbf{B'} = \mathbf{B}[1, 2, \cdots, X_1]$ be the back-off counter values of DSRC nodes in 802.11ac's sensing range, and $B^{(1)}$ be $W$'s back-off counter value. We sort $\mathbf{B}$ in ascending order and denote these values as $B_0, B_1, B_2, \cdots, B_N$, where $B_0 = 0$, $B_1 \leq B_2 \leq \cdots \leq B_N$. Suppose that the back-off counter of $W$ is the $I_1^{th}$ smallest among all DSRC nodes in its transmission range, and the $I_2^{th}$ smallest among all DSRC nodes in 802.11ac's sensing range. Note that we add

**Algorithm 1** Monte Carlo sampling algorithm

**Input:** $\text{IFS}_2$ of 802.11ac, PIFS, CW
**Output:** $P_c, P_{\text{tran}}$.
Define $k = \lfloor \frac{\text{IFS}_2 - \text{PIFS}}{\sigma} \rfloor$, $l = \lfloor \frac{\text{CW}}{k} \rfloor$, $\beta_1 = 2\lambda R$, $\beta_2 = 2\lambda S$
Initialize $P_{\text{tran}} = 0$,
$\gamma_1 = \min\{\beta_1, \beta_2\}$, $\gamma_2 = |\beta_1 - \beta_2|$
**for** $t = 1, 2, \cdots, T$ **do**
    Sample $X_1 \sim \text{Poi}(\gamma_1)$, $X_2 \sim \text{Poi}(\gamma_2)$, $N = X_1 + X_2$
    Sample $B^{(i)} \sim \text{unif}[0, \text{CW} - 1]$, $i = 1, 2, \cdots, N$
    Add $B^{(0)} = 0$, let $\mathbf{B} = [B^{(0)}, B^{(1)}, \cdots, B^{(N)}]$
    $\mathbf{B}' = \mathbf{B}[1, 2, \cdots, X_1]$
    **if** $\beta_1 > \beta_2$ **then**
        Find the indexes of $B^{(1)}$ in $\mathbf{B}$ and $\mathbf{B}'$, denoted as $I_1$ and $I_2$
    **else**
        Find the indexes of $B^{(1)}$ in $\mathbf{B}$ and $\mathbf{B}'$, denoted as $I_2$ and $I_1$
    **end if**
    Sort $B^{(0)}, \cdots, B^{(N)}$ in ascending order $B_0, \cdots, B_N$
    Initialize $\mathbf{Q} = [0, 0, \cdots, 0]_{1 \times l}$.
    **for** $j = 1, 2, \cdots, l$ **do**
        **for** $m = 1, 2, \cdots, N_2$ **do**
            **if** $k \cdot j \leq B_m - B_{m-1} < k \cdot (j + 1)$ **then**
                **if** $m \leq I_2$ **then**
                $\mathbf{Q}(j) = \mathbf{Q}(j) + 1$
                **end if**
            **end if**
        **end for**
    **end for**
    $n_{ac} = [1, 2, \cdots, l] \cdot \mathbf{Q}^T$
    **if** $n_{ac} \cdot T_2 + I_1 \cdot (T_1 + \text{PIFS}) + B^{(1)} \cdot \sigma \leq T_c$ **then**
        $P_{\text{tran}} = P_{\text{tran}} + 1$
        **if** $B^{(1)} == B_{I_1+1}$ or $B^{(1)} == B_{I_1-1}$ **then**
            $P_c = P_c + 1$
        **end if**
    **end if**
**end for**
$P_c = P_c / P_{\text{tran}}$, $P_{\text{tran}} = P_{\text{tran}} / T$

$B_0 = 0$ because we need to consider the scenario where an 802.11ac transmitter gains access to the channel before all DSRC nodes.

For any $m$, if $j.k \leq (B_m - B_{m-1}) < (j+1).k$, a Wi-Fi transmitter can send $k$ packets before all DSRC nodes in its sensing range with a back-off counter value no less than $B_m$. Let $n_{ac}$ denote the number of packets that the 802.11ac node transmits before $W$. We define a matrix $\mathbf{Q}$, such that $\mathbf{Q}(j)$ is the number of times that 802.11ac successfully transmits $j$ packets between two DSRC packet transmissions. For example, as shown in Fig. 4.3, if 5 packets are sent out by 802.11ac transmitter between two consecutive DSRC transmissions, then $\mathbf{Q}(5)$ is increased by one. In our analysis, we focus on a particular transmitter $W$ which is the $I_2^{th}$ DSRC node in 802.11ac's sensing range to send its BSM. In order to check whether the BSM from $W$ is expired, we only need to calculate the number of packets transmitted by the 802.11ac node before $W$, i.e., we only need to consider the case $m \leq I_2$.

Since the maximum value of the back-off counter is CW, an 802.11ac node can transmit at most $l = \lfloor \frac{\text{CW}}{k} \rfloor$ packets between two consecutive DSRC transmissions. Hence, $n_{ac} = \sum_{i=1}^{l} i \cdot \mathbf{Q}(i)$. If $\left(n_{ac} \cdot T_2 + I_1 \cdot (T_1 + \text{PIFS}) + B^{(1)} \cdot \sigma\right) > T_c$ at the instant when $W$ wishes to transmit a BSM, more than $T_c$ amount of time has elapsed since the generation of the packet; in this scenario, $W$ cannot get access to the channel in the current inter-broadcast interval, and must drop its packet. Otherwise, $P_{\text{tran}}$ is incremented by 1. We divide $P_{\text{tran}}$ by the total number of iterations $T$ to obtain the value of $P_{\text{tran}}$.

In Algorithm 1, two DSRC nodes having the same back-off counter value indicates a concurrent transmission. Given that $W$ successfully sends its BSM, if $B^{(1)} = B_{I_1-1}$ or $B^{(1)} = B_{I_1+1}$, $W$ has the same back-off counter value with at least one of its neighbors, resulting in a collision due to concurrent transmission. We divide the number of collisions by the number of unexpired packets to obtain $P_c$.

The value of $P_H$ cannot be sampled from Algorithm 1. However, having obtained $P_{\text{tran}}$, using results from [268], $P_H$ can be approximated as, $P_H = e^{-\frac{2P_{\text{tran}}\lambda x T_1}{T_c}}$. From the values of $P_{\text{tran}}$, $P_c$ and $P_H$, we can obtain the PDR from Equation 4.1.

## 4.6 Simulation Results

We generate quantitative results on the impact of Wi-Fi transmissions on DSRC performance using ns-3 simulations. The simulation setup is shown in Fig. 4.4. We consider a 1000 meter long six-lane road with different traffic densities. The impact of 802.11ac's transmissions on DSRC performance is evaluated using a single DSRC transmitter-receiver pair as shown in Fig. 4.4. The simulation parameters are summarized in Table 4.1. As pointed out in [270], the default value of CW size (CW = 7) for DSRC nodes currently proposed in the 802.11p standard for BSM packets is far from optimal. The authors suggest setting the value of CW to 127. Following this recommendation, we set the CW size of DSRC nodes to 127.

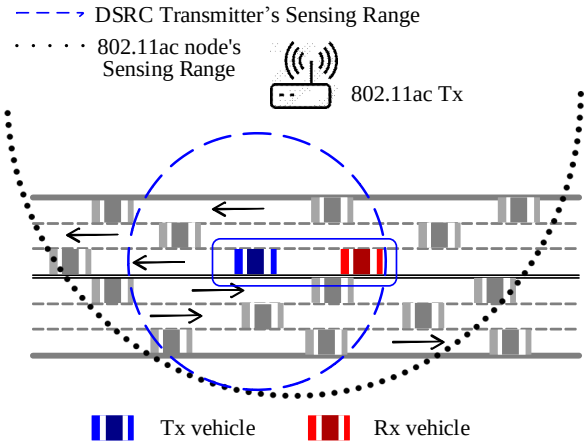


Figure 4.4: Simulation scenario.

The extended alternating channel access scheme with 50 ms CCH and 50 ms SCH, as prescribed in the IEEE 1609.4 standard, is used in the simulations. The DSRC transmitter broadcasts a packet once in every inter-broadcast interval over a CCH. Transmissions over an SCH are not considered in the simulations (since we are focusing on the performance of safety applications that use CCHs). Each simulation run consists of 100 packet broadcasts (i.e., 100 inter-broadcast intervals). We assume that the Wi-Fi transmitter always contends for the channel. The metrics used to evaluate the performance of DSRC are PDR and the Packet Expiration Ratio. These metrics are first computed in the absence of the Wi-Fi transmitter to obtain a baseline for comparison. Each computation is averaged over 10 simulation runs with different seed values. We then switch on the Wi-Fi transmitter and compare the corresponding values for different values of the Wi-Fi node's IFS and sensing range.

Fig. 4.5 shows the percentage of the packets delivered (in blue), lost due to collisions (in green), and expired (in brown) for different values of Wi-Fi IFS. The red line indicates the PDR of DSRC in the absence of any Wi-Fi transmissions. The solid magenta and cyan lines indicate the numerically computed values (as described in Sec. 4.5) of the number of unexpired packets transmitted by $W$, and delivered to $V$, respectively.

We first observe that *if the parameters of the 802.11ac transmitter are set to the default values (i.e., IFS = 23 $\mu s$, time slot = 9 $\mu s$), performance of the DSRC network degrades significantly.* For example, when the sensing range of Wi-Fi transmitter is 300 meters (same as its transmission range), the PDR of DSRC is lower than 10% (Fig. 4.5a, 4.5c, 4.5e). Even if the sensing range of the 802.11ac transmitter is increased to 500 meters, the PDR of DSRC is lower than 40% in all cases (Fig. 4.5b, 4.5d, 4.5f). These values of PDR are significantly lower than the PDR in the absence of 802.11ac transmissions.

We observe that PDR of the DSRC network tends to converge to fixed values as the Wi-Fi IFS increases. When the IFS of the Wi-Fi transmitter is larger than a threshold value, 802.11ac transmissions have no influence on the DSRC network, and the performance degradation of the DSRC network is due to the contention among the DSRC nodes themselves. The step-

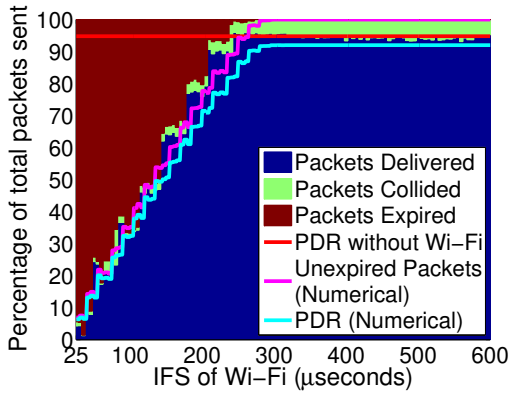


(a) 30 vehicles/km, SR = 300

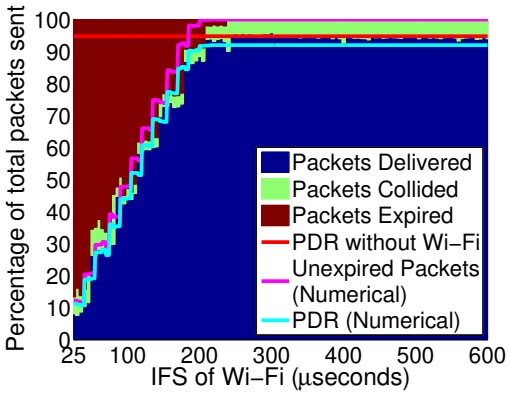


(b) 30 vehicles/km, SR = 500

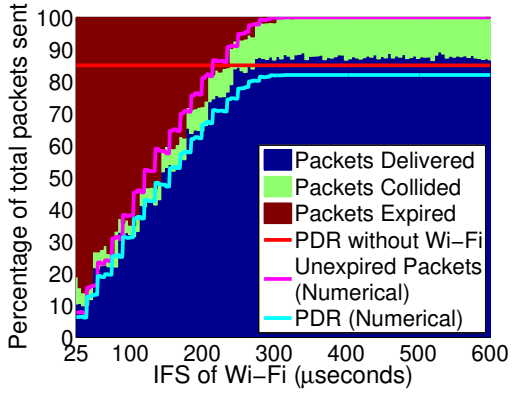


(c) 60 vehicles/km, SR = 300

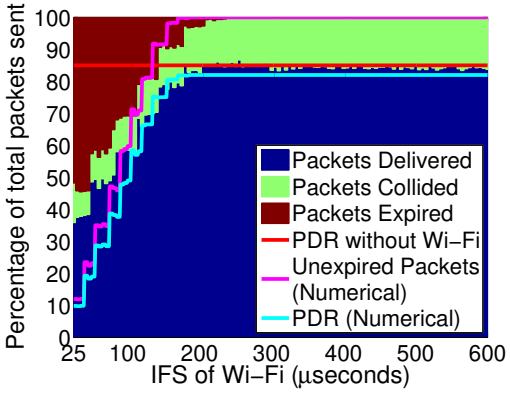


(d) 60 vehicles/km, SR = 500

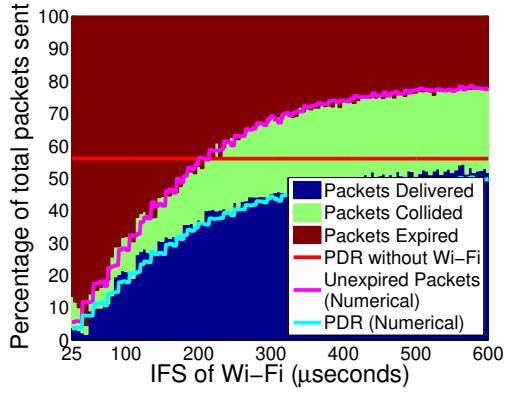


(e) 120 vehicles/km, SR = 300

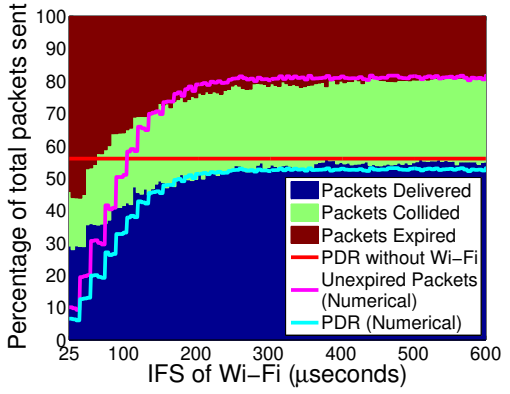


(f) 120 vehicles/km, SR = 500

Figure 4.5: Percentage of Delivered, Collided and Expired Packets

Table 4.1: Simulation parameters for evaluating DSRC – Wi-Fi coexistence

| **Parameter** | **Value** |
|---|---|
| **Road** | |
| Length of the road | 1000 meters |
| Vehicle densities | {30,60,120} vehicles/km |
| Number of lanes | 6 |
| Lane width | 3 meters |
| **DSRC** | |
| Transmitter Gain | 10 dB |
| Receiver Gain | 4.3 dB |
| Transmission Range | 300 meters |
| Sensing Range | 300 meters |
| Packet Length | 500 bytes |
| Data Rate | 6 Mbps |
| PIFS | 45 $\mu$seconds |
| Slot Duration ($\sigma$) | 16 $\mu$seconds |
| Contention Window | 127 |
| Inter-Broadcast Interval | 0.1 seconds |
| Distance between Tx & Rx | 50 meters |
| **IEEE 802.11ac** | |
| Transmitter Gain | 10 dB |
| Receiver Gain | 4.3 dB |
| Transmission Range | 300 meters |
| Sensing Range | {300,400,500} meters |
| Packet Length | 7,500 bytes |
| Data Rate | 78 Mbps |
| IFS | 23 to 2032$\mu$s (23 to CW $\cdot \sigma$) |
| Distance from DSRC | 150 meters |

like pattern for the number of unexpired packets can be attributed to the virtual back-off counter value ($k$) of Wi-Fi.

Figures 4.5a-4.5f suggest that as the IFS of Wi-Fi increases, the PDR of DSRC converges to the red line faster for a larger sensing range. Thus, *the sensitivity threshold of a Wi-Fi transmitter should be decreased so that its sensing range is larger than its transmission range. Under these circumstances, we can infer from Fig. 4.5 that for a Wi-Fi IFS value around* 200$\mu s$*, the performance of the DSRC network approaches its performance in the absence of any Wi-Fi transmissions.*

An interesting observation drawn from Figures 4.5a-4.5f is that the influence of Wi-Fi transmissions (specially for low IFS values) is more severe in low vehicle density scenarios as

compared to high vehicle density. If there are fewer vehicles in the Wi-Fi transmitter's sensing range, the time interval between two consecutive DSRC packet transmissions is larger than that in high vehicle density scenarios. The Wi-Fi transmitter, thus, has more opportunities to transmit packets during the idle channel interval, thus causing more DSRC packets to expire.

## 4.7 Testbed Setup

We created and configured a testbed comprising of four 802.11ac nodes and six 802.11p nodes. In this section, we describe the testbed setup in terms of the configuration of the hardware, the spectral scan and analysis procedure, and the performance evaluation of DSRC and Wi-Fi devices.

### 4.7.1 Hardware Configuration

We use off-the-shelf hardware for 802.11ac and 802.11p. The RouterBoard RB911G-5HPacD is used as the 802.11ac AP as well as the client. The RB911G-5HPacD has two Radio Frequency (RF) chains, thus enabling 2 × 2 MIMO. It uses Qualcomm Atheros QCA9882 chipset for 802.11ac. We use an embedded Linux distribution—OpenWrt (Chaos Calmer 15.05.1) as the operating system with ath10k drivers on the 802.11ac hardware.

The 802.11p hardware comprises of RouterBoard RB433AH as the processor and RouterBoard RB52H as the RF card. The RF card is compatible with 802.11a/b/g and operates in the 2.4 GHz and 5 GHz band. We use an OpenWrt distribution (Attitude Adjustment 12.09) with ath5k drivers provided by open-source vendor Componentiality on the 802.11p devices. This distribution modifies the 802.11a hardware to operate as 802.11p with 10 MHz-wide channels.

As discussed in Sec. 4.3, 802.11p operates in Ch. 172-184. The current regulations on 802.11ac, however, does not permit Wi-Fi operation above Ch. 165. Therefore, we configured the 802.11p nodes to operate on 10 MHz channels in the U-NII-3 band (Ch. 149-165). In this way, we created the spectrum sharing scenario of the U-NII-4 band in the U-NII-3 band. Although two 802.11p channels overlap with one 802.11ac channel in the U-NII-4 band, since partial overlap of 20 MHz channels is not allowed in the 5 GHz band, 802.11 hardware can operate only on certain fixed channels. Specifically, in our testbed, the 802.11p hardware can operate on Ch. 153, 157, and 161 with a channel width of 10 MHz. Although this channelization deviates from the one proposed for the U-NII-4 band (due to constraints imposed by the hardware and firmware), we believe that this does not negatively impact our study, because an 802.11ac transmitter must declare a 20 MHz channel to be busy if either of the two overlapping 10 MHz DSRC channels are occupied. In the rest of this work, we refer to the channels by their original 10 MHz and 20 MHz channel numbers in the U-NII-4

band, i.e., Ch. 172-184 (for DSRC) and Ch. 169-181 (for Wi-Fi).

### 4.7.2 Spectrum Scan and Analysis

Each Wi-Fi radio senses the channel before its transmission. We believe that this spectral information can be leveraged to make an informed channel and bandwidth allocations in Wi-Fi networks. The spectral information is required at the MAC layer and is implemented at the kernel level. However, some Wi-Fi chipset manufacturers provide access to this spectral information at the user-space.

In our testbed, we access the raw spectral information available from the 802.11ac QCA9882 chipset and analyze this data using a custom user-space application (based on [271]) to quantify spectral utilization. The 80 MHz spectrum (Ch. 169-181) is scanned approx. 1000 times in 1 sec. In each scan, 256 sample points are distributed across the 80 MHz spectrum. The scan and analysis are performed at the Wi-Fi AP itself; thus, permitting real-time usage of the spectral information.

For each 20 MHz channel, the spectral utilization is calculated as the fraction of time for which the signal level is above the energy detection threshold of the Wi-Fi AP (energy detection threshold is used because Wi-Fi AP cannot detect 802.11p preambles). For each 40 MHz channel, the spectral utilization is calculated as the fraction of time for which signal levels on any one of the two 20 MHz sub-channels is above the energy detection threshold. The spectral utilization for the 80 MHz channel is calculated similarly.

By analyzing the spectral information, an AP can learn the usage of the spectrum, and adjust its channelization in an informed manner. Thus, the spectral scan and analysis enable the AP to take into account the interference from other devices.

### 4.7.3 Performance Evaluation

Different metrics such as Packet Error Rate (PER), PDR, link throughput, etc. can be used to characterize a wireless link. We use the wireless link throughput as the metric for performance evaluation of 802.11ac links because 802.11ac has been primarily developed for high data-rate applications. On the other hand, we use the PER to analyze the performance of 802.11p systems, since 802.11p is expected to be used mainly for safety applications where low PER is of critical importance.

We use the packet generation tool Iperf for generating synthetic traffic and measuring the throughput and PER on the Wi-Fi and DSRC nodes. Only User Datagram Protocol (UDP) traffic is generated because we wish to ignore the performance loss due to Transmission Control Protocol (TCP) overheads (handshake, congestion control, TCP retransmissions, etc). In the case of 802.11ac links, unless otherwise mentioned, we generate UDP traffic

from the client to the AP.

The traffic patterns and topology of nodes for 802.11ac and DSRC are described alongside each test scenario. In all cases, we assume that a Wi-Fi AP and a client are both stationary. This is a reasonable assumption in most enterprise networks. The DSRC nodes are also stationary in our testbed. In practice, however, the DSRC nodes are mobile. We emulate this in our testbed using varying traffic patterns on DSRC channels.

Dynamic change of channelizations can lead to large switching delays due to hardware reconfigurations, dissociation, and re-association of the client(s). To minimize such delays, we leverage the Channel Switch Announcement (CSA) feature of IEEE 802.11. In a BSS, CSA can be used by an AP to notify the clients of the exact time of switch and channel information of the new channel. By using CSA, the switching delay can be reduced to a few hundred milliseconds.

### 4.7.4 Custom Modifications

In Sec. 4.6, we describe the need to adjust the AIFS value of the Wi-Fi transmitter based on the operating primary channel. We enable this change in the AIFS from the user-space by extending the *iw* command-line utility.

The IEEE 802.11 standard specifies the procedure for selection of primary and secondary channels in case of channel bonding [181]. If multiple APs share the same 40 MHz (or 80 MHz) channels, all the APs must set the same primary and secondary channels. However, as explained in Sec. 4.8.2, we need to set specific primary and secondary channels in our testbed. We achieve this by disabling the automatic shift of primary and secondary channels in the *hostapd* daemon.

## 4.8 Experimental Results

In the coexistence scenario between DSRC and Wi-Fi, DSRC is the primary user. In the preceding sections, our inherent assumption was that when DSRC and Wi-Fi users share the spectrum, the shared channel corresponds to the primary channel of Wi-Fi. Thus, the analysis presented in Sec. 4.5 is valid when DSRC devices operate in the primary channel of 802.11ac users. However, as described in Sec. 2.2.2, the secondary channel of 802.11ac uses a considerably different channel access mechanism. Thus, the impact of 802.11ac operation on DSRC system performance will be different if the shared spectrum corresponds to the secondary channel of an 802.11ac network. We verify the above claims in this section. As a consequence, we show that to provide adequate protection to DSRC transmissions, certain channelization options must be disabled at Wi-Fi transmitters.

### 4.8.1 DSRC in the Primary Channel of 802.11ac

One of the conclusions made in the previous studies [106, 272] is that increasing the AIFS of the Wi-Fi transmitter to a sufficiently large value can be used to mitigate the impact of Wi-Fi transmissions on DSRC performance. This is, however, valid only when the DSRC channel of operation overlaps with the primary channel of the Wi-Fi transmitters. We discuss DSRC's performance when it operates on a secondary Wi-Fi channel in the next subsection. In this subsection, using experimental results obtained from our testbed, we show that the conclusion made by investigators in the previous studies is indeed correct. However, we show that the value of AIFS must be increased to a value that is much higher than that suggested in [272], and justify this claim.

We consider a network comprising of 2 DSRC nodes and a Wi-Fi AP-client pair as shown in Fig. 4.6. The DSRC transmitter generates traffic on the CCH (Ch. 178), and the Wi-Fi AP operates on the 20 MHz channel that overlaps with the CCH (Ch. 177). The direction of the arrows on the solid lines indicates the direction of communication. The distance between the nodes is such that all nodes are within the transmission and sensing range of each other.

The source node sends UDP traffic to the sink node using Iperf such that the channel is fully saturated, but has a very small PER ($0 - 1\%$), i.e. any further increase in the packet transmission rate from the source node will lead to non-zero PER. The length of each DSRC packet is 200 bytes, and the packets are transmitted at a fixed PHY-layer rate of 6 Mbps.

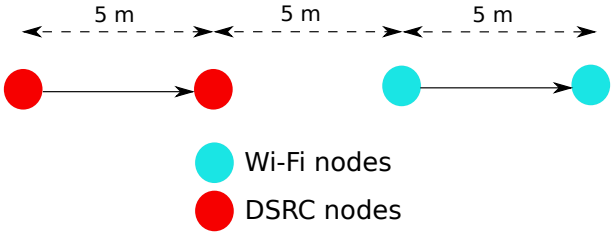


Figure 4.6: Topology for testing DSRC system performance

We first observe the performance of DSRC nodes in the absence of Wi-Fi transmissions. The Wi-Fi transmitter then starts a UDP stream of 1500 byte packets to the receiver. The Wi-Fi transmitter uses its rate adaptation algorithm to identify the best MCS for its transmissions. Fig. 4.7a shows the PER at the DSRC receiver as a function of Wi-Fi AIFSN. AIFS is related to AIFSN by

$$\text{AIFS} = \text{SIFS} + \text{AIFSN} \times \text{slot\_time}, \tag{4.2}$$

where SIFS is the short IFS used for acknowledgment packets and slot_time is the time duration of each Wi-Fi slot.

DSRC's medium access priority can be increased by increasing the AIFS value of Wi-Fi. The optimal AIFS value that the Wi-Fi transmitters must use to adequately protect DSRC would depend on several factors, including vehicle density, network topology, etc. In our setup, we

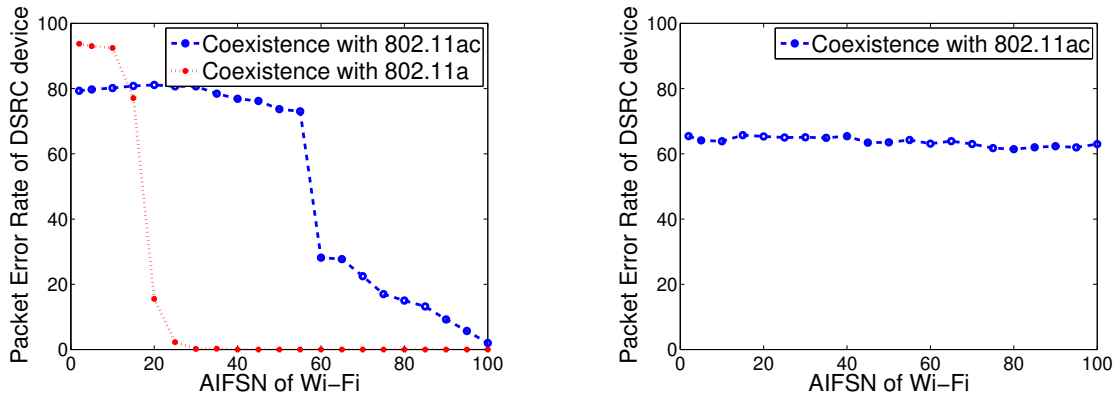


(a) DSRC on primary channel

(b) DSRC on secondary channel

Figure 4.7: PER of DSRC node on primary and secondary channel

observe from Fig. 4.7a that beyond AIFSN = 100, the impact of Wi-Fi transmissions on DSRC's PER is negligible. Henceforth, we set the AIFSN value to 100 (AIFS = 916$\mu$s) for Wi-Fi transmitters when they share the spectrum with DSRC.

We believe that the value of AIFSN required for prioritizing DSRC transmissions in our setup is much higher than that suggested in [272] due to frame aggregation in 802.11ac. To verify this, we let the interferer operate in 802.11a mode, where frame aggregation is disabled. The PER at the DSRC receiver, in this case, is also shown in Fig 4.7a. We infer that frame aggregation has a severe impact on DSRC performance. This is because single channel access of an aggregated frame is equivalent to the access of multiple non-aggregated Wi-Fi frames as far as DSRC performance is concerned.

### 4.8.2 DSRC in a Secondary Channel of 802.11ac

We claim that even a sufficiently large increase in the AIFS value of Wi-Fi transmitters would fail to protect DSRC from priority reversal (i.e. when both, Wi-Fi and DSRC nodes, have a packet to transmit, the Wi-Fi node transmits before the DSRC node), if the DSRC transmitters operate in the secondary channels of the Wi-Fi transmitter. We verify the legitimacy of our claim using experimental results. We use the same topology as shown in Fig. 4.6. The DSRC source node transmits packets to the sink node on the CCH such that the channel is saturated and the PER is very low. The Wi-Fi nodes operate on a 40 MHz link such that the CCH overlaps with the secondary channel of the Wi-Fi link. The curve in Fig. 4.7b represents the PER at the DSRC sink node operating in the secondary channel of the Wi-Fi link.

Results in Fig. 4.7b show that a sufficiently large increase in the Wi-Fi AIFS does not protect DSRC users (against performance degradation) if the shared channel is a secondary Wi-Fi channel. In such cases, reliable DSRC performance can be guaranteed if the *full*

*backoff procedure* (AIFS+backoff) [200] is followed on the secondary channels along with the primary channel[1], although this is not supported by the current Wi-Fi standards. From these results, we can make an important conclusion. *Under the current Wi-Fi standards, certain channelization schemes cannot be used by Wi-Fi networks without causing significant degradation in the performance of DSRC nodes that share the secondary Wi-Fi channels.*

Table 4.2: Permissible channelizations for Wi-Fi in the shared 5.9 GHz band

| **Channel** | 169 | 173 | 177 | 181 | 173(P) + 169(S) |
|---|---|---|---|---|---|
| **Channel Index** | $C_1$ | $C_2$ | $C_3$ | $C_4$ | $C_5$ |
| **HT mode** | HT20 | HT20 | HT20 | HT20 | HT40 |
| **AIFSN** | 2 | 100 | 100 | 100 | 100 |

**Summary:** Given that DSRC nodes are the primary users of the shared spectrum, and considering the importance of safety applications supported by DSRC networks, Wi-Fi transmissions must not degrade DSRC performance. From the experimental findings presented in this section, we conclude that while Wi-Fi nodes can share the spectrum with DSRC nodes, *a Wi-Fi AP should not be configured to operate its secondary channel(s) on the shared spectrum.* Consequently, Ch. 171 (80 MHz) and 175 (40 MHz) shown in Fig. 4.1 should not be used by Wi-Fi APs. The only channel bonding configuration available at the Wi-Fi AP is to bond Ch. 169 and 173 as the secondary and primary channels respectively. The possible channelizations are listed in Table 4.2.

## 4.9 Proposed Real-time Channelization Algorithm (RCA)

The increased AIFS value for Wi-Fi transmitters in the shared spectrum can have severe implications for Wi-Fi system performance. In the presence of high DSRC traffic, Wi-Fi APs operating in the shared spectrum could experience a substantial loss in throughput. In some cases, it might be beneficial for the Wi-Fi AP to operate on the 20 MHz non-shared spectrum. On the other hand, if DSRC nodes are absent, or if DSRC traffic is low, using the shared spectrum could yield satisfactory throughput despite the increased AIFS. Thus, efficient utilization of the spectrum relies on informed channelization allocation at the Wi-Fi AP. In this section, we describe our proposed RCA that makes use of the spectral information available at the Wi-Fi AP to determine the best channelization for an AP operating in the U-NII-4 band.

[1]This could not be verified in our testbed as the secondary channel access procedure is implemented in the proprietary firmware of QCA9882 (as is the case with most other chipsets).

Table 4.3: Real-time Channelization Algorithm Parameters

| Param. | Description | Value |
|---|---|---|
| $L_{data}$ | Length of data packets | 1500 bytes |
| $L_{ack}$ | Length of ACK packets | 100 bytes |
| $K$ | Number of aggregated frames | $2-32$ |
| $R_i$ | Data rate used in previous transmission | $6.5-400$ Mbps |
| $PRR$ | Packet Reception Ratio | $0-1$ |
| $R_{cur}$ | PHY Layer Rate used in the current session | $6.5-400$ Mbps |
| $U_i$ | Utilization ratio | $0-1$ |
| SIFS | SIFS time of Wi-Fi transmitter | $16\mu$s |
| AIFS | AIFS time of Wi-Fi transmitter | Eq. (4.2) |
| $E^i_{Th}$ | Expected throughput of the $i$th channel | Eq. (4.3) |
| $\beta$ | Throughput reduction factor | 0.4 |
| $\Delta(Th_{ch})$ | Two-window throughput difference | *variable* |
| $\Delta_{max}$ | Threshold for two-window throughput diff. | 0.15 |
| $T_{\max}$ | Maximum time before next scan process | Eq. (4.4) |
| $t_{analyze}$ | Time required to analyze sensing data | $3-4$ sec |
| $\tau_{ch}$ | Sojourn time on channel $ch$ | $0-T_{\max}$ |
| $E^{\max}_{Th}$ | Expected throughput at highest MCS | 400 Mbps |
| $t_{data}$ | Time to transmit data frames at $R_{cur}$ | $K \cdot L_{data}/R_{cur}$ |
| $t_{BO}$ | Expected time spent in backoff process | $\mathbb{E}[\text{CW}]$ |
| $t_{ack}$ | Time to transmit block acknowledgement | $L_{ack}/R_{cur}$ |

### 4.9.1 Problem Statement

We consider a shared spectrum network with 6 DSRC nodes and 2 Wi-Fi BSSs. Each BSS comprises of an AP and an associated client. Each AP can select a primary channel and bandwidth from $C = \{C_1, \cdots, C_k\}$ combinations, as shown in Table 4.2. The objective of RCA is to pick the best channel combination (in terms of its achievable throughput) among the permitted combinations using the locally available real-time spectral information. We only consider static channel access mechanism in this work since most channel bonding options are not available at the Wi-Fi AP in the U-NII-4 band. In the dynamic channel access mechanism, the AP determines the channel bandwidth for each transmission opportunity based on their availability. If the use of the secondary channel is permissible, RCA can be used to determine the best primary channel, and the secondary channels can be selected as available.

### 4.9.2 Approach

The performance of a Wi-Fi link depends on factors such as the surrounding environment, and particularly on the number of DSRC nodes or vehicles in its vicinity, DSRC traffic pattern, etc. Under such circumstances, the optimal channel combination at the AP cannot be determined without prior knowledge of the DSRC nodes. At best, the Wi-Fi AP can change its channelization in response to increased DSRC traffic on certain channels. RCA seeks to do just that — scan and analyze the spectrum to calculate the spectral utilization, estimate a bound on the achievable throughput on each channelization, and select the channelization that yields the highest throughput.

RCA keeps repeating the above process in varying traffic conditions. The main task of RCA is to look for a better channelization every time the link throughput drops. Additionally, RCA regularly tries to check for better channelization even if the channel conditions do not fluctuate. The finer details of RCA are described next.

**Algorithm 2** Real-time Channelization Algorithm (RCA)

1: Initialize: Hop across all $C_i$ to determine $R_i$, $i = 1, \cdots, k$.
2: **while** *true* **do**
3: Scan the 80 MHz spectrum.
4: Compute $U_i$, and $E^i_{Th}$, for $i = 1, \cdots, k$.
5: Update $R_{ch} = R_{cur}$.
6: Switch to Channel $ch = \arg\max_i([E^1_{Th}, \cdots, E^k_{Th}])$.
7: Initialize: $\tau_{ch} = 0$
8: **while** $\left(\Delta(Th_{ch}) \leq \Delta_{max}\right)$ and $\left(Th_{ch} \geq \beta E^{ch}_{Th}\right)$ and $\left(\tau_{ch} \leq T_{max}\right)$ **do**
9: Transmit on channel $ch$.
10: **end while**
11: **end while**

### 4.9.3 Proposed Algorithm

The detailed steps in RCA are shown in Algorithm 2. The variables used are listed in Table 4.3. For each parameter, the presence of a subscript or superscript $i$ indicates that the parameter is specific to channelization $i$, for $i = 1, \cdots, k$.

*Line 1:* In practical settings, Wi-Fi transmitters use some form of rate adaptation algorithm to minimize the PER or maximize the throughput. In RCA, we let the transmitter use its default rate adaptation algorithm to determine the best MCS scheme for its transmission. RCA starts by initializing the rates $R_i$ for all $C_i, i = 1, \cdots, k$. The AP hops across all channelizations to determine the client PHY rate on each channelization. The AP notifies the client of the channel switch using RCA; thus, minimizing the impact of channel switching.

*Lines* 3−4*:* The AP scans the 80 MHz spectrum. Using this scan data, spectral utilization of each channelization is computed as described in Sec. 4.7.2. The AP then calculates a bound on the expected throughput on each channelization using these utilization ratios. We use Eq. (4.3) to calculate the expected throughput for each channelization. In [198], the authors show that in the absence of external interference, except for the higher order MCS schemes, the actual throughput closely matches the expected throughput computed using Eq. (4.3). We introduce the term $(1 - U_i)$ in Eq. (4.3) to take external interference into consideration.

$$E_{Th}^{i} = \frac{K \cdot L_{data} \cdot (1 - U_i) \cdot PRR}{\text{AIFS} + t_{BO} + t_{data} + \text{SIFS} + t_{ack}} \tag{4.3}$$

The value of $K$, the number of aggregated frames, depends on the transmitter MCS scheme. Using Wireshark traces, we determine $K$ for each MCS scheme.

*Lines* 5−6*:* The AP tunes its RF front-end to the channelization that is expected to achieve the highest throughput. Before the AP moves to the new channel, the AP (i) announces the channel switch decision to all the associated client(s) using CSA, and (ii) stores the value of the PHY layer transmission rate used by the client on the current channel for subsequent computations of the expected throughput.

*Lines* 8 − 10*:* The objective of RCA is to determine the best channelization for an AP in real-time. A scan process is, thus, initiated in the following two cases.

Case (1): The link throughput drops due to an increase in the utilization of the operating channel. This sudden drop can be attributed to the entry of additional nodes using that channel. To identify a better channel, a scan process is initiated. We use the following two mechanisms for detecting an increase in spectrum utilization of the operating channel.

(a) A sudden drop in the throughput can be detected by maintaining two windows for calculating the average throughput. The first window averages over a larger interval (say $w_1$), while the second window averages over a smaller interval (say $w_2$). A sudden drop in link throughput will cause the average over a smaller window to drop faster than the average over a larger window. If the difference in average throughput over the two windows, $\Delta(Th_{ch})$, is greater than some threshold $\Delta_{\max}$, we trigger a scan process. In our experiments, we use $w_1 = 10, w_2 = 3$. For these window sizes, we observe that $\Delta_{\max} = 0.15$ accurately detects a sudden drop in throughput.

(b) There is a time delay of $t_{analyze}$ between the scan process and reconfiguration of the hardware to the new channelization. There is a possibility that certain nodes start operating on the new channel within this time interval. If the entry of these nodes causes the actual throughput to be significantly lower than the expected throughput, we infer that the channel conditions have changed since the previous scan, and initiate a new spectrum scan. We quantify this using a parameter $\beta$. A scan process is triggered if $Th_{ch} \leq \beta \cdot E_{Th}^{ch}$. A high value of $\beta$ can lead to frequent scans in the absence of any interference, especially at higher MCS schemes where the actual throughput can be less than the expected throughput. On

the other hand, a small value of $\beta$ can fail to detect the entry of other nodes in the operating channel. Using experiments, we observe that the value of $\beta = 0.4$ serves as a good indicator of external interference on the operating channel.

Case (2): $T_{\max}$ amount of time has elapsed since the previous scan. Although the throughput does not drop, there might exist another channelization that yields a higher throughput. Thus, after every $T_{\max}$ interval, the RCA scans the spectrum for better channelization despite no drop in throughput.

RCA calculates the value of $T_{\max}$ based on the expected throughput of the current channelization. If the expected throughput is equal to the maximum possible throughput, a spectral scan and analysis can lead to no increase in throughput. Ideally, if $Th_{ch} = Th_{\max}$, $T_{\max}$ should be infinite. On the other hand, the utilization of the entire 80 MHz spectrum can be high, resulting in a small throughput even on the best channel. When the expected throughput is close to zero, we let the device operate on the operating channel for at least $t_{analyze}$ amount of time. In such cases, frequent scans can detect a better channelization as soon as its utilization decreases. Keeping these conditions in mind, $T_{\max}$ is calculated as,

$$T_{\max} = \frac{t_{analyze}}{1 - \left(\frac{E_{Th}^{ch}}{Th_{\max}}\right)}, \tag{4.4}$$

where $Th_{max}$ is the maximum possible throughput. Since only 20 and 40 MHz channels are allowed, we let $Th_{max} = 400$ Mbps (corresponding to the highest MCS scheme at 40 MHz).

### 4.9.4 RCA Implementation

We implement RCA completely at the AP, with no modifications required at the associated client(s). This is important because it is infeasible to change software packages and drivers at all clients; however, the AP can enable RCA using a simple patch. Since RCA uses real-time spectral information to adapt the channelization, it is implemented with low response time on commodity hardware using custom user-space scripts. In our implementation, given that the AP detects a significant drop in throughput in the operating channel, the spectrum is scanned and the best channel is selected within $4 - 5$ sec. The main sources of delay at the AP are the scan process (approx. 1 sec), and the processing time of spectral information (approx. $3 - 4$ sec). During the scan and analysis phases of RCA, communication between AP and client continues over the previous operating channel. If the AP switches to a new channel, it notifies the clients(s) of the switch using CSA.

## 4.10 Evaluation of RCA

### 4.10.1 Experimental Characterization

The topology used to evaluate the performance of RCA is shown in Fig. 4.8. One DSRC transmitter-receiver pair operates on each of the Ch. 172, 178, and 182.[2] We use two pairs of Wi-Fi nodes in our experiments — an interfering pair that operates with saturated traffic on Ch. 169, and an observation pair, which is used to evaluate the performance of RCA. All the nodes are within the sensing range of each other.

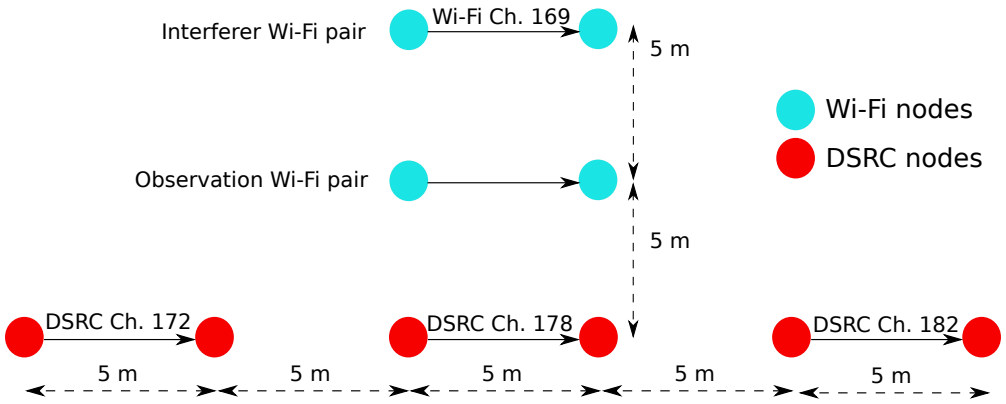


Figure 4.8: Topology for evaluating RCA performance.

Traffic on DSRC channels largely depends on the number of DSRC nodes in the vicinity of the Wi-Fi AP. The larger the number of DSRC nodes, the higher the utilization on the DSRC channels. While traffic on Ch. 172 (BSM traffic) and 178 (control traffic) are directly related to the number of vehicles, traffic on the SCH (Ch. 182) can be arbitrary. The traffic patterns of the four channels generated for our testbed experiments are shown in Fig. 4.9. The numbers inside each block indicate the spectrum utilization ratio at the observation AP as a fraction of saturated traffic. We change the traffic pattern every $T$ seconds; by changing the value of $T$, we can emulate fast and slow varying traffic conditions. The duration of each experiment is $8T$.

The utilization of Ch. 173 and 177 first gradually increase and then decrease. On the other hand, the utilization of Ch. 181 is either 0% or 50%. We operate an interfering Wi-Fi BSS on Ch. 169 with saturated traffic. As a result, utilization of Ch. 169 varies in the range $30-60\%$. Using these traffic patterns, we emulate several types of varying traffic conditions.

First, we evaluate the performance of each static channelization allocation (shown in Table 4.2) separately. We keep the channelization fixed throughout the duration of the experiment ($8T$). Next, we run RCA on the observed AP and test its performance. The

[2]Wi-Fi channels are odd-numbered, while DSRC channels are even-numbered. DSRC Ch. 172 overlaps with Wi-Fi Ch. 173, Ch. 178 with Ch. 177, and Ch. 182 with Ch. 181.

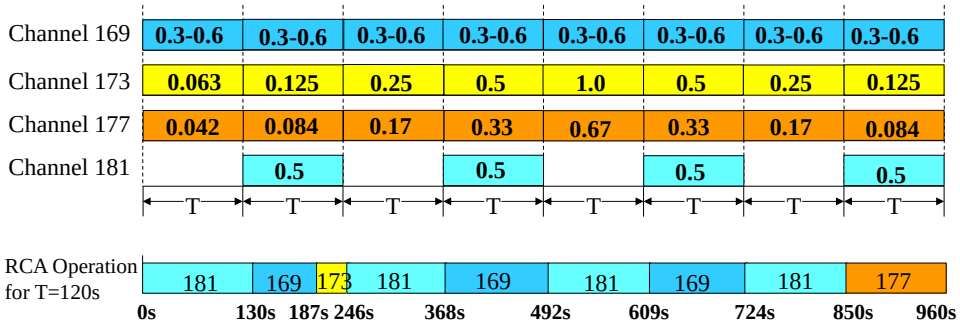


Figure 4.9: Traffic pattern generated for RCA evaluation

performance of RCA in comparison with all static allocations for different values of $T$ is shown in Fig. 4.11a. Each bar represents the average throughput for the duration of the experiment averaged over 10 independent trials. For each value of $T$, the first five bars show the performance of static allocation to channelizations $1-5$. The sixth bar shows the average across the five static channelizations, and the sixth bar represents the performance of RCA.

Different values of time interval $T$ have no impact on the performance of static channelization schemes because the same periodic pattern is generated, and only the duration of the experiment run changes. The performance of the 40 MHz bonded channel is poor because the interfering Wi-Fi AP always operates on its secondary channel (Ch. 169). Fig. 4.11a shows that for $T = 120$ sec, under the given traffic conditions, RCA outperforms the best static allocation by approx. 12%, and the average across all static allocations by approx. 50%. RCA efficiently uses the spectrum by using Ch. 169 when DSRC nodes occupy the shared spectrum while exploiting the idle time periods on Ch. 173, 177, and 181 whenever these channels can yield higher throughput.

The operation of RCA on the observed AP for one instance of $T = 120$ sec is shown at the bottom of Fig. 4.9. At the onset, the spectral analysis reveals low utilization on Ch. 181; thus, RCA uses Ch. 181 with AIFSN = 100. Since the channel conditions do not change, the spectrum is scanned every $T_{\max}$ interval of time; however, Ch. 181 is picked every time due to its near-zero utilization. At $T = 120$ sec, a DSRC node starts transmitting on Ch. 182 (overlapping with Ch. 181). The high AIFSN of the observation pair leads to a sudden drop in throughput, triggering the scan process. Next, Ch. 169 is picked as the best channel. Although the utilization of Ch. 169 is higher, RCA predicts that the low AIFSN (AIFSN = 2) when using this channel would result in a higher throughput in Ch. 169. In the next scan, RCA predicts a higher throughput in Ch. 173, and thus, switches to that channel. RCA continues operation in Ch. 173 until Ch. 183 becomes idle once again. The rest of the RCA operation is shown in Fig. 4.9.

Our experimental findings indicate that the Wi-Fi's opportunistic access to channels that are lightly utilized by DSRC can provide a significant increase in throughput. As the value of $T$ decreases, the performance gain of RCA over the best static allocation scheme decreases.

However, even in the worst-case (i.e., when $T = 10$ sec), the throughput achieved by RCA is approx. 95% of that using the best static allocation scheme, and performs better than all other static allocation schemes. This drop in the relative gain of RCA over the best static assignment is because $T$ becomes comparable to $t_{analyze}$. When an AP detects a throughput drop in the current channel, it takes about $4 - 5$ sec to tune to a new channel. Thus, the throughput gain in the new channel is just sufficient to compensate for the loss in throughput during the RCA analysis phase while the link continues to operate over the busy channel. In the next subsection, we evaluate RCA under more general settings via simulations.

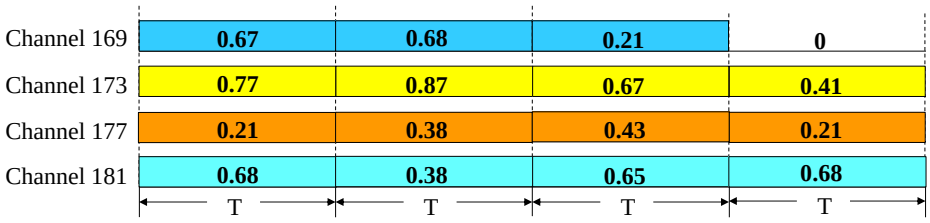


Figure 4.10: Channel utilization ratio of the four channels

### 4.10.2 Simulation Study

We evaluate RCA at scale using *ns-3*. We observe the throughput of a particular Wi-Fi pair operating with saturated traffic. All DSRC nodes move along a straight road with a velocity of 20 m/s. The lane is 20m away from the Wi-Fi transmitter. We disable the rate adaptation algorithm and fix the MCS scheme to MCS-7. The 80 MHz spectrum is sampled $10,000$ times every second to compute the utilization ratio for each channel. 20 DSRC nodes operate in each of Ch. 173, 177, and 181, while two Wi-Fi APs operate on Ch. 169. All other parameters are similar to those used in the testbed experiments.

Results from our simulation studies are shown in Fig. 4.11b. While it is infeasible to validate RCA against all DSRC traffic patterns, we consider two special cases and two arbitrary traffic patterns. The four sets of bars in Fig. 4.11b show the performance of RCA in comparison with each static channelization allocation in the following four cases. In Case I, the utilization ratio is constant across the entire simulation run. The utilization ratios are as shown in the first time interval $0 - T$ in Fig. 4.10 (i.e. 0.67, 0.77, 0.21, 0.68 respectively). In this case, static allocation to Ch. 177 is arguably the best choice (due to its lowest utilization). If the Wi-Fi AP uses RCA, some performance loss results due to periodic scanning of the spectrum. Thus, in this extreme case, the throughput using RCA is smaller (approx. 7%) than the best static allocation scheme, but outperforms all other static allocation schemes.

Next, we generate arbitrary traffic patterns on the four channels (utilizations shown in Fig. 4.10). We set $T = 60$ sec in Case II, and $T = 90$ sec in Case III. In Case IV, we show the upper bound of the performance gain achieved by RCA. In the first time interval of $T$ (we use $T = 60$ sec), Ch. 169 is idle, while all other channels have full utilization. In the

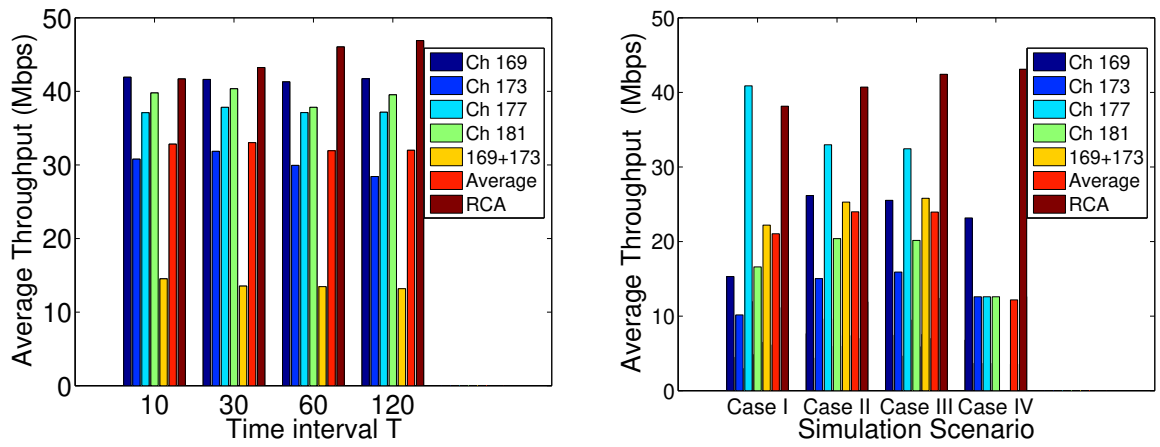


(a) Experimental results (b) Simulation results

Figure 4.11: Evaluation of RCA

second time interval of $T$, Ch. 173 is idle, and the other three channels have full utilization. Similar traffic patterns are generated for Ch. 177 and 181 in the third and fourth intervals respectively. In each of Case II, III, and IV, we observe that the average throughput using RCA is higher than the best static allocation scheme, while the performance gains over other static allocation schemes are even higher.

**Summary:** We see that informed channelization allocation at Wi-Fi APs can yield a substantial increase in the throughput over static channel allocation schemes, except in cases where traffic conditions remain constant forever or change over time intervals smaller than the analyzing delay. In practice, such frequent transitions in traffic patterns can occur at Wi-Fi APs located close to stop lights (depending on the interval of red and green lights). If this interval is small (order of $t_{analyze}$), certain static channel allocations can lead to higher throughput compared to RCA. However, this performance gap is very small as seen in Sec. 4.10.1.

## 4.11 Recommendations on the U-NII-4 Band Channelization

The Tiger Team, in its report [182], could not reach a consensus on band sharing options between DSRC and Wi-Fi. Based on the findings of this work, we suggest the following recommendations for coexistence between DSRC and Wi-Fi in the U-NII-4 band.

In Sec. 4.8.2, it was shown that DSRC nodes experience a high level of packet errors if the shared spectrum is configured as a secondary channel of some Wi-Fi AP. This renders the 80 MHz and one 40 MHz channelizations unusable by Wi-Fi APs. We propose a *combination*

*of the two solutions* proposed in the Tiger Team report to enable harmonious coexistence between DSRC and Wi-Fi users; this approach is described below.

First, as proposed in [183], Wi-Fi transmitters must be able to detect 10 MHz wide 802.11p preambles. Enabling detection of 802.11p preambles at Wi-Fi transmitters will increase the sensing range of Wi-Fi with respect to DSRC nodes (due to a lower threshold of preamble detection as compared to ED). This can also help in alleviating hidden node problems between Wi-Fi and DSRC nodes. Secondly, additional channelization options can be unlocked if the 802.11ac standard mandates full backoff on the secondary channels along with the primary channel. Finally, as suggested in [49], safety-critical applications must have exclusive access to the highest three DSRC channels (i.e., channels 180, 182, and 184). On the other hand, the lower four channels, which can be shared with Wi-Fi, should be used for non-safety applications, since they can tolerate a higher level of packet loss.

Referring to Fig. 4.1, we note that the above recommendations exclude only one 20 MHz channel (Ch. 181) for Wi-Fi usage. On the other hand, all 40 MHz and 80 MHz channelizations can be used by Wi-Fi, thus enabling the use of wider bandwidth channels for supporting high data-rate applications.

# Chapter 5

# Coexistence of Cellular V2X and Wi-Fi

## 5.1 Introduction

The two key technologies that support direct vehicular communications are DSRC and C-V2X. Primarily designed for V2V and V2I, DSRC has been the *de facto* technology for connecting vehicles for over a decade. However, in recent years, C-V2X has emerged as a viable candidate for enabling V2X communications. is a cellular-based V2X technology alternative to DSRC that can enable vehicular communications both in the presence and absence of cellular infrastructure.

Both DSRC and C-V2X are designed to operate in the 5.9 GHz ITS band[1]. Even though this band was allocated for ITS applications in the US as early as 1999, the commercialization of V2X-capable vehicles has been slow. As discussed in Chapter 3, citing this under-utilization, regulators in the US and Europe started considerations to allow unlicensed secondary operations, such as those from Wi-Fi devices, in the ITS band. In the US, FCC issued an NPRM [40] in 2013 that solicited proposals for unlicensed operations in the $5.85-5.925$ GHz band. The unlicensed Wi-Fi devices would operate as secondary users of the spectrum, transmitting only when its incumbent users did not occupy the band. In August 2013, the *DSRC Coexistence Tiger Team* was formed to investigate techniques for harmonious DSRC–Wi-Fi coexistence. In their final report [182], the Tiger Team proposed two mechanisms for DSRC–Wi-Fi coexistence. In Europe, on the other hand, the European Telecommunications Standards Institute (ETSI) has already standardized two mechanisms for DSRC–Wi-Fi coexistence [48].

In addition to the aforementioned co-channel operating scenario, ITS band (i.e., currently DSRC) devices are prone to interference from Wi-Fi devices operating in the adjacent bands due to out-of-band emissions (OOBE), especially if such Wi-Fi devices are located in the proximity of ITS band receivers. In the US, the ITS band spans from $5.85-5.925$ GHz. At the lower end of the ITS band lies the Unlicensed National Information Infrastructure 3 (U-NII-3) band ($5.725-5.85$ GHz), which is used by Wi-Fi devices to service wireless local area networks. Furthermore, to cater to the growing demand for unlicensed spectrum, the FCC in

[1]In addition to the 5.9 GHz band, C-V2X can also operate in a cellular operator's licensed spectrum.

the US is considering a proposal to allow Wi-Fi operations in parts of the $5.925 - 7.125$ GHz band [35], which is, again, adjacent to the ITS band. At the lower end of this spectrum is the U-NII-5 band ($5.925 - 6.425$ GHz) where outdoor operations of Wi-Fi devices may be permitted. To make matters worse, one of the two Tiger Team proposals for DSRC–Wi-Fi coexistence mechanisms places Wi-Fi and DSRC devices in adjacent bands with no guard band! It is, thus, clear that the efficacy of V2X communications is at risk from Wi-Fi-induced interference both due to co-channel and adjacent channel operations. Except for adjacent channel interference from U-NII-3 Wi-Fi devices, all other scenarios discussed above are still in the proposal phase. Thus, a detailed investigation of the impact of Wi-Fi transmissions on the performance of the V2X communications technology is critical.

Because C-V2X is a relatively new technology, studies that have looked at the impact of Wi-Fi transmissions on V2X communications' performance have, to this date, considered DSRC as the default V2X technology. However, it is arguable that C-V2X offers certain advantages over DSRC such as an increased communication range, eNodeB-assisted resource management, well-defined evolutionary paths etc [17]. While the merits and demerits of DSRC and C-V2X are still under debate, a scenario where Wi-Fi-like unlicensed devices coexist with C-V2X in and around the ITS band is a plausible one. Considering the new trends in the automotive industry, the popularity of Wi-Fi, and the development of new V2X use-cases, the FCC has started to take a fresh look at the 5.9 GHz band in the US. Under these circumstances, knowledge of whether and how much Wi-Fi devices' operations in co-channel and adjacent channel scenarios impact the performance of C-V2X is critical in the regulatory decision-making process.

In this chapter, through a systematic simulation study, we investigate the impact of Wi-Fi on C-V2X system performance. The main contributions of this chapter are summarized below.

- We first study the suitability of mechanisms, which were previously developed for DSRC–Wi-Fi coexistence, for the coexistence of C-V2X and Wi-Fi. Naturally, it is expected that such coexistence mechanisms may be inadequate at protecting C-V2X receivers from Wi-Fi interference. Using simulation results derived from our network simulator-3 (ns-3) based simulator, we demonstrate that this indeed the case.

- Using the same simulation platform, we show that Wi-Fi devices operating in channels (both existing and proposed) adjacent to the ITS band can significantly raise the noise floor of C-V2X receivers, thereby causing a considerable loss in the C-V2X system performance.

To the best of our knowledge, ours is the first effort to study and quantify the impact of Wi-Fi devices on the system-level performance of C-V2X. In this chapter, we keep our discussions limited to C-V2X devices using sidelink mode 4, i.e., C-V2X operations without assistance from the cellular infrastructure.

## 5.2 Related Work

The study of coexistence between Wi-Fi and the incumbent ITS technology has garnered considerable attention in the literature. However, existing studies almost exclusively consider DSRC as the ITS technology. At the time of writing this chapter, therefore, studies on the coexistence of C-V2X and Wi-Fi are limited in the literature.

Existing research works predominantly study the impact of Wi-Fi on DSRC under co-channel operating conditions. For example, it has been shown in [185] that if Wi-Fi devices vacate the ITS band for 10 seconds as soon as any DSRC activity is detected, a sufficient degree of protection can be provided to near-by DSRC devices. This has been verified by the FCC in its initial phase of experimental testing for DSRC and Wi-Fi coexistence [273]. While such *sense and vacate* mechanisms are expected to protect DSRC transmissions, the resulting Wi-Fi throughput makes the band unusable for Wi-Fi devices even at moderate vehicular densities. Since the purpose of allowing spectrum sharing between ITS band devices and Wi-Fi is to cater to the ever-growing demand for unlicensed spectrum, such coexistence mechanisms defeat the purpose of opening up additional bands.

To consider the performance of Wi-Fi, different coexistence mechanisms have been proposed, which rely on theoretical models [274], simulation studies [188] and experimental evaluations [189] and provide varying degrees of interference mitigation to DSRC devices while maximizing the Wi-Fi throughput. In addition, ETSI has proposed a range of coexistence mechanisms [48], which, depending on the degree of protection desired for DSRC devices, can strike a balance between Wi-Fi performance and interference mitigation to DSRC devices. In contrast, however, the issue of interference from Wi-Fi devices operating in the adjacent bands has received limited attention in the literature.

In the context of coexistence between C-V2X and Wi-Fi, this issue has only been briefly discussed in [10]. To the best of our knowledge, the question of how well existing coexistence mechanisms fare for C-V2X and Wi-Fi coexistence is unanswered in today's literature. On the other hand, Wi-Fi-induced adjacent channel interference to DSRC and C-V2X devices has been experimentally studied in [275]. Specifically, it has been shown that in the presence of a Wi-Fi Access Point (AP) operating in the U-NII-3 band, the performance of both DSRC and C-V2X, drops significantly. However, experiments in [275] only evaluate the impact of interference due to Wi-Fi transmissions in the U-NII-3 band. The impact of Wi-Fi transmitters operating in the U-NII-4 and U-NII-5 bands, which have a smaller frequency separation from ITS channels is unexplored in the literature.

## 5.3 Background

### 5.3.1 Potential Mechanisms for Co-channel Coexistence

#### 5.3.1.1 Tiger Team Proposals

In the US, the *DSRC Coexistence Tiger Team* was formed in 2013 to study mechanisms by which Wi-Fi devices could operate in the 5.9 GHz band without causing harmful interference to DSRC users operating in the band. The Tiger Team published their final report [182] on mechanisms for DSRC–Wi-Fi coexistence in March 2015. The report described two key proposals.

The first proposal [183], which we refer to as the *sense and vacate* proposal, recommends that Wi-Fi devices operating in the ITS band must be capable of detecting 10 MHz DSRC preambles as *valid* Wi-Fi frames, thereby causing the Wi-Fi transmitters to use the carrier sensing threshold (−85 dBm/10 MHz) to declare the channel busy in the presence of DSRC transmitters. Furthermore, if a Wi-Fi device detects a DSRC frame, it must cease transmissions on all seven ITS channels for an interval of 10 seconds. Following this idle time, the Wi-Fi transmitter can operate on the ITS channels as long as DSRC signals are not detected.

The second proposal [49], which is referred to as the *re-channelization* proposal, recommends re-farming of the ITS band. According to [49], all vehicular *safety* applications should be moved to the upper three ITS channels, i.e., channels 180, 182, and 184 (see Fig. 5.2), while the lower four ITS channels should be used for vehicular non-safety applications. Wi-Fi devices can then be allowed to operate in and share the spectrum with DSRC users in the lower four ITS channels. If this proposal is to be adopted, because Wi-Fi devices coexist only with vehicular non-safety applications, less conservative coexistence mechanisms (i.e., mechanisms that allow for a higher probability of Wi-Fi transmissions) can be adopted.

In the final Tiger Team report, a consensus was not arrived at either of the two coexistence mechanisms. Consequently, both the aforementioned proposals are under consideration in the US for DSRC–Wi-Fi coexistence.

#### 5.3.1.2 ETSI Proposals

As noted in Sec. 3.3, the ETSI in Europe finalized two mechanisms for coexistence between DSRC and Wi-Fi systems. These mechanisms, known as Detect and Mitigate (DAM), and Detect and Vacate (DAV) work with the basic principle that secondary Wi-Fi devices must first sense the channel for DSRC activity, and if DSRC activity is detected, they must deploy the respective coexistence mechanism. Based on the choice of the mechanism (between DAM and DAV), varying degrees of protection can be provided to DSRC systems operating in the vicinity of secondary Wi-Fi devices.

*Detect and Mitigate:* In Wi-Fi devices post 802.11n, Enhanced Distributed Channel Access (EDCA) parameters control the probability with which Wi-Fi transmitters access the channel. EDCA divides packets generated by various applications into four access categories—voice (VO), video (VI), best effort (BE), and background (BK). Each access category has an associated priority, with VO having the highest and BK the lowest priority. This is reflected in the channel access parameters, i.e., minimum and maximum contention windows and arbitration inter-frame spacing (AIFS). The larger the values of these parameters for a traffic type, the smaller is the priority of channel access for that category.

In DAM, if a DSRC frame is detected during Wi-Fi carrier sensing, Wi-Fi transmitters can continue to operate on the ITS channels, but with larger EDCA parameters. Two versions of the DAM have been standardized by ETSI—the *reduced DAM* and *absolute DAM*. The EDCA parameters (i.e., minimum and maximum contention window and AIFS number, or AIFSN) for reduced and absolute DAM along with default EDCA parameters are shown in Table 5.1. If a DSRC frame is detected, the Wi-Fi transmitter must use the DAM (reduced or absolute) parameters for a period of 2 seconds, after which the Wi-Fi device can resume the use of default EDCA parameters. If, however, another DSRC signal is detected during this 2 second interval, the 2 second timer is reset. Depending on the level of interference mitigation required, the reduced DAM (low interference mitigation) or the absolute DAM (high interference mitigation) can be used by Wi-Fi devices.

| **Coexistence Mechanism** | **Parameter** | **BK** | **BE** | **VI** | **VO** |
|---|---|---|---|---|---|
| Default | $CW_{min}$ | 15 | 15 | 7 | 3 |
| | $CW_{max}$ | 1023 | 1023 | 15 | 7 |
| | AIFSN | 7 | 3 | 2 | 2 |
| | TXOP | 0 | 0 | 3.008 msec | 1.504 msec |
| Reduced DAM | $CW_{min}$ | 31 | 31 | 15 | 7 |
| | $CW_{max}$ | 2047 | 2047 | 31 | 15 |
| | AIFSN | 49 | 43 | 31 | 11 |
| | TXOP | 2.528 msec | 2.528 msec | 3.000 msec | 2.080 msec |
| Absolute DAM | $CW_{min}$ | 31 | 31 | 15 | 7 |
| | $CW_{max}$ | 2047 | 2047 | 31 | 15 |
| | AIFSN | 2065 | 2059 | 1029 | 515 |
| | TXOP | 2.258 msec | 2.258 msec | 3.008 msec | 1.504 msec |

Table 5.1: EDCA parameters for default Wi-Fi, reduced DAM and absolute DAM

*Detect and Vacate:* In scenarios where the interference protection offered by DAM is insufficient, ETSI proposes the use of DAV, which is similar in principle to the Tiger Team's sense and vacate proposal but with additional measures for preventing the hidden node problem. A Wi-Fi device using the DAV mechanism, when using one of the ITS channel for the first time, must sense the channel using carrier sensing to detect the presence of DSRC transmit-

ters in its vicinity. If no DSRC transmissions are detected, the Wi-Fi transmitter must send a *probe frame* to detect the presence of *hidden* DSRC terminals. The maximum duration of this probe frame must be 250 $\mu$sec. If the reception of the probe frame is acknowledged, then the Wi-Fi device can operate on the ITS channel with an AIFS of 300 $\mu$sec and a maximum packet duration of 6 msec. If, however, the probe frame is not acknowledged, or if a DSRC frame is detected during the Wi-Fi device's operation, the Wi-Fi device must vacate all ITS channels for an interval of 10 seconds (similar to Tiger Team re-channelization proposal). Following this silent period, the Wi-Fi device must repeat the above procedure before attempting to access the channel.

## 5.3.2 Wi-Fi in Adjacent Bands

### 5.3.2.1 Wi-Fi Spectral Mask

When a Wi-Fi device transmits, it radiates some of its power in the adjacent bands in addition to transmitting on the intended channel. This behavior of Wi-Fi transmitters is dictated by the *spectral mask* of Wi-Fi, which is determined by regulatory agencies. The default spectral mask (class A mask [276]) for the U-NII bands is shown in Fig. 5.1. For different bandwidth configurations, points A, B, C, and D in Fig. 5.1 correspond to different frequency points around the center frequency as shown in Table 5.2.

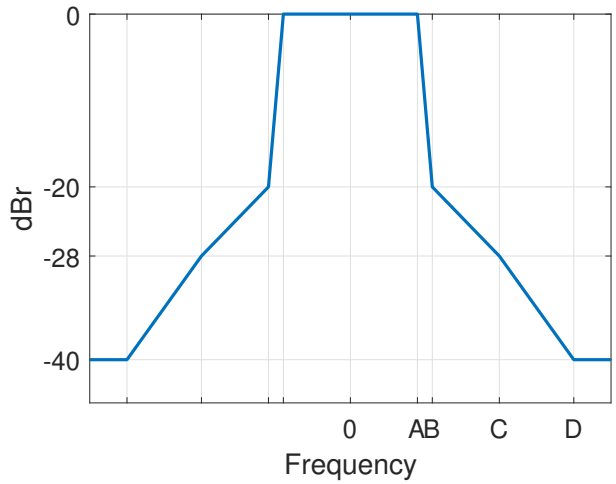


Figure 5.1: The default (class A) spectral mask for Wi-Fi

In the US, as per FCC regulations, the spectral mask shown in Fig. 5.1 represents the maximum power that can be radiated outside the desired band. Commercial devices typically radiate within these power limits, i.e. the actual spectral mask of most devices lies within the maximum permissible mask shown in Fig. 5.1. OOBE characteristics are governed by the device cost; low-cost devices tend to possess low-quality radio frequency (RF) filters,

Table 5.2: Frequency offsets A, B, C and D for the class A mask

| Bandwidth | A (0 dBr) | B (-20 dBr) | C (-28 dBr) | D (-40 dBr) |
|---|---|---|---|---|
| 20 MHz | 9 MHz | 11 MHz | 20 MHz | 30 MHz |
| 40 MHz | 19 MHz | 21 MHz | 40 MHz | 60 MHz |
| 80 MHz | 39 MHz | 41 MHz | 80 MHz | 120 MHz |
| 160 MHz | 79 MHz | 81 MHz | 160 MHz | 240 MHz |

radiating more power outside the desired channel. On the other hand, high-end Wi-Fi devices have superior RF filters, thereby radiating less power in the adjacent channels. Since a wide variety of devices are available commercially, we assume the worst-case spectral mask, i.e. *we assume that Wi-Fi devices transmit with the spectral mask shown in Fig. 5.1.*

#### 5.3.2.2 Interfering Wi-Fi Channels

The granularity of Wi-Fi channels in the 5 GHz bands is 20 MHz. There are no overlapping 20 MHz channels in the 5 GHz bands, unlike the 2.4 GHz bands. The center frequency, $f_c$, of each channel is decided by the channel number, $c$, as $f_c = 5000 + 5 \times \mathrm{c}$. The set of Wi-Fi channels in the U-NII-3, U-NII-4, and U-NII-5 bands is shown in Fig. 5.2.

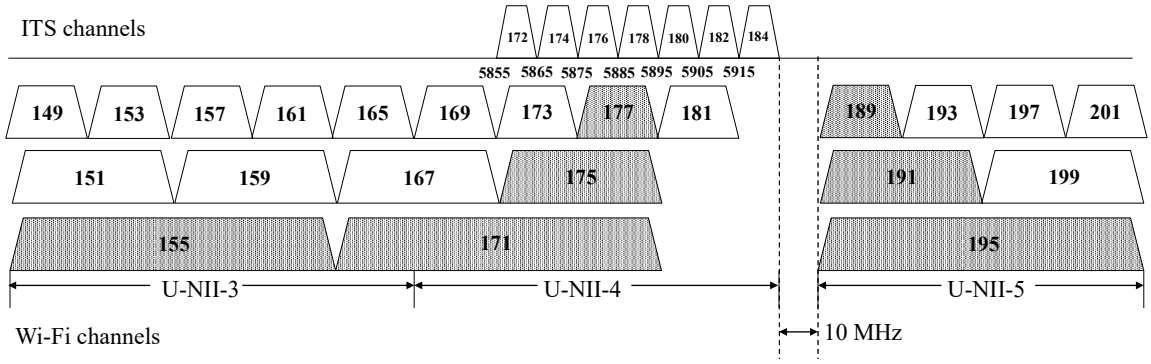


Figure 5.2: ITS channels and U-NII Wi-Fi channels. The shaded channels indicate those adjacent channels that can interfere with ongoing C-V2X operations.

Assuming that Wi-Fi devices radiate negligible power beyond point D in Fig. 5.1, only a few Wi-Fi channels shown in Fig. 5.2 can interfere with C-V2X receivers operating in the ITS band. For example, a Wi-Fi device operating in channel 165 ($f_c = 5825$ MHz) radiates almost all of its power in the $5795 - 5855$ MHz band, which does not cause interference to any of the ITS channels. However, a Wi-Fi device operating in channel 155 ($f_c = 5775$ MHz) radiates most of its power in the $5735 - 5805$ MHz band with undesired emissions in the $5655 - 5735$ MHz and $5805 - 5895$ bands. These undesired emissions can potentially interfere with C-V2X devices receiving packets in ch. 172, 174, 176, or 178. In Fig. 5.2, the shaded

channels are those that can interfere with ongoing C-V2X operations on one of the seven ITS channels.

Note that if U-NII-4 devices are permitted to operate as per the re-channelization proposal, C-V2X safety applications will be confined to ch. 180, 182, and 184. As a result, adjacent band Wi-Fi transmissions will interfere with C-V2X operations only if C-V2X devices use one of these channels. In this case, a Wi-Fi device operating in ch. 173 will not leak any of its power on to ch. 180, 182, or 184. Furthermore, under this proposal, the use of ch. 181 for Wi-Fi operations will be prohibited. Consequently, ch. 173 and 181 do not cause any adjacent channel interference to the C-V2X system even though they may cause interference in co-channel operating scenarios.

## 5.4 Simulation Setup

To perform our simulation study, we implement the C-V2X mode 4 algorithm in network simulator 3 (ns-3). We extended support for sidelink mode 4 over the simulator developed in [277], where the authors extend the ns-3 simulator to support sidelink modes 1 and 2. Our simulator conforms to all 3GPP Release 14 specifications for sidelink mode 4 as per [26, 27, 28]. To simulate interference from Wi-Fi transmissions in the adjacent bands, we implement the spectral mask for Wi-Fi for different bandwidths as discussed in Sec. 5.3.2.1. Furthermore, for all coexistence mechanisms described in Sec. 5.3.1, we assume that the same mechanisms apply if the incumbent ITS technology is C-V2X. For example, in all co-channel coexistence proposals, the Wi-Fi transmitters can detect C-V2X transmissions and use a carrier sensing threshold of $-85$ dBm/10 MHz.

We consider the *urban* scenario defined in [278] to perform our simulation study. The importance of this scenario stems from the fact that most roadside Wi-Fi deployments can be observed in urban areas, while at the same time, these areas are prone to high vehicular densities. Thus, among the various scenarios in which C-V2X and Wi-Fi users operate in each others' vicinity, the urban scenario is the most likely.

The simulation setup consists of a Manhattan grid layout shown in Fig. 5.3, where each block size is $250 \times 433$ m as recommended in [278]. Vehicles are dropped using Poisson distribution, with the inter-vehicle distance computed from the average vehicle velocity (the inter-vehicle distance is equal to the distance traveled by a vehicle in 2.5 seconds [278]). The total number of vehicles simulated is 600. Four Wi-Fi networks are simulated along the roads as indicated in Fig. 5.3. The number of Wi-Fi clients associated with the AP in each network is ten, and these clients are distributed uniformly around the AP in a circle of radius 10 m. To understand the worst-case impact of Wi-Fi transmissions on C-V2X performance, we assume saturated traffic at all Wi-Fi devices of traffic class BE ($\sim 90\%$ duty cycle). The performance metric chosen in our study is the packet delivery ratio (PDR), which is the ratio of the number of packets received at a C-V2X receiver from a given transmitter to the

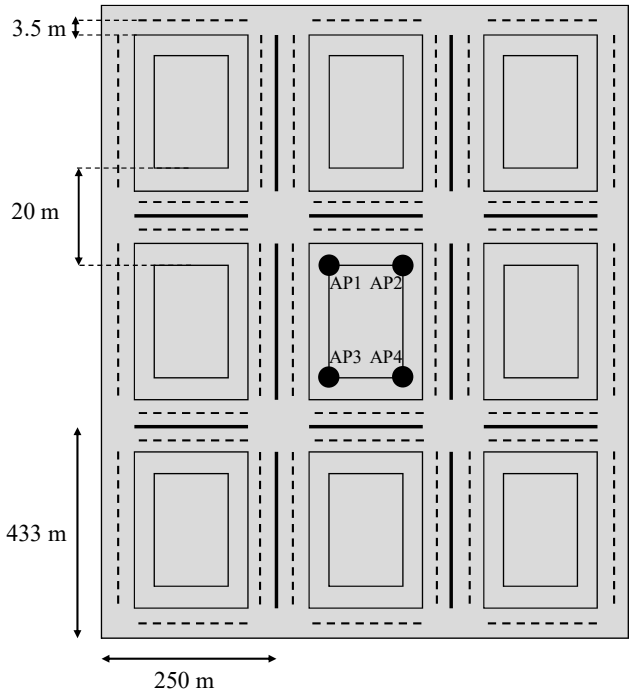


Figure 5.3: The Manhattan grid layout and location of Wi-Fi APs

number of packets transmitted by that transmitter. Each simulation run lasts for an interval of 20 sec., where Wi-Fi devices begin to transmit at t=1 sec. and C-V2X devices transmit from t=2 sec. to t=17 sec. All simulation parameters used in this chapter are outlined in Table 5.3. These simulation parameters and the performance metric, i.e. PDR, are widely used in other works such as in [30]. Unless explicitly stated otherwise, the Wi-Fi power is set to 30 dBm. For all simulation results presented in Sec. 5.5, the performance of C-V2X is averaged over C-V2X receivers located in the intersection region next to the four Wi-Fi APs shown in Fig. 5.3.

Table 5.3: Simulation parameters for evaluating C-V2X – Wi-Fi coexistence

| **Parameter** | **Value** | **Parameter** | **Value** |
|---|---|---|---|
| Avg. Velocity | 60 kmph | Inter-vehicle dist. | 41.67 m |
| Propagation Loss | WINNER+ B1 | C-V2X Tx. power | 23 dBm |
| C-V2X periodicity | 10 Hz | C-V2X bandwidth | 10 MHz |
| C-V2X pkt. size | 190, 300 bytes | Wi-Fi PHY rate | 24 Mbps |
| Wi-Fi pkt. size | 1024 bytes | Wi-Fi traffic | Saturated |

## 5.5 Simulation Results

### 5.5.1 Co-channel Coexistence

In this sub-section, we take a look at the performance of C-V2X sidelink mode 4 when Wi-Fi devices share the spectrum using coexistence mechanisms described in Sec. 5.3.1.

Fig. 5.4a shows the average PDR observed across all C-V2X receivers located in the four intersection regions as a function of the distance between that receiver and a C-V2X transmitter. As a baseline for comparison, we show the performance of C-V2X sidelink mode 4 in the *no Wi-Fi* scenario, i.e., scenarios where C-V2X devices are free from any external interference. In such scenarios, any losses in C-V2X performance are due to propagation effects and packet collisions resulting from the use of the C-V2X resource reservation algorithm.

We begin by observing that unhindered transmissions from Wi-Fi devices operating in the same channel (i.e., with no coexistence mechanism) significantly bring down the PDR of C-V2X receivers. In fact, the average 90 % reliability range is reduced merely to 20 meters! It must be noted that for urban scenarios, the 3GPP sets a PDR requirement of 90 % for transmitter-receiver distances up to 120 m [115]. In the absence of co-channel Wi-Fi transmitters, the observed PDR at this transmitter-receiver distance is 85 %. However, this is reduced to only about 20 % in the presence of Wi-Fi transmissions. It is, thus, clear that if C-V2X and Wi-Fi devices are to share the spectrum, effective coexistence mechanisms that mitigate interference at C-V2X receivers are needed.

In light of the aforementioned discussions, Fig. 5.4a indicates that the reduced DAM mechanism is completely ineffective in preventing interference at C-V2X receivers. In fact, the average PDR observed at a C-V2X receiver is only marginally better than the case where Wi-Fi devices use no coexistence mechanism. The reduced DAM mechanism fails at interference mitigation because it was designed for DSRC–Wi-Fi coexistence bearing the similarities between the MAC protocols of DSRC and Wi-Fi. Because DSRC and Wi-Fi both use Carrier Sense Multiple Access for channel access, by moderately increasing the contention parameters of Wi-Fi transmitters (as is the case in reduced DAM, see Table 5.1), the probability of Wi-Fi channel access can be substantially lowered. However, C-V2X uses a considerably different MAC protocol from Wi-Fi. C-V2X transmitters sense and reserve the spectrum and once reserved, C-V2X devices transmit on the reserved resource without any further sensing. As a result, even if Wi-Fi devices are already transmitting on the channel, C-V2X devices proceed with their transmissions, thereby potentially causing interference at C-V2X receivers. Furthermore, the choice of contention parameters for reduced DAM as shown in Table 5.1 results in AIFS of 0.4 msec[2], which is smaller than a C-V2X sub-frame duration (1 msec). As a result, if no C-V2X device within the sensing range of the Wi-Fi transmitter transmits in a given sub-frame, the Wi-Fi device will get access to the channel in that sub-frame. Since reduced DAM allows a maximum transmit opportunity of 2.5 msec, C-V2X

[2]AIFS = 16 $\mu$sec + (AIFSN $\times$ 9) $\mu$sec.

transmissions in the next two sub-frames are at risk from Wi-Fi interference. Thus, for every single idle C-V2X sub-frame, the next two sub-frames are at risk from Wi-Fi-induced interference. This manifests itself in the ineffectiveness of reduced DAM in mitigating interference at C-V2X receivers.

On the other hand, Fig. 5.4a shows that when Wi-Fi devices use one of the other three coexistence mechanisms, the C-V2X performance is practically unaffected. This is expected with the ETSI DAV and Tiger Team's sense and vacate mechanisms since Wi-Fi devices vacate the spectrum as soon as C-V2X activity is detected. In this work, we assume 100 % probability of detection of C-V2X signals at the Wi-Fi transmitter (as long as the Wi-Fi device is not in the transmit state). Consequently, Wi-Fi devices cease transmissions as soon as C-V2X transmissions are detected, thereby resulting in negligible Wi-Fi-induced performance loss to the C-V2X system.

A more interesting behavior is observed when Wi-Fi devices use the absolute DAM mechanism for coexistence. Since we simulate BE traffic at Wi-Fi devices, Wi-Fi transmitters use AIFSN of 2065, which translates to AIFS of 18.5 msec (i.e., 18.5 sub-frames). Even in modest vehicular traffic conditions, the probability that there are no C-V2X transmissions in 18 consecutive sub-frames is very small. As a result, while a Wi-Fi device continues to defer channel access for 18.5 milliseconds (after a C-V2X transmission is first detected), it is likely to detect at least one C-V2X transmission during this interval and consequently continue to use the extended contention parameters. Furthermore, every time a C-V2X transmission is detected, the AIFS countdown is reset and as soon as the C-V2X transmission ends, the Wi-Fi device must wait for an additional AIFS duration (i.e., additional 18.5 sub-frames) before resuming its back-off countdown. As a result, Wi-Fi devices continue to defer channel access to C-V2X devices as long as the C-V2X traffic density is sufficient enough that there is at least one C-V2X transmission (within the Wi-Fi device's sensing range) in every 18 consecutive sub-frames. Thus, even though the absolute DAM mechanism is fundamentally similar to the reduced DAM mechanism and was originally designed by leveraging the similarities in MAC protocols of DSRC and Wi-Fi, the same mechanism also effectively mitigates interference to C-V2X users.

While interference mitigation at the C-V2X receivers is an absolute necessity, it is also essential to look at the Wi-Fi performance resulting from the use of the above coexistence mechanisms. The eventual goal of allowing Wi-Fi access in the ITS band is to provide additional unlicensed bands so that emerging bandwidth-intensive applications can be effectively supported. Fig. 5.4b shows the aggregate Wi-Fi throughput as a result of using the different coexistence mechanisms. All mechanisms that provide a sufficient degree of protection to the C-V2X system do so at the cost of complete loss in Wi-Fi throughput. Note that the small Wi-Fi throughput observed in these cases is due to Wi-Fi transmissions in intervals before and after the C-V2X devices are turned on (i.e., t=1 sec to t=2 sec for all mechanisms and t=19 sec to t=20 sec for the absolute DAM). Thus, *even though conservative schemes such as the absolute DAM, DAV or the Tiger Team's sense & vacate can achieve interference mitigation, these mechanisms render the channel unusable for any meaningful Wi-Fi*

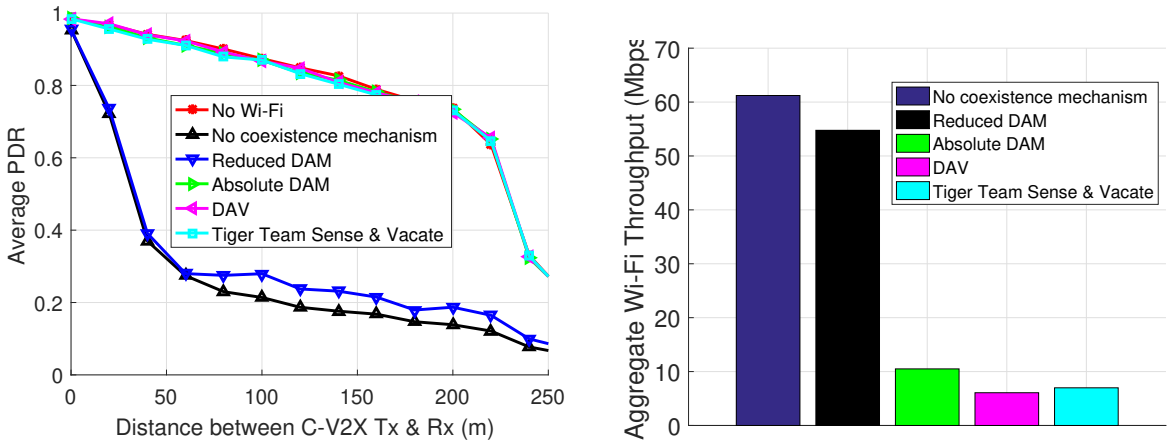


(a) Impact on C-V2X performance

(b) Wi-Fi throughput

Figure 5.4: Evaluation of co-channel coexistence mechanisms

*applications.*

### 5.5.2 Adjacent Channel Interference

Interference from Wi-Fi device(s) operating in the adjacent band can affect C-V2X performance in two ways. First, OOBE from Wi-Fi transmitters can raise the noise floor of a C-V2X receiver, which will result in the lowering of the Signal-to-Interference-plus-Noise Ratio (SINR) of the received C-V2X packet. This can result in the loss of a C-V2X packet, which could have been received successfully if not for the adjacent band Wi-Fi device. Second, adjacent channel Wi-Fi transmissions will increase the energy content of resources within the sensing window, which can lead to the selection of a non-ideal resource from the selection window (see Sec. 2.2.5.1). The resulting C-V2X system level performance will drop due to the combined effect of the two aforementioned factors. We investigate this performance drop in this sub-section.

#### 5.5.2.1 Interference from U-NII-3 Wi-Fi

We first look at the impact of adjacent channel interference resulting from Wi-Fi operations in the U-NII-3 band. What distinguishes this scenario from Wi-Fi's (proposed) operations in the U-NII-4 and U-NII-5 bands is that in the US and many other countries, Wi-Fi operations in the U-NII-3 band are already present, whereas those in the U-NII-4/5 band are still under consideration. Consequently, C-V2X devices operating in one of the channels affected by Wi-Fi transmissions in the U-NII-3 band are already set to suffer from Wi-Fi-induced interference.

It must be noted that the only U-NII-3 channel that can cause interference at a C-V2X

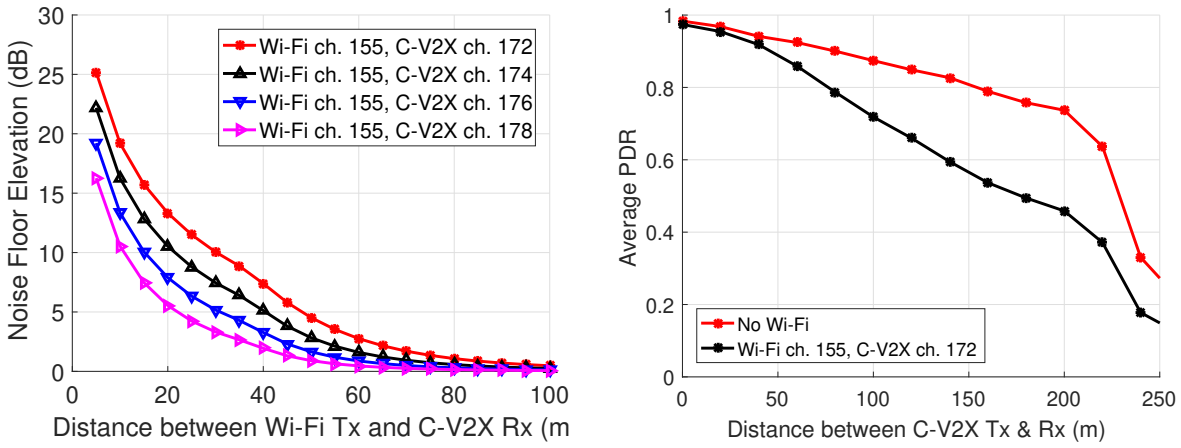


(a) Noise floor elevation (b) System performance

Figure 5.5: Impact of U-NII-3 adjacent channel interference on C-V2X performance

receiver is channel 155[3], OOBE from which stretches up to 5.895 MHz, potentially interfering with C-V2X operations in ch. 172, 174, 176, and 178. Fig. 5.5a shows the elevation in the noise floor observed at a C-V2X receiver as a function of its distance from the Wi-Fi transmitter. This is computed as the difference between the noise floor at the C-V2X receiver when the Wi-Fi device in the adjacent channel transmits and when there is no Wi-Fi device in the adjacent channel (both in the absence of C-V2X transmissions). It is seen that for a C-V2X receiver operating on ch. 172 and located very close to the Wi-Fi transmitter ($< 10$ m), its noise floor can be elevated by as much as 25 dB! As the frequency separation between the Wi-Fi and C-V2X operating channel increases (i.e., from ch. 172 through 178), Wi-Fi transmissions begin to have a smaller impact on the C-V2X receivers' noise floor. Nevertheless, as long as the Wi-Fi transmitter operates close to the C-V2X receivers, the C-V2X performance remains susceptible to Wi-Fi interference.

Fig. 5.5b shows the impact of the aforementioned elevated noise floor on the system level performance of C-V2X operating in ch. 172, where the impact of Wi-Fi devices operating in ch. 155 is the largest. For short distances between the C-V2X transmitter and receiver, the received signal strength is usually large enough to overcome the negative effects of the elevated noise floor. However, as the distance between the C-V2X transmitter and receiver increases, the interference power due to adjacent channel Wi-Fi operations becomes significant compared to the desired C-V2X signal power, thereby resulting in a large fraction of C-V2X packets being dropped at the C-V2X receiver. In the simulated scenario, the 90 % reliability range (i.e., the C-V2X transmitter-receiver distance up to which the PDR is greater than 90 %) is reduced to nearly half (from $\sim 80$ m to $\sim 45$ m)!

[3]For all other U-NII-3 channels, all ITS channels fall beyond point D in Fig. 5.1. We ignore the impact of such Wi-Fi channels on C-V2X performance.

#### 5.5.2.2 Interference from U-NII-4 and U-NII-5 Wi-Fi

Next, we look at the impact of transmissions from Wi-Fi devices operating in those bands that are yet to be finalized for unlicensed use. Since Wi-Fi operations in these channels are yet to be standardized, results presented in this section can be used to make an informed decision on future channelizations of the U-NII-4 and U-NII-5 bands. In terms of Wi-Fi U-NII-4 channels, we first note that if the re-channelization mechanism is permitted by regulations, all ITS safety applications will be moved to channels 180, 182, and 184, allowing Wi-Fi devices to operate in the newly opened up U-NII-4 channels shown in Fig. 5.2. As a result, the only C-V2X channels affected by U-NII-4 Wi-Fi transmissions are 180, 182, and 184. On the other hand, there is a 10 MHz guard band between channel 184 and the lower edge of the U-NII-5 band. Depending on the channel bandwidth of the U-NII-5 channels, these channels can affect some or all of the seven ITS channels.

Fig. 5.6 shows the elevation in the noise floor for different Wi-Fi and C-V2X channel configurations. In each case, the Wi-Fi transmitter is located 10 m away from the C-V2X receiver. As shown in Fig. 5.5a, for a C-V2X receiver operating on ch. 172, a Wi-Fi transmitter located 10 m away and operating on ch. 155 raises the noise floor by 20 dB. What is interesting to note is that C-V2X ch. 172, even though being the lowermost of all ITS channels, is affected by Wi-Fi transmissions in ch. 195, which is the first 80 MHz channel in the U-NII-5 band! Like ch. 172, ch. 174, 176, and 178 are only affected by Wi-Fi operations in ch. 155 and 195 due to their large bandwidths.

On the other hand, C-V2X ch. 180 through 184 are impacted differently by different Wi-Fi channels depending on the Wi-Fi channel width and the frequency separation between the Wi-Fi and C-V2X channels. The C-V2X ch. 180 is affected heavily by Wi-Fi transmissions on ch. 171, 175, and 177, with ch. 177 creating the largest interference on ch. 180 among all Wi-Fi and C-V2X channel configurations. When we look at the impact on ch. 182, on the other hand, Wi-Fi ch. 171 and 175 create larger interference than ch. 177. This highlights an important fact that OOBE resulting from Wi-Fi operations on a 20 MHz channel create the maximum interference at the immediately adjacent channel (e.g., Wi-Fi ch. 177 and C-V2X ch. 180). This can be explained by the fact that when a Wi-Fi device doubles its bandwidth, the power per sub-carrier is reduced by 3 dB for the same total radiated power. Consequently, the narrowest channel configuration, i.e. 20 MHz, is likely to leak the maximum power on to the immediately adjacent channel. However, interference due to wider Wi-Fi channels (such as ch. 171 or 175) span a larger number of ITS channels and consequently, have a larger impact on far-away ITS channels. Similarly, the Wi-Fi ch. 191 and 195 in the U-NII-5 band have a larger impact on C-V2X ch. 184 than the Wi-Fi ch. 189 (due to the 10 MHz guard band).

Important observations from Fig. 5.6 are summarized in Table 5.4, which shows the set of Wi-Fi channels that interfere with different ITS channels and the Wi-Fi channel that results in the largest interference at each of the seven ITS channels.

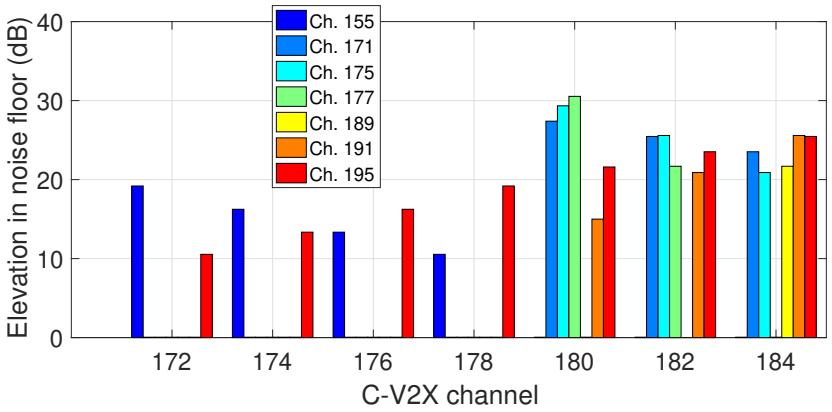


Figure 5.6: Elevation in the noise floor for C-V2X receiver

| **C-V2X channel** | **Wi-Fi channels impacting C-V2X performance** | **Maximum impact channel** |
|---|---|---|
| 172 | 155, 195 | 155 |
| 174 | 155, 195 | 155 |
| 176 | 155, 195 | 195 |
| 178 | 155, 195 | 195 |
| 180 | 171, 175, 177, 191, 195 | 177 |
| 182 | 171, 175, 177, 189, 191, 195 | 175 |
| 184 | 171, 175, 177, 189, 191, 195 | 191 |

Table 5.4: Summary of the impact of adjacent channel Wi-Fi interference

The impact of adjacent channel interference from Wi-Fi devices operating in the U-NII-4 and U-NII-5 bands on the system-level performance of C-V2X is shown in Fig. 5.7. Note that the reduction in the PDR of the C-V2X system at a given distance in the presence of Wi-Fi is directly related to the elevation in the noise floor observed at the C-V2X receiver as shown in Fig. 5.6. Thus, the C-V2X system performance drops the most when C-V2X and Wi-Fi operate in ch. 180 and ch. 177, respectively for the U-NII-4 band scenario (see Fig. 5.7a). On the other hand, the impact of U-NII-5 transmissions is maximum when C-V2X and Wi-Fi operate in ch. 184 and ch. 191, respectively (see Fig. 5.7b).

### 5.5.3 Interference Mitigation

In what follows, we describe two ways by which adjacent channel interference from Wi-Fi devices can be minimized.

*Tighter Masks:* By controlling OOBE from Wi-Fi transmitters operating in the U-NII bands, less power can be radiated into channels reserved for ITS applications. The tighter the

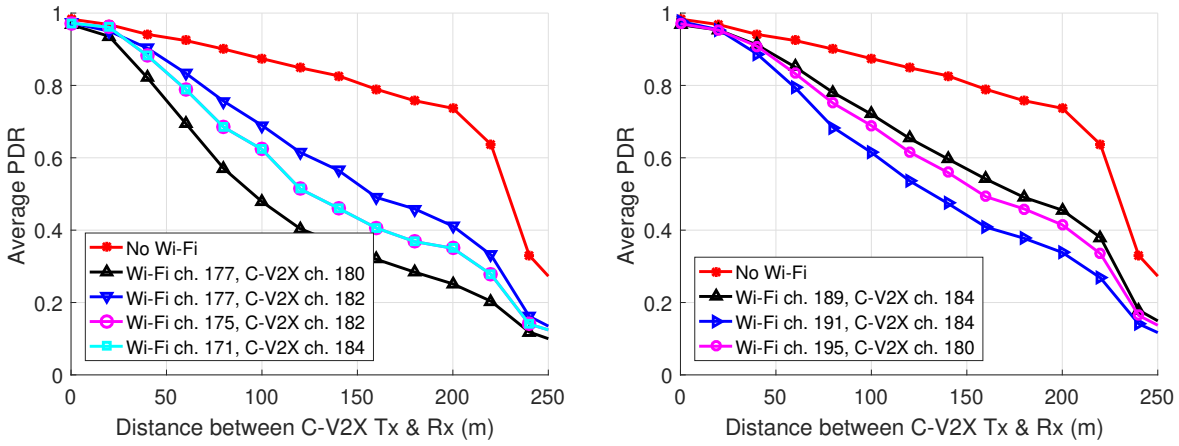


(a) U-NII-4 (b) U-NII-5

Figure 5.7: Impact of U-NII-4 and U-NII-5 adjacent channel interference on C-V2X performance

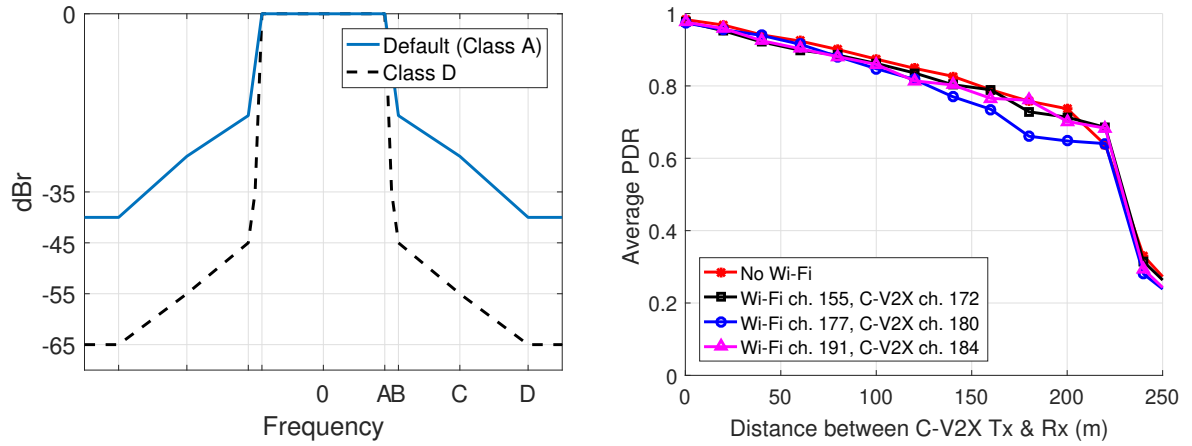


(a) Class D spectral mask (b) Impact on C-V2X system performance

Figure 5.8: Impact of Class D mask on C-V2X performance

spectral mask, the lower will be the impact of Wi-Fi transmissions on C-V2X performance. The *Class D* spectral mask [276] (see Fig. 5.8a) has the most stringent OOBE requirements among all Wi-Fi spectral masks, leaking the least power into adjacent channels. Fig. 5.8b shows that in the presence of a Wi-Fi network operating on any of the adjacent channels and using the class D mask, the interference at a C-V2X receiver largely alleviated. In fact, when Wi-Fi and C-V2X devices operate in channels 177 and 180, respectively, which is the case of maximum adjacent channel interference (see Fig. 5.6), the 90% PDR range is reduced by only 5 meters.

*Reduced Wi-Fi Transmission Power/Indoor Operations:* The disadvantage of using tighter spectral masks is that to use such masks, high-quality RF filters need to be used, which leads to an increase in the cost of Wi-Fi devices. Such an increase in the cost can be

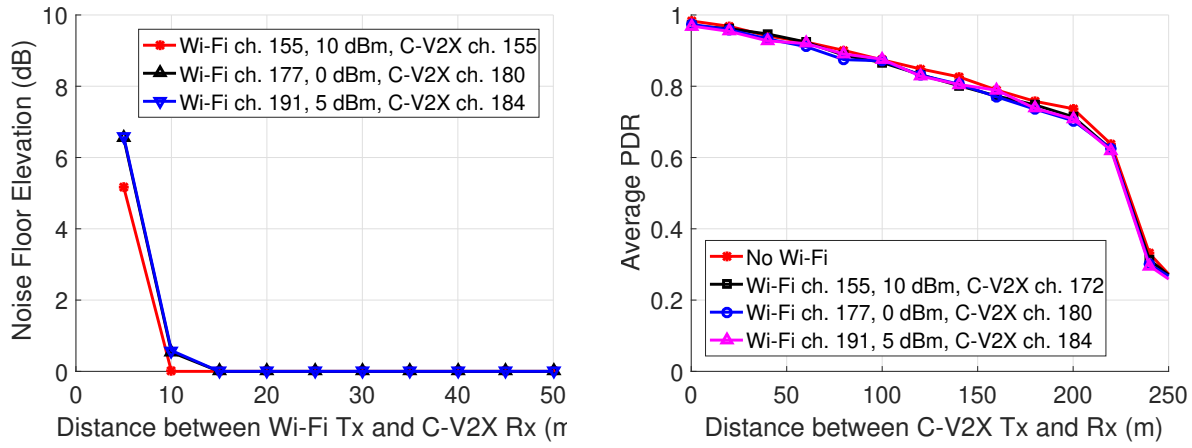


(a) Elevation in C-V2X receiver noise floor (b) Impact on system level performance

Figure 5.9: Impact of Wi-Fi power on C-V2X performance

prohibitive to provisioning Wi-Fi services as is reported in [279]. A simpler alternative to tighter spectral masks is to reduce the maximum permissible transmission power of Wi-Fi devices in channels that can potentially interfere with C-V2X operations. Fig. 5.9a shows that the elevation in the noise floor due to adjacent channel Wi-Fi transmissions can be reduced to zero by reducing the Wi-Fi transmission power (U-NII-3, U-NII-4 and U-NII-5 power levels of 10 dBm, 0 dBm and 5 dBm, respectively) beyond a distance of 10 m between the Wi-Fi transmitter and the C-V2X receiver. Fig. 5.9b shows that the resulting loss in the performance of C-V2X is negligible. Further, by restricting the usage of such Wi-Fi devices to indoor environments, a separation of 10 m between Wi-Fi devices and C-V2X receivers can be achieved. Additionally, the confinement of Wi-Fi to indoor environments provides additional protection to C-V2X devices due to attenuation from walls ($\sim$ 10 dB), windows ($\sim$ 6 dB), and doors ($\sim$ 6 dB).

While reducing the power of Wi-Fi devices to $0-10$ dBm may reduce the interference to C-V2X devices, the lower Wi-Fi transmission power will substantially reduce the signal strength at Wi-Fi receivers, thereby resulting in lower SINR of received Wi-Fi packets. Consequently, Wi-Fi devices may be unable to use higher-order modulation and coding schemes (MCS) that are enabled by the latest Wi-Fi technologies, such as 256-QAM in 802.11ac. Furthermore, for the same MCS, the reduction in power from 30 dBm to $0-10$ dBm can reduce the transmission range in indoor environments by nearly a factor of 8 [280]. Therefore, *a reduction in Wi-Fi power to mitigate interference to C-V2X may reduce the lucrativeness of those Wi-Fi channels that are adjacent to C-V2X channels.* Eventually, it is up to the regional regulators as to which alternative to select (i.e., tighter masks or lower transmit power). However, from the discussions in this section, it is clear that without employing such mechanisms, the only other option to sufficiently protect C-V2X devices in the vicinity is to prohibit Wi-Fi operations in all those channels that are adjacent to the ITS band. If the latter is the case, the Wi-Fi community will have to let go of three 80 MHz channels (ch. 155, 171 & 195), two 40 MHz channels (ch. 175 & 191) and two 20 MHz

channels (ch. 177 & 189)!

## 5.6 Summary & Discussions

### 5.6.1 Co-channel Coexistence

Results presented in Sec. 5.5.1 indicate that existing coexistence mechanisms fall into two categories. On one hand, a technique such as the reduced DAM fails at mitigating Wi-Fi-induced interference at C-V2X receivers owing to the mechanism's reliance on DSRC and Wi-Fi MAC protocol similarities. On the other hand, the DAV and Tiger Team's sense & vacate mechanisms use a conservative approach, whereby Wi-Fi devices must completely cease transmissions in the ITS band for a large interval of time. Consequently, as long as the ITS technology signal is reliably detected, mechanisms such as DAV and sense & vacate are agnostic to the choice of the incumbent ITS technology.

The absolute DAM mechanism is a notable exception to the above discussion. Even though this mechanism was developed for DSRC–Wi-Fi coexistence, the choice of very large contention parameters minimizes the impact of Wi-Fi on the C-V2X system performance. A common link, however, between the absolute DAM, DAV and sense & vacate is that these mechanisms practically result in no utilization of the ITS band by Wi-Fi devices. It is, thus, clear that existing coexistence mechanisms are not effective at enabling *harmonious* and meaningful coexistence between C-V2X and Wi-Fi devices. Unsurprisingly, this is an expected conclusion because these mechanisms were originally designed for DSRC–Wi-Fi coexistence. An effective C-V2X–Wi-Fi coexistence mechanism is one that lets Wi-Fi devices utilize time-gaps between C-V2X transmissions, thereby optimizing Wi-Fi performance while ensuring that C-V2X system performance remains unaffected. Whether such a mechanism can be developed with reasonable implementation complexity remains an interesting research problem, which we will investigate in our future work. Nevertheless, it can be concluded that unless novel coexistence mechanisms, which are tailored to the specifics of C-V2X and Wi-Fi MAC protocols, are developed, *Wi-Fi and C-V2X devices cannot meaningfully coexist in the same spectrum.*

### 5.6.2 Adjacent Channel Interference

We first note that because U-NII-3 Wi-Fi devices are already deployed, not much can be done about interference resulting from such devices. At best, it must be ensured that the use of channel 155 must be avoided in all scenarios where the Wi-Fi AP or clients can come in the proximity of vehicles.

To ensure that such adjacent channel U-NII-4 transmissions do not affect C-V2X perfor-

mance, proactive measures must be taken. For example, if channel 180 is selected for C-V2X safety applications, Wi-Fi devices must strictly avoid using all adjacent channels. On the other hand, if channel 182 or 184 is chosen for C-V2X safety applications, the use of ch. 171 and 175 must be restricted, whereas ch. 177 may be permitted at lower transmission powers. Furthermore, based on our findings in Sec. 5.5.3, if permitted, it is best to confine U-NII-4 devices within indoor environments.

Interference from Wi-Fi users in the U-NII-5 band is of grave concern in the US considering that the 5G Automotive Association (5GAA) is considering C-V2X operations in ch. 182 and 184 [51]. The current 6 GHz FCC NPRM [35] only considers the impact of co-channel Wi-Fi transmissions on the incumbent technologies in the U-NII-5 band. As a preliminary approach, the use of geo-location databases to ascertain the absence of incumbent users is considered. If the channel is found to be idle after querying the database, Wi-Fi devices are free to transmit, even in outdoor environments. However, outdoor U-NII-5 installments can place Wi-Fi transmitters in close proximity to C-V2X receivers. From our discussions in Sec. 5.5.2.2, it is evident that in such cases, the C-V2X system performance can be significantly degraded. It is, therefore, critical that all stakeholders must consider the impact of allowing Wi-Fi operations in the U-NII-5 band on C-V2X system performance. Regulations must either restrict (i.e., impose tighter masks or lower transmit powers) or prohibit the use of ch. 189, 191, and 195 in all deployment scenarios where Wi-Fi and C-V2X can operate in close proximity.

## 5.7 Chapter Summary

In this chapter, we perform a comprehensive simulation study on the impact of Wi-Fi transmissions in and around the 5.9 GHz ITS band on the system-wide performance of C-V2X sidelink mode 4. Our work, being the first of its kind, is driven by an objective to help inform the regulatory process in its decision to allow Wi-Fi operations in co-channel scenarios with C-V2X (i.e., in the U-NII-4 band) and in adjacent channel scenarios (i.e., in the U-NII-4 and U-NII-5 bands). Our evaluation of existing co-channel coexistence mechanisms, which were originally developed for DSRC–Wi-Fi coexistence, unsurprisingly leads to the conclusion that these mechanisms are not suitable for C-V2X–Wi-Fi coexistence. This calls for the design of novel mechanisms that enable harmonious and meaningful C-V2X–Wi-Fi coexistence. Furthermore, our simulation study indicates that the C-V2X system performance is also at risk from Wi-Fi operations in the adjacent bands. While not much can be done regarding interference from existing Wi-Fi devices in the U-NII-3 band, we highlight the need for regulators to take into consideration the impact of U-NII-4 and U-NII-5 band Wi-Fi transmitters on the C-V2X performance.

# Chapter 6

# Coexistence of New Radio Unlicensed and Wi-Fi in the 6 GHz Bands

The FCC in the US recently approved spectrum sharing rules for the 6 GHz bands in its 6 GHz Report & Order [2]. Similarly, regulators in Europe are considering to allow unlicensed operations in the 6 GHz bands [34]. Arguably, Wi-Fi is the most popular unlicensed RAT in use today. Naturally, the IEEE 802.11 Working Group is actively working on 6 GHz rules for the upcoming IEEE 802.11ax standard of devices [53]. Wi-Fi devices certified as per the 802.11ax specifications are referred to as Wi-Fi 6 devices, while those capable of operating in the 6 GHz bands will be referred to as Wi-Fi 6E devices. Furthermore, the next generation of Wi-Fi devices—which will be based on IEEE 802.11be— is likely to be equipped with several features tailored for operations in the 6 GHz bands [72, 76]. Simultaneously, the 3GPP recently released the specifications for the 5G NR-U in its Release 16 [33], which includes provisions for NR-U devices to operate in the 6 GHz bands [96, 281]. Thus, spectrum sharing between Wi-Fi 6E and NR-U devices is imminent in the 6 GHz bands.

Spectrum sharing between Wi-Fi and 3GPP-based unlicensed RATs is hardly a new challenge. As discussed in Chapter 3, during the design of previous 3GPP-based unlicensed RATs—LTE LAA in Release 13 and enhanced LAA in Release 14—there was significant debate on whether these cellular-based RATs can coexist harmoniously with the millions of existing Wi-Fi networks in the 5 GHz bands [245]. After careful deliberations, to ensure that the existing Wi-Fi deployments remain unharmed, theMAC protocol of LAA was designed to be similar to that of Wi-Fi [32]. Thus, at their core, both Wi-Fi and LAA use LBT-based MAC protocols for channel arbitration[1].

The 6 GHz unlicensed spectrum, on the other hand, is *greenfield* spectrum, i.e., these are bands where neither Wi-Fi nor any 3GPP-based unlicensed RATs presently operate. This has significant implications for the design of unlicensed RATs that will share the 6 GHz bands. Firstly, NR-U is no longer constrained to provide an additional degree of protection to Wi-Fi devices[2] operating in these new bands. Secondly, for the first time since the design of IEEE 802.11a, Wi-Fi 6E devices operating in the 6 GHz bands need not be backward

[1]Note that the LBT-based MAC protocol in Wi-Fi is known as CSMA/CA. Due to their functional similarities, we use the terms LBT and CSMA/CA interchangeably.

[2]In the 5 GHz bands, compared to the detection threshold used by Wi-Fi devices to detect LAA signals (−62 dBm), LAA networks used a 10 dB lower detection threshold (−72 dBm) to detect Wi-Fi signals on the air.

compatible with older generations of Wi-Fi devices. Thus, the 6 GHz bands provide a rare opportunity for the design of *novel* coexistence mechanisms between unlicensed RATs.

In this chapter, we use tools from stochastic geometry to derive an analytical model to assess the performance of Wi-Fi 6E and NR-U when they coexist. Our derived analytical model can be applied to all frequency bands in which Wi-Fi 6E and NR-U systems can operate. However, we interpret the results from our model in the context of the 6 GHz bands because these bands allow us to take measures that are otherwise not possible in the 5 GHz bands. For example, one of the critical findings in this chapter is that MU OFDMA—a feature introduced to Wi-Fi in 802.11ax—can be used to improve the performance of NR-U as well as that of uplink Wi-Fi 6E transmissions. While exclusive use of MU OFDMA (i.e., disabling the LBT-based legacy contention) for uplink access is not possible in the 5 GHz bands due to the millions of already deployed Wi-Fi users, this is indeed feasible in the greenfield 6 GHz bands.

In the formulation of our analytical model, we seek an answer to the following question—*given that an NR-U or Wi-Fi 6E device has gained access to the medium, what is the probability that its transmission will be successful?* An NR-U or Wi-Fi 6E packet transmission is successful if the SINR of that packet observed at the desired receiver is greater than the threshold SINR value. In the pursuit of this answer, we identify two critical factors that significantly impact NR-U and Wi-Fi 6E performance when they coexist: (i) NR-U networks benefit when Wi-Fi 6E restricts its uplink transmissions to the schedule-based MU OFDMA mode. At the same time Wi-Fi 6E devices can themselves benefit when they use the MU OFDMA mode (as opposed to LBT-based contention) for uplink transmissions, and (ii) in both NR-U and Wi-Fi 6E networks, the entity that schedules uplink users must accurately sense the channel. If not, the very factors that improve the RAT's uplink performance contribute negatively to the success of the other RAT's ongoing transmissions.

In contrast to related research, we look at the coexistence of Wi-Fi 6E and NR-U on a per-transmission basis when one NR-U network coexists with a Wi-Fi Basic Service Set (BSS). This framework gives us the flexibility to individually study the impact of coexistence on both RATs under all possible combinations of transmission and interference directions (i.e., uplink and downlink), both operational modes of Wi-Fi 6E (i.e., LBT-based legacy contention and MU OFDMA), and the impact of transmit power control—a mandatory requirement in both uplink MU OFDMA Wi-Fi 6E and NR-U. Furthermore, we see that insights derived from this simplified scenario hold even when multiple Wi-Fi 6E and NR-U networks coexist.

The main contributions of this work are as follows:

- To the best of our knowledge, this is the first 6 GHz-centric study on the coexistence of Wi-Fi 6E and NR-U.
- We use a stochastic geometry-based coexistence model and our in-house simulator to study the impact of MU OFDMA in Wi-Fi 6E on the coexistence performance.

- We show that two features—MU OFDMA and transmit power control—which are traditionally used to improve a given RAT's performance, also benefit Wi-Fi 6E and NR-U performance when they coexist.

- We identify two critical factors that significantly impact the performance of Wi-Fi 6E and NR-U when they coexist: (i) transmit power control used by uplink devices, and (ii) the number of scheduled uplink users.

## 6.1 Related Work

There is rich literature on the coexistence between the predecessors of Wi-Fi 6/6E and NR-U, i.e., IEEE 802.11ac and LAA, respectively. These studies derive their results through experimental studies, system-level simulations, and/or analytical modeling. We reviewed some of these works in Chapter 3. Chen et al. provide a comprehensive survey on the related work on LAA–Wi-Fi coexistence in [32].

In terms of stochastic geometry-based coexistence modeling, Li et al. [265] derive expressions for the medium access probability and the coverage probability for the two RATs when they coexist. Ajami et al. [266] derive expressions for similar metrics but additionally consider 802.11ax as the Wi-Fi standard, thereby considering MU OFDMA transmissions and the use of spatial re-use techniques introduced in 802.11ax. Mbengue et al. [282] study the impact of the detection threshold on LAA and Wi-Fi performance. Wang et al. [283] and Bhorkar et al. [284] leverage stochastic geometry to evaluate coexistence between LTE-U[3] and Wi-Fi in the 5 GHz bands.

The focus of the aforementioned studies is on analyzing the performance of existing protocols rather than optimizing parameters/settings that influence coexistence, which is critical when unlicensed RATs begin to operate in a new band. Furthermore, references [265, 266, 282, 283, 284] consider LAA traffic only in the downlink, while uplink LAA traffic is ignored. Additionally, the only reference that considers MU OFDMA in IEEE 802.11ax is [266], while others look at the performance of Wi-Fi with Carrier Sense Multiple Access with Collision Avoidance (CSMA/CA). Finally, the most significant difference between related literature and our work is the studied performance metric—we look at the coexistence problem on a per-transmission basis, which allows us to look at the NR-U–Wi-Fi 6E coexistence problem at a more granular level.

[3]LTE-U is an unlicensed flavor of LTE developed by an industry forum that uses adaptive duty-cycling instead of LBT for coexistence.

## 6.2 System Model

### 6.2.1 Notations

An italicized variable $t$ denotes an instance of a random variable $T$. The probability density function (pdf), cumulative distribution function (cdf) and moment generating function (mgf) of $T$ are denoted as $f_T(.)$, $\mathbb{F}_T(.)$ and $\Phi_T(.)$, respectively. $\mathcal{L}^{-1}(.)$ is the Laplace inverse operator and Re$\{.\}$ denotes the real part of a complex quantity. Further, $|.|$ indicates the cardinality of a set. A parameter or random variable written as $T^{\mathrm{YZ}}$ or $T_{\mathrm{YZ}}$ indicates that the parameter/random variable is computed for a scenario where RAT Y device(s) is/are transmitting and RAT Z devices act as potential interferers.

### 6.2.2 Setup

We consider a scenario where a Wi-Fi 6E BSS operates in the close proximity of an NR-U network. The two networks operate on the same channel, thereby sharing the channel, and potentially interfering with each other. The Wi-Fi 6E BSS comprises of one AP and $\mathrm{M_W}$ STAs, while the NR-U network comprises of one gNB and $\mathrm{M_N}$ UEs. The devices are randomly and uniformly located inside a circular region $\mathcal{C}(o, \mathrm{R})$ of radius R and centered at the origin, $o$, as shown in Fig. 6.1. In practical networks, $\mathcal{C}(o, \mathrm{R})$ can be thought of as the smallest circular region that encloses all Wi-Fi 6E and NR-U devices associated with the Wi-Fi 6E AP and the NR-U gNB, respectively. The locations of Wi-Fi 6E and NR-U devices are modeled as two independent Binomial Point Processes (BPPs), $\Psi_{\mathrm{W}}$ and $\Psi_{\mathrm{N}}$, respectively, such that $|\Psi_{\mathrm{W}}| = \mathrm{M_W} + 1$ and $|\Psi_{\mathrm{N}}| = \mathrm{M_N} + 1$. The BPPs corresponding to the active Wi-Fi 6E and NR-U transmitters are denoted as $\Psi_{\mathrm{W}}^{\mathrm{T}}$ and $\Psi_{\mathrm{N}}^{\mathrm{T}}$, respectively, where $\Psi_{\mathrm{W}}^{\mathrm{T}} \subset \Psi_{\mathrm{W}}$ and $\Psi_{\mathrm{N}}^{\mathrm{T}} \subset \Psi_{\mathrm{N}}$. Let $|\Psi_{\mathrm{W}}^{\mathrm{T}}| = \mathrm{M_W^T}$ and $|\Psi_{\mathrm{N}}^{\mathrm{T}}| = \mathrm{M_N^T}$. The list of notations used in this chapter are outlined in Table 6.1.

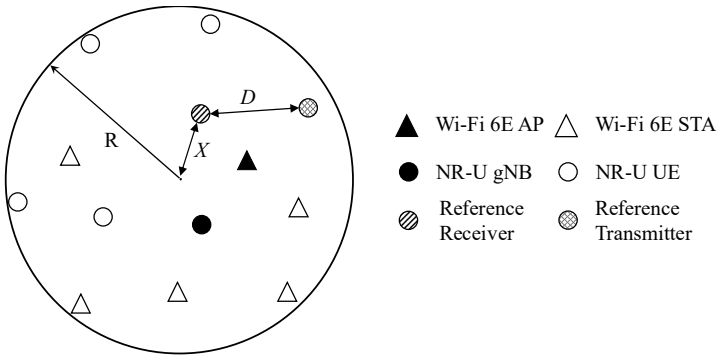


Figure 6.1: System model: uniform distribution within $\mathcal{C}(o, \mathrm{R})$.

Table 6.1: Summary of notations used in this chapter.

| Notation | Definition |
|---|---|
| $\mathcal{C}(o, \mathrm{R})$ | Circular region where all devices are located, centered at $o$ and of radius R |
| $\eta$ | Path loss exponent |
| $g$ | Constant path loss factor |
| $K$ | Fading coefficient |
| $\Psi_{\mathrm{W}}/\Psi_{\mathrm{N}}$ | BPP that defines Wi-Fi 6E/NR-U device locations |
| $\Psi_{\mathrm{W}}^{\mathrm{T}}/\Psi_{\mathrm{N}}^{\mathrm{T}}$ | BPP for the locations of active Wi-Fi 6E/NR-U transmitters |
| $\mathrm{M_W}/\mathrm{M_N}$ | Total number of Wi-Fi 6E STAs/NR-U UEs |
| $\mathrm{M_W^T}/\mathrm{M_N^T}$ | Number of active Wi-Fi 6E/NR-U transmitters |
| $\mathrm{P_{AP}}/\mathrm{P_{STA}}$ | Transmit power of Wi-Fi 6E AP/STA |
| $\mathrm{P_{gNB}}/\mathrm{P_{UE}}$ | Transmit power of NR-U gNB/UE |
| $\beta_{\mathrm{YZ}}$ | Threshold used by RAT Z devices to detect RAT Y transmissions |
| $\gamma_{\mathrm{Y}}$ | Min. SIR required to decode RAT Y transmissions |
| $\epsilon_{\mathrm{Y}}/\epsilon_{\mathrm{Z}}$ | Fractional power control parameter used by RAT Y/Z |
| $X$ | R.V. denoting the distance of a point from $o$ |
| $D$ | R.V. denoting the distance between two arbitrary points in $\mathcal{C}(o, \mathrm{R})$ given one of the points is at $X = x$ |
| $Q_{\mathrm{YZ}}$ | R.V. denoting the number of hidden RAT Z devices during ongoing RAT Y transmissions |
| $\mathrm{Q_{YZ}^{max}}$ | Max. number of hidden RAT Z devices when RAT Y transmits |
| $\mathrm{Q_Z^{sch}}$ | Number of scheduled uplink users, i.e., STAs for MU OFDMA uplink Wi-Fi 6E and UEs for uplink NR-U |
| $p_{\mathrm{H}}^{\mathrm{YZ}}$ | Prob. that a given device of RAT Z is hidden to ongoing RAT Y transmission(s) |
| $p_{\mathrm{H},x}^{\mathrm{YZ}}$ | Prob. that a given device of RAT Z, located at X = x, is hidden to ongoing RAT Y transmission(s) |
| $p_{\mathrm{S}}^{\mathrm{Y}}$ | Prob. that a given RAT Y transmission is successful |
| $p_{\mathrm{S},q}^{\mathrm{Y}}$ | Prob. that a given RAT Y transmission is successful given $q$ fixed RAT Z interferers |

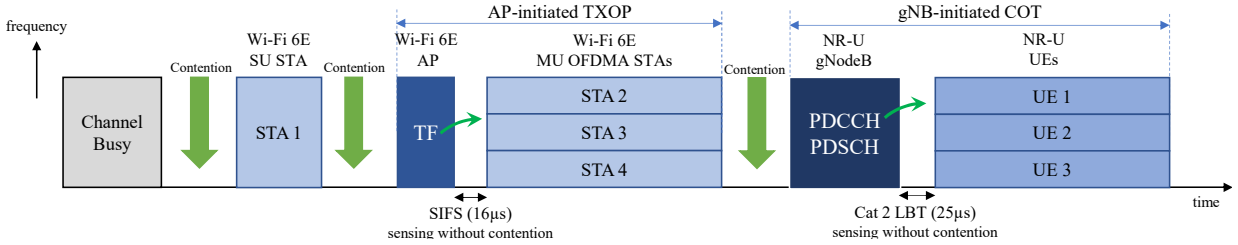


Figure 6.2: An illustration of SU and MU OFDMA transmissions in Wi-Fi 6E and NR-U transmissions. Packet ACKs are not shown.

### 6.2.3 Transmission Model

Transmissions in Wi-Fi 6 and NR-U are illustrated in Fig. 6.2. Downlink and uplink MU OFDMA transmissions are both initiated by the Wi-Fi 6 AP using a TF. As illustrated in Fig. 6.2, uplink MU OFDMA transmissions in Wi-Fi 6 are initiated by the AP by contending for the channel using CSMA/CA and transmitting the TF upon winning access. This TF contains resource allocation information required by the STAs to transmit in the uplink. MU OFDMA transmissions then occur at a fixed interval of 16 $\mu$sec after receiving the TF.

In downlink MU OFDMA, the AP transmits a single frame that contains packets addressed to all the assigned STAs. Upon reception, this packet is decoded by the relevant STAs. On the other hand, STAs *scheduled* by the AP for uplink start transmitting on their designated RUs. Since the channel availability can be different at the AP and the scheduled STA(s), each scheduled STA senses the medium once again before transmitting. If the channel is busy at the STA(s), the STA(s) will refrain from transmitting. However, if the channel is idle, the STA(s) do not perform exponential back-off and proceed with their transmissions. The exchange of TF, uplink MU OFDMA packets, and the ACK occurs in a single TXOP, which is initiated by the AP when it gains access to the channel during the transmission of the TF. It is worthwhile to note that uplink MU OFDMA transmissions in Wi-Fi 6 use a *hybrid* LBT (at the AP) and schedule-based (at the STAs) transmission approach.

In the uplink, the number of concurrently transmitting STAs can be more than one. Although these transmissions occur on orthogonal RUs, if the received signal strength on these RUs at the AP varies considerably, adjacent-RU interference can impair the reception of signals sent by far-away STAs. Therefore, the 802.11ax standard makes it mandatory for uplink MU OFDMA users to use transmit power control [53].

The channel access mechanism for data traffic in NR-U is based on Category 4 LBT—one of the four LBT categories defined by the 3GPP [33, 101], which is functionally similar to Wi-Fi's CSMA/CA protocol. To ensure fair channel access with Wi-Fi devices, the MAC protocol parameters chosen in NR-U are the same as those used by Wi-Fi [96]. Like the Wi-Fi 6/6E AP, the NR-U gNB transmits in the downlink by contending for the channel using LBT. Uplink NR-U transmissions, on the other hand, use the hybrid LBT and scheduled approach (similar to Wi-Fi 6/6E MU OFDMA, see Fig. 6.2), whereby the gNB first contends for the medium and, if the channel is idle, schedules a fixed number of NR-U UEs for uplink transmissions. The resource allocation information for uplink transmissions is contained in the PDCCH, which is the downlink logical control channel in NR (the downlink logical channel for data transmissions is referred to as the PDSCH). The assigned UEs can then transmit using category 2 LBT, wherein the UEs sense the medium for a fixed interval of 25 $\mu$sec, but do not perform random back-off. If the assigned resources are busy at a scheduled UE, it must cease its transmission and wait until the next uplink assignment. The entire exchange of PDSCH/PDCCH and the uplink transmissions is completed within the gNB-initiated Channel Occupancy Time (COT). Furthermore, like MU OFDMA STAs, UEs transmitting in the uplink use transmit power control.

### 6.2.4 Assumptions

To ensure that our analytical model remains tractable, we make the following assumptions.

1) *Path loss & fading:* We use the decaying path loss model with exponent $\eta$, where the received power ($P_R$) at a distance $d$ from the transmitter is $P_R = P_T g K d^{-\eta}$. Here, $P_T$ is the transmit power, $g$ is a constant, and $K$ is the fading coefficient. The channel is assumed to undergo Rayleigh fading, which is a widely made assumption [265, 266].

2) *Full buffer traffic:* We assume that all nodes in the network always have a packet to transmit. Despite this assumption, MU OFDMA STAs and NR-U UEs transmit only when scheduled by the AP/gNB. Further, even though IEEE 802.11ax has defined Target Wake Time (TWT) for power saving (whereby STAs negotiate wake times with the AP), STAs can transmit in the uplink using LBT-based contention [285].

3) *SU Wi-Fi 6E transmissions:* We assume that if one of the $\mathrm{M_W}$ SU STAs in the BSS transmits, the other STAs sense the signal and back-off. This is a fair assumption because Wi-Fi devices use preamble detection (with a threshold of $-82$dBm) and virtual carrier sensing [69] to detect other Wi-Fi signals (see Fig. 6.3(c)). We relax this assumption in our simulations.

4) *Independence of the hidden node probability:* We assume that the probability of a node being hidden to ongoing transmission(s) is independent of its location in $\mathcal{C}(o, \mathrm{R})$. This is not true in general [286]. In fact, Sec. 6.3.1 computes the hidden node probability by averaging over all possible node locations. However, we see in Sec. 6.4 that this assumption has a very small impact on the computed metrics.

5) *Interference-limited:* We assume that Wi-Fi 6E and NR-U are interference-limited—a widely used assumption [287, 288].

### 6.2.5 Distributions & Power Computation

For performance analysis, we look at the received signal strength at a device that is arbitrarily located inside $\mathcal{C}(o, \mathrm{R})$. The distance of this point (location) from the origin, $o$, is denoted by a random variable $X$, whose pdf is given by Eq. (6.1) [289]. Given that the location of this *reference* receiver is $X = x$, the distance between this receiver and an arbitrary *reference* transmitter in $\mathcal{C}(o, \mathrm{R})$ is denoted by a random variable $D$ (see Fig. 6.1), whose pdf is given by Eq. (6.2) [289].

$$f_X(x) = \frac{2x}{\mathrm{R}^2}, \qquad 0 \leq x \leq \mathrm{R}. \tag{6.1}$$

$$f_D(d) = \begin{cases} \frac{2d}{\mathrm{R}^2}, & 0 \leq d \leq \mathrm{R} - x, \\ \frac{2d}{\pi \mathrm{R}^2} \cos^{-1}\left(\frac{d^2 + x^2 - \mathrm{R}^2}{2xd}\right), & \mathrm{R} - x \leq d \leq \mathrm{R} + x. \end{cases} \tag{6.2}$$

The transmit powers of the AP, STAs, gNB and UEs are denoted as $\mathrm{P_{AP}}$, $\mathrm{P_{STA}}$, $\mathrm{P_{gNB}}$ and $\mathrm{P_{UE}}$, respectively. MU OFDMA Wi-Fi 6E STAs and NR-U UEs use fractional transmit power control with parameter $\epsilon$ for uplink transmissions [290]. The transmit power of a generic device located at a distance $\mathrm{d_1}$ from its intended receiver is given by Eq. (6.3), where $\mathrm{P_Y} \in \{\mathrm{P_{AP}}, \mathrm{P_{STA}}\}$ for Wi-Fi 6E devices and $\mathrm{P_Y} \in \{\mathrm{P_{gNB}}, \mathrm{P_{UE}}\}$ for NR-U devices. If the transmitting device is a Wi-Fi 6E AP, SU STA, or NR-U gNB, $\epsilon = 0$, i.e., no power control is used, while $\epsilon \geq 0$ for MU OFDMA STAs and NR-U UEs. Using the path loss model described in assumption 1, the received power from this transmission at an arbitrary device located at a distance $\mathrm{d_2}$ from the transmitter is then given by Eq. (6.4).

$$P_T(\mathrm{d_1}) = \mathrm{P_Y} \mathrm{d_1}^{\eta\epsilon}. \tag{6.3}$$

$$\begin{aligned} P_R(\mathrm{d_1}, \mathrm{d_2}) &= P_T(\mathrm{d_1}) g K \mathrm{d_2}^{-\eta} \\ &= g \mathrm{P_Y} K \mathrm{d_1}^{\eta\epsilon} \mathrm{d_2}^{-\eta}. \end{aligned} \tag{6.4}$$

## 6.3 Performance Analysis

In this section, we derive an expression for the success probability of a given (Wi-Fi 6E/NR-U) RAT's transmissions given that these devices have gained access to the channel. The RAT that gains access to the channel first is referred to as "Y", while the potentially interfering RAT is referred to as "Z". For example, when Wi-Fi 6E devices transmit, Y=W (i.e., Wi-Fi) and Z=N (i.e., NR-U), and vice-versa.

The two RATs coexist by sensing each other and ceasing their transmissions when the channel is detected as busy. If the strength of the signal transmitted by the RAT Y device(s) at a RAT Z device is lower than the detection threshold[4], $\beta_{\mathrm{YZ}}$, the devices are *hidden* to each other. Thereafter, the hidden RAT Z device can transmit and interfere with the RAT Y receiver.

Since we focus on the investigation of inter-RAT coexistence, we ignore intra-RAT hidden nodes, i.e., hidden Wi-Fi (or NR-U) nodes when other Wi-Fi (or NR-U) devices transmit. Note that in our system model, intra-RAT interference can only originate from SU Wi-Fi 6E STAs transmitting in the uplink. This is because uplink MU OFDMA and NR-U transmissions occur only when scheduled by the AP/gNB. Further, our implicit assumption in this section is that NR-U and Wi-Fi 6E devices contend on a 20 MHz channel. However, the analysis easily extends to wider channel bandwidths by selecting the appropriate detection threshold in Eq. (6.5) and considering only the overlapping interference in Eq. (6.18).

[4]The detection threshold is collectively defined by "Y" and "Z". In the 5 GHz bands, $\beta_{\mathrm{WW}}$=−82dBm, $\beta_{\mathrm{NW}}$=−62dBm, and $\beta_{\mathrm{WN}}$=$\beta_{\mathrm{NN}}$=−72dBm for a 20 MHz channel.

### 6.3.1 The Hidden Node Probability

An arbitrary RAT Z device is hidden to RAT Y transmissions if the total power received from these transmissions at the RAT Z device is less than the detection threshold, $\beta_{\mathrm{YZ}}$. Given that the reference RAT Z device is located at $X = x$, the probability that it is hidden to ongoing RAT Y transmissions is denoted as $p_{\mathrm{H},x}^{\mathrm{YZ}}$ and given by Eq. (6.5), where $D_{bi}$ denotes the RAT Y transmitter's distance from its intended receiver and $D_i$ denotes the distance between the RAT Y transmitter and the reference RAT Z receiver. The pdf of $D_{bi}$ and $D_i$ is given by Eq. (6.2). Further, $\beta'_{\mathrm{YZ}} = \frac{\beta_{\mathrm{YZ}}}{g\mathrm{P_Y}}$, and $T_x$ is a dummy random variable defined as: $T_x = \sum_{i=1}^{\mathrm{M_Y^T}} K_i D_i^{-\eta} D_{bi}^{\eta\epsilon_{\mathrm{Y}}}$.

$$\begin{aligned} p_{\mathrm{H},x}^{\mathrm{YZ}} &= \mathbb{P}\left(\sum_{i\in\Psi_{\mathrm{Y}}^{\mathrm{T}}} P_{\mathrm{T}}(D_{bi}) g K_i D_i^{-\eta} < \beta_{\mathrm{YZ}}\right) \\ &= \mathbb{P}\left(\sum_{i=1}^{\mathrm{M_Y^T}} K_i D_i^{-\eta} D_{bi}^{\eta\epsilon_{\mathrm{Y}}} < \beta'_{\mathrm{YZ}}\right) \\ &= \mathbb{P}\left(T_x < \beta'_{\mathrm{YZ}}\right) = \mathbb{F}_{T_x}\left(\beta'_{\mathrm{YZ}}\right). \end{aligned} \tag{6.5}$$

Averaging over all possible locations of the reference RAT Z device, we get the average hidden node probability in Eq. (6.6).

$$p_{\mathrm{H}}^{\mathrm{YZ}} = \mathbb{E}_X\left(p_{\mathrm{H},x}^{\mathrm{YZ}}\right) = \int_0^{\mathrm{R}} \frac{2x}{\mathrm{R}^2}\, p_{\mathrm{H},x}^{\mathrm{YZ}}\, \mathrm{d}x. \tag{6.6}$$

To compute the distribution of $T_x$, we first derive an expression for the mgf of $T_x$, i.e., $\Phi_{T_x}(s)$. The cdf of $T_x$ can then be obtained as,

$$\mathbb{F}_{T_x}(t) = \mathcal{L}^{-1}\left[\frac{\Phi_{T_x}(s)}{s}\right]. \tag{6.7}$$

Sources of randomness in $T_x$ are the fading coefficients $K_i$, the distance between the RAT Y transmitter(s) and the RAT Z device, $D_i$, and the distance between the RAT Y transmitter(s) and the desired receiver, $D_{bi}$. To compute the mgf of $T_x$, we need the joint pdf $f_{K_i,D_{bi},D_i}(k, d_{bi}, d_i)$. We assume that $K_i$, $D_{bi}$ and $D_i$ are independent of each other. Therefore, $f_{K_i,D_{bi},D_i}(k, d_{bi}, d_i) = f_K(k) \cdot f_D(d_{bi}) \cdot f_D(d_i)$. Further, due to the Rayleigh fading assumption, $K$ is an exponential random variable. We assume that the mean of $K$ is 1. Thus, the pdf of $K$ is given by $f_K(k) = e^{-k}, 0 \le k < \infty$ [265]. The mgf of $T_x$ can be obtained as shown in Eq. (6.8).

$$\begin{aligned}\Phi_{T_x}(s) &= \mathbb{E}_{K_i,D_{bi},D_i}\left\{\exp\left(-sT_x\right)\right\}\\ &= \mathbb{E}_{K_i,D_{bi},D_i}\left\{\exp\left(-s\sum_{i=1}^{\mathrm{M_Y^T}} k_i d_i^{-\eta} d_{bi}^{\eta\epsilon_{\mathrm{Y}}}\right)\right\}\\ &= \left(\mathbb{E}_{K_i,D_{bi},D_i}\left\{\exp\left(-sk_i d_i^{-\eta} d_{bi}^{\eta\epsilon_{\mathrm{Y}}}\right)\right\}\right)^{\mathrm{M_Y^T}}\\ &= \left(\int_{D_{bi}}\int_{D_i} f_D(d_{bi}) f_D(d_i)\left(\frac{1}{sd_i^{-\eta} d_{bi}^{\eta\epsilon_{\mathrm{Y}}}+1}\right)\,\mathrm{d}d_i\,\mathrm{d}d_{bi}\right)^{\mathrm{M_Y^T}}.\end{aligned} \tag{6.8}$$

The pdf of $D$ from Eq. (6.2) can be substituted in Eq. (6.8) to obtain an expression for $\Phi_{T_x}(s)$. The resulting expression is a summation of four double integrals (since the pdf of $D$ is defined over two intervals, i.e., 0 to $\mathrm{R}-x$, and $\mathrm{R}-x$ to $\mathrm{R}+x$). Due to the presence of the $\cos^{-1}$ term in Eq. (6.2), however, Eq. (6.8) does not have a closed-form expression. Therefore, Eq. (6.8) and all subsequent integrals involving $\Phi_{T_x}(s)$ require numerical solution of integrals.

Eq. (6.8) can be substituted in Eq. (6.7) and evaluated at $\beta'_{\mathrm{YZ}}$ to obtain $p_{\mathrm{H},x}^{\mathrm{YZ}}$ (see Eq. (6.5)). Then, $p_{\mathrm{H}}^{\mathrm{YZ}}$ can be computed using Eq. (6.6). In order to get $\mathbb{F}_{T_x}(\beta'_{\mathrm{YZ}})$, however, a Laplace inverse operation is required, which must be computed numerically. We use the approach provided in [289] as shown in Eq. (6.9).

$$\mathbb{F}_{T_x}(\beta'_{\mathrm{YZ}}) = \frac{2^{-H}\exp(A/2)}{\beta'_{\mathrm{YZ}}}\sum_{h=0}^{H}\binom{H}{h}\sum_{c=0}^{C+h}\frac{(-1)^c}{E_c}\mathrm{Re}\left\{\frac{\Phi_{T_x}(s)}{s}\right\}, \tag{6.9}$$

where the parameters $A$, $H$ and $C$ are chosen as $\zeta\ln(A), 1.243\zeta-1$ and $1.467\zeta$, respectively, to achieve an estimation accuracy of $10^{-\zeta}$ (we use $\zeta$ =8). Further, $s=\frac{(A+\mathbf{i}2\pi c)}{2\beta'_{\mathrm{YZ}}}$, and the parameter $E_c=2$, if $c=0$, and $E_c=1$, otherwise.

### 6.3.2 Probability Mass Function for the Number of Interferers

We now estimate the number of RAT Z devices that are hidden to RAT Y transmission(s). From assumption 4, we have the same hidden node probability, $p_{\mathrm{H}}^{\mathrm{YZ}}$, for all RAT Z devices. Let $Q_{\mathrm{YZ}}$ and $\mathrm{Q}_{\mathrm{YZ}}^{\max}$ denote the actual and maximum number of RAT Z devices hidden to RAT Y transmissions, respectively.

First, consider the case where Wi-Fi 6E uses MU OFDMA in the uplink. In this scenario, the operations of Wi-Fi 6E and NR-U are similar. The AP/NR-U transmits in the downlink by using LBT to contend for the medium. Upon winning access, the AP/gNB transmits its packet. This implies that if RAT Z has traffic in the downlink, the only possible interferer is the AP/gNB, which interferes with RAT Y transmission(s) if it is hidden. Thus, the number

of interferers can be either 0 or 1, i.e., $\mathrm{Q}_{\mathrm{YZ}}^{\max} = 1$ for RAT Z downlink interference. The corresponding probabilities are given in Eq. (6.10) and Eq. (6.11).

For uplink transmissions, the AP/gNB first senses the channel and, if idle, schedules the STA(s)/UE(s) (see Fig. 6.2). This is followed by sensing at the STA(s)/UE(s). If the channel is idle at the STA(s)/UE(s) as well, an uplink transmission is initiated. If the AP/gNB is not hidden, it will not schedule uplink transmissions. However, if the AP/gNB is hidden it can schedule users in the uplink and any of these scheduled users can potentially be hidden to the ongoing RAT Y transmission(s). Thus, if RAT Z has traffic in the uplink, the maximum number of interferers is equal to the number of scheduled uplink devices (which we denote as $\mathrm{Q}_{\mathrm{Z}}^{\mathrm{sch}}$), i.e., $\mathrm{Q}_{\mathrm{YZ}}^{\max} = \mathrm{Q}_{\mathrm{Z}}^{\mathrm{sch}}$. The number of uplink interferers is 0 in two cases (see Eq. (6.12)), (i) the AP/gNB can sense ongoing RAT Y transmissions, or (ii) the AP/gNB is hidden but all of the $\mathrm{Q}_{\mathrm{YZ}}^{\max}(= \mathrm{Q}_{\mathrm{Z}}^{\mathrm{sch}})$ STAs/UEs can sense the ongoing RAT Y transmissions. On the other hand, the number of interferers is $j$, where $j > 0$, if (i) the AP/gNB is hidden, *and* (ii) $j$ of the $\mathrm{Q}_{\mathrm{Z}}^{\mathrm{sch}}$ scheduled uplink users are hidden. The resulting probability is given in Eq. (6.13).

Now consider the case where Wi-Fi 6E users operate in the SU mode using LBT-based legacy contention. In this scenario, since STAs need not be scheduled by the AP to transmit, any of the hidden STA(s) can initiate a transmission and act as a potential interferer. Using assumptions 2 and 3, the number of interferers is zero if none of the $\mathrm{M_W}$ Wi-Fi 6E STAs are hidden. On the other hand, the number of interferers is one if at least one of the $\mathrm{M_W}$ STAs is hidden to NR-U transmissions. The corresponding probabilities are given in Eq. (6.14) and (6.15).

Table 6.2: Probability mass function of $Q_{\mathrm{YZ}}$, $\mathbb{P}(Q_{\mathrm{YZ}} = q)$.

| **Case** | **Value** ($q$) | $\mathrm{Q}_{\mathrm{YZ}}^{\max}$ | **Probability**, $\mathbb{P}(Q_{\mathrm{YZ}} = q)$ |
|---|---|---|---|
| Down- | 0 | 1 | $(1 - \mathrm{p}_{\mathrm{H}}^{\mathrm{YZ}})^{\mathrm{Q}_{\mathrm{YZ}}^{\max}} = 1 - p_{\mathrm{H}}^{\mathrm{YZ}}$ (6.10) |
| link | 1 | | $1 - (1 - \mathrm{p}_{\mathrm{H}}^{\mathrm{YZ}})^{\mathrm{Q}_{\mathrm{YZ}}^{\max}} = p_{\mathrm{H}}^{\mathrm{YZ}}$ (6.11) |
| Up- | 0 | $\mathrm{Q}_{\mathrm{Z}}^{\mathrm{sch}}$ | $1 - \mathrm{p}_{\mathrm{H}}^{\mathrm{YZ}} + p_{\mathrm{H}}^{\mathrm{YZ}}(1 - p_{\mathrm{H}}^{\mathrm{YZ}})^{\mathrm{Q}_{\mathrm{YZ}}^{\max}}$ (6.12) |
| link | $j > 0$ | | $\mathrm{p}_{\mathrm{H}}^{\mathrm{YZ}}\binom{\mathrm{Q}_{\mathrm{YZ}}^{\max}}{j}\left(p_{\mathrm{H}}^{\mathrm{YZ}}\right)^{j}\left(1 - p_{\mathrm{H}}^{\mathrm{YZ}}\right)^{\mathrm{Q}_{\mathrm{YZ}}^{\max} - j}$ (6.13) |
| SU | 0 | 1 | $(1 - \mathrm{p}_{\mathrm{H}}^{\mathrm{YZ}})^{\mathrm{M_W}}$ (6.14) |
| Wi-Fi | 1 | | $1 - (1 - \mathrm{p}_{\mathrm{H}}^{\mathrm{YZ}})^{\mathrm{M_W}}$ (6.15) |

### 6.3.3 Success Probability

Finally, we compute the success probability of a given RAT Y transmission, which is denoted as $p_{\mathrm{S}}^{\mathrm{Y}}$. First, we let the number of RAT Z interferers be fixed to $q$ and compute the resulting RAT Y success probability, denoted by $p_{\mathrm{S,q}}^{\mathrm{Y}}$. The probability $p_{\mathrm{S}}^{\mathrm{Y}}$ can then be computed as given by Eq. (6.16).

$$p_{\mathrm{S}}^{\mathrm{Y}} = \sum_{q=0}^{\mathrm{Q}_{\mathrm{YZ}}^{\max}} \mathbb{P}(Q_{\mathrm{YZ}} = q) \times p_{\mathrm{S,q}}^{\mathrm{Y}}, \tag{6.16}$$

In Eq. (6.16), $\mathbb{P}(Q_{\mathrm{YZ}} = q)$ is computed using Table 6.2. From assumption 5, we have $p_{\mathrm{S},0}^{\mathrm{Y}} = 1$. Given that the number of RAT Z interferers is fixed to $q$, the probability that the RAT Y transmission is successful can be computed as follows.

$$p_{\mathrm{S,q}}^{\mathrm{Y}} = \mathbb{E}_X \left\{ p_{\mathrm{S,q,x}}^{\mathrm{Y}} \right\} = \int_0^{\mathrm{R}} f_X(x)\, p_{\mathrm{S,q,x}}^{\mathrm{Y}}\, \mathrm{d}x, \tag{6.17}$$

where $p_{\mathrm{S,q,x}}^{\mathrm{Y}}$ denotes the probability that a given transmission of RAT Y is successful given that the number of interferers is fixed to $Q_{\mathrm{YZ}} = q$ and the RAT Y receiver is located at $X = x$. The expression for $p_{\mathrm{S,q,x}}^{\mathrm{Y}}$ can be derived as shown in Eq. (6.18).

$$\begin{aligned} p_{\mathrm{S,q,x}}^{\mathrm{Y}} &= \mathbb{P}\left( \frac{\mathrm{P_Y} g K_b D_b^{\eta(\epsilon_{\mathrm{Y}}-1)}}{\sum_{l=1}^{q} \mathrm{P_Z} g K_l D_{(2l-1)}^{\eta\epsilon_{\mathrm{Z}}} D_{(2l)}^{-\eta}} \geq \gamma_{\mathrm{Y}} \right) \\ &= \mathbb{E}\left\{ \mathbb{P}\left( K_b \geq \gamma'_{\mathrm{Y}} d_b^{\eta(1-\epsilon_{\mathrm{Y}})} \left[ \sum_{l=1}^{q} k_l d_{(2l-1)}^{\eta\epsilon_{\mathrm{Z}}} d_{(2l)}^{-\eta} \right] \right) \right\} \\ &\overset{(a)}{=} \mathbb{E}\left\{ \exp\left( -\gamma'_{\mathrm{Y}} d_b^{\eta(1-\epsilon_{\mathrm{Y}})} \left[ \sum_{l=1}^{q} k_l d_{(2l-1)}^{\eta\epsilon_{\mathrm{Z}}} d_{(2l)}^{-\eta} \right] \right) \right\} \\ &\overset{(b)}{=} \mathbb{E}\left\{ \prod_{l=1}^{q} \left( \frac{1}{1 + \gamma'_{\mathrm{Y}} d_b^{\eta(1-\epsilon_{\mathrm{Y}})} d_{(2l-1)}^{\eta\epsilon_{\mathrm{Z}}} d_{(2l)}^{-\eta}} \right) \right\}, \end{aligned} \tag{6.18}$$

where $\gamma_{\mathrm{Y}}$ is the minimum SIR required to decode the RAT Y signal at the receiver, $D_b$ is the distance between the RAT Y transmitter and its desired receiver, and $\gamma'_{\mathrm{Y}} = \frac{\mathrm{P_Z}\gamma_{\mathrm{Y}}}{\mathrm{P_Y}}$. Note that the denominator of Eq. (6.18) contains $D_{(2l-1)}$ and $D_{(2l)}$, which denote the distance between the interferer and its desired receiver, and the distance between the interferer and RAT Y receiver, respectively. However, since these two represent the same distance for the RAT Y transmitter, there is only one such term in the numerator (i.e., $D_b$). Further, (a) follows from the complementary cdf of an exponential random variable, while (b) is obtained by taking expectation over all $K_l$, and given that $\int_0^{\infty} e^{-k} e^{-tk}\, dk = \frac{1}{1+t}$ for $t \geq 0$. Taking expectations over $D_b$, $D_{(2l-1)}$, $D_{(2l)}$ and finally over $X$ (see Eq. (6.17)), we get the expression for $p_{\mathrm{S,q}}^{\mathrm{Y}}$ as shown in Eq. (6.19).

$$p_{\mathrm{S,q}}^{\mathrm{Y}} = \int_X \int_{D_b} \underbrace{\int_{D_1} \int_{D_2} \cdots \int_{D_{(2q)}}}_{2 \times \mathrm{q\ integrals}} \Bigg\{ f_X(x) f_D(d_b) \underbrace{f_D(d_1) f_D(d_2) \cdots f_D(d_{(2q)})}_{2 \times \mathrm{q\ terms}} \times \prod_{l=1}^{q} \left( \frac{1}{1 + \gamma'_{\mathrm{Y}} d_b^{\eta(1-\epsilon_{\mathrm{Y}})} d_{(2l-1)}^{\eta\epsilon_{\mathrm{Z}}} d_{(2l)}^{-\eta}} \right) \Bigg\} \mathrm{d}d_{(2q)} \ \cdots \ \mathrm{d}d_1 \ \mathrm{d}d_b \ \mathrm{d}x \tag{6.19}$$

## 6.4 Simulation and Numerical Results

The numerical results presented in this section are generated using Matlab's numerical integration functions for up to four definite integrals. When the number of definite integrals is more than four, we use Monte Carlo integration with uniform sampling within the integration region. Simulation results have been generated using our Matlab-based in-house NR-U and Wi-Fi 6E simulator. The PHY layer is abstracted such that all packets received above the threshold SIR are forwarded to the MAC layer, while those below the threshold SIR are dropped.

Unless explicitly stated otherwise, lines with error bars indicate simulation results, where the error bars show the 95% confidence interval. Throughout this section, we refer to Wi-Fi 6E devices simply as Wi-Fi devices. Wi-Fi and NR-U parameters used in this section are outlined in Table 6.3. We choose the parameters $g = 10^{-4}$ and $\eta = 4$ in Eq. (6.4) such that the path loss (without fading) predicted by Eq. (6.4) matches with the predictions of the WINNER+ A1 non-line-of-sight model [167], which emulates an office-like indoor setting.

Table 6.3: Simulation parameters for evaluating NR-U – Wi-Fi coexistence in the 6 GHz Bands

| **Parameter** | **Value** | **Parameter** | **Value** |
|---|---|---|---|
| R | 4 to 25 | $\gamma_{\mathrm{W}}$, $\gamma_{\mathrm{N}}$ | 4.3 dB |
| $g$ | $10^{-4}$ | $\eta$ | 4 |
| $\mathrm{P_{AP}}$, $\mathrm{P_{gNB}}$ | 23 dBm | $\mathrm{P_{STA}}$, $\mathrm{P_{UE}}$ | 14 dBm [291] |
| $\mathrm{M_W}$, $\mathrm{M_N}$ | 1 to 9 | $\mathrm{M_W^T}$, $\mathrm{M_N^T}$ | 1,3,9 |
| $\epsilon_{\mathrm{W}}$, $\epsilon_{\mathrm{N}}$ | 0, 0.2, 0.5, 1 (uplink)<br>0 (downlink) | $\mathrm{Q_W^{sch}}$, $\mathrm{Q_N^{sch}}$ | 1 to 5 |
| Pkt. size | 1000 Bytes | PHY rate | 24 Mbps |

### 6.4.1 Validation of Analysis

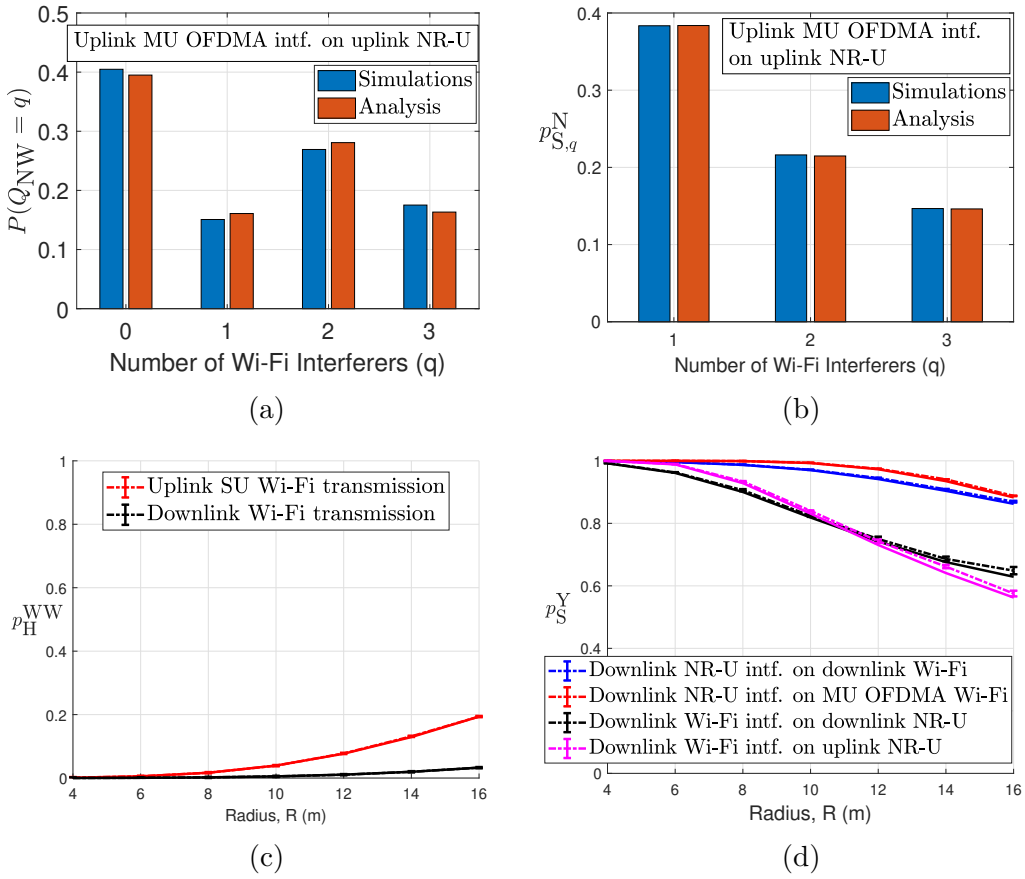


Figure 6.3: Validation of analysis, $\epsilon_{W}$=$\epsilon_{N}$=0 for all plots, (a) No. of interferers when MU OFDMA Wi-Fi STAs interfere with NR-U uplink, $M^{T}_{N}$=1, $Q^{sch}_{W}$ = 3, $\beta_{NW}$=−62dBm, (b) Success prob. when no. of interferers is fixed, $M^{T}_{N}$=1, $Q^{sch}_{W}$ = 3, (c) Hidden node prob. for Wi-Fi devices when other Wi-Fi devices transmit, $\beta_{WW}$=−82 dBm, (d) Impact of 5 GHz detection thresholds, Wi-Fi 6E in the MU OFDMA mode, $\beta_{NW}$=−62dBm, and $\beta_{WN}$=−72dBm, $M^{T}_{W}$=$M^{T}_{N}$=3 for uplink RAT Y transmissions.

We begin by validating the correctness of our analysis against simulation results. In Fig. 6.3(a) and Fig. 6.3(b), we report results for a scenario where Wi-Fi STAs transmitting in the uplink MU OFDMA mode interfere with ongoing uplink NR-U transmissions. Fig. 6.3(a) shows that despite our assumption that the hidden node probability $p^{NW}_{H}$ is independent of the location of the RAT Z (Wi-Fi, in this case) interferer, i.e., assumption 4, there is a close match in the analytical and simulated values for $\mathbb{P}(Q_{NW} = q)$. Similarly, Fig. 6.3(b) shows that for a fixed number of interferers, the success probability derived in Eq. (6.19) matches exactly with the simulation results. Fig. 6.3(c) shows that $p^{WW}_{H}$, i.e., the probability that Wi-Fi devices are hidden to other Wi-Fi transmissions is very small (due to $\beta_{WW}$=−82dBm), thereby

justifying assumption 3. Finally, Fig. 6.3(d) and Fig. 6.4 through Fig. 6.6 show that the derived expressions for $p_{\mathrm{S}}^{\mathrm{Y}}$ for various cases agree closely with the simulation results, thereby validating our analysis.

### 6.4.2 Unfairness of 5 GHz Detection Thresholds

Fig. 6.3(d) shows the performance of NR-U and Wi-Fi for the 5 GHz detection thresholds. We see that in the presence of downlink Wi-Fi (or NR-U) interference, as the radius, R, increases, the success probability of both uplink and downlink NR-U (or Wi-Fi) drops. This drop comes from the increase in the hidden node probability $p_{\mathrm{H}}^{\mathrm{NW}}$ (or $p_{\mathrm{H}}^{\mathrm{WN}}$) as R increases. However, due to the different thresholds used by Wi-Fi and NR-U to detect each other in the 5 GHz bands ($\beta_{\mathrm{NW}}$=−62dBm and $\beta_{\mathrm{WN}}$=−72dBm), when all other Wi-Fi and NR-U operational aspects are identical (for e.g. when the number of scheduled RAT Y users in the uplink is the same, $\mathrm{M}_{\mathrm{W}}^{\mathrm{T}}$=$\mathrm{M}_{\mathrm{N}}^{\mathrm{T}}$=3, or when RAT Y transmits in the downlink) *for most values of R, the success probability of NR-U is consistently 20-30% lower than that of Wi-Fi.* Although this unfairness issue is widely known in the literature [243], certain contributions (such as [256]) argue for maintaining the *status quo* for channel access parameters in the 6 GHz bands. However, Fig. 6.3(d) reiterates the need to use the same detection threshold across all coexisting technologies in the 6 GHz bands. Hereafter, unless explicitly stated otherwise, we use $\beta_{\mathrm{WN}}$=$\beta_{\mathrm{NW}}$=−72dBm.

### 6.4.3 Benefits of MU OFDMA over LBT-based contention

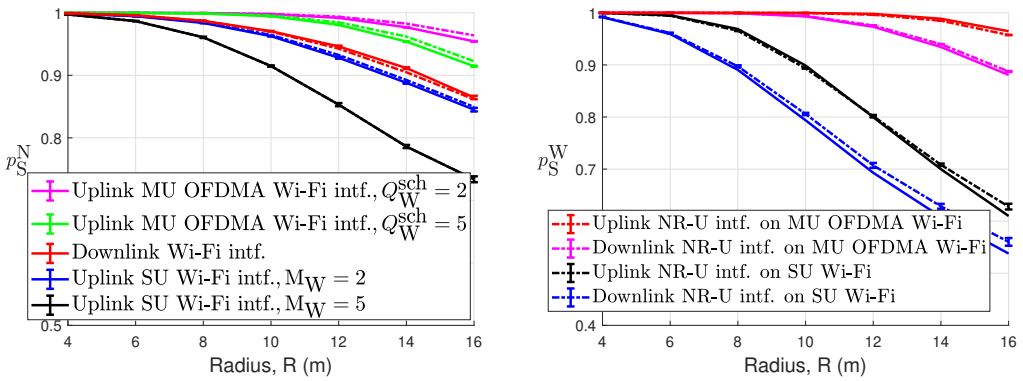


(a) (b)

Figure 6.4: Legacy contention (SU) vs MU OFDMA for Wi-Fi, $\epsilon_{\mathrm{W}}$=$\epsilon_{\mathrm{N}}$=0, (a) Impact of Wi-Fi intf. on NR-U downlink, (b) Impact of NR-U on Wi-Fi uplink, $\mathrm{M}_{\mathrm{W}}^{\mathrm{T}}$=3 for MU OFDMA, $\mathrm{Q}_{\mathrm{N}}^{\mathrm{sch}}$=3 for uplink intf.

#### 6.4.3.1 Performance for a given set of detection thresholds

Fig. 6.4(a) shows the impact of Wi-Fi interference on NR-U downlink. The interfering RAT (Wi-Fi) can operate in three settings: (i) downlink[5], (ii) uplink SU, and (iii) uplink MU OFDMA. For a fair comparison between the latter two cases, power control is disabled for uplink MU OFDMA STAs (since $\epsilon_W$=0 for SU STAs), and we present results on the impact of uplink Wi-Fi interference (in the SU and MU OFDMA cases) when the number of *potential* interferers is the same for the two cases. Thus, if the *hidden* Wi-Fi AP schedules 2 (or 5) STAs, we compare the resulting impact with the scenario where there are 2 (or 5) SU STAs in the BSS.

Fig. 6.4(a) shows that even if there are only two SU Wi-Fi STAs in the BSS, their impact on NR-U is worse than downlink Wi-Fi interference. This is despite the 9 dB higher power used by the AP (see Table 6.3). If there are more than two STAs in the BSS (e.g., 5 STAs), we see that uplink SU STAs have a far worse impact on NR-U performance than either downlink or uplink MU OFDMA interference. Furthermore, compared to uplink SU STAs, for the same number of potential interferers, uplink MU OFDMA STAs have a significantly lower impact on NR-U performance. This is because: for a MU OFDMA STA to interfere at the UE, the transmitting gNB must be hidden to the AP *as well as* at the MU OFDMA STA. On the other hand, SU STAs transmit in a distributed fashion. If *any* of the SU STAs in the BSS is hidden, it senses the channel idle and can initiate a transmission, thereby interfering at the UE. Thus, the added requirement of sensing at the AP (in addition to the STAs) for initiating uplink transmissions in the MU OFDMA mode offers better protection to NR-U transmissions.

Although Fig. 6.4(a) shows the impact of Wi-Fi interference on downlink NR-U, we have verified that the same phenomenon is true for uplink NR-U transmissions—for the same number of potential interferers, interference from uplink SU STAs is significantly worse than interference from uplink MU OFDMA STAs. For the parameters chosen in Table 6.3, the only scenario where downlink Wi-Fi has a worse impact on NR-U transmissions (than uplink SU Wi-Fi) is when $M_W$=1, i.e., there is only one potential SU interferer in the BSS.

Fig. 6.4(b) further reveals that MU OFDMA transmissions in Wi-Fi are not only beneficial for NR-U performance (when Wi-Fi is the interfering RAT) but also for the success of uplink Wi-Fi transmissions. Specifically, we see that as long as the AP schedules more than one MU OFDMA STA ($M_W^T$=3 in Fig. 6.4(b)), the success probability of resulting uplink Wi-Fi transmissions is considerably higher than uplink SU transmissions. This improvement stems from the increase in the number simultaneously active transmitters (3 in Fig. 6.4(b)) as we will discuss in Sec. 6.4.4.1. Note that if only one MU OFDMA STA is scheduled (i.e., if $M_W^T$=1), the resulting Wi-Fi success probability is the same as in the uplink SU scenario. However, since MU OFDMA was introduced in Wi-Fi for improving the Wi-Fi MAC layer

[5]Note that as far as Wi-Fi downlink is concerned, there is no difference between downlink MU OFDMA and downlink SU transmissions.

efficiency, the AP has a strong incentive to always schedule more than one STA in the uplink.

#### 6.4.3.2 Relative impact of the detection threshold

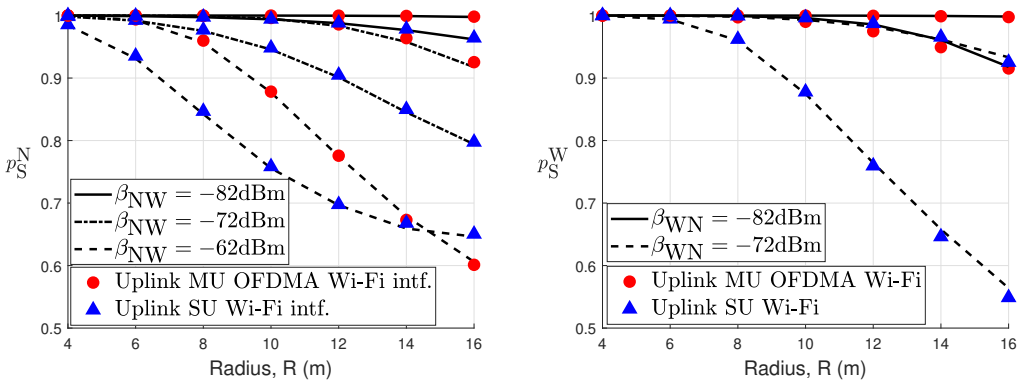


(a) (b)

Figure 6.5: Relative impact of different detection thresholds, markers indicate simulation results, (a) Impact of uplink Wi-Fi intf. on NR-U downlink, $\epsilon_W$=0.2, $Q_W^{sch}$=3, (b) Impact of uplink NR-U intf. on Wi-Fi uplink, $\epsilon_W$=$\epsilon_N$=0.2, $M_W^T$=1, $Q_N^{sch}$=3.

Fig. 6.5(a) shows the impact of uplink Wi-Fi interference on the success probability of downlink NR-U transmissions. Unsurprisingly, we see that as $\beta_{NW}$ is lowered, the hidden node probability, $p_{NW}^H$, reduces and consequently, the success probability of NR-U, $p_S^N$, increases. Similarly, we see in Fig. 6.5(b), which shows the impact of uplink NR-U interference on uplink Wi-Fi performance, that a lower $\beta_{WN}$ increases the success probability of both SU and MU OFDMA uplink Wi-Fi transmissions, $p_S^W$.

The key observation in Fig. 6.5(a), however, is that the performance of NR-U remains practically unaffected for small (and more practical) values of the radius, R, if the detection threshold is raised by 10dB (from $\beta_{NW} = -82$dBm to $\beta_{NW} = -72$dBm) while switching Wi-Fi interference from the SU mode to the MU OFDMA mode. This is also true when NR-U UEs transmit in the uplink (not shown). Similarly, Fig. 6.5(b) reveals that the impact of uplink NR-U interference on uplink Wi-Fi performance is the same when $\beta_{WN} = -82$dBm for the SU mode and $\beta_{WN} = -72$dBm for the MU OFDMA mode. *Although these discussions have been presented through Fig. 6.5 for a specific set of parameters, we verify that they are also true for other choices of* $M_Y^T$, $Q_Y^{sch}$, $\epsilon_Y$, *and* $\beta_{YZ}$.

**Summary:** We conclude that for a given number of potential interferers, NR-U performance in the presence of potential uplink Wi-Fi interference is strictly better when Wi-Fi STAs use the MU OFDMA mode instead of the SU mode. At the same time, the uplink performance in Wi-Fi is also significantly better when Wi-Fi uses the MU OFDMA mode and schedules more

than one STAs at a time. The benefits for NR-U arise from the added sensing requirement at the AP when MU OFDMA-based uplink transmissions are scheduled, while those for Wi-Fi arise from reduced hidden node probability due to more than one simultaneous transmitters. Further, when the MU OFDMA mode is used for Wi-Fi uplink transmissions, NR-U (both uplink and downlink) and uplink Wi-Fi achieve the same success probability at $-72$dBm, which would otherwise require a detection threshold of $-82$dBm if uplink Wi-Fi STAs were to use the SU mode. The only case where there are no benefits from switching to the MU OFDMA mode is the Wi-Fi downlink.

### 6.4.4 Importance of accurate sensing at the AP/gNB

Having established that schedule-based uplink transmissions at the interfering RAT are beneficial in increasing the success probability of RAT Y, we now look at the importance of accurate sensing at the entity that schedules these transmissions.

#### 6.4.4.1 Impact of number of scheduled uplink transmitters

Fig. 6.6(a) shows the impact of the number of scheduled uplink transmitters on the success probability of RAT Y. In Fig. 6.6(a), Y is Wi-Fi while the interfering RAT Z is NR-U. Observe that as the number of scheduled transmitters increases, the success probability of each of these transmissions increases. This can be understood intuitively as follows: as the number of active Wi-Fi STAs increases, the probability that *at least one* of them is within the sensing range of NR-U devices increases, thereby reducing the hidden node probability, $p_{\mathrm{H}}^{\mathrm{WN}}$. Thus, from the AP's perspective, it is more likely to receive uplink packets successfully if it schedules more STAs in the TF. Now consider a scenario where there are ongoing NR-U transmission(s) but the AP falsely infers the channel to be idle and schedules uplink users. Such a scenario can arise if the AP is hidden to the ongoing NR-U transmission(s). Fig. 6.6(b) shows the success probability of downlink NR-U transmissions in the presence of uplink MU OFDMA Wi-Fi interferers. Observe that as the hidden AP schedules more number of uplink STAs, the resulting impact on downlink NR-U worsens.

#### 6.4.4.2 Impact of transmit power control

Next, we look at the impact of transmit power control, which is a mandatory feature in both MU OFDMA and NR-U uplink transmissions. Fig. 6.6(c) shows the impact of transmit power control used in uplink MU OFDMA Wi-Fi transmissions in the presence of downlink NR-U interference. We observe that as far as the success probability of Wi-Fi is concerned, the higher the value of $\epsilon_{\mathrm{W}}$ used by the STAs, the more probable is the successful reception of these packets at the AP. This follows from observing Eq. (6.4). A higher value of $\epsilon_{\mathrm{W}}$ provides more compensation for the path loss encountered in transmitting a signal. If $\epsilon_{\mathrm{W}} = 1$, the

path loss from the transmitter to the desired receiver is completely compensated for at the receiver. Thus, to compensate for the high path loss, STAs located far from the AP transmit at a much higher power than those located close to the AP. This leads to high transmission powers at STAs located far from the AP, which diminishes the probability of these STAs being hidden to other devices. The probability of such transmissions being hidden to other devices diminishes rapidly and consequently, they are practically guaranteed to be successfully decoded at the receiver. On the other hand, if the Wi-Fi AP has falsely concluded that the channel is idle, when, in fact, there are ongoing NR-U transmissions, a higher $\epsilon_W$ has the opposite effect on NR-U transmissions. This is shown in Fig. 6.6(b), which shows the impact of uplink Wi-Fi interference on downlink NR-U transmissions. Note that all the aforementioned discussions on Fig. 6.6 also apply to uplink NR-U transmissions.

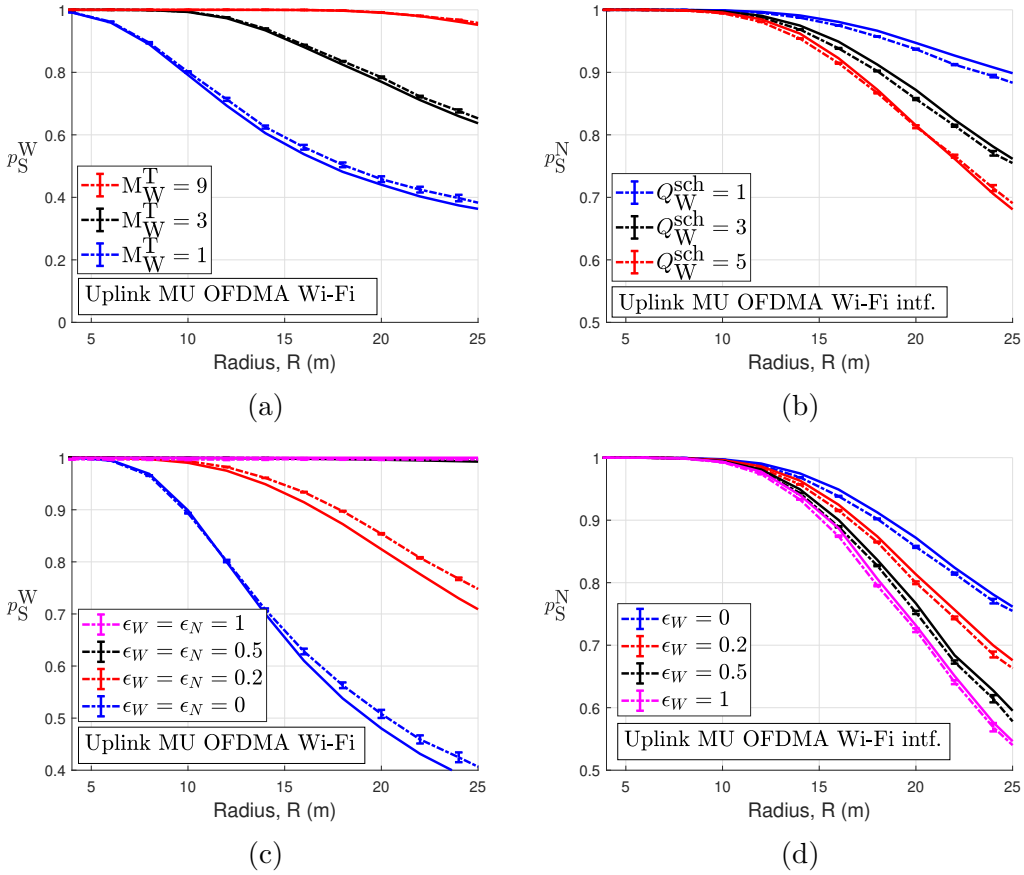


Figure 6.6: (a) Impact of number of scheduled RAT Y (Wi-Fi) transmitters, downlink NR-U intf., $\epsilon_W$=0 (b) Impact of number of scheduled RAT Z (Wi-Fi) interferers on downlink NR-U, (c) Impact of power control at RAT Y (Wi-Fi), $M_W^T$=3, downlink NR-U intf., (d) Impact of power control at RAT Z (Wi-Fi) on downlink NR-U, $Q_W^{sch}$=3.

**Summary:** We conclude that both factors: (i) a higher number of scheduled users, and

(ii) transmit power control, are beneficial in increasing the success probability of uplink transmissions. However, if the channel is busy, and the AP/gNB falsely concludes that the channel is idle, both of these factors exacerbate the interference at the other RAT's receiver.

### 6.4.5 Coexistence of Multiple Wi-Fi and NR-U Networks

In the simulation results discussed next, we randomly place three Wi-Fi APs and NR-U gNBs each in a square region of length 100 m. We place 15 Wi-Fi STAs and 15 NR-U UEs randomly in this region. Each STA/UE is associated with its nearest AP/gNB. All nodes detect each other using a detection threshold of $-72$ dBm, i.e., $\beta_{\mathrm{WW}}{=}\beta_{\mathrm{WN}}{=}\beta_{\mathrm{NW}}{=}\beta_{\mathrm{NN}}{=}-72$ dBm.

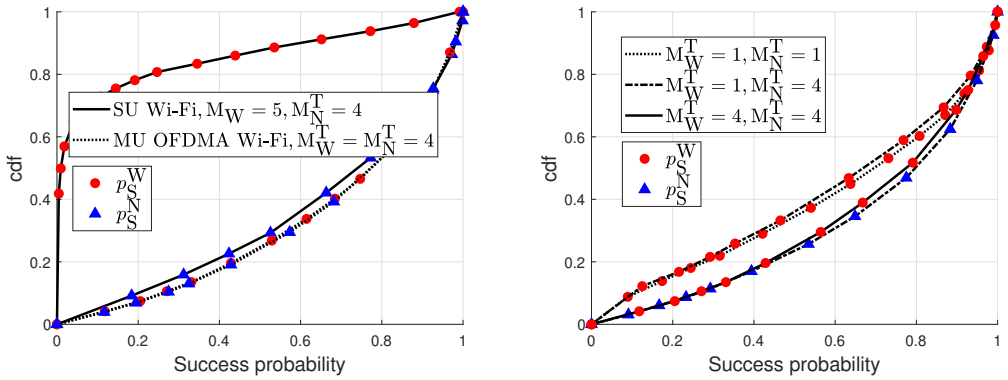


(a) (b)

Figure 6.7: Simulation results for three co-channel Wi-Fi and NR-U networks, $\epsilon_{\mathrm{W}}{=}\epsilon_{\mathrm{N}}{=}0.2$, (a) legacy contention (SU) vs MU OFDMA for uplink Wi-Fi, (b) impact of number of scheduled transmitters.

Fig. 6.7(a) shows the cdf of the success probabilities observed by the Wi-Fi STAs and NR-U UEs under different conditions. The success probability observed at a device is zero if none of its transmitted packets are successfully decoded at the receiver during the simulation interval. First, observe that the success probability of Wi-Fi STAs dramatically improves when they switch from the legacy contention mode to the MU OFDMA mode. Furthermore, as discussed in Sec. 6.4.3, we observe that this switch also increases the success probability of NR-U UEs, albeit by a modest amount. Next, Fig. 6.7(b) shows the cdf of Wi-Fi STAs and NR-U UEs under a different number of scheduled transmitters. In all cases reported in Fig. 6.7(b) Wi-Fi STAs transmit using MU OFDMA. Observe that when the number of scheduled transmitters are equal for both RATs, an increase in $\mathrm{M_Y^T}$ (from 1 to 4) increases the success probability of both RAT's transmissions[6]. On the other hand, if one of the RATs schedules more users than the other (NR-U in Fig. 6.7(b)), we observe that the success probability of that RAT's

[6]In the MU OFDMA mode, when $\mathrm{M_W^T}{=}\mathrm{M_N^T}$, $p_{\mathrm{S}}^{\mathrm{W}}{=}p_{\mathrm{S}}^{\mathrm{N}}$ (see Fig. 6.7(a) for $\mathrm{M_W^T}{=}\mathrm{M_N^T}{=}4$). Hence, for cases where $\mathrm{M_W^T}{=}\mathrm{M_N^T}$, we only show $p_{\mathrm{S}}^{\mathrm{W}}$ in Fig. 6.7(b).

transmissions (i.e., NR-U) increases while that of the other RAT (i.e., Wi-Fi) drops by a small amount. Thus, scheduling more uplink transmitters results in an increase in the success probability of their transmissions. We observe the same phenomenon with transmit power control (as discussed in Sec. 6.4.4.2). We omit these results in the interest of space.

We note that the above results differ from those discussed in the preceding subsections. Results in Fig. 6.7 also account for packet losses due to the simultaneous countdown of the back-off counter to zero, whereas we ignore these in our analysis. Nevertheless, the above discussions highlight that *although our analysis was derived for the case of only one co-channel Wi-Fi and NR-U networks, the insights derived from the model also apply when more than one Wi-Fi and NR-U networks coexist.*

## 6.5 Chapter Summary

In this chapter, using a stochastic geometry-based model and extensive simulations, we investigated the factors that critically affect the success probability of Wi-Fi 6E and NR-U transmissions when the two technologies coexist in the 6 GHz bands. We identify that compared to CSMA/CA, schedule-based uplink MU OFDMA transmissions improve the success probability of NR-U transmissions as well as those of Wi-Fi 6E uplink. This is a critical finding for the 6 GHz bands, where there are no current Wi-Fi or 3GPP-based unlicensed technologies in operation. Consequently, CSMA/CA for uplink access can indeed be disabled in these bands. Additionally, we observe that the same factors that are responsible for the superior performance of schedule-based uplink transmissions worsen the performance of the other technology's transmissions if the AP/gNB incorrectly detects the channel to be idle.

We limit our work in this chapter to the success probability of individual transmissions. Although this has implications on user-perceived system-level metrics like the throughput and the latency, other factors can come into play in LBT-based networks. For example, we ignore the exposed node problem in our work, which, in many cases, is known to contribute negatively to the overall system performance. We leave the extension of our work to include a study on the exposed node problem and system-level metrics to future work.

# Chapter 7

# Performance Evaluation of Cellular V2X

## 7.1 Introduction

The benefits of V2X communications in terms of reducing vehicle crashes and fatalities and improving traffic efficiency are well known. During the conception of DSRC—the first radio access technology to enable direct V2X communications—the focus was on enabling safety applications that alerted drivers in potentially hazardous situations. Today, however, connected vehicles are considered far more important not only in terms of enabling basic safety applications but also as a precursor to fully autonomous driving. A quick look at the standardization activities around V2X technologies bears testimony to the growing importance of V2X communications. The underlying standard for DSRC—IEEE 802.11p is evolving to IEEE 802.11bd, while the recently developed C-V2X is already undergoing enhancements in NR V2X [50].

C-V2X was developed by the 3GPP in its Release 14, while the standardization of it's successor, NR V2X, was recently completed in 3GPP Release 16. Throughout this chapter, We collectively refer to C-V2X and NR V2X as 3GPP-based V2X technologies. Direct vehicular communications in these technologies are supported over the sidelink[1] interface. 3GPP-based V2X technologies have an added advantage over IEEE 802.11-based technologies in that vehicles equipped with C-V2X or NR V2X can rely on the widespread cellular infrastructure for centralized resource allocation wherever possible. However, since the presence of cellular coverage cannot always be relied upon, both C-V2X and NR V2X support direct vehicular communications in the absence of the cellular infrastructure as well. Direct V2X communications in the absence of cellular coverage are enabled through sidelink mode 4 in C-V2X and sidelink mode 2 in NR V2X [50].

One of the fundamental challenges in the design of robust V2X systems is the design of a MAC protocol that is efficient, distributed, and scalable. In distributed systems, the MAC protocol remains a major bottleneck in translating the high performance of the PHY layer into reliable application layer performance. Therefore, efforts are underway to improve the

[1]This interface, defined in 3GPP Release 12, enables direct communications between user equipment without the involvement of the cellular infrastructure.

MAC efficiency in NR V2X. As such, NR V2X is set to introduce several new features derived from 5G NR. However, the fundamental aspects of the MAC layer design are likely to remain similar across the two 3GPP-based V2X technologies [50]. One key reliability-enhancing mechanism that is considered in both, C-V2X and NR V2X, is the use of packet re-transmissions. In the broadcast mode of communications (the default mode in C-V2X and one of the three modes in NR V2X), re-transmissions are also referred to as *blind* re-transmissions because if configured to do so, transmitters re-transmit every packet regardless of whether the earlier transmission(s) are received successfully or not. This differentiates re-transmissions in C-V2X and NR V2X from the conventional hybrid automatic repeat request (HARQ) used in cellular 3GPP technologies.

Re-transmissions are beneficial from the PHY layer perspective because multiple copies of a packet can provide frequency and time-domain diversity. At the receiver, a packet is successfully received as long as one of its copies is correctly decoded by the receiver. Thus, the probability of packet errors is reduced, thereby enhancing the link-level performance. From the MAC layer perspective, however, it has been shown in the context of C-V2X that the benefit of achieving higher transmission reliability diminishes as the traffic density[2] increases [30]. The 3GPP Release 14 allows for static configuration of a UE, i.e., vehicle, to transmit each packet once (i.e., no re-transmissions) or twice (i.e., one re-transmission) as well as a dynamic configuration whereby UEs can autonomously decide whether or not to re-transmit a packet. Similar provisions are likely to be provided in 3GPP Release 16 as well, except the number of permissible re-transmissions is likely to be more than one [50]. However, to the best of our knowledge, the problem of how to enable UEs to autonomously (i.e., without assistance from the cellular infrastructure) decide when to activate re-transmissions remains unaddressed, and it is the subject of this chapter.

In this chapter, through an extensive simulation study carried out using network simulator-3 (ns-3), we show that static re-transmission configurations provide superior performance only in specific scenarios. Although in theory, re-transmissions are beneficial (especially from the PHY layer perspective) and are often claimed to be a key reliability-enhancing feature in C-V2X and NR V2X [292], in practice, this feature can have the opposite effect and seriously degrade system performance if it is not implemented carefully. Thus, we argue the need for a re-transmission control mechanism, i.e., a mechanism that allows the vehicles to autonomously decide whether or not to re-transmit packets based on locally available information. We then propose Channel Congestion-based Re-transmission Control ($C^2RC$)—a simple, yet effective, probabilistic re-transmission control mechanism using which the UEs can use re-transmissions to maximize system performance in lightly-loaded scenarios while avoiding re-transmitting in heavily loaded conditions, thereby avoiding performance degradation. Although the discussions in our work on the impact of re-transmissions and the proposed re-transmission control mechanism apply to both C-V2X and NR V2X, our simulation study is restricted to C-V2X sidelink mode 4. Throughout this chapter, we refer

[2]We say that the transmission density increases when the number of vehicles increases and/or the packet transmission rate (in Hz) increases.

to the terms vehicles and UEs interchangeably. The main contributions of our work are as follows.

- We investigate the impact of re-transmissions on C-V2X sidelink mode 4 performance. Based on our observations, we motivate the need for re-transmission control mechanisms in C-V2X sidelink mode 4.
- We perform a systematic study on the impact of re-transmissions on the observed channel congestion. We show that beyond a certain congestion level, switching on re-transmissions leads to the re-use of resources, which can potentially degrade the overall system performance.
- We propose C$^2$RC—a mechanism that allows C-V2X UEs to enjoy the benefits of using packet re-transmissions when they are truly beneficial while minimizing the impact of re-transmissions in congested environments.

## 7.2 Related Work

The authors in [293] and [294] study the performance of C-V2X sidelink mode 3, where the UEs are within cellular coverage. On the other hand, the authors in reference [30] and [295] evaluate the performance of C-V2X mode 4 in the highway and urban scenarios, respectively. In [30], the authors show that packet re-transmissions are not always helpful. Furthermore, the authors show the impact of several transmission parameters such as the packet transmission rate, modulation and coding scheme, etc. on the system performance of sidelink mode 4 in highway scenarios. The authors in [296] perform a comprehensive study on the impact of different PHY and MAC layer parameters on the system performance of C-V2X sidelink mode 4.

An analytical model to capture the performance of C-V2X mode 4 has been developed in [297]. Through their analytical model, the authors accurately characterize the performance of C-V2X mode 4 in different scenarios. However, due to the complexity of the model, the performance gain (or lack thereof) due to re-transmissions is ignored in [297]. The aforementioned works provide several insights on the performance of C-V2X. However, the study of re-transmissions in C-V2X as a reliability-enhancing mechanism has not received much attention in the literature, with only brief discussions in [30].

## 7.3 Background & Simulation Setup

The C-V2X sidelink mode 4 algorithm is defined in 3GPP Release 14. We describe this algorithm in detail in Sec. 2.2.5. In what follows, we provide a brief overview of the algorithm required to understand the re-transmission control mechanism, C$^2$RC, proposed in Sec. 7.5.

When the C-V2X sidelink mode 4 algorithm is triggered by a UE, it first senses the operating channel for a fixed 1 second interval (this interval is referred to as the *sensing window*) and uses these sensing results to select a *resource* within the *selection window*[3]. A resource in C-V2X constitutes a group of contiguous Resource Blocks (RBs) in the frequency domain and lasts for 1 sub-frame (i.e., 1 msec) in time. Each time a resource is selected, the UE reserves the selected resource for a number of subsequent transmissions. This number is referred to as the re-selection counter (denoted as $C_{\text{resel}}$ in [27]). $C_{\text{resel}}$ is randomly chosen in [5, 15] if the packet transmission rate is 10 Hz, in [10, 30] for 20 Hz and in [25, 75] for 50 Hz. After each packet transmission, $C_{\text{resel}}$ is decremented by 1, and if $C_{\text{resel}}$ becomes zero, the mode 4 algorithm is triggered to select a new resource with a probability known as the *reselection probability*, $p_{\text{resel}}$. Finally, when the UE transmits a packet, in addition to the actual payload, it broadcasts the resource selection information to aid other UEs in selecting the best resource for their respective transmissions.

The results presented in this chapter have been obtained using our ns-3 simulator. Our ns-3 simulator implements all functionalities of C-V2X sidelink mode 4, including the mode 4 algorithm as per the 3GPP specifications [26, 27]. This algorithm can be used in all deployment scenarios. However, in urban environments, vehicles are more likely to be within cellular coverage. Therefore, the resource allocation of vehicle-generated packets can be done by the eNodeB using sidelink mode 3. In the rest of this chapter, we restrict our focus to the performance of C-V2X mode 4 in highway environments.

The performance metric chosen in our study is the packet delivery ratio (PDR)—the ratio of the number of packets received from a certain transmitter to the number of packets sent by that transmitter. In cases where a transmitter sends each packet twice, each packet is successfully decoded at the receiver as long as one of its copies is received successfully. Losses in a wireless communication system can either occur due to packet collisions or wireless channel characteristics. Our ns-3 simulator handles both types of losses. The wireless channel for a transmitter-receiver pair is modeled as per [298], which provides a look-up table for the probability of packet error for a given SINR. For each received packet, the SINR is computed as the ratio of the signal power to the noise power (in case of no collisions) or noise plus interference power (in case of packet collisions).

The 3GPP provides guidelines on simulation topologies for the performance evaluation of C-V2X [299]. For the highway scenario, 3GPP recommends that at least a 2 kilometer (km) road-stretch must be simulated, with three 4 m wide lanes in each direction. Scenarios are identified by the average velocity of vehicles. Given the average velocity, the inter-vehicle distance in each lane is computed as the distance traveled by a vehicle in 2.5 seconds. The two standard scenarios specified in [299] are for 70 km/hr and 140 km/hr, which represent medium (120 vehicles/km) and sparse (60 vehicles/km) density of vehicles, respectively. The simulation parameters used in this chapter are as outlined in Table 7.1.

[3]The selection window is the time duration within which the packet must be transmitted to satisfy its latency requirement.

Table 7.1: Simulation Parameters for performance evaluation of C-V2X sidelink mode 4

| Parameter | Value | Parameter | Value |
|---|---|---|---|
| Noise Figure | 9 dB | Bandwidth | 10 MHz |
| Sub-channel size | 24 RBs | Packet size | 190/300 Bytes |
| Loss Model | WINNER+ B1 | Tx power | 23 dBm |
| Modulation scheme | QPSK | Code rate | 0.7 (190 B)<br>0.5 (300 B) |
| RSRP Thresh. see [296] | −110 dBm | $p_{\text{resel}}$ see [30, 296] | 1 |

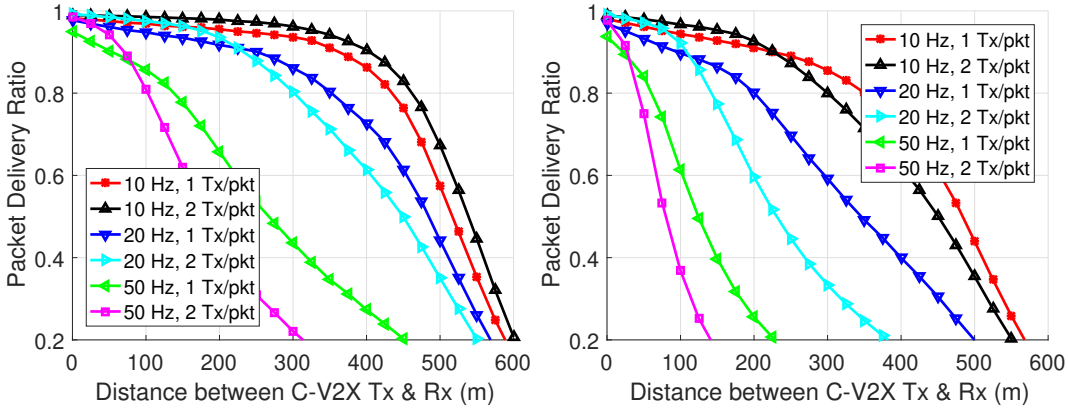


(a) Highway Fast (b) Highway Slow

Figure 7.1: C-V2X mode 4 performance in 3GPP-defined scenarios

## 7.4 Is Re-transmission Control Needed?

### 7.4.1 Impact of Re-transmissions on System Performance

We first study the performance of C-V2X sidelink mode 4 in the two standard highway scenarios given in [299]. The purpose of this study is to understand if re-transmission control mechanisms are needed and if so, under what scenarios are such mechanisms useful. Consistent with [295], we refer to the 70 km/hr and 140 km/hr scenarios as the *Highway Slow* and *Highway Fast* scenarios, respectively. For these two highway scenarios, Fig. 7.1 shows the average PDR observed across all C-V2X receivers as a function of the receiver's distance from a given transmitter. The packet transmission rate, specified in Hz (10, 20, or 50) indicates the number of packets transmitted by each C-V2X UE every second. 1 Tx/-packet indicates that each packet is transmitted only once, whereas 2 Tx/packet indicates that each packet is always re-transmitted. Hereafter, we refer to the static configuration where re-transmissions are always disabled or enabled at all UEs as the always OFF and always ON modes, respectively.

Fig. 7.1 shows that except for the 10 Hz, Highway Fast scenario, the always ON mode performs inferior to the always OFF mode beyond a certain distance between the transmitter and receiver. For example, in the Highway Fast scenario with 20 Hz transmission rate, if a transmitter has to communicate with a receiver greater than 220 m away, the transmitter is better off in sending each packet only once (as opposed to sending each packet twice) in terms of the average PDR observed at the receiver. The primary reason for this behavior is channel congestion. The always ON mode can require up to twice[4] the number of resources used in the always OFF mode. Beyond a certain traffic density, when re-transmissions are switched ON, C-V2X UEs end up re-using a fraction of resources (i.e., a C-V2X UE re-uses a resource already reserved by another C-V2X UE), which leads to packet collisions and consequently, performance degradation.

Further, we see that in all scenarios, the always ON mode results in a higher PDR at small transmitter-receiver distances. For small distances, even if a collision occurs on a particular resource, the SINR can be sufficient to decode the strongest signal, which is typically sent by the transmitter located very close to the receiver. Therefore, packets transmitted by UEs that are located close to the receiver have a high probability of being successfully decoded, especially if each packet is transmitted twice. However, as the traffic density increases, the always ON mode results in the re-use of a significant number of resources, i.e., a large fraction of resources suffer from collisions. In such cases, packets sent by far-away transmitters are less likely to be decoded, resulting in poor performance relative to the always OFF mode at large distances.

### 7.4.2 Need for Re-transmission Control

It must be noted from Fig. 7.1 that at relatively low densities (e.g., Highway Fast, 10 Hz), re-transmissions improve the system performance for all transmitter-receiver distances. It is only when the traffic density exceeds a certain limit that the always ON mode begins to perform inferior to the always OFF mode for large transmitter-receiver distances. We leave the determination of the exact traffic density and the distance at which this behavior occurs to future work. Our focus in this work, rather, is to develop a mechanism using which UEs can autonomously decide whether or not to enable re-transmissions, thereby leading to superior performance in sparse scenarios, while mitigating the negative impact of re-transmissions on performance in dense conditions.

The communication requirements of vehicular safety applications differ in terms of latency, reliability, and range. Some applications require high reliability with a short range. For such applications, the always ON mode is suitable. However, this performance gain at short distances comes at the cost of significant loss at larger distances as shown in Fig. 7.1. For certain safety applications, a large communication range is desired. Thus, high reliability at

[4]Ideally, as long as UEs in the always OFF mode cumulatively use up less than 50% of the available resources, switching from the always OFF to the always ON mode should double the number of used resources.

short distances alone is not sufficient to support all safety applications. In practical scenarios, vehicles are likely to participate in multiple safety applications simultaneously. For example, each vehicle will process packets received from near-by vehicles to detect another vehicle in its blind spot, while using a packet from a far-away vehicle to detect an approaching emergency vehicle. Considering this diverse set of safety applications, to guarantee performance across a wide range of transmitter-receiver distances, a re-transmission control mechanism is necessary.

## 7.5 Design of C$^2$RC

### 7.5.1 Channel Congestion due to Re-Transmissions

A detailed explanation of the impact of re-transmissions on system performance, particularly the observed performance loss at certain densities, requires a closer look at the congestion level observed in the channel when the C-V2X mode 4 algorithm is used. Toward this objective, we conduct simulations for a hypothetical scenario where all vehicles can sense each other. In this scenario, each vehicle must account for every other vehicle's transmissions while selecting a resource for its transmissions. The objective of studying this hypothetical scenario is to study the impact of switching ON re-transmissions on resource utilization when the C-V2X mode 4 algorithm is used. Before we do so, however, we must define a metric to quantify the congestion level in the network. We use the 3GPP-defined metric—Channel Busy Ratio (CBR), which is defined at any time instant as the ratio of the number of resources *utilized* in the previous 100 sub-frames (i.e., 100 milliseconds) to the total number of resources available in previous 100 sub-frames. Note that this definition of CBR requires a threshold energy value beyond which a resource is declared as utilized. We elaborate on what threshold to use in the next sub-section. For the sake of the following discussions, it can be assumed that all UEs sense each other at above the chosen energy threshold.

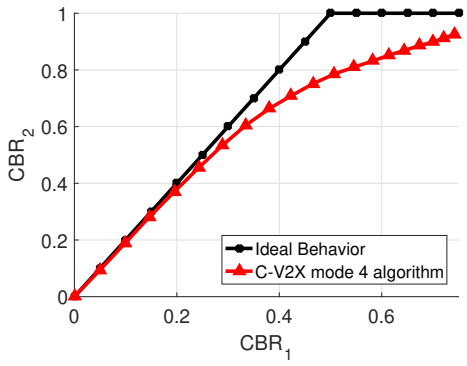


Figure 7.2: Effect of re-transmissions on the observed CBR. All UEs can sense each other at above the energy threshold.

For a given network configuration, let $CBR_1$ be the average CBR observed at a UE in the always OFF mode, while $CBR_2$ denotes the average CBR observed in the always ON mode. Fig. 7.2 shows the variation in $CBR_2$ as a function of $CBR_1$. Observe that as long as $CBR_1$ is under $\sim$0.3, transmitting a packet twice nearly doubles the observed congestion level, which is intuitive behavior. However, beyond this $CBR_1$ level, switching on re-transmissions leads to re-utilization of some of the resources, leading to packet collisions on some of the utilized resources even as other resources in the channel remain idle. When $CBR_1$ increases further, the curve significantly deviates from linear behavior, implying that a non-negligible fraction of resources is, in fact, re-used. Thus, we can infer from Fig. 7.2 that after the observed CBR level at a UE exceeds a certain level (not necessarily 0.3 as we show in Sec. 7.5.4), using the always ON mode is likely to negatively impact the overall system performance. Consequently, if the observed CBR is large enough, re-transmissions should be disabled, at least for some UEs, to prevent performance degradation.

### 7.5.2 Choice of Energy Threshold

In the previous sub-section, we noted that the definition of CBR requires the selection of an energy threshold (say $\gamma$) such that if the resource energy is greater than $\gamma$, the resource is declared as occupied. In the following discussions, we elaborate on the choice of an appropriate energy threshold.

For the simulations reported in this sub-section, we vary the number of vehicles in the 2 km stretch, with the inter-vehicle distance maintained such that vehicles are distributed uniformly along the 2 km road length. Fig. 7.3 shows the ratio of $CBR_2$ to $CBR_1$ as a function of the number of vehicles for two different packet transmission rates (i.e., 10 Hz and 20 Hz). Note from our discussions in the previous sub-section that re-transmissions begin to negatively affect the system performance when doubling the number of transmissions does not result in a corresponding increase in the observed congestion level. The number of UEs after which re-transmissions hurt the overall system performance is 125 and 70 for the 10 Hz and 20 Hz packet transmission rates (not shown in Fig. 7.3), respectively. For values of $\gamma$ above $-105$ dBm, the ratio of $CBR_2$ to $CBR_1$ does not vary significantly with the number of vehicles. The non-linear behavior of ratio becomes prominent only at $\gamma = -105$ dBm and below. Although results are presented in this chapter only for two specific cases, a similar trend was observed when parameters such as packet transmission rate and sub-channel size were varied. Thus, *an energy threshold, i.e., $\gamma$, of $-105$ dBm is suitable for estimating the congestion level on the operating channel.*

### 7.5.3 Channel Congestion-based Re-transmission Control

In C$^2$RC, when the UE uses the C-V2X mode 4 algorithm for resource selection, it decides on whether to enable or disable re-transmissions for the upcoming $C_{\text{resel}}$ transmissions (see

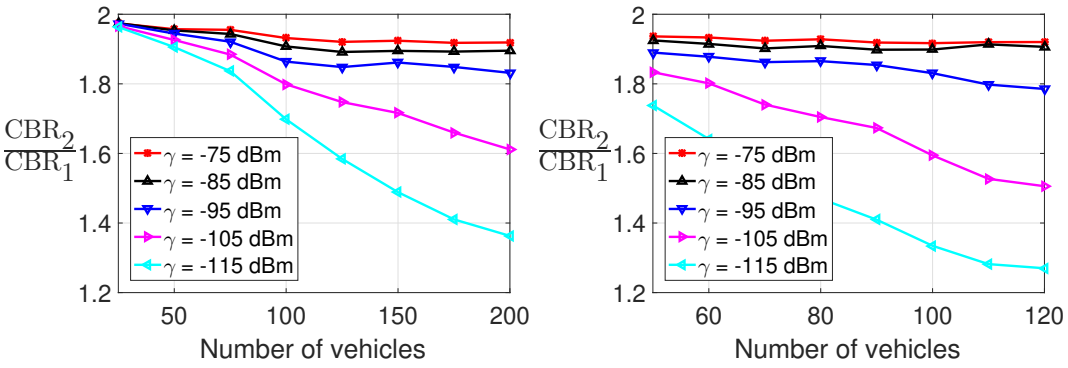


(a) 10 Hz (b) 20 Hz

Figure 7.3: Impact of energy threshold, i.e., $\gamma$.

Sec. 7.3) based on the CBR level observed in the cycle of previous $C_{\text{resel}}$ transmissions. Let the average CBR observed over the previous $C_{\text{resel}}$ transmissions be $\text{CBR}_{\text{obs}}$. This $\text{CBR}_{\text{obs}}$ can readily be computed at C-V2X UEs since its computation only depends on the measurement of Sidelink Received Signal Strength Indicator (S-RSSI) [300], which is measured during each cycle of $C_{\text{resel}}$ transmissions. The C-V2X UE then computes a probability, $p_{\text{re-tx}}$, with which the it will enable re-transmissions for the upcoming $C_{\text{resel}}$ transmissions. Based on our discussions in Sec. 7.5.1, it is clear that UEs must re-transmit packets if $\text{CBR}_{\text{obs}}$ is low and refrain from re-transmitting packets if $\text{CBR}_{\text{obs}}$ is too high. Thus, the probability $p_{\text{re-tx}}$ must meet the following criteria.

- The probability $p_{\text{re-tx}}$ must be a non-increasing function of the observed CBR level, $\text{CBR}_{\text{obs}}$.
- The rate at which $p_{\text{re-tx}}$ drops from 1 to 0 with $\text{CBR}_{\text{obs}}$ must be configurable.

In this work, we choose the shifted and inverted logistic function to define $p_{\text{re-tx}}$ as follows:

$$p_{\text{re-tx}} = 1 - \frac{1}{1 + e^{-2\beta(\text{CBR}_{\text{obs}} - \text{CBR}_{\Delta})}},$$

where $\text{CBR}_{\Delta} \in [0, 1]$ and $\beta \in (0, \infty)$ are tunable parameters. The significance of $\text{CBR}_{\Delta}$ and $\beta$ can be understood from Fig. 7.4. $\text{CBR}_{\Delta}$ signifies the CBR level at which $p_{\text{re-tx}}$ drops to 0.5, while $\beta$ controls the rate at which $p_{\text{re-tx}}$ drops from 1 to 0. If $\beta = \infty$, $p_{\text{re-tx}}$ resembles a shifted and inverted unit step function at $\text{CBR}_{\Delta}$, while for small values of $\beta$, $p_{\text{re-tx}}$ smoothly transitions from 1 to 0.

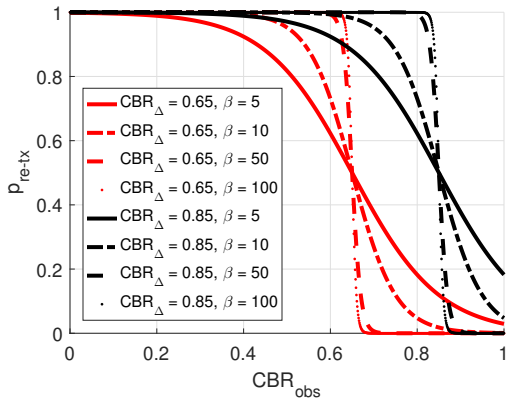


Figure 7.4: Impact of $\text{CBR}_\Delta$ and $\beta$ on $p_{\text{re-tx}}$.

### 7.5.4 Selection of C$^2$RC Parameters

Fig. 7.5 shows the performance of C$^2$RC in comparison to the static re-transmission modes for three different traffic densities. Fig. 7.5a represents a lightly loaded scenario where 100 UEs (10 Hz periodicity) are spread out over the 2 km stretch. As expected, the always ON mode outperforms the always OFF mode for all distances between the transmitter and the receiver. This is because the channel congestion is low enough that switching on re-transmissions does not lead to significant re-use of resources. The choice of parameters $\text{CBR}_\Delta$ and $\beta$ in this scenario must be such that C$^2$RC must enable re-transmissions with a high probability in this scenario. We see that as $\text{CBR}_\Delta$ progressively increases, the resulting C-V2X system performance keeps improving and approaches the performance of the always ON mode as $\text{CBR}_\Delta = 0.65$. A $\text{CBR}_\Delta$ value beyond 0.65 yields no performance improvement as the performance is bounded by that of the always ON mode.

Next, Fig. 7.5b represents a moderately loaded scenario with 200 UEs, each transmitting at 20 Hz. We see that as the channel load increases (from what was shown in Fig. 7.5a), an increase in $\text{CBR}_\Delta$ leads to a deterioration in system performance, albeit marginally (when $\beta = 100$). This is because the channel congestion is now large enough that doubling the number of transmissions (as a result of always re-transmitting) leads to significant re-use of resources and contributes negatively to the system performance. This trend is the reverse of what was shown in Fig. 7.5a. Further, although not shown in Fig. 7.5b, the parameter $\beta$ has negligible impact on the system performance if $\text{CBR}_\Delta$ is small (0.1 through 0.55). However, at large values of $\text{CBR}_\Delta$ (such as 0.65), choosing a small $\beta$ results in a non-negligible probability of re-transmissions even if the observed CBR is very high. For example, Fig. 7.4 shows that even if the CBR at a UE is 0.8, $\text{CBR}_\Delta = 0.65, \beta = 5$ results in $p_{\text{re-tx}} = 0.2$. This results in a slightly inferior system performance when $\beta = 5$ is selected.

Finally, Fig. 7.5c shows the performance in a heavily loaded scenario where 300 UEs transmit at 50 Hz. In this case, the observed CBR at all UEs in the always OFF mode is very

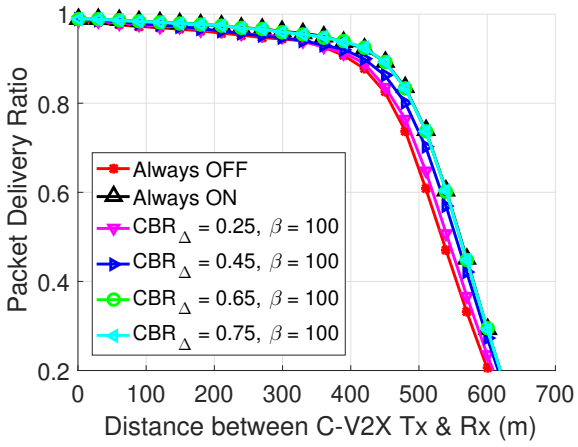


(a)

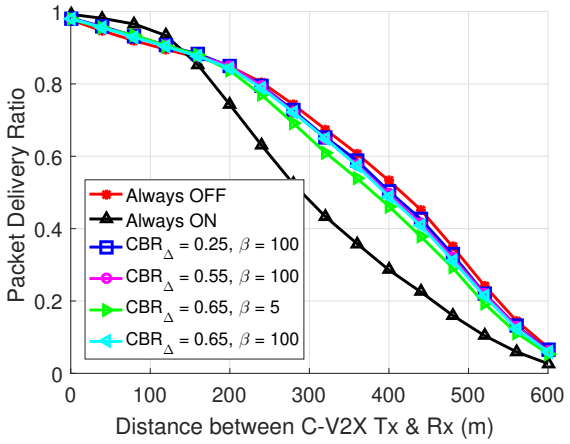


(b)

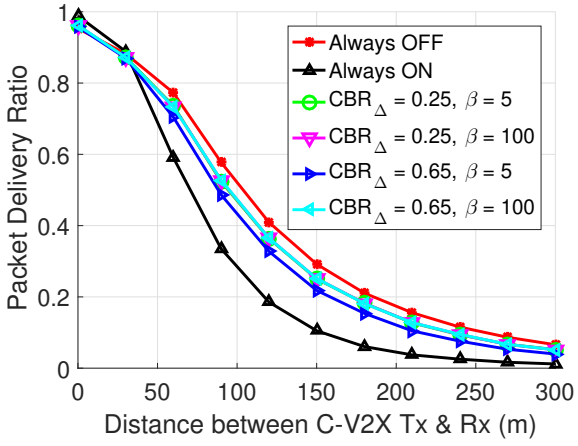


(c)

Figure 7.5: Performance of C$^2$RC in different traffic densities, (a) Light, 10 Hz, 100 vehicles, (b) Moderate, 20 Hz, 200 vehicles, (c) Heavy, 50 Hz, 300 vehicles.

high (∼0.9). Consequently, any reasonable choice[5] of $CBR_{\Delta}$ has a negligible impact on the resulting system performance. However, similar to the moderately loaded scenario, if a small value of $\beta$ is chosen at large values of $CBR_{\Delta}$ (e.g., 0.65), the system performance will deteriorate as shown in Fig. 7.5c.

Note from Fig. 7.5b and 7.5c that when $C^2RC$ is used, the average PDR at C-V2X transmitter-receiver distances in the [0-160] m (moderate scenario) and [0-30] m (dense scenario) range[6] is in-between the average PDR of the two static modes. Thus, a small improvement over the always OFF mode is observed for smaller transmitter-receiver distances. However, a substantial improvement is observed over the always ON mode for large transmitter-receiver distances. Because the UEs are randomly dropped along the road, in some instances, certain sections of the road can be less congested than others, which is likely in real-life scenarios as well. A marginal performance loss relative to the always OFF mode at larger distances occurs due to re-transmissions from a few C-V2X UEs that re-transmit because the locally observed CBR may be low enough to trigger the second transmission even though the channel is congested at far-away receivers.

Based on the above discussions, we infer that a small value of $CBR_{\Delta}$ is more suitable for moderate channel loads, while a large value of $CBR_{\Delta}$ is optimal for low channel loads. Yet, increasing $CBR_{\Delta} > 0.65$ yields very little performance improvement in light conditions. Furthermore, at moderate densities, even though an increase in $CBR_{\Delta}$ degrades the performance, this degradation is negligible as long as $\beta$ is large. Based on our simulation results, $\beta \geq 100$ prevents performance degradation even when $CBR_{\Delta}$ is as high as 0.65.

In summary, *our simulations reveal that* $CBR_{\Delta} = 0.65$ *and* $\beta = 100$ *strikes a balance between avoiding performance loss at high densities and improving performance at low densities.* This is, however, true as long as the chosen energy threshold for declaring a resource as occupied is $\gamma = -105$ dBm. Although simulation results for a limited set of scenarios have been shown in Fig. 7.5, the implications of selecting different values for $CBR_{\Delta}$ and $\beta$ as discussed here were tested to be true in a wide range of traffic densities.

## 7.6 Chapter Summary

In this chapter, we take an in-depth look at the performance implications of packet re-transmissions, which is used in C-V2X and is likely to be re-used in NR V2X. We show that this feature, although useful, must be used with caution. Since both C-V2X and NR V2X must operate in distributed environments without any assistance from the cellular infrastructure, the UEs must decide on whether or not to re-transmit packets based only on

[5]Naturally, this is true when $CBR_{\Delta} < 0.9$. However, at such congestion levels, it is obvious that re-transmissions will hurt the system performance.

[6]160 m and 30 m are the distances beyond which the always ON mode performs worse in the moderate and heavy load scenarios, respectively.

the locally observed channel congestion. To address this, we propose and evaluate C$^2$RC—a probabilistic re-transmission control mechanism that allows the UEs to maximize performance when re-transmissions are truly beneficial while preventing performance degradation in scenarios where UEs are better off transmitting only once.

# Chapter 8

# Performance Analysis of MU OFDMA in IEEE 802.11ax

## 8.1 Introduction

Wi-Fi has experienced tremendous growth in the past two decades and has become ubiquitous in today's home and enterprise networks. It has been estimated that the global worth of the Wi-Fi market will reach USD 33.6 billion by 2020 [301]. This huge success of Wi-Fi has, however, at the same time, led to a degradation in its performance, particularly in dense deployment scenarios. For instance, a Wi-Fi hotspot in a crowded street (e.g., Times Square), an airport, a stadium, or a concert offers poor performance because of severe collisions arising due to channel contention from a large number of associated Wi-Fi STAs. Motivated by the growing need for improved performance, the IEEE 802.11 working group has actively continued to release new protocols for Wi-Fi starting from 802.11a to the more recent 802.11ac. Additionally, to take Wi-Fi a step further, in 2014, the High Efficiency (HE) WLAN task group (a.k.a. TGax) was formed to develop standards for the next generation Wi-Fi, namely IEEE 802.11ax [302]. According to its functional requirements, 802.11ax should support a ten-fold increase in the number of supported users over the same unlicensed spectrum, increase average user throughput by four times, and improve outdoor and multi-path signal robustness [303].

Although most of the previous 802.11 amendments have improved the PHY layer throughput by adopting advanced techniques, such as higher-order modulation and coding schemes, OFDM, MIMO, etc., the MAC layer protocol used in all amendments have been fairly similar to each other. Admittedly, the MAC protocols of 802.11 have been unable to keep up with the progress made at its PHY layer. Therefore, the inefficiency of the MAC layer presents a major bottleneck in translating the high PHY layer throughput into high throughput at the transport and application layers in real-world scenarios, particularly when the Wi-Fi deployment is dense [304]. To address this issue, the 802.11ax TGax has introduced several modifications to the 802.11 MAC layer protocol. The most notable feature is the adoption of OFDMA in both the uplink (UL) (i.e., from STAs to the AP) and the downlink (DL) (i.e., from the AP to STAs). OFDMA divides the available physical resource, i.e., spectrum, into multiple orthogonal sub-channels—referred to as an RU in the 802.11ax terminology. The 20 MHz, 40 MHz, 80 MHz and 160 MHz Wi-Fi channels can be divided into 9, 18,

37 and 74 RUs, respectively. These RUs can then be allocated to different users as per their traffic demands, thereby enabling concurrent MU transmissions. This is in contrast to previous Wi-Fi standards wherein all devices transmit, one at a time, in the entire channel bandwidth.

For facilitating MU transmissions, the 802.11ax capable AP serves as a central controller and triggers the MU OFDMA mode by transmitting a TF [305]. A TF is an 802.11ax frame structure that contains fields related to RU allocation for STAs, associated power control, and transmission timing information. In the DL, the AP has the global knowledge of the packet queue status for each associated STA. Therefore, 802.11ax provisions purely schedule-based transmissions in the DL; one or more RUs are dedicated for packet transmission to a particular STA. However, in the UL, the STAs must explicitly communicate their traffic requirements to the AP by transmitting a regular buffer status report (BSR). BSR information can either be elicited by the AP or piggybacked by STAs in certain transmitted packets. 802.11ax supports two modes in which packets can be transmitted in the UL: i) scheduled access (SA), in which the AP schedules a set of STAs to transmit on dedicated contention-free RUs, and ii) random access (RA) in which, multiple STAs contend to transmit their packet using the exponential backoff-based DCF, similar to the one used in legacy[1] 802.11 MAC.

SA mode preempts channel contention from STAs and helps in improving the overall 802.11ax throughput. On the other hand, RA mode facilitates the 802.11ax network in allowing transmissions from those STAs whose BSR information is not available at the AP. For example, newly joined STAs that have control frames to transmit or other STAs who haven't transmitted any packets for a while may not be scheduled in any SA RUs by the AP because of the unavailability of their BSR information. However, using RA mode, such STAs can contend and transmit their packets (along with piggybacked BSR information) in RA RUs. Thus, the use of RA RUs not only allows STAs to transmit their packets but also provides the required information to the AP so that the AP can schedule SA RUs to those STAs in the subsequent TFs. Therefore, in all practical implementations of 802.11ax, the AP dynamically allocates some of the RUs as SA RUs and the remaining ones as RA RUs such that it can collect enough BSRs for scheduling STAs in the SA RUs. It is important to note that maintaining a balance between RA RUs and SA RUs is key to meet 802.11ax's functional requirements. In this work, we investigate this resource allocation problem in detail and devise an algorithm that facilitates the dynamic and optimized allocation of RUs such that the 802.11ax network throughput is maximized in different deployment scenarios.

Furthermore, we envision that at least during the initial deployments of 802.11ax networks, an 802.11ax capable AP would need to simultaneously serve both legacy 802.11 and 802.11ax STAs. Although 802.11ax devices are backward compatible with legacy 802.11 protocols, legacy STAs cannot understand and support MU OFDMA transmissions. They can only decode transmissions done on the entire 20 MHz channel. Therefore, in order to jointly

[1]Recall that the term "legacy Wi-Fi" refers to all previous versions of Wi-Fi including 802.11a/b/g/n/ac.

serve both legacy 802.11 and 802.11ax STAs, the AP has to allocate different fractions of airtime for single-user (to support legacy STAs) and multi-user (to support 802.11ax STAs) transmission modes. In this work, we study the issue of fair distribution of airtime between legacy 802.11 and 802.11ax transmissions when they operate in networks with different traffic requirements.

The core contributions of this work are summarized in the following bullets:

(1) We describe the novel MU-OFDMA based 802.11ax MAC that is being studied for 802.11ax in the TGax. We provide a detailed analysis of the MAC protocol and derive an expression for throughput achieved at the MAC layer.

(2) We investigate the impact of different distributions of RA RUs and SA RUs on the overall performance of 802.11ax MAC. Based on our findings, we devise an algorithm for the optimal allocation of RUs as SA RUs and RA RUs that maximizes the overall throughput of an 802.11ax network in all use-case scenarios.

(3) We envision that during the initial deployments of 802.11ax, an 802.11ax capable AP would need to serve both legacy 802.11 and 802.11ax STAs. In such settings, we analyze how to fairly distribute the airtime for jointly serving legacy 802.11 and 802.11ax STAs in networks with different traffic requirements.

(4) We enhance several PHY and MAC layer modules of ns-3 for supporting MU OFDMA transmissions as described in the latest TGax documents. We validate our analyses by comparing the performance of an 802.11ax network obtained from theoretical results with those obtained from extensive ns-3 simulations.

## 8.2 Related Work

The performance of 802.11-based networks has been extensively studied in the literature. The foundation of such analyses was laid by Bianchi in [306], where the author proposes a two-dimensional Markov chain model to characterize the throughput performance (in saturated conditions) of the 802.11 DCF. Extensions to this model have been proposed for 802.11ax networks, particularly for the UL MU OFDMA mode of operation. For example, Bellalta et al. [213] compute the 802.11ax saturated throughput when the 802.11ax AP uses both, MU MIMO as well as MU OFDMA transmissions. The authors show that there exists an optimal number of active users that maximizes the aggregate network throughput. Additionally, Lanante et al. [214] compute the saturated throughput in the UL under the assumption that UL OFDMA-based RA (UORA)[2] is the only mechanism for transmitting UL packets. On the other hand, DL throughput in 802.11ax is essentially deterministic (under saturated assumptions), which is verified by the authors in [307].

[2]We describe the UORA scheme in Sec. 8.3

The existing literature on 802.11ax provides deeper insights into 802.11ax performance. However, each of the aforementioned works restricts their focus on a sub-problem of the overall network performance. For example, the authors in [213] and [307] do not consider UORA – that enables stations to contend over a subset of the total RUs. The authors in [214] consider an RA-only UL system, thus failing to capture the behavior of a practical 802.11ax network which uses both RA and SA mechanisms simultaneously. Note that the RA mechanism informs BSR information to the AP and facilitates SA transmissions. Hence, we argue that a study that does not consider RA and SA transmissions jointly is incomplete and does not reflect the practical behavior of 802.11ax networks. In addition, the existing works focus on the performance of an 802.11ax-only network and do not study the network performance in the presence of legacy 802.11 users. We believe that the latter is a more practical scenario, at least in the initial phases of 802.11ax deployments.

In this work, we consider a system model that is accurate as per the latest TGax submissions and consider a scenario where UORA is used in conjunction with SA, i.e. when the AP transmits a TF, it provides scheduling information for STAs on a subset of RUs, while the remaining RUs are used for RA. Along with the saturated system throughput, we characterize 802.11ax performance in terms of *BSR delivery rate*—a metric that is important in dynamic network environments. Furthermore, we study the 802.11ax system performance under different use-case scenarios where the traffic requirements in the UL and DL are asymmetric. Finally, we analyze the performance of a heterogeneous network comprising of legacy 802.11 as well as 802.11ax STAs, both of which are jointly served by a single 802.11ax-capable AP.

## 8.3 MAC Scheme

The granularity of a frequency resource in the legacy 802.11 standards is a 20 MHz-wide channel that is composed of 64 OFDM sub-carriers, each of which is 312.5 kHz wide. This is set to change in 802.11ax, where the sub-carrier width will be reduced by a factor of four to 78.125 kHz. This improves the robustness of 802.11ax against multi-path fading in outdoor environments. Further, a block of 26 sub-carriers constitutes the smallest unit of frequency resource—i.e., RU—that can be assigned independently to different users, thereby enabling multiple concurrent transmissions, also known as MU OFDMA transmissions. Thanks to MU OFDMA, a 20 MHz-wide channel can support a maximum of 9 parallel transmissions, while the 40, 80, and 160 MHz wide channels can support up to 18, 37, and 74 concurrent transmissions, respectively.

802.11ax will support MU OFDMA in the UL as well as DL. In both cases, the MU OFDMA mode of operation is initiated when the AP broadcasts a TF. Since all DL traffic is routed to the STAs through the AP, the AP can transmit packets concurrently to multiple STAs over different RUs while taking into consideration performance requirements (such as latency, throughput, etc.) of individual STAs. On the other hand, efficient allocation of RUs to the STAs in UL requires the AP to have a knowledge of the buffer occupancy status of the

associated STAs. This is facilitated in 802.11ax using a BSR frame that is sent by the STAs to the AP to notify the current occupancy status of their transmit buffers. BSR delivery to the AP can be AP-invoked (where the AP explicitly requests BSRs from its STAs) or unelicited (when the STAs transmit their BSRs without the AP's request). For the former case, any QoS-enabled frame can act as the BSR where the TXOP field in the QoS Control sub-frame is re-used (when the network operates in MU OFDMA mode) as the BSR. In the latter case, STAs transmit their BSR information by piggybacking it along with their regular payload packets.

The UL MU OFDMA mode in 802.11ax will provision two types of RUs—SA RUs, on which the AP specifies (using the TF) an exact sub-set of STAs that can transmit in the UL without any contention, and RA RUs, on which those STAs can contend that have packets to transmit, but are not scheduled to transmit in the current MU OFDMA cycle because their BSR information is not available at the AP[3]. A TF that supports at least one RA RU is referred to as a Trigger Frame-Random Access (TF-R). In a TF-R, RA RUs are identified by a value 0 in the Association ID (AID) field, while each SA RU is identified by a non-zero AID value (corresponding to the AID of the STA that is scheduled to transmit on that particular RU). RA RUs can be used by: i) STAs that seek to join the network (to send control frames such as Association Requests), or ii) STAs that have recently joined the network or have just woken from a sleep state and have not been scheduled by the AP for transmissions in the UL (to send their BSR information).

The contention process used by STAs for transmitting their packets on RA RUs is referred to as UORA. Note that UORA occurs in conjunction with the SA procedure in the UL OFDMA mode of 802.11ax. Each contending STA picks a random integer—the OFDMA Backoff Counter (OBO) uniformly in the range [0, OCW−1], where OCW stands for OFDMA Contention Window. On reception of the TF-R, STAs that have not been assigned to SA RUs but have a packet to transmit contend for transmission on the RA RUs. Every contending STA decrements its OBO by the number of advertised RA RUs ($N_{RA}$). If the OBO decrements to zero, the packet is transmitted on a randomly chosen RA RU. If not, the contention process is ceased until the reception of the next TF-R. Much like the contention procedure used in legacy 802.11 standards, OCW is reset to $\text{OCW}_{\text{min}}$ following a successful transmission and is doubled for every collision until the OCW reaches $\text{OCW}_{\text{max}}$. We assume that STAs that contend on RA RUs transmit their respective payload frames with the TXOP field in the QoS Control sub-frame set to indicate their respective transmit buffer occupancy status. Once an STA successfully transmits a packet (along with piggybacked BSR), it does not contend on RA RUs until the AP assigns enough SA RUs for the STA to be able to transmit all the packets reported in its latest BSR. Note that once the AP knows BSR information of an STA, the former will allocate required resources to the later based on its QoS requirements such as latency, throughput, etc. Fig. 8.1 provides an illustrative example of UORA operation in conjunction with SA in 802.11ax UL OFDMA.

[3]In our work, we assume that STAs who have successfully reported their BSR information to the AP but are not scheduled for transmission in the current MU OFDMA cycle do not contend for RA RUs.

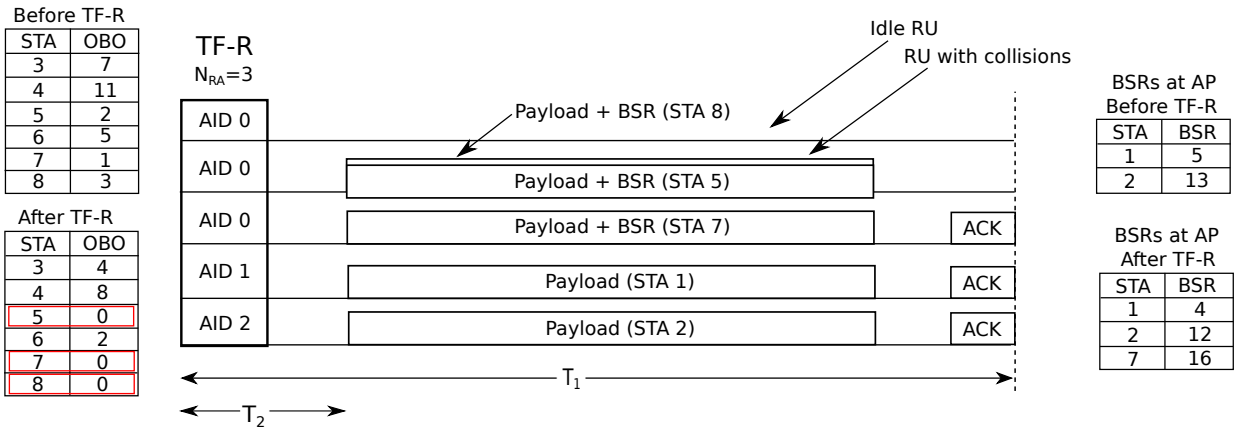


Figure 8.1: UORA used jointly with SA transmissions. STAs 1 and 2 are assigned RUs for SA, while the remaining STAs contend for transmissions on the three RA RUs. STAs 5, 7 and 8 decrement their OBOs to zero, and transmit on randomly selected RUs. This leads to a collision on the second RA RU, and successful transmission on the third RA RU; the first RA RU remains idle.

Transmissions shown in Fig. 8.1 correspond to one cycle of UL MU OFDMA transmissions. Throughout this chapter, we refer to this cycle as *TF cycle*. The AP can assign RUs for SA in the TF-R because it is aware of the transmission queue status of STAs 1 and 2. On the completion of the TF cycle, the AP knows STA 7's buffer status and can assign STA 7 SA RUs in subsequent TF cycles.

Throughout this chapter, we assume that the only mechanism for BSR delivery available at the STAs is by piggybacking the BSR information on payload frames. We make this assumption because although a null QoS frame (i.e. a QoS frame with no payload) can be used to convey the BSR to the AP if the TF-R assigns any of the RUs for SA, the time taken for the completion of the TF cycle will depend on the time taken for the STAs that are assigned SA RUs to complete their payload transmissions. By transmitting the null QoS frame, the remainder of the air-time in the TF cycle is wasted even if the transmission is successful. The only pragmatic use-case where the null QoS frame can be used for BSR delivery is when all RUs are assigned for RA. In such circumstances, it is advantageous to use a null QoS frame because if transmissions on all RUs collide, then the air-time wasted is small. This procedure is similar in spirit to the use of RTS/CTS frame in legacy transmissions whereby payload transmissions can be preceded by RTS/CTS exchange so that if the RTS/CTS frames collide, the wasted air-time is minimized.

Furthermore, we assume that only the RA RUs are used for BSR transmissions. This is because the sub-field (TXOP duration) in the QoS Control sub-frame that is used for conveying the BSR can have different interpretations based on the mode in which the 802.11ax AP operates. The TXOP sub-field is normally used by the STAs to request a specific TXOP duration for subsequent transmissions. However, the 802.11ax standard requires the AP

to interpret the TXOP sub-field as the BSR of the corresponding STA when the network operates in MU OFDMA mode. Although BSRs can be transmitted piggybacked on payload frames on SA RUs, STAs can potentially use the TXOP field in the regular context. Therefore, the AP can be certain of the TXOP sub-field interpretation (as a BSR) only when the BSR is delivered on one of the RA RUs.

From the aforementioned discussions, it is clear that the AP can schedule UL MU OFDMA transmissions effectively only if the STAs are successful in delivering their respective BSRs over the RA RUs. Consequently, the choice of the division of RUs between RA and SA RUs is a critical factor influencing the overall network performance. We look at the impact of this design choice in the next section.

## 8.4 Performance Analysis

In this section, we analyze the performance of the MU OFDMA scheme described in the previous section. In particular, we derive expressions for the following two key performance metrics: i) Throughput, and ii) BSR delivery rate.

Let us consider an 802.11ax network consisting of a single AP and $n$ STAs. Assume a saturated network, where the transmission queue of every STA is always non-empty. Nevertheless, STAs still need to inform the AP about their BSR information because the AP only schedules those STAs in the UL SA RUs whose BSR is known to it. Since MU transmissions are one of the characteristic features of 802.11ax MAC, we assume that the AP as well as all STAs support MU transmissions in both UL and DL. However, since the DL MU OFDMA is based on purely schedule-based transmissions, the DL throughput is invariant to network parameters and we will discuss it briefly towards the end of the section. First, we focus our attention on the UL throughput of the 802.11ax MAC.

Suppose that the 802.11ax channel is divided into $N_{\mathrm{RU}}$ RUs, where $N_{\mathrm{RA}}$ RUs are allocated for RA and the remaining $N_{\mathrm{SA}} = N_{\mathrm{RU}} - N_{\mathrm{RA}}$ RUs are allocated for SA. Since there is one STA assigned to each $N_{\mathrm{SA}}$ RU in a TF cycle, the remaining $n_{\mathrm{ra}} = n - N_{\mathrm{SA}}$ STAs contend for transmission on $N_{\mathrm{RA}}$ RUs. Similar to many previous works on 802.11, let us assume that all nodes can hear transmissions from other nodes; i.e., there are no hidden nodes. Also, we assume that channel conditions are ideal, i.e. there are no PHY layer impairments. Thus, in our model, packet errors occur only when multiple STAs transmit at the same time in the same RU.

Let us use the notation $W_i = 2^i W$ to denote the size of the OCW, where $W_i$ denotes the OCW for back-off state $i$ and $W$ denotes the $\mathrm{OCW}_{\mathrm{min}}$. Let $m$ be the maximum back-off state and $W_{\mathrm{max}} = 2^m W$ be $\mathrm{OCW}_{\mathrm{max}}$. An STA transmits a frame when its OBO decrements to 0. As opposed to the back-off procedure in legacy 802.11, in 802.11ax, the OBO is decremented by $N_{\mathrm{RA}}$ after receiving the TF. The back-off process can then be modeled by a two-dimensional Markov chain, and the probability that an STA transmits its BSR in any of the $N_{\mathrm{RA}}$ RUs

can be computed as follows [306, 308],

$$\tau = \frac{2(1-2p)}{(1-2p)\left(\frac{W}{N_{\mathrm{RA}}}+1\right)+p\frac{W}{N_{\mathrm{RA}}}(1-(2p)^m)}. \tag{8.1}$$

where, $p$ denotes probability that a transmitted packet collides.

Similar to legacy 802.11, there is only one contention process running in the 802.11ax MAC. However, there are $N_{\mathrm{RA}}$ RA RUs, and collision among transmissions from multiple STAs occur only when they transmit at the same time on the same RA RU. Assuming that a packet is transmitted on a randomly chosen RA RU among $N_{\mathrm{RA}}$ available RA RUs, the probability that a transmitted packet results in a collision can be computed as,

$$p = 1 - \left(1 - \frac{\tau}{N_{\mathrm{RA}}}\right)^{n_{\mathrm{ra}}-1}. \tag{8.2}$$

Equations (8.1) and (8.2) can be solved using numerical methods for given values of $W$, $m$, $N_{\mathrm{RA}}$ and $n_{\mathrm{ra}}$. Using the values of $\tau$ and $p$, we can compute the probability that at least one STA transmits in a considered RA RU during the TF as follows,

$$P_{tr} = 1 - \left(1 - \frac{\tau}{N_{\mathrm{RA}}}\right)^{n_{\mathrm{ra}}}. \tag{8.3}$$

Now, the probability $P_s$ that a transmission in an RA RU is successful is given by the probability of exactly one transmission given that there has been a transmission on the considered RA RU.

$$P_s = \frac{n_{\mathrm{ra}}\frac{\tau}{N_{\mathrm{RA}}}\left(1-\frac{\tau}{N_{\mathrm{RA}}}\right)^{n_{\mathrm{ra}}-1}}{1-\left(1-\frac{\tau}{N_{\mathrm{RA}}}\right)^{n_{\mathrm{ra}}}}. \tag{8.4}$$

Similarly, the probability $P_{\mathrm{idle}}$ that all RA RUs are idle because none of the STAs were able to complete their back-off procedure is given as,

$$P_{\mathrm{idle}} = (1-P_{tr})^{N_{\mathrm{RA}}}. \tag{8.5}$$

Next, we define the following two time periods $T_1$ and $T_2$ (see Equation (8.6)) based on the TF cycle of Figure 8.1.

$$\begin{aligned} T_1 &= T_H + (T_{\mathrm{TF}} + \mathrm{SIFS} + T_\delta) + (T_P + \mathrm{SIFS} + T_\delta) + (T_{\mathrm{ACK}} + \mathrm{SIFS} + T_\delta) \\ T_2 &= T_H + (T_{\mathrm{TF}} + \mathrm{AIFS} + T_\delta) \end{aligned} \tag{8.6}$$

where, $T_H$ and $T_\delta$ refer to the time taken to transmit frame header bits and the propagation delay respectively.

- $T_1$**:** $T_1$ represents the time spanned by a TF cycle when there is at least one RU on which a packet is transmitted. This includes two cases: i) a TF cycle that allocates at least one RU as SA RU (this case always results in transmissions in the allocated SA RUs), and ii) a TF cycle that allocates all RUs as RA RUs and there is at least one STA that transmits on an RA RU. In either case, the duration of a TF cycle is $T_1$.
- $T_2$**:** $T_2$ denotes the time duration of a TF cycle for which all RUs are assigned as RA RUs (i.e., $N_{RA} = N_{RU}$) but none of the STAs transmits a packet due to non-zero OCW values. In this case, the AP can transmit a new TF with the same/different RU assignments after sensing the channel idle for an AIFS duration.

Based on the allocation of RUs as RA RUs and SA RUs in a TF cycle, the following throughput expressions can be derived.

1. $1 \leq N_{\text{SA}} \leq N_{\text{RU}}$ (at least one RU assigned for SA and the rest are assigned for RA):
   When a TF comprises of at least one SA RU, irrespective of whether transmissions occur in RA RUs, the AP must reserve the channel for $T_1$ duration to allow transmissions in the SA RUs. In this case, the throughput is computed as,
   $$S_{ul} = \frac{(N_{\text{SA}} + N_{\text{RA}} P_{tr} P_s) E[P]}{T_1}. \tag{8.7}$$
   where $E[P]$ denotes the expected packet size in bits.
2. $N_{\text{RA}} = N_{\text{RU}}$ (all RUs are assigned as RA RUs):
   This case includes two sub-cases: i) none of the STAs can finish their respective back-off procedure, resulting in no packets being transmitted on any of the RA RUs (this event occurs with probability $P_{\text{idle}}$), and ii) at least one STA completes its back-off procedure and transmits on an RA RU. Combining these mutually-exclusive events, the throughput of a TF cycle can be computed.
   $$S_{ul} = \frac{N_{\text{RA}} P_{tr} P_s E[P]}{(1 - P_{\text{idle}}) T_1 + P_{\text{idle}} T_2}. \tag{8.8}$$

Finally, let us use the notation $S_{dl}$ to denote the downlink throughput of 802.11ax. Since 802.11ax DL transmissions are purely schedule-based, $S_{dl}$ is independent of $n$ and is computed as $S_{dl} = \frac{N_{\text{RU}} E[P]}{T_1}$. Note that each TF cycle used for DL transmissions delivers $N_{RU}$ packets whereas each TF cycle designated for UL transmissions delivers $(P_{tr} P_s N_{RA} + N_{SA})$ packets on average. Therefore, if the the DL to UL traffic/packet ratio in an 802.11ax network is $\eta : 1$, then the aggregate 802.11ax throughput can be computed using Equation (8.9).

$$S_{11ax} = \frac{\eta (P_{tr} P_s N_{RA} + N_{SA}) S_{dl} + N_{RU} S_{ul}}{\eta (P_{tr} P_s N_{RA} + N_{SA}) + N_{RU}} \tag{8.9}$$

Consider a highly dense and dynamic use-case scenario for 802.11ax, such as a wireless hotspot in a crowded street (e.g., Times Square in New York City)[4]. In such settings, due to severe contention on RA RUs, many STAs might fail to successfully report their BSR information to the AP. Thus, the AP cannot schedule them in the SA RUs of subsequent TF cycles. This effect is more pronounced for STAs that need to join (by sending control packets on an RA RU) or have just joined the network but haven't reported their BSR to the AP. To assess how well an 802.11ax network supports such STAs in dense and dynamic use-cases, quantifying the UL throughput itself is not sufficient. Rather, the efficiency of the MAC layer in terms of the average number of BSRs collected per TF cycle must be analyzed. We coin a new metric, namely *BSR delivery rate*, denoted by $\beta$ for facilitating this measurement. In particular, $\beta$ can be calculated using Equation (8.10).

$$\beta = N_{\mathrm{RA}} P_{tr} P_s. \tag{8.10}$$

Ideally, an 802.11ax network delivers the best performance to STAs by simultaneously offering high throughput and $\beta$. However, we must note that these two are conflicting requirements in the UL. If the goal is to maximize the UL throughput, the AP must allocate all RUs as SA RUs, but that will lead to $\beta = 0$. When $\beta = 0$, the AP cannot schedule enough STAs in the subsequent TF cycles, thus lowering the throughput. On the other hand, if the objective is to maximize $\beta$, i.e., maximally support new STAs for reducing their latency, then all RUs should be allocated as RA RUs. However, this would reduce the UL throughput because the efficiency of RA RUs in successfully transmitting a packet is significantly low due to contention. An optimal balance between throughput and $\beta$ can be achieved by carefully allocating RA RUs and SA RUs. We study this issue in detail in the next section.

## 8.5 Optimal RU Allocation Scheme

As discussed in the previous section, striking an optimal balance between $N_{\mathrm{SA}}$ and $N_{\mathrm{RA}}$ is critical in achieving a stable UL throughput in 802.11ax networks. On one hand, to increase the aggregate throughput, the AP can choose to assign a large fraction of the RUs as SA RUs—as contention-free transmissions on the SA RUs provide the maximum possible throughput. On the other hand, the AP cannot assign STAs for schedule-based transmissions unless it knows the BSRs of the corresponding STAs. Since we assume that the only mechanism for BSR delivery is through contention on the RA RUs (recall this discussion from Sec. 8.3), the AP must select $N_{\mathrm{SA}}$ and $N_{\mathrm{RA}}$ such that it never runs out of BSR values. An arbitrarily chosen division of RUs may imply that the network either lacks enough resources to meet STAs' demand for transmission (when it assigns a larger $N_{\mathrm{RA}}$ than is required). It may also imply that the network wastes some resources because of the unavailability of STAs' BSR information (when it assigns small $N_{\mathrm{RA}}$).

[4]We use the term "dynamic" to refer to a network use-case scenario where STAs join/leave the network frequently.

If the objective is to maximize the throughput, the AP must select $N_{\text{SA}}$ and $N_{\text{RA}}$ such that BSRs are collected from STAs at exactly the same rate at which these STAs can be scheduled on SA RUs, at least on an average sense. We refer to such a system state as the *steady state* of the system. We now outline the requirement for a system to be in a steady state. Suppose that the AP uses $N_{\text{RA}}$ RA RUs and, on an average, successfully collects BSR information from $\beta = P_{tr}P_sN_{RA}$ STAs in each TF cycle. The AP allocates the remaining $N_{SA}$ SA RUs for serving the UL traffic demand of STAs whose BSR information is known to the AP.

We assume that STAs report BSRs to the AP in terms of the number of available packets in its transmit buffer. Further, we assume that the mean length of the BSR field is $\lambda$. This implies that if one SA RU allocation to an STA results in the transmission of one packet, then that STA must be scheduled in $\lambda$ TF cycles before its UL buffer is empty. Further, if an STA $s$ reports a BSR of $\lambda_s$, we assume that the STA will not contend for transmissions on RA RUs until it is scheduled for transmitting $\lambda_s$ packets in the subsequent UL TF cycles by the AP. We claim that this assumption is pragmatic because the AP has a knowledge of at least $\lambda_s$ packets available in the buffer of STA $s$. Therefore, any further transmission attempt from the same STA on RA RUs will only increase the overall contention.

Given this, for an 802.11ax network to be stable, the demand from STAs—i.e., $\beta \times \lambda$ packet transmission requests—must be equal to the supply—i.e., $N_{SA}$ packet transmission opportunities. If this condition is not satisfied, either the AP collects BSR information from a larger number of STAs on average than can be assigned using the available SA RUs, or there might a fewer number of STAs for which the AP knows the BSR information than the available SA RUs. Equation (8.11) concisely characterizes the mathematical representation of a stable 802.11ax network.

$$N_{SA} = \lambda\beta \implies N_{SA} = \lambda P_{tr}P_sN_{RA} \tag{8.11}$$

Given that a system is in the steady state, on an average, the AP knows the BSR values of exactly as many STAs that are assigned SA RUs for transmissions. Equation (8.11) further implies that, on an average, the AP only knows the BSR information of $N_{\text{SA}}$ STAs. Thus, if there are a total of $n$ nodes, in the steady state, $n - N_{SA}$ nodes contend for transmission on $N_{RA}$ RA RUs and $N_{SA}$ nodes transmit on contention-free SA RUs.

From Equation (8.11), it is clear that the optimal values of $N_{\text{SA}}$ and $N_{\text{RA}}$ depend on $\lambda$. Further, since $P_{tr}$ and $P_s$ depend on the network size ($n$), the optimal $N_{\text{SA}}$ and $N_{\text{RA}}$ also depend on $n$. In practical 802.11ax networks, $\lambda$ for each STA might be different and change with respect to time. Generally speaking, the AP may not be able to track this information for all associated STAs. Consequently, although an optimal $N_{RA}$ can be computed theoretically by jointly solving Equations (8.1), (8.2) and (8.11), a real-world AP does not have this luxury. Therefore, an AP must be able to learn the changing network dynamics on the fly and arrive at the steady-state regardless of $n$ and the distribution of $\lambda$ across STAs. Towards this objective, we now describe an algorithm, Algorithm 1, that can be implemented at an

802.11ax AP for achieving the optimal distribution of SA RUs and RA RUs.

In Algorithm 1, $\Psi$ denotes the set of STAs whose non-zero BSRs are known at the AP. Further, in a given TF cycle, let $\phi$ and $\psi$ denote the set of STAs that have been assigned SA RUs and the set of STAs that successfully deliver a BSR to the AP, respectively.

**Algorithm 3** Algorithm for optimal allocation of RU in 802.11ax.

**Initialize:** $\Psi \leftarrow \{\}$
**while** true **do**
  Compute $N_{\text{SA}} = \min(|\Psi|, N_{\text{RU}})$
  Sort BSRs in descending order
  Select $N_{\text{SA}}$ STAs with largest BSRs in $\Psi$
  BSR[$s$] = BSR[$s$] - #scheduled_packets $\forall s \in \phi$
  **if** BSR[$s$] = 0, $\forall s \in \Psi$ **then**
    $\Psi = \Psi \setminus \{s\}$
  **end if**
  Allocate $N_{\text{RA}} = N_{\text{RU}} - N_{\text{SA}}$ RUs for random access
  Transmit Trigger Frame
  **if** $N_{\text{RA}} > 0$ and BSR received on RA RU $k$ **then**
    $\Psi \cup \{k\}$ $\forall k \in \psi$
    Update BSR[$k$] $\forall k \in \psi$
  **end if**
**end while**

In each TF cycle, the AP updates the BSR values of all scheduled STAs by decrementing their respective BSR values by the number of scheduled packets. Further, following the successful reception of BSR(s) from contending STA(s) on one or more of the RA RUs, BSR values of the corresponding STA(s) are updated.

The core idea used in Algorithm 1 is that as long as the AP is aware of the BSR information of $N_{\text{RU}}$ STAs, the AP assigns all RUs for schedule-based transmissions, one for each STA. If not, the AP assigns a SA RU, one for each of those STAs whose BSR information is available at the AP, while the remaining RUs are assigned for RA. BSRs, once delivered, are valid at the AP until $\lambda$ packets are scheduled in the UL. Thus, after $\lambda$ packets have been scheduled in the UL for a particular STA, the AP no longer knows its buffer status. In Algorithm 1, $N_{\text{RA}} > 0$ only when there are fewer than $N_{\text{RU}}$ BSRs are known to the AP. These conditions ensure that the AP collects just the right number of BSRs that it can schedule on the SA RUs. In Section 8.7, we evaluate the performance of Algorithm 1 by implementing it in ns-3 and performing simulations therein.

## 8.6 Airtime Distribution between Legacy Wi-Fi and 802.11ax

In this section, we leverage the analysis presented in previous sections and study a key practical issue in 802.11ax deployments—i.e., the appropriate distribution of airtime between legacy Wi-Fi and 802.11ax when both categories of STAs are jointly served by a single AP. Consider a scenario where a single 802.11ax capable AP needs to serve both legacy Wi-Fi as well as 802.11ax STAs. This will indeed be the case during the initial deployments of 802.11ax where the newly introduced devices will be 802.11ax capable whereas the existing devices will not support MU-OFDMA based 802.11ax transmissions. Therefore, to support both categories of devices, an 802.11ax capable AP needs to facilitate two disjoint operation modes: i) single-user mode, which allows transmissions to/from legacy Wi-Fi devices, and ii) multi-user mode intended for 802.11ax devices.

In single-user mode, transmission from each STA occurs over the entire channel bandwidth. Since 802.11ax devices are backward compatible with legacy 802.11 protocols, the former can decode the legacy 802.11 packet headers and back-off their transmissions. More specifically, 802.11ax devices can decode the network allocation vector (NAV) field in the MAC header and enter into power-saving mode. Note that there have been discussions in the TGax on whether to allow 802.11ax devices to contend for the channel during both single-user and multi-user modes of operation[5]. Permitting 802.11ax STAs to contend during both single-user and multi-user modes of operations allows them to transmit more frequently leading to fairness issues. Therefore, the TGax discussions advocate permitting only legacy 802.11 STAs to contend for the channel when the AP provisions single user mode of operation. Therefore, we establish our subsequent discussions based on the same assumption.

The single-user and multi-user modes operate dis-jointly and facilitate transmissions from legacy and 802.11ax STAs, respectively. In such settings, throughput and fairness are the key performance metrics that need to be considered while designing the system. It is often desired that the overall throughput of the network be maximized, but such a throughput maximization scheme might not be fair for all users. For instance, in a network composed of legacy and 802.11ax STAs, allowing the network to operate only in multi-user mode maximizes the overall network throughput, but doing so will be unfair to legacy STAs. Also, it has been shown that systems employing throughput fairness—i.e., each STA transmits the same number of packets on average—reduces the overall throughput of the network when some STAs (e.g., legacy STAs) only support lower rates. For example, an STA with a very low rate occupies the channel most of the time, thereby lowering the aggregate network throughput. Research has shown that Airtime Fairness (AF)—a fairness scheme that allows an equal fraction of air time to each STA—achieves a proper balance between throughput maximization and fairness consideration in 802.11 networks. In particular, it has been shown

[5]Since 802.11ax STAs can also operate in legacy mode (i.e., single-user mode), they can contend for the entire channel if permitted to do so during the single-user mode.

both analytically and experimentally that: i) traditional notion of proportional fairness [309] translates to airtime fairness in CSMA/CA-based system such as Wi-Fi [310], and ii) airtime fairness improves the aggregate performance of the network [311].

Let us assume there are $n_{leg}$ legacy and $n_{11ax}$ 802.11ax STAs associated to a single 802.11ax capable AP. Denote the total MAC-layer throughput of a purely legacy network having $n_{leg}$ nodes by $S_{leg}$ and that of a purely 802.11ax network having $n_{11ax}$ nodes by $S_{11ax}$. Suppose that the AP operates in a single-user mode for $\alpha$ fraction of time and multi-user mode for the remaining $(1-\alpha)$ fraction. Then, the throughput fairness between legacy Wi-Fi transmissions and 802.11ax transmissions in a heterogeneous Wi-Fi network is achieved if the airtime distribution satisfies Equation (8.12).

$$\frac{\alpha S_{leg}}{n_{leg}} = \frac{(1-\alpha)S_{11ax}}{n_{11ax}} \implies \alpha = \frac{n_{leg}S_{11ax}}{n_{leg}S_{11ax} + n_{11ax}S_{leg}} \tag{8.12}$$

Similarly, airtime fairness between legacy Wi-Fi transmissions and 802.11ax transmissions is achieved if the airtime distribution satisfies Equation (8.13).

$$\frac{\alpha}{n_{leg}} = \frac{(1-\alpha)}{n_{11ax}} \implies \alpha = \frac{n_{leg}}{n_{leg} + n_{11ax}} \tag{8.13}$$

Consequently, the aggregate throughput achieved by a heterogeneous network consisting of both legacy and 802.11ax STAs is given by Equation (8.14).

$$S_{agg} = \alpha S_{leg} + (1-\alpha)S_{11ax} \tag{8.14}$$

We shall discuss the implications of Equation (8.14) for different network deployment scenarios in the next section.

## 8.7 Results and Discussions

In this section, we investigate the MAC layer performance of 802.11ax by applying the analysis presented in previous sections. We then validate our analysis by implementing the MU OFDMA based 802.11ax MAC in ns-3 and comparing analytical results with those obtained from extensive ns-3 simulations for various use-case scenarios. Finally, based on our results, we provide key insights on some practical issues that might arise during the initial deployments of 802.11ax. Henceforth, unless explicitly stated otherwise, we use the following set of parameters (see Table 8.1) for all of our simulations.

Throughout this section, results pertaining to throughput represent the normalized throughput (ratio of payload size in bits to the time taken to transmit the payload) observed at the MAC layer, assuming that the underlying PHY layer uses a rate of 1 Mbps. In the case of

ns-3 simulations, this is achieved by using the same fixed PHY rate for control and data frames and scaling the resulting throughput by the fixed PHY rate. Each simulation run lasts for 90 seconds, and the results presented are averaged over 10 simulation runs with different seed values. In each plot, unless explicitly stated otherwise, markers represent results from ns-3 simulations whereas the lines without markers correspond to analytical results.

### 8.7.1 ns-3 Implementation of 802.11ax

For validating the analytical results derived throughout this chapter, we extend the capabilities of the ns-3 simulator to support MU OFDMA transmissions in the UL as well as DL. To achieve this, modules for PHY and MAC layer in the default ns-3 implementation were significantly modified. In legacy 802.11, all transmissions (in the UL as well as DL) occur over a single channel. In the MU OFDMA mode, however, these transmissions can occur in parallel, which necessitates the creation of separate transmit and receive chains for each RU. Furthermore, contending STAs in legacy 802.11 contend for a single channel. However, for the 802.11ax UL MU OFDMA to function, STAs contend for RA RUs. Therefore, state management functions such as the PHY state (e.g. IDLE/BUSY, etc.) need to be implemented on a per-RU basis. We use the newly introduced *SpectrumWifiPhy* module to enable transmission and reception on specific OFDM sub-carriers. The use of this module also enables simulation of interference across transmissions from legacy (on an entire channel) and 802.11ax (on specific sub-channels) devices.

In order to facilitate other researchers in conducting 802.11ax based simulations, we have released the source code of the modified ns-3 simulator [312]. In the near future, we also plan to make an official submission of our extended ns-3 modules to the ns-3 community.

Table 8.1: Simulation parameters for evaluating IEEE 802.11ax MAC performance

| **Parameter** | **Value** | **Parameter** | **Value** |
|---|---|---|---|
| Prop. loss model | Okumura Hata | SIFS | 16 $\mu s$ |
| AP coverage | 40 meters | $T_\delta$ | 3 $\mu s$ |
| $N_{\text{RA}}/N_{\text{SA}}$ | From Alg. 1 | $N_{\text{RU}}$ | 9 |
| $\text{CW}_{\text{min}}/\text{OCW}_{\text{min}}$ | 32 | $m$ | 5 |
| $\text{CW}_{\text{max}}/\text{OCW}_{\text{max}}$ | 1024 | TF-R | 140 bytes |
| $\alpha$ | From Eq. (8.13) | $P$ | 1023 bytes |
| ACK | 14 bytes | $H$ | 44 bytes |

### 8.7.2 Performance of the 802.11ax MAC

Figure 8.2 shows the performance of UL MU OFDMA for a network that consists of only 802.11ax STAs. As described in the previous sections, $\lambda$ represents the mean number of

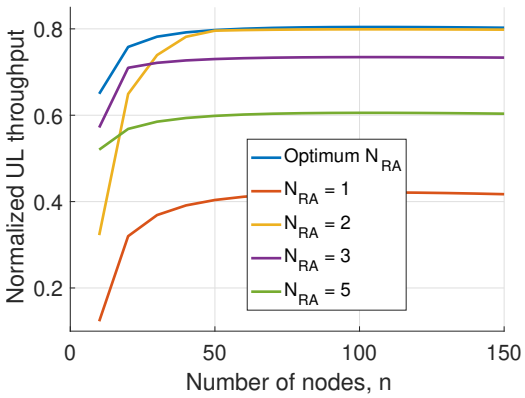


(a) Performance of Algorithm 1.

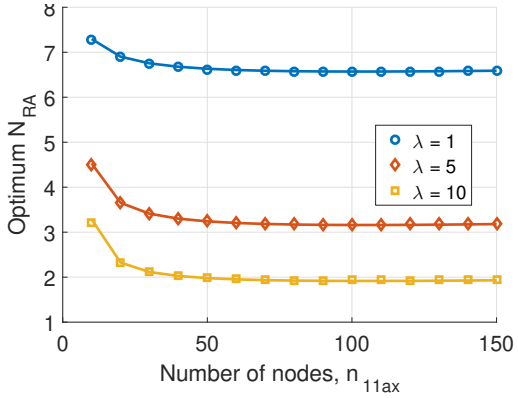


(b) Optimum $N_{RA}$ versus $n_{11ax}$.

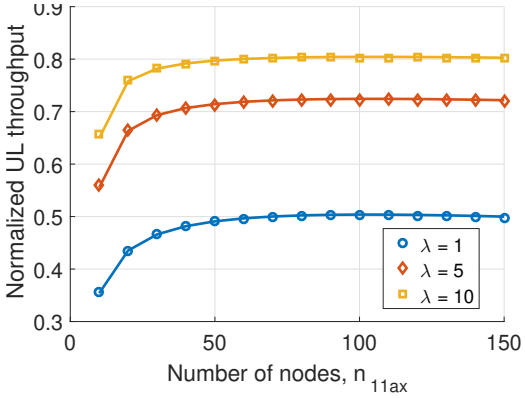


(c) UL throughput for different $\lambda$.

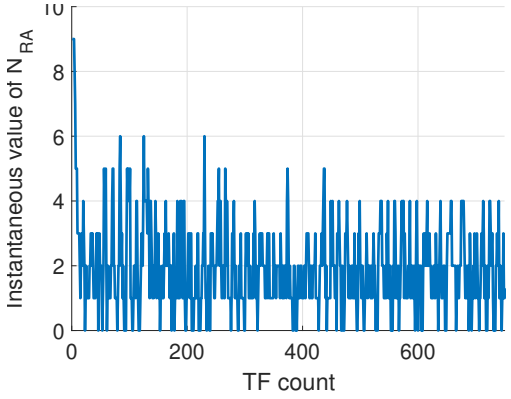


(d) Variations in instantaneous values of $N_{\mathrm{RA}}$.

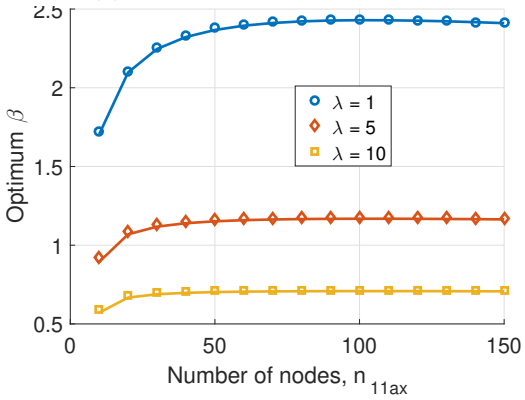


(e) Optimum $\beta$ versus $n_{11ax}$.

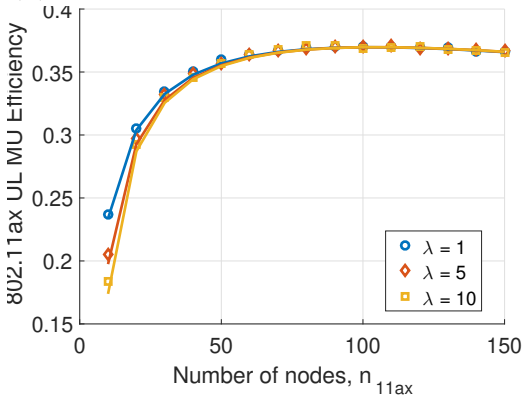


(f) MU Efficiency of 802.11ax.

Figure 8.2: UL performance of the 802.11ax MAC.

packets available in the transmit buffer of 802.11ax STAs. Figure 8.2a shows the MAC layer UL throughput of the network when $\lambda = 10$ and fixed $N_{\text{RA}}$ values are used by the AP. The performance of these fixed allocations of RA RUs is compared with that of Algorithm 1. We first note that no fixed $N_{\text{RA}}$ allocation offers throughput performance comparable to that of Algorithm 1. This is owing to the fact that the optimal $N_{\text{RA}}$ value depends on $\lambda$ as well as the network size, i.e., $n_{11\text{ax}}$. Thus, for each value of $\lambda$ and $n_{11\text{ax}}$, the optimal $N_{\text{RA}}$ is different. Furthermore, as discussed in Sec. 8.5, for the optimal allocation of RA RUs and SA RUs, the number of BSRs available at the AP must be $N_{\text{SA}}$ on an average. To achieve this, Algorithm 1 dynamically changes the value of $N_{\text{RA}}$ so as to maintain the steady-state condition (Equation (8.11)). The variation of $N_{\text{RA}}$ across TF cycles when an AP uses Algorithm 1 is shown in Figure 8.2d. As seen in the figure, the instantaneous value of $N_{\text{RA}}$ varies considerably, but its mean value converges to the optimal value obtained from Equation (8.11). This validates that Algorithm 1 indeed facilitates the optimal allocation of UL RUs in 802.11ax.

Figure 8.2b shows the optimal value (on an average) of $N_{\text{RA}}$ for different values of $\lambda$, and the corresponding optimal throughputs are shown in Figure 8.2c. For small values of $\lambda$, for example, $\lambda = 1$ (which means, on average, when an STA transmits a BSR, it informs the AP that it has one packet available in its buffer), the optimal $N_{\text{RA}}$ value is much higher than that for larger values of $\lambda$ (for example $\lambda = 10$). This is intuitive because a small value of $\lambda$ implies that the AP can schedule only a few packets on SA RUs in the UL based on the corresponding BSR. As a result, the AP needs to provision RA RUs frequently to collect enough BSRs and strike a balance between the demand on RA RUs and supply on the SA RUs. Further, a large value of $N_{\text{RA}}$ implies that a larger fraction of RUs are used as RA RUs. This is corroborated by Figure 8.2e, which shows the value of $\beta$, i.e. the number of packets transmitted on RA RUs, for different values of $\lambda$. Now, since the efficiency of the random access mechanism in UL MU OFDMA can at best be around 38%, as seen in Figure 8.2f, the throughput achieved is significantly lower than cases where $N_{\text{RA}}$ is small.

Thus, in summary, a larger throughput can be achieved in UL MU OFDMA when $\lambda$ is large. Large $\lambda$ implies that the AP does not need to frequently collect BSRs from an STA, thereby allowing the former to allocate a large fraction of RUs as contention-free SA RUs. Additionally, Algorithm 1 facilitates the AP in optimally allocating RUs in the UL. The AP uses Algorithm 1 to dynamically adjust the value of $N_{RA}$ on the fly and achieves optimal throughput for all values of $n_{11\text{ax}}$ and $\lambda$. In all plots, the overlap between the markers (results from ns-3 simulations) and solid lines (results from analysis) validate the correctness of our analysis.

Next, we look at the aggregate (i.e., combined UL and DL) throughput performance of 802.11ax for different values of $\lambda$ and $\eta$ (i.e. DL to UL traffic ratio) and compare with legacy 802.11. Figure 8.4 summarizes our results. An important observation is that for legacy 802.11 networks, the aggregate throughput falls sharply as the network size increases, thus highlighting its lack of scalability to the network size. In contrast, an 802.11ax network scales well with the network size, which suggests that it can be deployed in use-case scenarios where

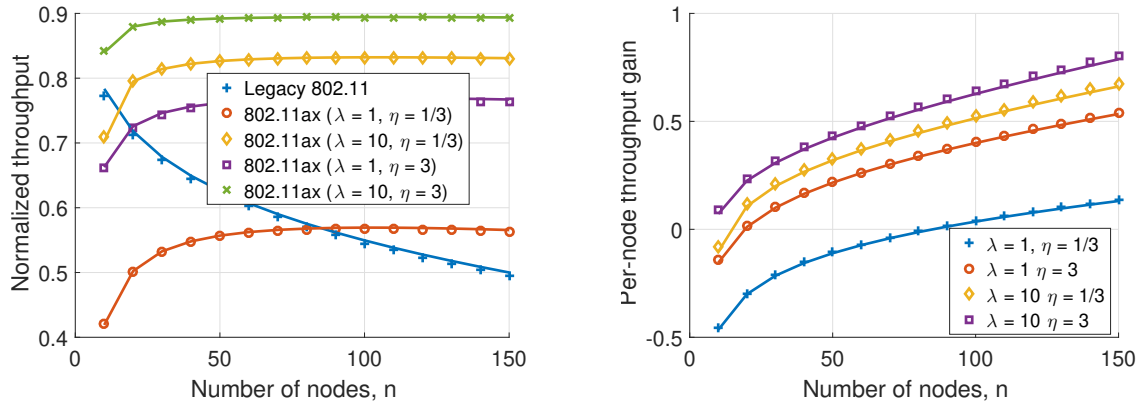


(a) Aggregate throughput.

(b) Gain in per-node throughput offered by 802.11ax.

Figure 8.3: Aggregate MAC-layer throughput of legacy Wi-Fi and 802.11ax.

an AP needs to support a large number of STAs (e.g., concerts, stadiums, etc.). However, it is also noteworthy that for certain values of $\lambda$ and $\eta$, the performance of 802.11ax may not be as good as that of the legacy network. For instance, when UL dominates the DL traffic (i.e., small $\eta$) and $\lambda$ (packet arrival rate at the MAC layer) is small, the AP must allocate a large number of RA RUs for collecting BSRs which hurts the network throughput. *Thus, although in general, 802.11ax offers improved performance over its legacy counterpart, our results indicate that a naive usage of 802.11ax without consideration of the network size and use-case scenario ($\eta$ and $\lambda$) may lead to poor throughput performance in some cases.*

It must be noted that for legacy 802.11 systems, there is no explicit differentiation between UL and DL traffic. In most implementations of Wi-Fi, the legacy AP and STAs use the same set of contention parameters, resulting in the same priority for UL and DL traffic. On the other hand, in 802.11ax systems, the DL traffic comprises of schedule-based transmissions, resulting in a deterministic and high DL throughput in comparison to UL traffic that comprises of both schedule-based and contention-based transmissions. Consequently, it follows that the larger the value of $\eta$, the higher is the aggregate network throughput. In most practical scenarios, the traffic in the DL indeed dominates traffic in the UL [313], which implies that in most scenarios, for an 802.11 network of given network size (particularly, larger values of $n_{11ax}$), the aggregate network throughput in 802.11ax will be higher than that in a legacy network of same network size. Figure 8.3b shows the relative gain in per-STA throughput at the MAC layer for an 802.11ax network compared to a legacy 802.11 network. Thus, the per-node-throughput-gain, as specified in the functional requirements of 802.11ax, can be achieved in many scenarios. Admittedly, the gain reported in Figure 8.3b is further amplified if we consider the PHY-layer enhancements adopted by 802.11ax. A key observation is that *the gain in per-node-throughput is more pronounced for larger network sizes and large $\eta$ values.*

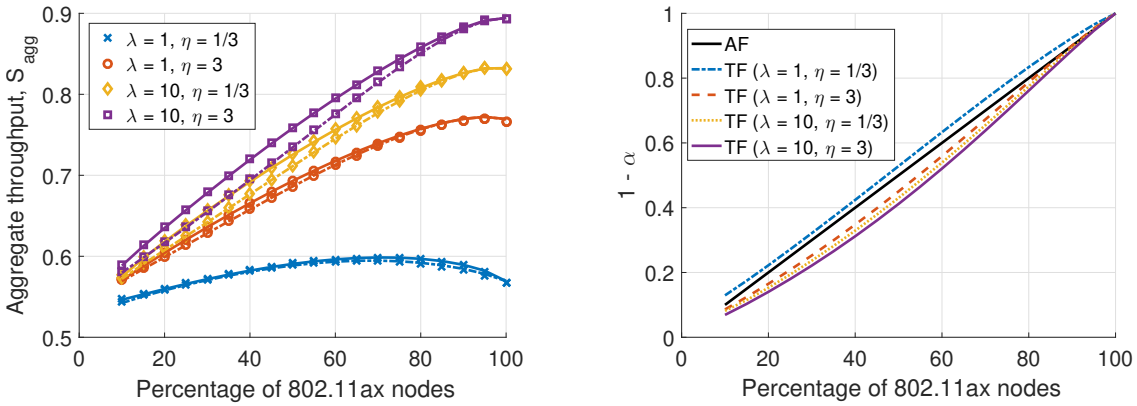


(a) Aggregate network throughput.

(b) Airtime allocated for 802.11ax transmissions.

Figure 8.4: Performance of a heterogeneous Wi-Fi network.

### 8.7.3 Joint Operation of Legacy Wi-Fi and 802.11ax

Now, we look at the joint operation of legacy 802.11 and 802.11ax when both categories of STAs are served by a single Wi-Fi AP. Figure 8.4a shows the aggregate throughput of such a network. For this study, we assume that the total number of STAs is fixed at 100 while we vary the proportion of 802.11ax and legacy STAs. In particular, we evaluate the aggregate throughput performance of such a heterogeneous Wi-Fi network by considering two fairness requirements: (i) the airtime is shared between legacy and 802.11ax STAs based on airtime fairness as described in Sec. 8.6, and (ii) the airtime is shared between the two types of STAs based on throughput fairness. In general, as expected, increasing the proportion of 802.11ax STAs in the network increases the aggregate network throughput. However, for small $\lambda$ (e.g., $\lambda = 1$) and small $\eta$ values, the aggregate throughput is not maximum when the fraction of 802.11ax nodes is 100%. Specially for small $\eta$, as seen in Figure 8.3a, a legacy network with a small number of nodes (say 20 nodes) offers better throughput than an 802.11ax network with large number of nodes (say 80 nodes). In such cases, it is advantageous not to have too many nodes contending on 802.11ax. This observation indicates that based on the network dynamics, it may be beneficial at times to let some of the 802.11ax STAs contend in the legacy mode (since 802.11ax STAs can operate in single-user/legacy mode) so that the overall network throughput is maximized.

Finally, we show in Figure 8.4b the distribution of airtime between legacy Wi-Fi and 802.11ax when throughput fairness (TF) and airtime fairness (AF) are considered. Matching with our intuition, when AF is considered, the airtime is divided based on the proportion of legacy and 802.11ax STAs, resulting in a straight line. On the other hand, for achieving TF, the airtime must be divided not only based on the proportion of STAs of a particular category but also based on the throughput achieved by that class of STAs. For instance, 802.11ax

achieves better throughput for large $\lambda$ and $\eta$ values. However, since the airtime dedicated to 802.11ax based on TF is small, this results in reduced overall network throughput (see Figure 8.4a). Thus, our results show that in a heterogeneous Wi-Fi network, AF achieves the best aggregate network throughput in all use-case scenarios.

### 8.7.4 Latency of 802.11ax STAs

Although the SA RU - RA RU division algorithm presented in Sec. 8.5 achieves the optimal throughput for a given 802.11ax network, one limitation of the algorithm in its current form is that it favors those STAs whose BSR is already known at the AP. This can be unfair towards those STAs that are waiting to transmit their packets/BSRs on the RA RUs, particularly when $\lambda$ is large. In practical scenarios, $\lambda$ is large for applications that are bandwidth-intensive (such as file transfer and downloads). However, such applications usually dominate DL traffic. Moreover, these applications are less sensitive to delay; consequently making the algorithm practical in most realistic scenarios. A class of applications that can be bandwidth-intensive, as well as delay-sensitive, is media streaming. Algorithm 1 may likely offer poor performance in such scenarios, and alternative approaches to maximize throughput in such scenarios remains a part of our future work.

## 8.8 Chapter Summary

In this chapter, we present a detailed analysis of the performance of MU OFDMA-based MAC of IEEE 802.11ax for a wide range of deployment scenarios. We consider the performance of 802.11ax networks when the network comprises of only 802.11ax as well as a combination of 802.11ax and legacy stations. The latter is a practical scenario, especially during the initial phases of 802.11ax deployments. Simulation results, obtained from our ns-3 based simulator, give encouraging signs for 802.11ax performance in many real-world scenarios. That being said, there are some scenarios where naive usage of MU OFDMA by an 802.11ax-capable Wi-Fi AP can be detrimental to the overall system performance. Our results indicate that careful consideration of network dynamics is critical in exploiting the best performance, especially in a heterogeneous Wi-Fi network.

# Chapter 9

# Performance Analysis of Multi Link Aggregation in IEEE 802.11be

## 9.1 Introduction

The global augmented reality (AR) and virtual reality (VR) market is estimated to be worth over $570 billion by 2025 [314]. In the US alone, the market is estimated to be worth over $85 billion [315]. AR/VR and other real-time applications (RTA) place stringent quality of service (QoS) constraints on the underlying communication technology, often demanding high throughput, low latency, and high reliability simultaneously [316]. While 5G is likely to be the main driving technology for wireless AR and VR [317] in outdoor environments, the Wi-Fi community has accelerated its efforts to develop features and techniques that support wireless RTA in next-generation Wi-Fi. This is best demonstrated in the Project Authorization Report of IEEE 802.11be [318], which outlines two of its objectives (among others) to be to define at least one mode of operation that supports (i) a maximum throughput of at least 30 Gbps, and (ii) improved worst-case latency and jitter.

One of the critical features being designed with the aforementioned objectives for next-generation Wi-Fi 7 systems is Multi Link Aggregation (MLA)[1] [76]. MLA belongs to a class of techniques in IEEE 802.11be that are referred to as Multi Link Operations (MLO). The design of MLO is motivated by the fact that most of today's Wi-Fi devices are capable of operating in multiple bands such as the 2.4 GHz band and different parts of the 5 GHz bands. Additionally, the 6 GHz bands (5.925–7.125 GHz) were recently added to the pool of unlicensed bands in the US, while similar considerations are ongoing in Europe [13]. Thus, future Wi-Fi devices are likely to support operations in at least three bands—namely 2.4 GHz, 5 GHz, and 6 GHz. Even though the current 802.11 architecture includes provisions for devices to operate in multiple bands[2], Wi-Fi device operations are currently limited to a single band at a given time. Thus, Wi-Fi devices that support multiple bands cannot use them simultaneously even if channels across different bands are idle and available for transmission, resulting in sub-optimal spectral utilization.

[1] MLA is also referred to as multi-channel aggregation or multi-band aggregation in some references.

[2] This provision was included to support Fast Session Transfer (FST) [319]—a feature that allows IEEE 802.11ad devices to rapidly switch between mmWave bands and sub-6 GHz bands.

In contrast, IEEE 802.11be devices that support MLA will be allowed to transmit (or receive) frames at the same time on all their supported links. Such devices will be referred to as Multi Link Devices (MLDs). Links aggregated in MLA can be two or more channels in the same band (such as in the 2.4 GHz band) or two or more channels in different bands.

Since MLA enables IEEE 802.11be devices to operate over multiple links at the same time, the operational bandwidth of MLDs increases. Thus, MLA is expected to yield significant throughput gains and these gains are expected to be proportional to the aggregated bandwidth [320]. However, a far more interesting consequence of MLA is the resulting latency reduction. The traditional Medium Access Control (MAC) layer of Wi-Fi uses a truncated binary exponential back-off protocol [10]. Even with MAC enhancements like Enhanced Distributed Channel Access (EDCA)—which prioritizes packets that belong to certain traffic categories—Wi-Fi devices are often unable to meet the stringent latency requirements of RTA. This is especially true for the worst-case latency requirements [318], which are on the order of 10 msec for most RTA [316]. Allowing Wi-Fi devices to concurrently compete for channel access on multiple links enables them to flush the queued packets as soon as any of the links are available, and is expected to yield substantial latency reductions [321].

While the fact that MLA can facilitate lower end-to-end latencies is known, there is a lack of research in how impactful these latency reductions are, and whether they will be sufficient for supporting RTA. To address these gaps, the questions that we seek to answer in this dissertation are (i) *How much can MLA contribute to decreasing the worst-case latency in Wi-Fi networks?* and (ii) *Is the latency reduction sufficient to support RTA?* To answer these questions, we have built a custom MATLAB-based simulator that implements the physical (PHY) and MAC layer functionalities of MLA that are consistent with their descriptions in IEEE 802.11be documents. Using this simulator, we have performed a comprehensive study on the performance of MLA under various network configurations and report our findings in this dissertation. We make the following key observations: (i) unlike throughput gains, latency reductions from MLA seem to be non-linear and less sensitive to parameters such as the aggregated bandwidth and/or the modulation and coding scheme (MCS), (ii) the addition of a second link alone leads to an order of magnitude reduction in the worst-case latency in many scenarios, and (ii) while the addition of subsequent links is beneficial, the resulting reductions in latency seem to follow the law of diminishing marginal returns. We summarize our main contributions below.

- To the best of our knowledge, the analysis of MLA performance—specifically in the context of its ability to improve the latency in future Wi-Fi networks—done in this dissertation represents the first such systematic study.
- Using our simulator, we investigate the impact of traditional throughput-enhancing techniques like increasing the bandwidth and/or MCS on Wi-Fi latency and compare their latency reductions with that obtained from MLA.
- We show that even in dense traffic, MLA can help future Wi-Fi devices meet the

worst-case latency requirement of 10 msec demanded by most RTA.

## 9.2 Related Work

At the time of writing this dissertation, studies on the performance of MLA are largely limited to industry contributions within TGbe. For example, references [85, 320] highlight the throughput gains of using MLA, while [321, 322] report significant latency gains. While the central message of these contributions—*MLA brings throughput and latency gains*—is clear, the quantification of these gains remains somewhat unclear due to the lack of consistency across simulation settings and the choice of network parameters.

In addition to the aforementioned references, the basic principles of MLA and its schemes have been described in [13, 72, 76, 323]. However, discussions in these dissertations are brief and there are no MLA-related performance evaluation studies. Yang et al. [79] study the performance of MLA in 802.11be but restrict their focus to throughput improvements. On the other hand, while Adame et al. [75] study the low-latency enabling features in IEEE 802.11be and describe MLA to be one of them, simulation results in the dissertation are limited to single-link operations. Furthermore, Avdotin et al. [324] study the ability of IEEE 802.11be to support RTA. However, they restrict their focus to Multi-User Orthogonal Frequency Division Multiple Access (MU OFDMA) in the uplink and propose modifications to the channel access rules for uplink MU OFDMA to provision better support for RTA.

## 9.3 Background

### 9.3.1 Latency Components in Wi-Fi

Wi-Fi uses Carrier Sense Multiple Access with Collision Avoidance (CSMA/CA) as its MAC protocol. CSMA/CA is fundamentally a *listen-before-talk* protocol, wherein a device with pending packets senses the channel and transmits if the channel is idle. The channel is sensed for a minimum duration referred to as the *inter-frame spacing* (IFS)[3] followed by a random backoff procedure. During the backoff phase, the Wi-Fi device picks the value of the *backoff counter* (BO) randomly in [0, CW-1], where CW refers to the parameter *Contention Window*. The device then decrements the value of BO for each idle slot (9 $\mu$sec) and transmits when BO decrements to 0. If the channel is busy, the BO value is frozen until the channel is idle and the device re-enters the backoff phase. CW lies in the range [$\text{CW}_{\text{min}}$, $\text{CW}_{\text{max}}$] and is reset/doubled each time the packet transmission succeeds/fails. The success of a particular transmission is inferred when the *acknowledgment frame* (ACK) is received. If transmission attempt(s) for a given packet fails, the packet is re-transmitted until a maximum retry limit

[3]The value of IFS differs with the type of packet at the transmitter.

is reached. If the packet is not successfully delivered to the receiver even after this limit is reached, it is dropped and the CW of the device is reset to $CW_{min}$. We refer the interested readers to [69] for additional details on the CSMA/CA protocol.

The end-to-end latency in Wi-Fi systems is composed of four major components. These are the queuing, channel access, transmission, and re-transmission latencies[4] as illustrated in Fig. 9.1. The queuing latency is the difference between the time at which a queued packet moves to the front of the queue and the time at which that packet was queued. Thereafter, the duration until the packet is attempted for the first time constitutes the channel access latency. If the transmission attempt succeeds, the re-transmission latency for the packet is zero. In this case, the only other latency component is the transmission latency, which is the time it takes for the transmitter to send the packet over-the-air and receive the ACK frame from the receiver. However, if the transmission attempt fails the time duration between the start of the first transmission attempt and the start of the final (i.e., successful) transmission attempt constitutes the re-transmission latency.

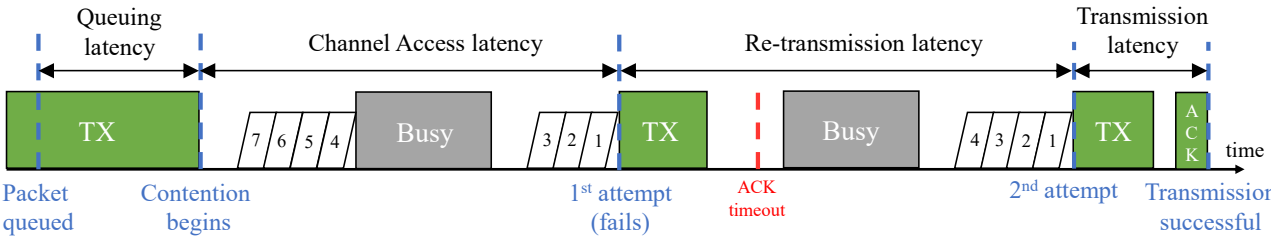


Figure 9.1: Illustration of latency components in Wi-Fi; $(CW_{min}, BO) = (16, 7)$ for attempt 1, and (32, 4) for attempt 2.

### 9.3.2 Channel Contention Rules for MLA in IEEE 802.11be

In principle, MLA in Wi-Fi 7 will be similar to carrier aggregation supported in cellular Long Term Evolution (LTE) [325]. However, unlike cellular networks, Wi-Fi devices operate in the unlicensed bands where channel availability across different links cannot be guaranteed. Consequently, coordinating channel access across different links is a challenging task in Wi-Fi. In the following discussions, we describe how IEEE 802.11be extends the channel contention rules used by contemporary Wi-Fi devices to provision support for MLA.

The protocol for channel contention in MLDs depends on the choice of the MLA scheme. At present, there are three MLA schemes under consideration for IEEE 802.11be [13]. These are (i) independent MLA, (ii) synchronous single-primary MLA, and (iii) synchronous multi-primary MLA.

MLDs that support independent MLA perform channel contention independently (i.e., without any coordination) on all links. The contention parameters BO, CW, $CW_{min}$, and $CW_{max}$

[4]We ignore propagation and processing delays because they are much smaller than the four listed latency components.

are separately maintained and independently updated for each link. This implies that even if an MLD is in the transmit state on one or more links if its queue is non-empty it will continue to contend for channel access on the remaining links. Independent MLA operations for a three-link scenario are illustrated in Fig. 9.2. Observe that because there is no information exchange across the links, transmissions are unlikely to be synchronized. Therefore, independent MLA is also referred to as asynchronous MLA. Due to this asynchronous transmit and receive behavior of independent MLA, it is suitable when there is a large frequency separation between the aggregated links. If independent MLA is used when the frequency separation between the aggregated links is small, the in-device interference from the transmitting link(s) at the receiving link(s) can be significantly high and can impair the reception of packets on the receiving link(s).

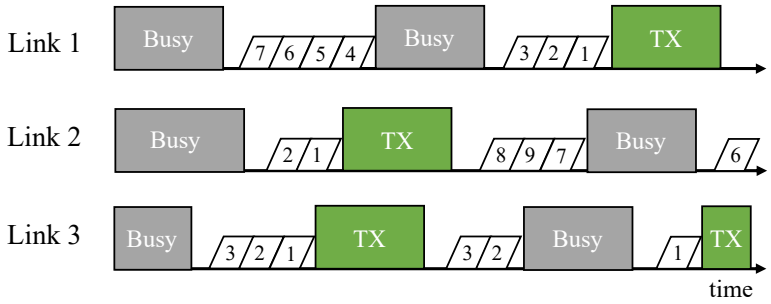


Figure 9.2: Independent MLA for three links in IEEE 802.11be.

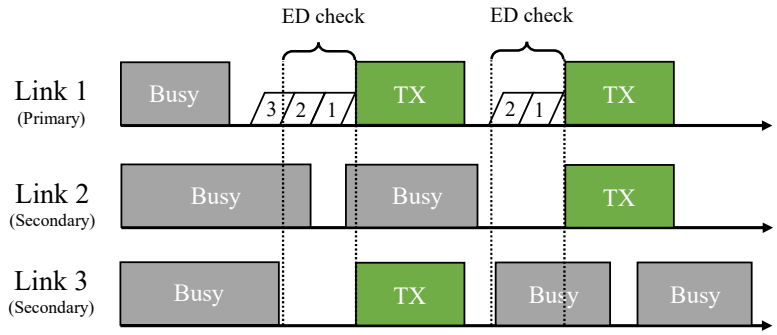


Figure 9.3: Synchronous single-primary MLA in IEEE 802.11be.

Synchronous MLA schemes attempt to synchronize transmission attempts across the aggregated links [13]. This is done by extending the 802.11 channel bonding mechanism, which is used for combining two or more 20 MHz channels to form a wider bandwidth channel [10]. In channel bonding, an 802.11 device contends for channel access only on a single 20 MHz *primary* channel. The remaining 20 MHz channels are referred to as the *secondary* channels. Following this convention, in synchronous single-primary MLA, the MLD contends for the channel on only one of the links, which is referred to as the primary link. The contention parameters, therefore, need to be maintained only for the primary link. An energy detection

(ED) check is performed on the remaining (secondary) links for a duration of PIFS[5] right before the BO value reaches zero on the primary link. All idle links are then aggregated. This is illustrated in Fig. 9.3. Operations of synchronous multi-primary are similar to those shown in Fig. 9.3, except contention is now allowed on more than one link (i.e., more than one links can be primary) and when the BO value counts down to zero on any one link, an ED check is performed on all other links. Synchronous MLA schemes are suitable in configurations where the frequency separation between the links is small. The principle in the design of these schemes is that if most of the links (ideally all) are in the transmit state at the same time, scenarios, where packet losses occur due to simultaneous transmission and reception (across links with small frequency gaps), can be avoided. Nevertheless, there are several challenges associated with these schemes—as highlighted in [326, 327]—that must be resolved before they can be adopted in the IEEE 802.11be specifications. Independent MLA is the more likely of the three schemes that will be adopted in Draft 1.0 of IEEE 802.11be specifications, which is expected to be released by May 2021 [328]. Thus, for the remainder of this dissertation, we limit our attention to independent MLA.

## 9.4 System Model

### 9.4.1 System Model

In this dissertation, we limit our attention to MLA operations in a single Wi-Fi Basic Service Set (BSS). We consider a BSS with one IEEE 802.11be AP, $M_{SL}$ single-link STAs, and $M_{MLD}$ MLDs. These single-link devices can be Wi-Fi STAs that pre-date the IEEE 802.11be (i.e., IEEE 802.11ax and older) specifications or IEEE 802.11be devices that do not support MLO. We assume that all MLDs can contend using independent MLA on $N_L$ links. All STAs are randomly placed in a square region of length 10 m, with the AP placed at the center. A sample realization of the simulation topology with $M_{SL} = M_{MLD} = 5$ is shown in Fig. 9.4.

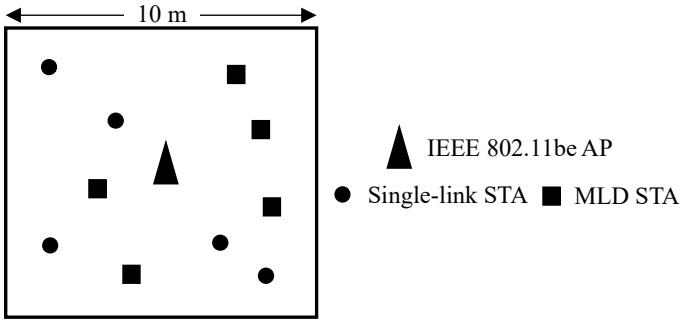


Figure 9.4: Simulation Topology

[5]The duration of PIFS is 25 $\mu$sec.

Table 9.1: Simulation parameters for evaluation of MLA performance

| Parameter | Value | Parameter | Value |
|---|---|---|---|
| $N_L$ | 1 to 5 | Max. retry limit | 10 |
| Power (AP) | 24 dBm | Path loss model | WINNER A1 |
| Power (STA) | 14 dBm | Thresh SIR (MCS 2) | 8 dB |
| MCS | 2,10 | Thresh SIR (MCS 10) | 31 dB |
| ED thresh | -62 dBm | Sensitivity (MCS 2) | -90 dBm |
| PD thresh | -82 dBm | Sensitivity (MCS 10) | -67 dBm |
| $L_{MLD}$ | 1-50 Mbps | Load (single-link) | full-buffer |
| Packet size | 1500 Bytes | Rate Adaptation | No |

Arguably, the latency experienced by a particular Wi-Fi device increases when other Wi-Fi devices in the network aggressively compete for the channel. Since the focus of our study is to evaluate MLA performance in such *worst-case* scenarios, we assume that all the single-link devices in the BSS have saturated traffic, i.e., they always have a packet to transmit in their respective queues. Further, we also assume saturated traffic at the AP. To model real-time traffic patterns at the MLD STAs, we assume constant bit-rate (CBR) traffic of $L_{MLD}$ Mbps at the MLD STAs (consistent with references such as [321, 322]), where fixed-sized packets are queued with a fixed inter-arrival time. This inter-arrival time is computed from the offered load at the MLDs. For example, if the fixed packet size is 1500 Bytes and $L_{MLD}$ is 10 Mbps, packets are queued at the MLDs once every 1.2 msec. Finally, for simplicity, we assume that all the relevant parameters (e.g., $N_L$, $L_{MLD}$, etc.) are the same for all MLDs. Simulation parameters used in the following section are outlined in Table 9.1.

## 9.5 Performance Evaluation

### 9.5.1 The Simulator

To simulate the impact of independent MLA on the end-to-end packet latency, we implemented a modular and configurable software simulator in MATLAB. The traffic generated at all devices and queued at the MAC layer can be individually customized. We model the Wi-Fi MAC layer mechanisms such as the CSMA/CA protocol, channel bonding, frame aggregation, and traffic class prioritization using EDCA [10] for single-link Wi-Fi operations as well as independent MLA. At the PHY layer, we model channel sensing (both physical and virtual [69]), and packet collisions. For each packet transmitted by a Wi-Fi device, the signal-to-interference ratio (SIR) is computed at the receiver. The effects of the PHY layer are abstracted such that a packet is forwarded to the MAC layer if the received signal strength indicator (RSSI) of the packet is above the receiver sensitivity and the SIR of the packet is above an SIR threshold. These RSSI and SIR threshold values are obtained

from [329]. If either of these conditions fails (i.e., the RSSI is below the receiver sensitivity, or the SIR is below the threshold value) the packet is dropped at the PHY layer.

In the following subsections, we restrict our performance evaluation to the cumulative distribution function (CDF) of the end-to-end latency experienced by the MLDs' packets. Since the focus of this dissertation is on the performance of MLA, we do not discuss the performance of the single-link STAs in the BSS. Unless explicitly stated otherwise, in the CDF plots we refer to the *90 percentile latency* as the *worst-case latency*.

### 9.5.2 Single MLD competing with single-link devices

In this subsection, we assume that there is no traffic class prioritization for the MLD STA's packets, i.e., the MLD STA, the single-link STAs, and the AP use the same channel access parameters (corresponding to Best Effort traffic).

Fig. 9.5(a) and Fig. 9.5(b) shows the impact of traditional throughput-enhancing mechanisms such as increasing the channel bandwidth and/or the MCS on the distribution of packet latency and compares them to the gains achieved using MLA. We first look at a scenario where the offered load at the MLD STA is small ($L_{MLD}$ = 1 Mbps) in Fig. 9.5(a). Observe that when $N_L = 1$, the 90 percentile latency obtained using a 20 MHz channel and MCS 2 is extremely high (800 msec). While increasing the bandwidth (to 80 MHz) and the MCS (to MCS 10) helps in reducing this worst-case latency (to 550 sec and 300 msec, respectively), we see that adding a second 20 MHz link (with MCS 2) alone yields a far greater latency reduction (the 90 percentile latency is reduced to ≈100 msec). Furthermore, when $N_L = 2$, the additional latency reduction obtained from increasing the bandwidth and the MCS is small.

Fig. 9.5(b), on the other hand, shows that if the offered load at the MLD STA is high ($L_{MLD}$ = 20 Mbps), adding a second low-bandwidth link does very little to reduce the latency tail. However, a substantial latency gain is observed when the bandwidth and the MCS are increased to 80 MHz and MCS 10, respectively. This is despite the fact that increasing the MCS (from 2 to 10) decreases the resilience of the transmissions to packet collisions (see SIR threshold and sensitivity values in Table 9.1). Adding a second 80 MHz, MCS 10 link results in a substantial further reduction in the worst-case latency. Overall, the 90 percentile latency shows an order-of-magnitude improvement from 5 seconds[6] for $N_L = 1$, 20 MHz, and MCS 2 to 100 msec for $N_L = 2$, 80 MHz, and MCS 10.

The fundamental difference between the two aforementioned cases is queuing latency. When the MLD competes for channel access with other Wi-Fi devices, the link capacity is divided across all contenders. When $L_{MLD}$ = 1 Mbps, the MLD's share of the link with a single 20 MHz channel and MCS 2 is sufficient to flush the queued packets at a fast enough rate.

[6]The root cause for such high latency values is the large number of packet collisions due to many full-buffer contenders (which is 8 including the AP).

Table 9.2: MLD throughput for cases shown in Fig. 9.5(b).

| **Case I** | **Case II** | **Case III** | **Case IV** | **Case V** |
|---|---|---|---|---|
| $\mathbf{N_L = 1}$<br>20 MHz<br>MCS 2 | $\mathbf{N_L = 1}$<br>80 MHz<br>MCS 2 | $\mathbf{N_L = 1}$<br>80 MHz<br>MCS 10 | $\mathbf{N_L = 2}$<br>20+20 MHz<br>MCS 2 | $\mathbf{N_L = 2}$<br>80+80 MHz<br>MCS 10 |
| 1.9 Mbps | 7.8 Mbps | 19.1 Mbps | 3.8 Mbps | 19.8 Mbps |

This can be verified from the throughput of the MLD, which is ≈1 Mbps. The predominant latency components, in this case, are the channel access and re-transmission latencies, which are substantially lowered by adding a second 20 MHz link. Consequently, adding a second 20 MHz link alone results in substantial reduction in the worst-case latency.

On the other hand, when $L_{MLD} = 20$ Mbps, the average MLD throughput in the five cases presented in Fig. 9.5(b) is given in Table 9.2. Observe in Table 9.2 that in Cases I, II, and IV, the capacity requirement of the MLD is not met and MLD throughput $\ll L_{MLD}$ (i.e., 20 Mbps). The only two cases where the MLD throughput $\approx$ 20 Mbps are those where the worst-case latency in Fig. 9.5(b) is substantially lower (i.e., Cases III and V). Furthermore, observe that even though the MLD throughput is $\approx$ 20 Mbps in Cases III and V, adding a second link (with the same bandwidth and MCS) yields substantial reduction in the end-to-end latency through reductions in the channel access and re-transmission latencies. The 90 percentile latency is reduced from 620 msec when $N_L = 1$ to 95 msec when $N_L = 2$. In summary, as long as the capacity requirement of the MLD is met (by increasing the bandwidth, MCS, or both), MLA can yield substantial latency improvements by lowering the channel access and re-transmission latencies.

Next, in Fig. 9.5(c), we look at the impact of the number of aggregated links, i.e., $N_L$ on the latency. From the above discussions, we know that the queuing latency can be controlled only if the offered load at the MLD, $L_{MLD}$, is smaller than its share of the channel capacity. Thus, in Fig. 9.5(c), we minimize the impact of queuing by setting $L_{MLD} = 1$ Mbps. The bandwidth of all but one links is set to 80 MHz and the MCS on all links is set to MCS 2. For $N_L \geq 2$, we set the bandwidth of one link to 20 MHz to emulate a 2.4 GHz link[7]. We observe in Fig. 9.5(c) that while the addition of each link contributes positively toward the reduction of latency, the relative gains decrease with the addition of each successive link. The 90 percentile latency is reduced from 600 msec in the single-link scenario to 40 msec in the three-link scenario, which is a 93% reduction. However, increasing $N_L$ to 5 yields only a 50% further reduction in the 90 percentile latency.

While increasing the number of links is indeed beneficial in scenarios where the offered load at the MLD is high, the reduction in latency in such cases can be primarily attributed to a reduction in the queuing latency. Addressing capacity issues, which is the fundamental cause for the increased queuing latency, is far more appealing by increasing the channel

[7]The typical channel bandwidth in the 2.4 GHz band is 20 MHz.

bandwidth (which is available in abundance in the 6 GHz bands [13]), modulation order, and the number of spatial streams. This is due to two main reasons, (i) increasing the number of radio frequency front-ends available in future Wi-Fi 7 devices to more than 3 may be infeasible, especially in power-limited devices like smartphones and VR headsets, and (ii) the number of links that have large enough frequency gaps and support simultaneous transmission and reception, which is a fundamental requirement for independent MLA, is likely to be three (one each in the 2.4 GHz, 5 GHz, and 6 GHz bands).

### 9.5.3 Multiple MLD competing with single-link devices

While the aforementioned results and discussions provide interesting insights on the worst-case performance of MLA, the setup used in these simulations is not entirely practical for two reasons, (i) the number of MLDs in a BSS is likely to be more than one, especially with the widespread adoption of Wi-Fi 7 and Wi-Fi 7-based RTA, and (ii) in practice, RTA packets are likely to be transmitted with a higher priority than others to satisfy the QoS requirements of such applications. Therefore, in the following discussions, we introduce more than one MLD in the network and observe the resulting impact on the end-to-end latency of the MLDs' packets. At the same time, packets generated at all the MLDs are assigned the highest priority by transmitting these packets using the channel access parameters corresponding to voice traffic.

Fig. 9.6(a) shows the distribution of the end-to-end latency when three MLDs share the channel with seven single-link STAs. We observe that even in the presence of 7 full-buffer STAs and $L_{MLD}$ = 20 Mbps at each of the three MLDs, the 99 percentile latency of MLDs' packets is just over 10 msec for the single-link scenario. Compared to the results shown in Sec. 9.5.2, this is a substantial improvement and arises from traffic class prioritization used by the MLDs in the transmission of their packets. Furthermore, while the availability of additional links for contention reduces the latency, this reduction is not significant. Thus, in scenarios where the number of MLDs with RTA traffic is small, as long as MLDs use traffic prioritization to transmit their packets the QoS requirements of RTA can be met even when the number of full-buffer contenders (with lower priority traffic) is high.

The benefits of traffic class prioritization notwithstanding, the gains achieved by using this prioritization come at a cost when the density of high-priority traffic increases. This is evident in Fig. 9.6(b) and Fig. 9.6(c), which show the latency distribution of MLDs' packets when there are seven MLDs and seven single-link full-buffer STAs in the BSS for $L_{MLD}$ = 20 Mbps and $L_{MLD}$ = 50 Mbps, respectively.

First, we see from Fig. 9.6(a) and Fig. 9.6(b) that by increasing the number of MLDs from 3 to 7 for the same offered load, the 90 percentile latency when $N_L = 1$ jumps 300% from 5 msec to 20 msec. The corresponding increase in the latency when $L_{MLD}$ is increased to 50 Mbps is much worse (Fig. 9.6(c)). These effects can be attributed to the increase in the number of packet collisions among the MLDs, which lead to very high re-transmission

latencies. It must be noted that voice traffic packets are assigned a higher priority through the reduction of the channel access parameters (i.e., IFS, $CW_{min}$, and $CW_{max}$) values, which inevitably leads to a large number of collisions when many such STAs share the channel. Fig. 9.6(b) shows that 35% of the MLD packets experience 90 percentile latency of greater than 10 msec when $N_L = 1$ and $L_{MLD} = 20$ Mbps. However, the addition of a second link alone reduces the 90 percentile latency to 6 msec. On the other hand, even when $N_L = 3$, more than 90% of the packets experience an end-to-end latency of more than 10 msec when $L_{MLD} = 50$ Mbps. Nevertheless, even at such high RTA traffic densities, the 90 percentile latency can be brought to under 10 msec if $N_L \geq 4$.

## 9.6 Chapter Summary

In this chapter, we investigate the impact of Multi Link Aggregation—a key feature likely to be introduced in Wi-Fi 7—on the packet latency in Wi-Fi networks. The simulation results shown in this paper demonstrate that the use of MLA in future Wi-Fi networks can yield an order-of-magnitude reduction in the worst-case latency experienced by Wi-Fi devices. Furthermore, we highlight that even in dense traffic conditions, MLA can help Wi-Fi devices meet the challenging worst-case latency requirement of 10 msec demanded by most real-time applications. There are three natural extensions to the study conducted in this paper. First, we look at the performance of MLA in a single Wi-Fi 7 BSS. Thus, the exposed node problem, which is known to negatively affect Wi-Fi performance in dense environments, is ignored. Second, we consider only CSMA/CA-based Wi-Fi transmissions, whereas IEEE 802.11ax additionally allows uplink and downlink access using MU OFDMA. Finally, we evaluate the performance of only one of the three MLA schemes, i.e., independent MLA. We will address these shortcomings in our future work.

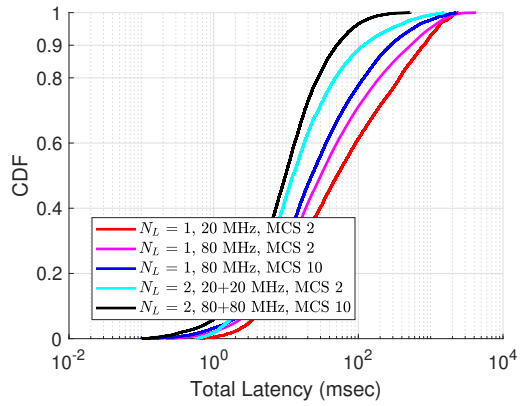


(a) $M_{SL} = 7$, $M_{MLD} = 1$, $L_{MLD} = 1$ Mbps

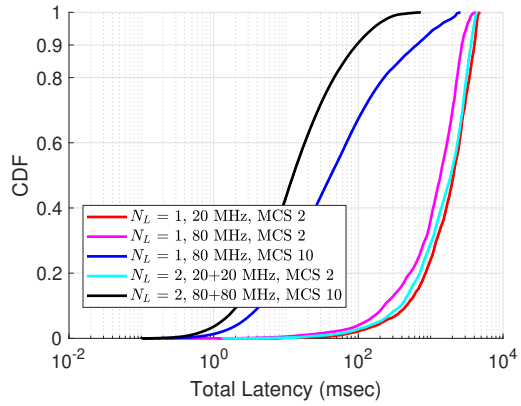


(b) $M_{SL} = 7$, $M_{MLD} = 1$, $L_{MLD} = 20$ Mbps

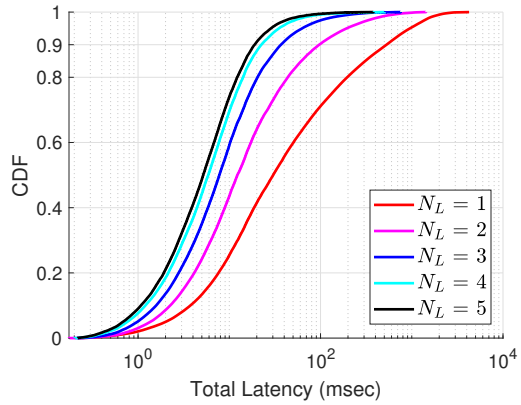


(c) $M_{SL} = 7$, $M_{MLD} = 1$, $L_{MLD} = 1$ Mbps

Figure 9.5: CDF of the end-to-end latency of the MLD's packets. One MLD competing for channel access with single-link STAs.

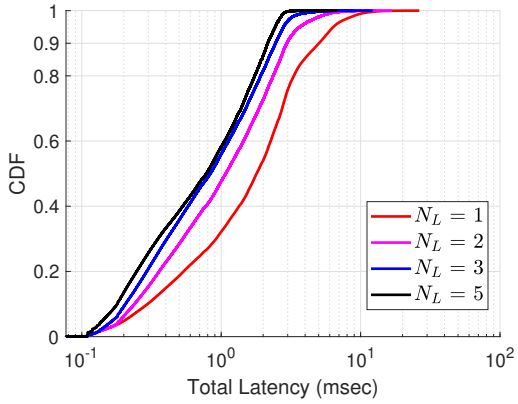


(a) $M_{MLD} = 3$, $L_{MLD} = 20$ Mbps

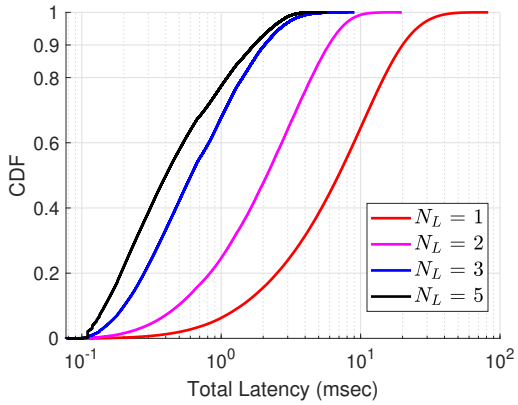


(b) $M_{MLD} = 7$, $L_{MLD} = 20$ Mbps

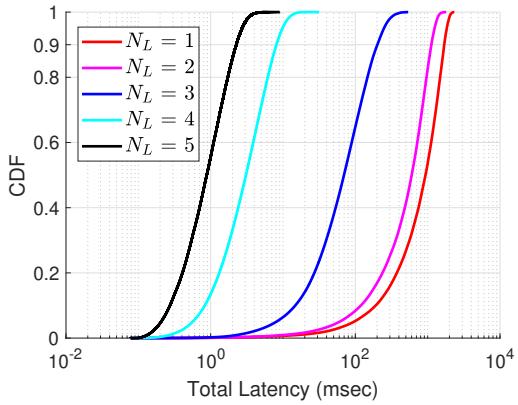


(c) $M_{MLD} = 7$, $L_{MLD} = 50$ Mbps

Figure 9.6: Impact of traffic prioritization and multiple MLDs on the MLDs' end-to-end latency, $M_{SL} = 7$.

# Chapter 10

# Conclusions

The demand for wireless connectivity has been ever-increasing and future trends are no likely to be different. Applications that are now used over wireless devices demand large amounts of bandwidth and often demand tight latency and reliability requirements. The wireless industry has largely been able to keep up with this demand with the design of new and innovative radio access technologies. Unlicensed wireless spectrum is particularly lucrative in delivering wireless applications and services because the service provides (and consequently the users) do not have to spend large sums of money on acquiring operational licenses. Nevertheless, the fundamental resource that is required to support these technologies and applications—unlicensed wireless spectrum, particularly those with favorable propagation characteristics—remains limited.

Regulators across the world have kept their efforts ongoing to identify potential bands where unlicensed operations can be allowed, and go through the often strenuous process of finalizing rules on how the operational integrity of the bands' incumbent users can be preserved. Frequency bands in the 5 GHz and 6 GHz range are two such examples. Over the last few years (especially since 2013), there has been considerable activity toward identifying new bands for unlicensed technologies (such as Wi-Fi) and facilitating their entry into these bands. A great testimony to these efforts is the fact that in the last two years alone, the FCC has added over 1.2 GHz of unlicensed spectrum in the US, thereby more than doubling the amount of unlicensed spectrum available in the US.

The availability of new unlicensed bands, however, comes with several challenges. Several technologies such as DSRC, radars, and Wi-Fi already operate in the 5 GHz bands, while the 6 GHz bands support many incumbent services such as fixed service links, satellite systems, television pickup stations as well as UWB-based unlicensed systems. Furthermore, the development and roll-out of many new technologies such as C-V2X, IEEE 802.11bd, NR V2X, and 5G NR-U is underway. Many of these technologies are built atop fundamentally different and incompatible radio access technologies. Thus, when spectrum sharing between these technologies is desired or mandated, many complex research challenges arise.

In Chapter 3, we describe in detail several such spectrum sharing scenarios: (i) coexistence of cellular-based unlicensed RATs (LAA, LTE-U, and NR-U) and Wi-Fi, (ii) coexistence of radar and Wi-Fi systems, (iii) coexistence between the 6 GHz incumbents and unlicensed devices (Wi-Fi and NR-U), (iv) coexistence between V2X technologies (DSRC and C-V2X) and Wi-Fi, (v) coexistence across different generations of Wi-Fi devices, and (vi) coexistence

across V2X technologies. The diversity of wireless technologies in the 5 GHz and 6 GHz bands implies that each of these coexistence scenarios is unique, and often requires a tailor-made solution. Consequently, solutions developed for one coexistence scenario cannot be extended or even easily modified to fit another coexistence scenario, even when the technologies are developed for similar use-cases. The best example for this is the coexistence between DSRC & Wi-Fi, and between C-V2X & Wi-Fi. Although the primary user in both cases is a V2X RAT, solutions that work well for DSRC and Wi-Fi coexistence (as seen in Chapter 3.3) do not suffice to protect C-V2X systems from Wi-Fi induced interference (as we see in Chapter 3.4).

In Chapter 3.3 and Chapter 3.4, we look at DSRC–Wi-Fi and C-V2X–Wi-Fi coexistence problems, respectively, in detail. We show that due to the similarities in the MAC protocols of DSRC and Wi-Fi, very simple, yet effective, coexistence mechanisms can be used to achieve harmonious coexistence between DSRC and Wi-Fi. This has considerable implications because if Wi-Fi and DSRC devices are allowed to share the ITS spectrum, Wi-Fi devices will have contiguous access to the entire 5 GHz and 6 GHz bands in the US. However, the same is not true for C-V2X and Wi-Fi coexistence. Since C-V2X is derived from LTE, it's MAC protocol significantly differs from that of Wi-Fi, and hence, to achieve effective coexistence between these two technologies, the design of novel coexistence mechanisms is necessary.

In Chapter 6, we use tools from stochastic geometry to study the coexistence between NR-U and Wi-Fi. Although the coexistence model developed in this chapter can be used to analyze the performance of the two RATs in any of the bands in which they operate, we interpret the results from the model in the context of the greenfield 6 GHz bands. The main reason to do so is that these greenfield bands provide a unique and rare opportunity to take a fresh look at the coexistence problem. Specifically, several MAC layer parameters, the choice of which in the 5 GHz bands is restricted by the millions of current Wi-Fi deployments, can be freshly chosen for the 5 GHz bands. Furthermore, MU OFDMA—which will be used for the first time in IEEE 802.11ax compliant Wi-Fi 6 devices—benefits both NR-U and Wi-Fi 6 users. This finding strongly motivates the disabling of LBT-based legacy contention used in Wi-Fi when they operate in the 6 GHz bands.

As new technologies continue to be designed, standardized, and rolled-out, existing technologies have continued to evolve. An accurate and thorough understanding of these new technologies, features, and mechanisms warrants a systematic study. During the study of coexistence scenarios arising in the 5 GHz and 6 GHz bands, we identified several gaps in the literature on the performance of IEEE 802.11ax (related to uplink MU OFDMA) and C-V2X (especially in the sidelink mode 4). In Chapter 7 and Chapter 8, we make an attempt to fill these gaps.

In Chapter 7, we study the performance of C-V2X sidelink mode 4 in highway environments. In doing so, we look at the impact of packet re-transmissions—a mechanism used to increase the reliability of packet transmissions—on the system-level performance in detail. We see

that although re-transmissions are beneficial from the system performance viewpoint, this is true only when the density of vehicles and the periodicity of packet transmissions are low. If either of these intensities increase, packet re-transmissions begin to negatively impact system performance. To address this issue, we propose and evaluate a simple—yet effective—re-transmission control mechanism named $C^2RC$.

In Chapter 8, we study the performance of UORA—the random access mechanism designed to be used alongside schedule-based uplink MU OFDMA transmissions in 802.11ax. We also present a detailed analysis of the performance of MU OFDMA-based MAC of IEEE 802.11ax for a wide range of deployment scenarios. We consider the performance of 802.11ax networks when the network comprises of only 802.11ax as well as a combination of 802.11ax and legacy stations. The latter is a practical scenario, especially during the initial phases of 802.11ax deployments. The results derived from our model give encouraging signs for 802.11ax performance in many real-world scenarios. That being said, there are some scenarios where naive usage of MU OFDMA by an 802.11ax-capable Wi-Fi AP can be detrimental to the overall system performance. Our results indicate that careful consideration of network dynamics is critical in exploiting the best performance, especially in a heterogeneous Wi-Fi network.

In Chapter 9, we perform a comprehensive simulation study to characterize the performance of Multi Link Aggregation (MLA) in IEEE 802.11be. We study the impact of different traffic densities on the 90 percentile latency of Wi-Fi packets and identify that the addition of a single link is sufficient to substantially bring down the 90 percentile latency in many practical scenarios. Furthermore, we show that while addition of subsequent links is beneficial, the largest latency gain in most scenarios is experienced when the second link (i.e., one additional) link is added. Finally, we show that even in extremely dense traffic conditions, if a sufficient number of links are available at the MLA-capable transmitter and receiver, MLA can help Wi-Fi devices to meet the latency requirements of most real-time applications.

In summary, the 5 GHz and 6 GHz bands provide several interesting research problems, some of which we have addressed in this dissertation, while others have been addressed in the literature. However, many of these open problems continue to act as significant hurdles to the success of future wireless applications, particularly in increasingly dense settings. The 6 GHz bands, in particular, are an exciting new frontier in unlicensed wireless communications due to their greenfield nature. Steps taken in the near future on these bands to enable coexistence across heterogeneous wireless technologies can be the deciding factor on how efficiently these bands cater to the demand for wireless applications and services.

# Bibliography


[1] Netmanias, "Analysis of LTE–WiFi aggregation solutions." Online: http://www.netmanias.com/en/post/reports/8532/laa-lte-lte-u-lwa-mptcp-wi-fi/analysis-of-lte-wifi-aggregation-solutions, March 2016 (accessed November 9, 2020).

[2] FCC, "Report and Order and Further Notice of Proposed Rulemaking; In the Matter of Unlicensed Use of the 6 GHz band (ET Docket No. 18-295); Expanding Flexible Use in Mid-Band Spectrum Between 3.7 and 24 GHz (GN Docket No. 17-183)." Online: https://docs.fcc.gov/public/attachments/FCC-20-51A1.pdf, April 2020 (accessed November 9, 2020).

[3] CEPT, "CEPT Report 73; Report from CEPT to the European Commission in response to the Mandate "to study feasibility and identify harmonised technical conditions for Wireless Access Systems including Radio Local Area Networks in the 5925-6425 MHz band for the provision of wireless broadband services"." https://www.ecodocdb.dk/download/0d0696a1-89ae/CEPT%20Report%2073.pdf, March 2020 (accessed November 9, 2020).

[4] K. Westcott, J. Loucks, D. Littmann, P. Wilson, S. Srivastava, and D. Ciampa, *Build it and they will embrace it; Consumers are preparing for 5G connectivity in the home and on the go*, December 2019.

[5] Cisco Systems Inc., *Cisco Annual Internet Report (2018–2023) White Paper*, March 2020.

[6] Ericsson, "Ericsson Mobility Report: Mobile data traffic outlook." Online: https://www.ericsson.com/en/mobility-report/reports/june-2020/mobile-data-traffic-outlook, June 2020.

[7] S. Simoens, P. Pellati, J. Gosteau, K. Gosse, and C. Ware, "The evolution of 5GHz WLAN toward higher throughputs," *IEEE Wireless Communications*, vol. 10, no. 6, pp. 6–13, 2003.

[8] E. Perahia and R. Stacey, *Next generation wireless LANs: 802.11 n and 802.11 ac*. Cambridge university press, 2013.

[9] E. Khorov, A. Kiryanov, A. Lyakhov, and G. Bianchi, "A tutorial on IEEE 802.11 ax high efficiency WLANs," *IEEE Communications Surveys & Tutorials*, vol. 21, no. 1, pp. 197–216, 2018.

[10] G. Naik, J. Liu, and J.-M. Park, "Coexistence of Wireless Technologies in the 5 GHz Bands: A Survey of Existing Solutions and a Roadmap for Future Research," *IEEE Communications Surveys & Tutorials*, 2018.

[11] A. Mukherjee, J.-F. Cheng, S. Falahati, H. Koorapaty, R. Karaki, L. Falconetti, D. Larsson, *et al.*, "Licensed-assisted access LTE: coexistence with IEEE 802.11 and the evolution toward 5G," *IEEE Communications Magazine*, vol. 54, no. 6, pp. 50–57, 2016.

[12] R. Zhang, M. Wang, L. X. Cai, Z. Zheng, X. Shen, and L.-L. Xie, "LTE-unlicensed: the future of spectrum aggregation for cellular networks," *IEEE Wireless Communications*, vol. 22, no. 3, pp. 150–159, 2015.

[13] G. Naik, J.-M. Park, J. Ashdown, and W. Lehr, "Next Generation Wi-Fi and 5G NR-U in the 6 GHz Bands: Opportunities & Challenges," *IEEE Access*, 2020.

[14] R. L. D. Hoover, S. J. Rao, G. Howe, and F. S. Barickman, "Heavy-vehicle lane departure warning test development," 2014.

[15] G. Forkenbrock, R. L. Hoover, E. Gerdus, T. R. Van Buskirk, M. Heitz, *et al.*, "Blind spot monitoring in light vehicles—System performance," tech. rep., United States. National Highway Traffic Safety Administration, 2014.

[16] T. Litman, *Autonomous vehicle implementation predictions*. Victoria Transport Policy Institute Victoria, Canada, 2017.

[17] X. Wang, S. Mao, and M. X. Gong, "An Overview of 3GPP Cellular Vehicle-to-Everything Standards," *GetMobile: Mobile Computing and Communications*, vol. 21, no. 3, pp. 19–25, 2017.

[18] US Department of Transportation, "Vehicle-to-vehicle communication technology." https://www.nhtsa.gov/sites/nhtsa.dot.gov/files/documents/v2v_fact_sheet_101414_v2a.pdf, July 2017 (accessed November 9, 2020).

[19] A. Amoroso, G. Marfia, M. Roccetti, and G. Pau, "To live and drive in LA: Measurements from a real intervehicular accident alert test," in *Wireless Communications and Networking Conference Workshops (WCNCW), 2012 IEEE*, pp. 328–332, IEEE, 2012.

[20] J. B. Kenney, "Dedicated short-range communications (DSRC) standards in the United States," *Proceedings of the IEEE*, vol. 99, no. 7, pp. 1162–1182, 2011.

[21] ETSI, "ETSI TR 102 638: Intelligent Transport Systems (ITS); Vehicular Communications; Basic Set of Applications; Definitions." Online: https://www.etsi.org/deliver/etsi_tr/102600_102699/102638/01.01.01_60/tr_102638v010101p.pdf, June 2009 (accessed November 9, 2020).

[22] 5GAA, "5G V2X, The automotive use-case for 5G." https://www.3gpp.org/ftp/information/presentations/Presentations_2017/A4Conf010_Dino%20Flore_5GAA_v1.pdf, 2017 (accessed November 9, 2020).

[23] 3GPP, "3GPP TR 22.886: Study on enhancement of 3GPP Support for 5G V2X Services (v16.2.0, Release 16)," Dec. 2018.

[24] FCC, "Notice of Proposed Rulemaking; In the Matter of Use of the 5.850-5.925 GHz Band (ET Docket No. 19-138)." Online: https://docs.fcc.gov/public/attachments/DOC-360940A1.pdf, November 2019 (accessed November 9, 2020).

[25] M. Chowdhury, M. Rahman, A. Rayamajhi, S. M. Khan, M. Islam, Z. Khan, and J. Martin, "Lessons Learned from the Real-world Deployment of a Connected Vehicle Testbed," *Transportation Research Record*, vol. 2672, no. 22, pp. 10–23, 2018.

[26] 3GPP, "3GPP TS 36.213: Evolved Universal Terrestrial Radio Access (E-UTRA); Physical layer procedures (v14.3.0, Release 14)," June 2017.

[27] 3GPP, "3GPP TS 36.321: Evolved Universal Terrestrial Radio Access (E-UTRA); Medium Access Control (MAC) protocol specification (v14.3.0, Release 14)," June 2017.

[28] 3GPP, "3GPP TS 36.331: Radio Resource Control (RRC); Protocol specification (v14.2.2, Release 14)," May 2017.

[29] K. A. Hafeez, L. Zhao, B. Ma, and J. W. Mark, "Performance analysis and enhancement of the DSRC for VANET's safety applications," *IEEE Trans. on Veh. Techn.*, vol. 62, no. 7, pp. 3069–3083, 2013.

[30] R. Molina-Masegosa and J. Gozalvez, "LTE-V for Sidelink 5G V2X Vehicular Communications: A New 5G Technology for Short-Range Vehicle-to-Everything Communications," *IEEE Vehicular Technology Magazine*, vol. 12, no. 4, pp. 30–39, 2017.

[31] A. M. Cavalcante, E. Almeida, R. D. Vieira, S. Choudhury, E. Tuomaala, K. Doppler, F. Chaves, R. C. Paiva, and F. Abinader, "Performance evaluation of LTE and Wi-Fi coexistence in unlicensed bands," in *2013 IEEE 77th Vehicular Technology Conference (VTC Spring)*, pp. 1–6, IEEE, 2013.

[32] B. Chen, J. Chen, Y. Gao, and J. Zhang, "Coexistence of LTE-LAA and Wi-Fi on 5 GHz with corresponding deployment scenarios: A survey," *IEEE Communications Surveys & Tutorials*, vol. 19, no. 1, pp. 7–32, 2016.

[33] 3GPP, "3GPP TS 37.213: Physical layer procedures for shared spectrum channel access (Release 15) ," July 2018.

[34] European Commission, "Mandate to CEPT to study feasibility and identify harmonized technical conditions for wireless access systems including radio local area networks in the 5925-6425 MHz band for the provision of wireless broadband services." Online: http://ec.europa.eu/newsroom/dae/document.cfm?doc_id=50343, December 2017 (accessed November 9, 2020).

[35] FCC, "Notice of Proposed Rulemaking; In the Matter of Unlicensed Use of the 6 GHz band (ET Docket No. 18-295); Expanding Flexible Use in Mid-Band Spectrum Between 3.7 and 24 GHz (GN Docket No. 17-183)." Online: https://docs.fcc.gov/public/attachments/FCC-18-147A1.pdf, October 2018 (accessed November 9, 2020).

[36] Y. Benkler, "Open wireless vs. licensed spectrum: Evidence from market adoption," *Harv. JL & Tech.*, vol. 26, p. 69, 2012.

[37] Fierce Wireless, "In 2017, how much low-, mid- and high-band spectrum do Verizon, AT&T, T-Mobile, Sprint and Dish own, and where?," May 2017 (accessed November 9, 2020).

[38] Y. Niu, Y. Li, D. Jin, L. Su, and A. V. Vasilakos, "A survey of millimeter wave communications (mmWave) for 5G: opportunities and challenges," *Wireless networks*, vol. 21, no. 8, pp. 2657–2676, 2015.

[39] M. Paolini and S. Fili, "LTE unlicensed and Wi-Fi: moving beyond coexistence." Online: https://ecfsapi.fcc.gov/file/60001076664.pdf, 2015.

[40] FCC, "Notice of Proposed Rulemaking; In the Matter of Revision of Part 15 of the Commission's Rules to Permit Unlicensed National Information Infrastructure (U-NII) Devices in the 5 GHz Band (ET Docket No. 13-49)." Online: https://docs.fcc.gov/public/attachments/FCC-13-22A1.pdf, February 2013 (accessed November 9, 2020).

[41] "CEPT Report 57; To study and identify harmonised compatibility and sharing conditions for Wireless Access Systems including Radio Local Area Networks in the bands 5350-5470 MHz and 5725-5925 MHz (WAS/RLAN extension bands) for the provision of wireless broadband services." Online: http://spectrum.welter.fr/international/cept/cept-reports/cept-report-057-5-GHz.pdf, March 2015 (accessed November 9, 2020).

[42] NetworkWorld, "Current developments in Wi-Fi spectrum." Online: https://www.networkworld.com/article/3188228/current-developments-in-wi-fi-spectrum.html, April 2017 (accessed November 9, 2020).

[43] J. Härri and J. Kenney, "Multi-channel operations, coexistence and spectrum sharing for vehicular communications," in *Vehicular ad hoc Networks*, pp. 193–218, Springer, 2015.

[44] ETSI, "ETSI EN 302 571: Intelligent Transport Systems (ITS); Radiocommunications equipment operating in the 5855 MHz to 5925 MHz frequency band; Harmonised Standard covering the essential requirements of article 3.2 of Directive 2014/53/EU." Online: https://www.etsi.org/deliver/etsi_en/302500_302599/302571/02.00.00_20/en_302571v020000a.pdf, March 2016 (accessed November 9, 2020).

[45] European Commission, "Commission Delegated Regulation (EU) of 13.3.2019 supplementing Directive 2010/40/EU of the European Parliament and of the Council with regard to the deployment and operational use of cooperative intelligent transport systems." Online: https://ec.europa.eu/transport/sites/transport/files/legislation/c20191789.pdf, March 2019 (accessed November 9, 2020).

[46] J. Yin, T. ElBatt, G. Yeung, B. Ryu, S. Habermas, H. Krishnan, and T. Talty, "Performance evaluation of safety applications over DSRC vehicular ad hoc networks," in *Proceedings of the 1st ACM international workshop on Vehicular ad hoc networks*, pp. 1–9, ACM, 2004.

[47] M. I. Hassan, H. L. Vu, and T. Sakurai, "Performance analysis of the IEEE 802.11 MAC protocol for DSRC safety applications," *IEEE Trans. on Vehicular Technology*, vol. 60, no. 8, pp. 3882–3896, 2011.

[48] ETSI, "ETSI TR 103 319: Mitigation techniques to enable sharing between RLANs and Road Tolling and Intelligent Transport Systems in the 5725 MHz to 5925 MHz band." Online: https://www.etsi.org/deliver/etsi_tr/103300_103399/103319/01.01.01_60/tr_103319v010101p.pdf, August 2017 (accessed November 9, 2020).

[49] T. Yucek, E. Perahia, V. Erceg, and X. Wu, "IEEE 802.11-13/1449r2: Proposal for UNII-4 band coexistence." contribution to the IEEE 802.11 Regulatory SC, Online: https://mentor.ieee.org/802.11/dcn/13/11-13-1449-02, November 2013.

[50] G. Naik, B. Choudhury, and J.-M. Park, "IEEE 802.11 bd & 5G NR V2X: Evolution of Radio Access Technologies for V2X Communications," *arXiv preprint arXiv:1903.08391*, 2019.

[51] 5GAA, "5GAA petition for waiver." https://ecfsapi.fcc.gov/file/11212224101742/5GAA%20Petition%20for%20Waiver%20-%20Final%2011.21.2018.pdf, November 2018.

[52] ——-, "EU opens road to 5G connected cars in boost to BMW, Qualcomm." Online: https://www.reuters.com/article/us-eu-autos-tech/eu-opens-road-to-5g-connected-cars-in-boost-to-bmw-qualcomm-idUSKCN1TZ11F, July 2019 (accessed November 9, 2020).

[53] IEEE, "IEEE P802.11ax/D6.0; Part 11: Wireless LAN Medium Access Control (MAC) and Physical Layer (PHY) Specifications; Amendment 1: Enhancements for High Efficiency WLAN," November 2019.

[54] ECC, "ECC Report 302; Sharing and compatibility studies related to Wireless Access Systems including Radio Local Area Networks (WAS/RLAN) in the frequency band 5925-6425 MHz." https://www.ecodocdb.dk/download/cc03c766-35f8/ECC%20Report%20302.pdf, May 2019 (accessed November 9, 2020).

[55] K. Meng, A. Jones, D. Cavalcanti, K. Iyer, C. Ji, K. Sakoda, A. Kishida, F. Hsu, J. Yee, L. Li, and E. Khorov, "IEEE 802.11-18/2009r6: IEEE 802.11 Real Time Applications TIG Report." report of the IEEE 802.11 RTA TIG, Online: https://mentor.ieee.org/802.11/dcn/18/11-18-2009-06, November 2018 (accessed November 9, 2020).

[56] IEEE, "Status of Project IEEE P802.11be." http://www.ieee802.org/11/Reports/tgbe_update.htm, 2019 (accessed November 9, 2020).

[57] Wi-Fi Alliance, "Wi-Fi Certified 6." https://www.wi-fi.org/discover-wi-fi/wi-fi-certified-6, 2019 (accessed November 9, 2020).

[58] Qualcomm, "Qualcomm Highlights Technology Leadership as Industry Readies for Wi-Fi 6E." https://www.qualcomm.com/news/releases/2020/02/25/qualcomm-highlights-technology-leadership-industry-readies-wi-fi-6e, February 2020 (accessed November 9, 2020).

[59] Broadcom, "Wi-Fi 6E: Faster Speed, Lower Latency and Higher Capacity." https://www.broadcom.com/info/wifi6e, January 2020 (accessed November 9, 2020).

[60] "Evaluation of the 5350-5470 MHz and 5850-5925 MHz Bands pursuant to Section 6406 (b) of the Middle Class Tax Relief and Job Creation Act of 2012." https://www.ntia.doc.gov/files/ntia/publications/ntia_5_ghz_report_01-25-2013.pdf, 2013 January.

[61] Ofcom, "Improving spectrum access for consumers in the 5 GHz band." Online: https://www.ofcom.org.uk/__data/assets/pdf_file/0037/79777/improving-spectrum-access-consumers-5ghz.pdf, May 2016 (accessed November 9, 2020).

[62] ITU-R Resolution 229 [COM5/16], "Use of the bands 5150-5250MHz, 5250-5350MHz and 5470-5725MHz by the mobile service for the implementation of wireless access systems including radio local area networks," *The World Radio-communication Conference (WRC-03)*, 2013.

[63] Wireless Innovation Forum, "Propagation Models and Interference Protection Criteria for Sharing between the Fixed Service and Unlicensed Devices in the 6 GHz Band." Technical Report, Document WINNF-TR-1002, Version V1.0.0, Online: https://www.wirelessinnovation.org/assets/work_products/Reports/winnf-tr-1002-v1.0.0%20propagation%20and%20ipc%20for%206%20ghz%20sharing.pdf, December 2019.

[64] Fixed Wireless Communications Coalition, "6 GHz RLAN Mitigation Issues." comments to the FCC GN Docket No. 17-183, Online: http://www.fwcc.us/pdffiles/17-183%20FWCC%20ExP%20Notice%202018-07-17%20--%20AS%20FILED%20(01214380xB3D1E).PDF, July 2018 (accessed November 9, 2020).

[65] Zebra Technologies, Inc., "Unlicensed use of the 6 GHz Band." comments to the FCC ET Docket No. 18-295 and GN Docket No. 17-183, Online: https://ecfsapi.fcc.gov/file/1218064643854/Zebra%20and%20NFL%20Presentation%206%20GHz%20Band.pdf, December 2019 (accessed November 9, 2020).

[66] Ultra Wide Band Alliance, "Presentation to FCC Office of Engineering and Technology (OET)." comments to the FCC ET Docket No. 18-295 and GN Docket No. 17-183, Online: Online:https://ecfsapi.fcc.gov/file/10216885901204/UWB%20Alliance%20FCC%206%20Ghz%20Comments%20and%20Preso%20Feb2019.pdf, February 2019 (accessed November 9, 2020).

[67] The Economist, "When wireless worlds collide. As Wi-Fi hotspots proliferate, who needs cellular wireless?." Online: https://www.economist.com/science-and-technology/2014/11/17/when-wireless-worlds-collide, April 2014 (accessed November 9, 2020).

[68] NetworkWorld, "What is 802.11ax (Wi-Fi 6), and what will it mean for 802.11ac." Online: https://www.networkworld.com/article/3258807/what-is-80211ax-wi-fi-6-and-what-will-it-mean-for-80211ac.html, February 2018 (accessed November 9, 2020).

[69] M. Burton and G. Hill, "802.11 Arbitration," *White Paper, Certified Wireless Network Professional Inc., Durham, NC, Online: https://www.cwnp.com/uploads/802-11_arbitration.pdf*, 2009.

[70] Cisco, *802.11ac: The Fifth Generation of Wi-Fi*, 2014.

[71] B. Bellalta, "IEEE 802.11 ax: High-efficiency WLANs," *IEEE Wireless Communications*, vol. 23, no. 1, pp. 38–46, 2016.

[72] E. Khorov, I. Levitsky, and I. F. Akyildiz, "Current Status and Directions of IEEE 802.11 be, the Future Wi-Fi 7," *IEEE Access*, 2020.

[73] L. Cariou, R. Stacey, C. Cordeiro, R. De Vegt, B. Tian, V. Erceg, and R. Porat, "IEEE 802.11-19/0787r2: 802.11be Timeline proposal." contribution to the IEEE TGbe, Online: https://mentor.ieee.org/802.11/dcn/19/11-19-0787-02, May 2019 (accessed November 9, 2020).

[74] A. Kishida, Y. Inoue, Y. Asai, Y. Takatori, S. Shinohara, K. Meng, X. Zuo, S. Kim, and D. Cavalcanti, "IEEE 802.11-19/1207r4: Views on Latency and Jitter Features in TGbe." contribution to the IEEE TGbe, Online: https://mentor.ieee.org/802.11/dcn/19/11-19-1207-04, July 2019 (accessed November 9, 2020).

[75] T. Adame, M. Carrascosa, and B. Bellalta, "Time-Sensitive Networking in IEEE 802.11be: On the Way to Low-latency WiFi 7," *arXiv preprint arXiv:1912.06086*, 2019.

[76] D. López-Pérez, A. Garcia-Rodriguez, L. Galati-Giordano, M. Kasslin, and K. Doppler, "IEEE 802.11be Extremely High Throughput: The Next Generation of Wi-Fi Technology Beyond 802.11 ax," *IEEE Communications Magazine*, vol. 57, no. 9, pp. 113–119, 2019.

[77] Y. Fang, B. Sun, Z. Han, and N. Li, "IEEE 802.11-19/1095: Multi-Link Architecture and Requirement Discussion." contribution to the IEEE TGbe, Online: https://mentor.ieee.org/802.11/dcn/19/11-19-1095, July 2019 (accessed November 9, 2020).

[78] J. Y. Gao, G. Huang, R. J. Yu, and P. Loc, "IEEE 802.11-19/0801r0: AP Coordination in EHT." contribution to the IEEE TGbe, Online: https://mentor.ieee.org/802.11/dcn/19/11-19-0801, March 2019 (accessed November 9, 2020).

[79] M. Yang, B. Li, Z. Yan, and Y. Yan, "AP Coordination and Full-duplex enabled Multi-band Operation for the Next Generation WLAN: IEEE 802.11 be (EHT)," in *2019 11th International Conference on Wireless Communications and Signal Processing (WCSP)*, pp. 1–7, IEEE, 2019.

[80] J. Suh, O. Aboul-Magd, and E. Au, "IEEE 802.11-19/0832r0: Performance Evaluation of 16 Spatial Stream based MU-MIMO." contribution to the IEEE TGbe, Online: https://mentor.ieee.org/802.11/dcn/19/11-19-0832, May 2019 (accessed November 9, 2020).

[81] S. Schelstraete, D. Dash, and I. Latif, "IEEE 802.11-19/0637: Feasibility of 4096QAM." contribution to the IEEE TGbe, Online: https://mentor.ieee.org/802.11/dcn/19/11-19-0637, May 2019 (accessed November 9, 2020).

[82] J. Kim, T. Song, E. Park, J. Kim, and J. Choi, "IEEE 802.11-19/0780r0: Consideration on HARQ." contribution to the IEEE TGbe, Online: https://mentor.ieee.org/802.11/dcn/19/11-19-0780, May 2019 (accessed November 9, 2020).

[83] E. Park, D. Lim, J. Kim, and J. Choi, "IEEE 802.11-19/1889r2: Discussion on 240MHz Bandwidth." contribution to the IEEE TGbe, Online: https://mentor.ieee.org/802.11/dcn/19/11-19-1889-02, November 2019 (accessed November 9, 2020).

[84] R. Hirata, Y. Tanaka, K. Aio, T. Handte, and D. Ciochina, "IEEE 802.11-19/0818r1: Discussion on Multi-band operation." contribution to the IEEE TGbe, Online: https://mentor.ieee.org/802.11/dcn/19/11-19-0818-01, July 2019 (accessed November 9, 2020).

[85] Y. Seok, W. Tsao, G. Bajko, J. Yee, J. Liu, P. Cheng, and T. Pare, "IEEE 802.11-19/0766r1: Enhanced Multi-band/Multi-channel Operation." contribution to the IEEE TGbe, Online: https://mentor.ieee.org/802.11/dcn/19/11-19-0766-01, May 2019 (accessed November 9, 2020).

[86] I. Jang, J. Choi, J. Kim, S. Kim, S. Park, and T. Song, "IEEE 802.11-19/1144r6: Channel Access for Multi-link Operation." contribution to the IEEE TGbe, Online: https://mentor.ieee.org/802.11/dcn/19/11-19-1144-06, July 2019 (accessed November 9, 2020).

[87] A. Al-Dulaimi, S. Al-Rubaye, Q. Ni, and E. Sousa, "5G communications race: Pursuit of more capacity triggers LTE in unlicensed band," *IEEE vehicular technology magazine*, vol. 10, no. 1, pp. 43–51, 2015.

[88] Qualcomm Technologies, Inc., *Qualcomm research LTE in unlicensed spectrum: harmonious coexistence with Wi-Fi*, June 2014 (accessed November 9, 2020).

[89] A. K. Sadek, "Carrier sense adaptive transmission (CSAT) in unlicensed spectrum," 2014. US Patent App. 14/486,855.

[90] M. Alliance, "MulteFire Release 1.0.1 Specification." Online: https://www.multefire.org/specification/, 2017.

[91] Qualcomm Inc, "Introducing MulteFire: LTE-like performance with Wi-Fi-like simplicity." https://www.qualcomm.com/news/onq/2015/06/11/introducing-multefire-lte-performance-wi-fi-simplicity, June 2015 (accessed November 9, 2020).

[92] M. Alliance, "MulteFire Release 1.0 Technical Paper." Online: https://www.multefire.org/specification/release-1-0-technical-paper-download/, 2017.

[93] D. Chambers, *MulteFire lights up the path for universal wireless service*, 2016.

[94] ETSI, "ETSI EN 301 893: Harmonized EN covering the essential requirements of article 3.2 of the R&TTE Directive." Online: http://www.etsi.org/deliver/etsi_en/301800_301899/301893/01.07.01_60/en_301893v010701p.pdf, June 2012 (accessed November 9, 2020).

[95] Qualcomm Inc., "RP-182878: New WID on NR-based Access to Unlicensed Spectrum ." 3GPP TSG RAN 82, Sorrento, Italy, Online: https://www.3gpp.org/ftp/TSG_RAN/TSG_RAN/TSGR_82/Docs/RP-182878.zip, December 2018 (accessed November 9, 2020).

[96] 3GPP, "3GPP TR 38.889: Technical Specification Group Radio Access Network; Study on NR-based access to unlicensed spectrum (Release 16) ," December 2018.

[97] S. Ahmadi, *5G NR: Architecture, Technology, Implementation, and Operation of 3GPP New Radio Standards*. Academic Press, 2019.

[98] S. Parkvall, E. Dahlman, A. Furuskar, and M. Frenne, "NR: The new 5G radio access technology," *IEEE Communications Standards Magazine*, vol. 1, no. 4, pp. 24–30, 2017.

[99] J. Zhang, M. Wang, M. Hua, T. Xia, W. Yang, and X. You, "Lte on license-exempt spectrum," *IEEE Communications Surveys & Tutorials*, vol. 20, no. 1, pp. 647–673, 2017.

[100] Y. Kim, Y. Kim, J. Oh, H. Ji, J. Yeo, S. Choi, H. Ryu, H. Noh, T. Kim, F. Sun, *et al.*, "New Radio (NR) and its Evolution toward 5G-Advanced," *IEEE Wireless Communications*, vol. 26, no. 3, pp. 2–7, 2019.

[101] M. Mehrnoush, V. Sathya, S. Roy, and M. Ghosh, "Analytical modeling of Wi-Fi and LTE-LAA coexistence: Throughput and impact of energy detection threshold," *IEEE/ACM Transactions on Networking (TON)*, vol. 26, no. 4, pp. 1990–2003, 2018.

[102] Q. Xu, T. Mak, J. Ko, and R. Sengupta, "Vehicle-to-vehicle safety messaging in DSRC," in *Proceedings of the 1st ACM international workshop on Vehicular ad hoc networks*, pp. 19–28, ACM, 2004.

[103] D. Jiang, V. Taliwal, A. Meier, W. Holfelder, and R. Herrtwich, "Design of 5.9 GHz DSRC-based vehicular safety communication," *IEEE Wireless Communications*, vol. 13, no. 5, 2006.

[104] H. Hartenstein and K. Laberteaux, *VANET vehicular applications and inter-networking technologies*, vol. 1. John Wiley & Sons, 2009.

[105] R. A. Uzcátegui, A. J. De Sucre, and G. Acosta-Marum, "Wave: A tutorial," *IEEE Communications magazine*, vol. 47, no. 5, 2009.

[106] J. Lansford, J. B. Kenney, and P. Ecclesine, "Coexistence of unlicensed devices with DSRC systems in the 5.9 GHz ITS band," in *Vehicular Networking Conference (VNC), 2013 IEEE*, pp. 9–16, IEEE, 2013.

[107] SAE International, *DSRC Implementation Guide, A guide to users of SAE J2735 message sets over DSRC*, February 2010.

[108] ———, "IEEE guide for wireless access in vehicular environments (WAVE) - architecture," *IEEE Std 1609.0-2013*, pp. 1–78, March 2014.

[109] H. Z. Bo Sun, "IEEE 802.11-18/0861r9: 802.11 NGV Proposed PAR." contribution to the IEEE NGV SG, https://mentor.ieee.org/802.11/dcn/18/11-18-0861-09, November 2019 (accessed November 9, 2020).

[110] F. Michael *et al.*, "IEEE 802.11-18/1186r0: Interoperable NGV PHY Improvements." contribution to the IEEE NGV SG, https://mentor.ieee.org/802.11/dcn/18/11-18-1186, July 2018 (accessed November 9, 2020).

[111] L. Dongguk *et al.*, "IEEE 802.11-19/0009r0: Consideration on Features for 11bd." contribution to the IEEE TGbd, Online: https://mentor.ieee.org/802.11/dcn/19/11-19-0009, January 2019 (accessed November 9, 2020).

[112] R. Jain, "Introduction to Introduction to 60 GHz Millimeter Wave 60 GHz Millimeter Wave Multi-Gigabit Wireless Networks." https://www.cse.wustl.edu/~jain/cse574-16/ftp/j_07sgh.pdf, 2016 (accessed November 9, 2020).

[113] M. Hiroyuki *et al.*, "IEEE 802.11-18/1187r3: mmW for V2X use cases." contribution to the IEEE NGV SG, https://mentor.ieee.org/802.11/dcn/18/11-18-1187.

[114] Q. Chen, D. Jiang, and L. Delgrossi, "IEEE 1609.4 DSRC multi-channel operations and its implications on vehicle safety communications," in *Vehicular Networking Conference (VNC), 2009 IEEE*, pp. 1–8, IEEE, 2009.

[115] 3GPP, "3GPP TS 23.285: Universal Mobile Telecommunications System (UMTS); Architecture enhancements for V2X services (v14.3.0, Release 14)," July 2017.

[116] A. Filippi, K. Moerman, V. Martinez, A. Turley, O. Haran, and R. Toledano, "IEEE802.11p ahead of LTE-V2V for safety applications." White Paper, Online: https://www.nxp.com/docs/en/white-paper/LTE-V2V-WP.pdf, 2017.

[117] Vodafone, "RP-181480: New SID: Study on NR V2X." 3GPP Planery Meeting 80, La Jolla, USA, June 2018.

[118] D. Butler, "How 'Talking' and 'Listening' Vehicles Could Make Roads Safer, Cities Better," Jan. 2019 (accessed November 9, 2020).

[119] ——, "R1-1810051: Final Report of 3GPP TSG RAN WG1 94 v1.0.0," Oct. 2018.

[120] Spreadtrum Communications, "R1-1811009: Consideration on sidelink unicast, groupcast and broadcast." 3GPP TSG RAN WG1 94b, Chengdu, China, Oct. 2018.

[121] ——, "Draft Report of 3GPP TSG RAN WG1 95 v0.3.0," Jan. 2019.

[122] LG Electronics, "R1-1903366: Feature lead summary for agenda item - 7.2.4.1.1 Physical layer structure." 3GPP TSG RAN WG1 96, Athens, Greece, Feb. 2019.

[123] Intel Corportation, "R1-1809867: Offline Summary for NR-V2X Agenda Item - 7.2.4.1.4 Resource Allocation Mechanism." 3GPP TSG RAN WG1 94, Gothenburg, Sweden, Aug. 2018.

[124] Huawei, HiSilicon, "R1-1812209: Sidelink resource allocation mode 2." 3GPP TSG RAN WG1 95, Spokane, USA, Nov. 2018.

[125] P. Joe, F. Whetten, J. Scott, and D. Whetten, "Airborne RLAN and weather radar interference at C-band," in *33rd Conf. on Radar Meteorology*, 2007.

[126] P. Joe, J. Scott, J. Sydor, A. Brandão, and A. Yongacoglu, "Radio local area network (RLAN) and C-band weather radar interference studies," in *Proc. 32nd AMS Radar Conference on Radar Meteorology*, 2005.

[127] M. Tercero, K. W. Sung, and J. Zander, "Impact of aggregate interference on meteorological radar from secondary users," in *2011 IEEE Wireless Communications and Networking Conference*, pp. 2167–2172, IEEE, 2011.

[128] Z. Horváth and D. Varga, "Elimination of RLAN interference on weather radars by channel allocation in 5 GHz band," in *2009 International Conference on Ultra Modern Telecommunications & Workshops*, pp. 1–6, IEEE, 2009.

[129] R. Keränen, L. Rojas, and P. Nyberg, "Progress in mitigation of WLAN interferences at weather radar," in *36th Conf. on Radar Meteorology*, 2013.

[130] M. Wen and L. Hanwen, "Radar detection for 802.11 a systems in 5 GHz band," in *Proceedings. 2005 International Conference on Wireless Communications, Networking and Mobile Computing, 2005.*, vol. 1, pp. 512–514, IEEE, 2005.

[131] M. Peura, "Computer vision methods for anomaly removal," in *Proc. ERAD*, pp. 312–317, 2002.

[132] M. Tercero, K. W. Sung, and J. Zander, "Temporal secondary access opportunities for WLAN in radar bands," in *Wireless Personal Multimedia Communications (WPMC), 2011 14th International Symposium on*, pp. 1–5, IEEE, 2011.

[133] M. Gast, "Why we lost the weather radar channels." http://boundless.aerohive.com/technology/why-we-lost-the-weather-radar-channels.html, 2013.

[134] E. Saltikoff, J. Y. Cho, P. Tristant, A. Huuskonen, L. Allmon, R. Cook, E. Becker, and P. Joe, "The Threat to Weather Radars by Wireless Technology," *Bulletin of the American Meteorological Society*, no. 2015, 2015.

[135] A. L. Brandão, J. Sydor, W. Brett, J. Scott, P. Joe, and D. Hung, "5 GHz RLAN interference on active meteorological radars," in *2005 IEEE 61st Vehicular Technology Conference*, vol. 2, pp. 1328–1332, IEEE, 2005.

[136] P. Tristant, "RLAN 5 GHz interference to C-band meteorological radars in Europe: solutions, lessons, follow-up," in *34th Conference on Radar Meteorology*, 2009.

[137] ECC, "ECC Report 192; The Current Status of DFS (Dynamic Frequency Selection) In the 5 GHz frequency range." Online: http://www.erodocdb.dk/Docs/doc98/official/pdf/ECCREP192.PDF, February 2014 (accessed November 9, 2020).

[138] P. Tristant, "RLAN 5 GHz interference to weather radars in Europe," in *ITU/WMO Seminar on use of radio spectrum for meteorology: Weather, Water and Climate monitoring and prediction*, 2009.

[139] D. Leiss, "Military radars and WLANs Wrestle with interference issues." http://archive.cotsjournalonline.com/articles/view/100225, 2004.

[140] T. Baykas, J. Wang, M. A. Rahman, H. N. Tran, C. Song, S. Filin, Y. Alemseged, C. Sun, G. P. Villardi, C.-S. Sum, *et al.*, "Overview of TV White Spaces: Current regulations, standards and coexistence between secondary users," in *Personal, Indoor and Mobile Radio Communications Workshops (PIMRC Workshops), 2010 IEEE 21st International Symposium on*, pp. 38–43, IEEE, 2010.

[141] D. Gurney, G. Buchwald, L. Ecklund, S. L. Kuffner, and J. Grosspietsch, "Geo-Location Database Techniques for Incumbent Protection in the TV White Space," in *2008 3rd IEEE Symposium on New Frontiers in Dynamic Spectrum Access Networks*, pp. 1–9, Oct 2008.

[142] C. Ghosh, S. Roy, and D. Cavalcanti, "Coexistence challenges for heterogeneous cognitive wireless networks in TV white spaces," *IEEE Wireless Communications*, vol. 18, pp. 22–31, August 2011.

[143] S. Ghosh, G. Naik, A. Kumar, and A. Karandikar, "OpenPAWS: An open source PAWS and UHF TV White Space database implementation for India," in *2015 Twenty First National Conference on Communications (NCC)*, pp. 1–6, Feb 2015.

[144] B. Bahrak, S. Bhattarai, A. Ullah, J.-M. Park, J. Reed, and D. Gurney, "Protecting the primary users' operational privacy in spectrum sharing," in *Dynamic Spectrum Access Networks (DYSPAN), 2014 IEEE International Symposium on*, pp. 236–247, IEEE, 2014.

[145] C. Dwork, "Differential privacy: A survey of results," in *International Conference on Theory and Applications of Models of Computation*, pp. 1–19, Springer, 2008.

[146] R. Mudumbai, D. R. B. Iii, U. Madhow, and H. V. Poor, "Distributed transmit beamforming: challenges and recent progress," *IEEE Communications Magazine*, vol. 47, no. 2, pp. 102–110, 2009.

[147] S. Bhattarai, G. Naik, and L. Hong, "A computationally efficient node-selection scheme for cooperative beamforming in Cognitive Radio enabled 5G systems," in *Computer Communications Workshops (INFOCOM WKSHPS), 2016 IEEE Conference on*, pp. 1021–1026, IEEE, 2016.

[148] 6GHz RLAN Group, "VLP Use Cases." comments to the FCC ET Docket No. 18-295 and GN Docket No. 17-183, Online: https://ecfsapi.fcc.gov/file/101312903918268/6%20GHz%20Ex%20Parte%20(Jan%2031%202020).pdf, January 2020 (accessed November 9, 2020).

[149] M. Grissa, A. A. Yavuz, and B. Hamdaoui, "TrustSAS: A Trustworthy Spectrum Access System for the 3.5 GHz CBRS Band," in *IEEE INFOCOM 2019-IEEE Conference on Computer Communications*, pp. 1495–1503, IEEE, 2019.

[150] Fixed Wireless Communications Coalition, "Deploying 6 GHz RLANs While Protecting the Fixed Service." comments to the FCC GN Docket No. 17-183, Online: https://www.fwcc.us/pdffiles/fl.%202019.06.19%20FWCC%20Ex%20Parte%2018-295%20FINAL%20(01325394xB3D1E).pdf, July 2019 (accessed November 9, 2020).

[151] CTIA, "6 GHz Proceeding." comments to the FCC ET Docket No. 18-295 and GN Docket No. 17-183, Online: https://ecfsapi.fcc.gov/file/1115974613804/191115%20CTIA%206%20GHz%20Ex%20Parte%20Letter.pdf, November 2019 (accessed November 9, 2020).

[152] CTIA, "6 GHz Interference Analysis." comments to the FCC ET Docket No. 18-295 and GN Docket No. 17-183, Online: https://ecfsapi.fcc.gov/file/10205257007112/200205%20CTIA%20Ex%20Parte.pdf, February 2020 (accessed November 9, 2020).

[153] Broadcom, "Duty Cycle Data." comments to the FCC ET Docket No. 18-295 and GN Docket No. 17-183, Online: https://ecfsapi.fcc.gov/file/12091349203272/12.5.19%206%20GHz%20VLP%20LPI%20Ex%20Parte.pdf, December 2019 (accessed November 9, 2020).

[154] 6GHz RLAN Group, "Reply Comments of Apple Inc., Broadcom Inc., Cisco Systems, Inc., Facebook, Inc., Google LLC, Hewlett Packard Enterprise, Intel Corporation, Marvell Semiconductor, Inc., Microsoft Corporation, Qualcomm Incorporated, and Ruckus Networks, An Arris Company." comments to the FCC ET Docket No. 18-295 and GN Docket No. 17-183, Online: https://ecfsapi.fcc.gov/file/10319225597381/6%20GHz%20RLAN%20Group%20Reply.pdf, March 2019 (accessed November 9, 2020).

[155] 6GHz RLAN Group, "The FCC's 6 GHz proceeding: Enabling the next wave of unlicensed innovation; Briefing for Aaron Goldberger." comments to the FCC ET Docket No. 18-295 and GN Docket No. 17-183, Online: https://ecfsapi.fcc.gov/file/10426170869390/Ex%20Parte%20Letter%204.24.19%206%20USC%20meetings.pdf, April 2019 (accessed November 9, 2020).

[156] 6GHz RLAN Group, "6 USC Presentation to the Office of Engineering and Technology; RLAN-FS Interactions." comments to the FCC ET Docket No. 18-295 and GN Docket No. 17-183, Online: https://ecfsapi.fcc.gov/file/106241674322296/6%20GHz%20ET%20Ex%20Parte%20(June%2024%202019).pdf, June 2019 (accessed November 9, 2020).

[157] 6GHz RLAN Group, "6GHz FS/WiFi coexistence testing." comments to the FCC ET Docket No. 18-295 and GN Docket No. 17-183, Online: https://ecfsapi.fcc.gov/file/108230735019254/6GHz%20FS%20coexistence%20study%20ex%20parte%20(final).pdf, August 2019 (accessed November 9, 2020).

[158] 6GHz RLAN Group, "6 GHz Spectrum Sharing: Los Angeles Dep't of Water & Power Interference Protection Case Study." comments to the FCC ET Docket No. 18-295 and GN Docket No. 17-183, Online: https://ecfsapi.fcc.gov/file/10705662603550/LADWP%20Ex%20Parte%202%20July%202019.pdf, July 2019 (accessed November 9, 2020).

[159] Hewlett Packard Enterprise, and Broadcom, Inc., "Demonstration of Low Power Indoor RLAN I/N from HighRise Buildings in New York City & Washington DC." comments to the FCC ET Docket No. 18-295 and GN Docket No. 17-183, Online: https://ecfsapi.fcc.gov/file/1082249498356/8.22.19%206USC%20HPE%20LPI%20Demo%20Ex%20Parte%20(final).pdf, August 2019 (accessed November 9, 2020).

[160] National Association of Broadcasters, "Broadcast Use of 6 GHz." comments to the FCC ET Docket No. 18-295 and GN Docket No. 17-183, Online: https://ecfsapi.fcc.gov/file/1020784361095/6%20GHz%20ex%20parte%202.7.2020.pdf, February 2020 (accessed November 9, 2020).

[161] Alion, "Analysis of Interference To Electronic News Gathering Receivers From Proposed 6 GHz RLAN Transmitters." Online: https://ecfsapi.fcc.gov/file/1205735216211/RESED-20-002_v9.pdf, October 2019 (accessed November 9, 2020).

[162] CableLabs, "Low Power Indoor (LPI) Wi-Fi Will Not Cause Harmful Interference to Broadcast Auxiliary Systems (BAS) in 6 GHz." Online: https://ecfsapi.fcc.gov/file/101171404403806/20200115_6GHz_further%20analysis_final.pdf, February 2020 (accessed November 9, 2020).

[163] RKF Engineering Solutions, LLC, "Frequency Sharing for Radio Local Area Networks in the 6 GHz Band." Online: https://s3.amazonaws.com/rkfengineering-web/6USC+Report+Release+-+24Jan2018.pdf, January 2018 (accessed November 9, 2020).

[164] S. Bhattarai, J.-M. J. Park, B. Gao, K. Bian, and W. Lehr, "An overview of dynamic spectrum sharing: Ongoing initiatives, challenges, and a roadmap for future research," *IEEE Transactions on Cognitive Communications and Networking*, vol. 2, no. 2, pp. 110–128, 2016.

[165] S. Bhattarai, A. Ullah, J.-M. J. Park, J. H. Reed, D. Gurney, and B. Gao, "Defining incumbent protection zones on the fly: Dynamic boundaries for spectrum sharing," in *2015 IEEE International Symposium on Dynamic Spectrum Access Networks (DySPAN)*, pp. 251–262, IEEE, 2015.

[166] F. Baccelli and B. Błaszczyszyn, *Stochastic geometry and wireless networks*, vol. 1. Now Publishers Inc, 2010.

[167] J. Meinila, P. Kyosti, L. Hentila, T. Jamsa, E. Suikkanen, E. Kunnari, and M. Narandzic, "D5. 3: WINNER+ final channel models," *Wireless World Initiative New Radio WINNER*, pp. 119–172, 2010.

[168] J.-M. Park, J. H. Reed, A. Beex, T. C. Clancy, V. Kumar, and B. Bahrak, "Security and enforcement in spectrum sharing," *Proceedings of the IEEE*, vol. 102, no. 3, pp. 270–281, 2014.

[169] V. Kumar, J.-M. Park, and K. Bian, "Blind transmitter authentication for spectrum security and enforcement," in *Proceedings of the 2014 ACM SIGSAC Conference on Computer and Communications Security*, pp. 787–798, 2014.

[170] V. Kumar, J.-M. J. Park, and K. Bian, "PHY-layer authentication using duobinary signaling for spectrum enforcement," *IEEE Transactions on Information Forensics and Security*, vol. 11, no. 5, pp. 1027–1038, 2016.

[171] X. Tan, K. Borle, W. Du, and B. Chen, "Cryptographic link signatures for spectrum usage authentication in cognitive radio," in *Proceedings of the fourth ACM conference on Wireless network security*, pp. 79–90, 2011.

[172] L. Yang, Z. Zhang, B. Y. Zhao, C. Kruegel, and H. Zheng, "Enforcing dynamic spectrum access with spectrum permits," in *Proceedings of the thirteenth ACM international symposium on Mobile Ad Hoc Networking and Computing*, pp. 195–204, 2012.

[173] V. Kumar, H. Li, J.-M. J. Park, and K. Bian, "Enforcement in spectrum sharing: Crowd-sourced blind authentication of co-channel transmitters," in *2018 IEEE International Symposium on Dynamic Spectrum Access Networks (DySPAN)*, pp. 1–10, IEEE, 2018.

[174] V. Kumar, H. Li, J.-M. J. Park, and K. Bian, "Crowd-Sourced Authentication for Enforcement in Dynamic Spectrum Sharing," *IEEE Transactions on Cognitive Communications and Networking*, vol. 5, no. 3, pp. 625–636, 2019.

[175] F. Awad, M. Al-Refai, and A. Al-Qerem, "Rogue access point localization using particle swarm optimization," in *2017 8th International Conference on Information and Communication Systems (ICICS)*, pp. 282–286, IEEE, 2017.

[176] T. M. Le, R. P. Liu, and M. Hedley, "Rogue access point detection and localization," in *2012 IEEE 23rd International Symposium on Personal, Indoor and Mobile Radio Communications-(PIMRC)*, pp. 2489–2493, IEEE, 2012.

[177] X. Zheng, C. Wang, Y. Chen, and J. Yang, "Accurate rogue access point localization leveraging fine-grained channel information," in *2014 IEEE conference on communications and network security*, pp. 211–219, IEEE, 2014.

[178] M. Khaledi, M. Khaledi, S. Sarkar, S. Kasera, N. Patwari, K. Derr, and S. Ramirez, "Simultaneous power-based localization of transmitters for crowdsourced spectrum monitoring," in *Proceedings of the 23rd Annual International Conference on Mobile Computing and Networking*, pp. 235–247, 2017.

[179] T. Zhou, Z. Cai, B. Xiao, Y. Chen, and M. Xu, "Detecting rogue ap with the crowd wisdom," in *2017 IEEE 37th International Conference on Distributed Computing Systems (ICDCS)*, pp. 2327–2332, IEEE, 2017.

[180] C. Wang, X. Zheng, Y. J. Chen, and J. Yang, "Locating rogue access point using fine-grained channel information," *IEEE Transactions on Mobile Computing*, vol. 16, no. 9, pp. 2560–2573, 2016.

[181] ———, "IEEE Standard for Information technology–Telecommunications and information exchange between systems Local and metropolitan area networks–Specific requirements Part 11: Wireless LAN Medium Access Control (MAC) and Physical Layer (PHY) Specifications," *IEEE Std 802.11-2012 (Revision of IEEE Std 802.11-2007)*, pp. 1–2793, March 2012.

[182] J. Lansford, J. Kenney, P. Ecclesine, T. Yucek, and P. Spaanderman, "IEEE 802.11-15/0347: Final Report of DSRC Coexistence Tiger Team." Final report of the IEEE 802.11 Regulatory SC, Online: https://mentor.ieee.org/802.11/dcn/15/11-15-0347, March 2015.

[183] J. Lansford and J. Kenney, "IEEE 802.11-13/0552: Coexistence issues between 802.11p and 802.11ac in the proposed UNII-4 band." contribution to the WNG SC, Online: https://mentor.ieee.org/802.11/dcn/13/11-13-0552, June 2013.

[184] J. Kenney, D. Jiang, N. Probert, B. Gallagher, R. Miucic, *et al.*, "IEEE 802.11-14/1101r1: A response to the re-channelization proposal." contribution to the IEEE 802.11 Regulatory SC, Online: https://mentor.ieee.org/802.11/dcn/14/11-14-1101-01, September 2014.

[185] J. Wang, T. Wu, Y. Liu, W. Deng, and H. Oh, "Modeling and performance analysis of dynamic spectrum sharing between DSRC and Wi-Fi systems," *Wireless Communications and Mobile Computing*, vol. 16, no. 16, pp. 2743–2758, 2016.

[186] K.-H. Chang, "Wireless communications for vehicular safety," *Wireless Communications, IEEE*, vol. 22, no. 1, pp. 6–7, 2015.

[187] Y. Park and H. Kim, "On the coexistence of IEEE 802.11 ac and WAVE in the 5.9 GHz Band," *IEEE Communications Magazine*, vol. 52, no. 6, pp. 162–168, 2014.

[188] J. Liu, G. Naik, and J.-M. J. Park, "Coexistence of DSRC and Wi-Fi: Impact on the performance of vehicular safety applications," in *Communications (ICC), 2017 IEEE Int'l Conf. on*, pp. 1–6, IEEE, 2017.

[189] G. Naik, J. Liu, and J.-M. J. Park, "Coexistence of Dedicated Short Range Communications (DSRC) and Wi-Fi: Implications to Wi-Fi Performance," in *Proc. IEEE INFOCOM*, 2017.

[190] U.S. Department of Transportation, "RP-180690: U.S. Department of Transportation Views on NR V2X SI." 3GPP Planery Meeting 80, La Jolla, USA, 2018.

[191] Qualcomm Inc., "R1-1812000: Summary of Coexistence Aspects in NR-V2X Study." 3GPP TSG RAN WG1 94b, Chengdu, China, 2018.

[192] ZTE, "R1-1813178: Coexistence between NR V2X and LTE V2X." 3GPP TSG RAN WG1 95, Spokane, USA, Nov. 2018.

[193] CATT, "R1-1812624: Discussion on coex. of LTE sidelink and NR sidelink in NR V2X." GPP TSG RAN WG1 95, Spokane, USA, 2018.

[194] Toyota, "Toyota and Lexus to Launch Technology to Connect Vehicles and Infrastructure in the U.S. in 2021," April 2018 (accessed November 9, 2020).

[195] J. B. Kenney, "An Update on V2X in the United States," Nov. 2018.

[196] G. Bianchi, I. Tinnirello, and L. Scalia, "Understanding 802.11e contention-based prioritization mechanisms and their coexistence with legacy 802.11 stations," *IEEE network*, vol. 19, no. 4, pp. 28–34, 2005.

[197] R. Chandra, R. Mahajan, T. Moscibroda, R. Raghavendra, and P. Bahl, "A case for adapting channel width in wireless networks," in *ACM SIGCOMM computer communication review*, vol. 38, pp. 135–146, ACM, 2008.

[198] L. Deek, E. Garcia-Villegas, E. Belding, S.-J. Lee, and K. Almeroth, "The impact of channel bonding on 802.11n network management," in *Proceedings of the Seventh COnference on emerging Networking EXperiments and Technologies*, p. 11, ACM, 2011.

[199] Y. Zeng, P. H. Pathak, and P. Mohapatra, "A first look at 802.11 ac in action: energy efficiency and interference characterization," in *Networking Conference, 2014 IFIP*, pp. 1–9, IEEE, 2014.

[200] M. Park, "IEEE 802.11ac: Dynamic bandwidth channel access," in *2011 IEEE international conference on communications (ICC)*, pp. 1–5, IEEE, 2011.

[201] M.-D. Dianu, J. Riihijärvi, and M. Petrova, "Measurement-based study of the performance of IEEE 802.11ac in an indoor environment," in *2014 IEEE International Conference on Communications (ICC)*, pp. 5771–5776, IEEE, 2014.

[202] W. Kim, J.-P. Jeong, and Y.-J. Suh, "Delayed Dynamic Bandwidth Channel Access scheme for IEEE 802.11ac WLANs," in *2017 International Conference on Information Networking (ICOIN)*, pp. 70–75, Jan 2017.

[203] A. Stelter, P. Szulakiewicz, R. Kotrys, M. Krasicki, and P. Remlein, "Dynamic 20/40/60/80 MHz Channel Access for 80 MHz 802.11ac," *Wireless Personal Communications*, vol. 79, no. 1, pp. 235–248, 2014.

[204] M. Heusse, F. Rousseau, G. Berger-Sabbatel, and A. Duda, "Performance anomaly of 802.11b," in *INFOCOM 2003. Twenty-Second Annual Joint Conference of the IEEE Computer and Communications. IEEE Societies*, vol. 2, pp. 836–843, IEEE, 2003.

[205] J. Fang and I.-T. Lu, "Efficient utilisation of extended bandwidth in 802.11ac with and without overlapping basic service sets," *Electronics Letters*, vol. 50, no. 24, pp. 1884–1886, 2014.

[206] L. Wang *et al.*, "IEEE 802.11-14/0567r3: Proposed 802.11ax Functional Requirements." contribution to the IEEE TGax, Online: https://mentor.ieee.org/802.11/dcn/14/11-14-0567-03, May 2014.

[207] I. Jamil, L. Cariou, and J.-F. Hélard, "Efficient MAC protocols optimization for future high density WLANs," in *2015 IEEE Wireless Communications and Networking Conference (WCNC)*, pp. 1054–1059, IEEE, 2015.

[208] M. S. Afaqui, E. Garcia-Villegas, and E. Lopez-Aguilera, "Dynamic sensitivity control algorithm leveraging adaptive RTS/CTS for IEEE 802.11ax," in *Wireless Communications and Networking Conference (WCNC), 2016 IEEE*, pp. 1–6, IEEE, 2016.

[209] Z. Zhong, F. Cao, P. Kulkarni, and Z. Fan, "Promise and perils of Dynamic Sensitivity control in IEEE 802.11 ax WLANs," in *Wireless Communication Systems (ISWCS), 2016 International Symposium on*, pp. 439–444, IEEE, 2016.

[210] J. Son *et al.*, "IEEE 802.11-15/0085: Legacy Fairness Issues of Enhanced CCA." contribution to the IEEE TGax, Online: https://mentor.ieee.org/802.11/dcn/15/11-15-0085, 2014 (accessed November 9, 2020).

[211] J. Wang *et al.*, "IEEE 802.11-14/0637: Spatial Reuse and Coexistence with Legacy Devices." contribution to the IEEE TGax, Online: https://mentor.ieee.org/802.11/dcn/14/11-14-0637, 2014 (accessed November 9, 2020).

[212] G. Wikstrom *et al.*, "IEEE 802.11-14/1426: DSC and Legacy Coexistence." contribution to the IEEE TGax, Online: https://mentor.ieee.org/802.11/dcn/14/11-14-1426, 2014 (accessed November 9, 2020).

[213] B. Bellalta and K. Kosek-Szott, "AP-initiated Multi-User Transmissions in IEEE 802.11ax WLANs," *CoRR*, vol. abs/1702.05397, 2017.

[214] L. Lanante, H. O. T. Uwai, Y. Nagao, M. Kurosaki, and C. Ghosh, "Performance analysis of the 802.11 ax UL OFDMA random access protocol in dense networks," in *Communications (ICC), 2017 IEEE International Conference on*, pp. 1–6, IEEE, 2017.

[215] R. Hedayat, Y. H. Kwon, Y. Seok, and V. Ferdowsi, "IEEE 802.11-15/0086r2: Uplink MU Transmission and Coexistence." contribution to the IEEE TGax, Online: https://mentor.ieee.org/802.11/dcn/15/11-15-0086-02, January 2015.

[216] Google Inc, *Google whitepaper on LTE-U/WiFi coexistence*, 2015.

[217] National Cable & Telecommunications Association, "Comments of the National Cable & Telecommunications Association." comments to the FCC ET Docket No. 15-105, https://ecfsapi.fcc.gov/file/60001078155.pdf, June 2015 (accessed November 9, 2020).

[218] Qualcomm, "CableLabs and Qualcomm Wi-Fi/LTE-U Coexistence Study – Test Results." Online: https://www.qualcomm.com/documents/cablelabs-and-qualcomm-wi-filte-u-coexistence-study-test-results, 2015 (accessed November 9, 2020).

[219] J. Brodkin, "LTE over Wi-Fi spectrum sets up industry-wide fight over interference." Online: https://arstechnica.com/information-technology/2015/08/verizon-and-t-mobile-join-forces-in-fight-for-wi-fi-airwaves/, August 2015 (accessed November 9, 2020).

[220] C. Chen, R. Ratasuk, and A. Ghosh, "Downlink performance analysis of LTE and WiFi coexistence in unlicensed bands with a simple listen-before-talk scheme," in *2015 IEEE 81st Vehicular Technology Conference (VTC Spring)*, pp. 1–5, IEEE, 2015.

[221] S.-Y. Lien, J. Lee, and Y.-C. Liang, "Random Access or Scheduling: Optimum LTE Licensed-Assisted Access to Unlicensed Spectrum," *IEEE Communications Letters*, vol. 20, no. 3, pp. 590–593, 2016.

[222] J. Jeon, H. Niu, Q. Li, A. Papathanassiou, and G. Wu, "LTE with listen-before-talk in unlicensed spectrum," in *2015 IEEE international conference on communication workshop (ICCW)*, pp. 2320–2324, IEEE, 2015.

[223] A. Bhorkar, C. Ibars, A. Papathanassiou, and P. Zong, "Medium access design for LTE in unlicensed band," in *2015 IEEE Wireless Communications and Networking Conference Workshops (WCNCW)*, pp. 369–373, IEEE, 2015.

[224] R. Ratasuk, N. Mangalvedhe, and A. Ghosh, "LTE in unlicensed spectrum using licensed-assisted access," in *2014 IEEE Globecom Workshops (GC Wkshps)*, pp. 746–751, IEEE, 2014.

[225] Y. Li, J. Zheng, and Q. Li, "Enhanced listen-before-talk scheme for frequency reuse of licensed-assisted access using LTE," in *Personal, Indoor, and Mobile Radio Communications (PIMRC), 2015 IEEE 26th Annual International Symposium on*, pp. 1918–1923, IEEE, 2015.

[226] N. Rupasinghe and I. Güvenç, "Licensed-assisted access for WiFi-LTE coexistence in the unlicensed spectrum," in *2014 IEEE Globecom Workshops (GC Wkshps)*, pp. 894–899, IEEE, 2014.

[227] N. Rupasinghe and İ. Güvenç, "Reinforcement learning for licensed-assisted access of LTE in the unlicensed spectrum," in *2015 IEEE Wireless Communications and Networking Conference (WCNC)*, pp. 1279–1284, IEEE, 2015.

[228] T. Tao, F. Han, and Y. Liu, "Enhanced LBT algorithm for LTE-LAA in unlicensed band," in *Personal, Indoor, and Mobile Radio Communications (PIMRC), 2015 IEEE 26th Annual International Symposium on*, pp. 1907–1911, IEEE, 2015.

[229] C. Cano, D. J. Leith, A. Garcia-Saavedra, and P. Serrano, "Fair coexistence of scheduled and random access wireless networks: Unlicensed LTE/WiFi," *IEEE/ACM Transactions on Networking*, vol. 25, no. 6, pp. 3267–3281, 2017.

[230] A. Mukherjee, J.-F. Cheng, S. Falahati, L. Falconetti, A. Furuskär, B. Godana, H. Koorapaty, D. Larsson, Y. Yang, *et al.*, "System architecture and coexistence evaluation of licensed-assisted access LTE with IEEE 802.11," in *2015 IEEE International Conference on Communication Workshop (ICCW)*, pp. 2350–2355, IEEE, 2015.

[231] E. Chai, K. Sundaresan, M. A. Khojastepour, and S. Rangarajan, "LTE in unlicensed spectrum: Are we there yet?," in *Proceedings of the 22nd Annual International Conference on Mobile Computing and Networking*, pp. 135–148, 2016.

[232] P. Xia, Z. Teng, and J. Wu, "How loud to talk and how hard to listen-before-talk in unlicensed LTE," in *2015 IEEE International Conference on Communication Workshop (ICCW)*, pp. 2314–2319, IEEE, 2015.

[233] H. Song, Q. Cui, Y. Gu, G. L. Stüber, Y. Li, Z. Fei, and C. Guo, "Cooperative LBT design and effective capacity analysis for 5G NR ultra dense networks in unlicensed spectrum," *IEEE Access*, vol. 7, pp. 50265–50279, 2019.

[234] X. Wang, S. Mao, and M. X. Gong, "A survey of LTE Wi-Fi coexistence in unlicensed bands," *GetMobile: Mobile Computing and Communications*, vol. 20, no. 3, pp. 17–23, 2017.

[235] Qualcomm CDMA Technologies, "BRAN(19)104018: Technology neutral synchronous access." presented at ETSI BRAN # 104, November 2019.

[236] ETSI, "ETSI EN 301 893: 5 GHz RLAN; Harmonized Standard covering the essential requirements of article 3.2 of Directive 2014/53/EU V2.1.1." Online: https://www.etsi.org/deliver/etsi_en/301800_301899/301893/02.01.01_60/en_301893v020101p.pdf, May 2017 (accessed November 9, 2020).

[237] ZTE, Sanechips, "R1-1911822: Remaining issues on channel access procedure for NR-U." 3GPP TSG RAN WG1 99, Reno, USA, Online: https://www.3gpp.org/ftp/tsg_ran/WG1_RL1/TSGR1_99/Docs/R1-1911822.zip, November 2019 (accessed November 9, 2020).

[238] MediaTek Inc., "R1-1912188: Remaining details in channel access procedures." 3GPP TSG RAN WG1 99, Reno, USA, Online: https://www.3gpp.org/ftp/tsg_ran/WG1_RL1/TSGR1_99/Docs/R1-1912088.zip, November 2019 (accessed November 9, 2020).

[239] Intel Corporation, "R1-1912197: Channel access mechanism for NR-unlicensed." 3GPP TSG RAN WG1 99, Reno, USA, Online: https://www.3gpp.org/ftp/tsg_ran/WG1_RL1/TSGR1_99/Docs/R1-1912197.zip, November 2019 (accessed November 9, 2020).

[240] Nokia, Nokia Shanghai Bell, "R1-1912257: Channel access and co-existence for NR-U operation." 3GPP TSG RAN WG1 99, Reno, USA, Online: https://www.3gpp.org/ftp/tsg_ran/WG1_RL1/TSGR1_99/Docs/R1-1912257.zip, November 2019 (accessed November 9, 2020).

[241] Q. Incorporated, "Comments of Qualcomm Incorporated." comments to the FCC ET Docket No. 18-295 and GN Docket No. 17-183, Online: https://ecfsapi.fcc.gov/file/1021644462961/Qualcomm%20Comments%20on%206GHz%20NPRM.pdf, February 2019 (accessed November 9, 2020).

[242] Vivo, "R1-1912012: Discussion on the channel access procedures." 3GPP TSG RAN WG1 99, Reno, USA, Online: https://www.3gpp.org/ftp/tsg_ran/WG1_RL1/TSGR1_99/Docs/R1-1912012.zip, November 2019 (accessed November 9, 2020).

[243] K. Kim, L. Li, E. Perahia, D. Stanley, S. Strickland, and C. Vlachou, "LAA/Wi-Fi Coexistence Evaluations With Commercial Hardware." presented at the P802.11

Coexistence SC workshop, Online: http://grouper.ieee.org/groups/802/11/Workshops/2019-July-Coex/2019_07_17_Coexistence_Workshop_HPE.pptx, July 2019 (accessed November 9, 2020).

[244] M. Ghosh, V. Sathya, M. Iqbal, M. Mehrnoush, and S. Roy, "Coexistence of LTE-LAA and Wi-Fi: analysis, simulation and experiments." presented at the P802.11 Coexistence SC workshop, Online: http://grouper.ieee.org/groups/802/11/Workshops/2019-July-Coex/2-2-UChicago_Coexistence%20Wkshp.pptx, July 2019 (accessed November 9, 2020).

[245] S. Falahati, G. Hiertz, and N. Madhavan, "IEEE 802.11-19/1083r1: Coexistence in 6 GHz License-exempt Spectrum." presented at the P802.11 Coexistence SC workshop, Online: https://mentor.ieee.org/802.11/dcn/19/11-19-1083-01, July 2019 (accessed November 9, 2020).

[246] Zhang, J and Fan, W and Mazzarese, D and Salem, M, "Performance Evaluation of Channel Access Mechanisms in 6 GHz Spectrum." presented at the P802.11 Coexistence SC workshop, Online: http://grouper.ieee.org/groups/802/11/Workshops/2019-July-Coex/Performance%20Evaluation%20of%20Channel%20Access%20Mechanisms%20in%206%20GHz%20Spectrum%20v4.pptx, July 2019 (accessed November 9, 2020).

[247] S. Falahati, G. Hiertz, and N. Madhavan, "IEEE 802.11-19/1088r1: Coexistence Mechanisms." presented at the P802.11 Coexistence SC workshop, Online: https://mentor.ieee.org/802.11/dcn/19/11-19-1088-01, July 2019 (accessed November 9, 2020).

[248] Ericsson, "BRAN(19)104010r1: Common ED for 6 GHz." presented at ETSI BRAN # 104, November 2019.

[249] CableLabs, Comcast, Cox Communications, Midco, "NR-U/Wi-Fi Coexistence in 5/6 GHz bands." presented at the P802.11 Coexistence SC workshop, Online: http://grouper.ieee.org/groups/802/11/Workshops/2019-July-Coex/Coexistence%20Workshop%20presentation%2007012019.pptx, July 2019 (accessed November 9, 2020).

[250] Quantenna Communications, "Efficient and Fair Medium Sharing Enabled by a Common Preamble." presented at the P802.11 Coexistence SC workshop, Online: http://grouper.ieee.org/groups/802/11/Workshops/2019-July-Coex/coex_Presentation_CP_Quantenna.pdf, July 2019 (accessed November 9, 2020).

[251] Orange, "Orange view on co-existence between NR-U and Wi-Fi." presented at the P802.11 Coexistence SC workshop, Online: http://grouper.ieee.org/groups/802/11/Workshops/2019-July-Coex/IEEE%20co-existence%20workshop%

20-%20Orange%20views%20-%2017th%20July%202019%20-final.pdf, July 2019 (accessed November 9, 2020).

[252] Broadcom, "Benefits of 802.11 preamble for Wi-Fi and NR-U coexistence." presented at the P802.11 Coexistence SC workshop, Online: http://grouper.ieee.org/groups/802/11/Workshops/2019-July-Coex/3-9-coex-workshop-presentation-common-preamble-Broadcom.pptx, July 2019 (accessed November 9, 2020).

[253] AT&T, "Common Preamble Design in the 6 GHz Band - Merits and Challenges." presented at the P802.11 Coexistence SC workshop, Online: http://grouper.ieee.org/groups/802/11/Workshops/2019-July-Coex/att_coex_ws_final.pdf, July 2019 (accessed November 9, 2020).

[254] S.-T. Hong, H. Lee, H. Kim, and H. J. Yang, "Lightweight Wi-Fi Frame Detection for Licensed Assisted Access LTE," *IEEE Access*, vol. 7, pp. 77618–77628, 2019.

[255] A. Myles, "IEEE 802.11-19/2150r6: Agenda for IEEE 802.11 Coexistence SC meeting in Irvine in January 2020." contribution to the IEEE Coex SC, Online: https://mentor.ieee.org/802.11/dcn/19/11-19-2150-06, January 2020 (accessed November 9, 2020).

[256] Cisco Systems Belgium, "BRAN(19)103023: Response to BRAN(19)103016." presented at ETSI BRAN # 103, October 2019.

[257] Nokia Corporation, "BRAN(19)103016: 6 GHz channel access simulation results." presented at ETSI BRAN # 103, September 2019.

[258] A. Myles, "IEEE 802.11-19/1111r0: LBT should remain the basis of fair & efficient coexistence in 6 GHz unlicensed spectrum." presented at the P802.11 Coexistence SC workshop, Online: https://mentor.ieee.org/802.11/dcn/19/11-19-1111, July 2019 (accessed November 9, 2020).

[259] P. Chatzimisios, V. Vitsas, and A. C. Boucouvalas, "Throughput and delay analysis of IEEE 802.11 protocol," in *Proceedings 3rd IEEE International Workshop on System-on-Chip for Real-Time Applications*, pp. 168–174, IEEE, 2002.

[260] T. Sakurai and H. L. Vu, "MAC access delay of IEEE 802.11 DCF," *IEEE Transactions on Wireless Communications*, vol. 6, no. 5, pp. 1702–1710, 2007.

[261] G. Bianchi, "Performance analysis of the IEEE 802.11 distributed coordination function," *IEEE Journal on selected areas in communications*, vol. 18, no. 3, pp. 535–547, 2000.

[262] L. Dai and X. Sun, "A unified analysis of IEEE 802.11 DCF networks: Stability, throughput, and delay," *IEEE Transactions on Mobile Computing*, vol. 12, no. 8, pp. 1558–1572, 2012.

[263] C.-L. Huang and W. Liao, "Throughput and delay performance of IEEE 802.11 e enhanced distributed channel access (EDCA) under saturation condition," *IEEE Transactions on wireless communications*, vol. 6, no. 1, pp. 136–145, 2007.

[264] D. Xu, T. Sakurai, and H. L. Vu, "An access delay model for IEEE 802.11 e EDCA," *IEEE transactions on mobile computing*, vol. 8, no. 2, pp. 261–275, 2008.

[265] Y. Li, F. Baccelli, J. G. Andrews, T. D. Novlan, and J. C. Zhang, "Modeling and analyzing the coexistence of Wi-Fi and LTE in unlicensed spectrum," *IEEE Transactions on Wireless Communications*, vol. 15, no. 9, pp. 6310–6326, 2016.

[266] A.-k. Ajami and H. Artail, "On the modeling and analysis of uplink and downlink IEEE 802.11 ax Wi-Fi with LTE in unlicensed spectrum," *IEEE Transactions on Wireless Communications*, vol. 16, no. 9, pp. 5779–5795, 2017.

[267] M. Y. Arslan, K. Pelechrinis, I. Broustis, S. V. Krishnamurthy, S. Addepalli, and K. Papagiannaki, "Auto-configuration of 802.11n WLANs," in *Proceedings of the 6th International Conference*, p. 27, ACM, 2010.

[268] X. Ma, J. Zhang, and T. Wu, "Reliability analysis of one-hop safety-critical broadcast services in vanets," *Vehicular Technology, IEEE Transactions on*, vol. 60, no. 8, pp. 3933–3946, 2011.

[269] R. P. Roess, E. S. Prassas, and W. R. McShane, *Traffic engineering*. Prentice Hall, 2004.

[270] R. Stanica, E. Chaput, and A.-L. Beylot, "Reverse back-off mechanism for safety vehicular ad hoc networks," *Ad Hoc Networks*, vol. 16, pp. 210–224, 2014.

[271] S. Wunderlich, "GitHub code for FFT evaluation in Atheros AR92xx and AR93xx devices." https://github.com/simonwunderlich/FFT_eval, (accessed November 9, 2020).

[272] Y. Park and H. Kim, "On the coexistence of IEEE 802.11 ac and wave in the 5.9 GHz band," *IEEE Communications Magazine*, vol. 52, no. 6, pp. 162–168, 2014.

[273] Office of Engineering and Technology, FCC, "Phase I Testing of Prototype U-NII-4 Devices." Online: https://docs.fcc.gov/public/attachments/DA-18-1111A2.pdf, October 2018 (accessed November 9, 2020).

[274] S. Gopal and S. K. Kaul, "A Game Theoretic Approach to DSRC and WiFi Coexistence," *arXiv preprint arXiv:1803.00552*, 2018.

[275] 5GAA, "V2X Technology Benchmark Testing ." https://www.fcc.gov/ecfs/filing/109271050222769, Sept. 2018.

[276] A. Malarky, "IEEE 802.11-08/0908r3: TGp LB 125 Comment Resolution Transmit Spectrum Mask CL-I-2-3." contribution to the IEEE TGp, Online: https://mentor.ieee.org/802.11/dcn/08/11-08-0908-03, July 2008 (accessed November 9, 2020).

[277] R. Rouil, F. J. Cintrón, A. Ben Mosbah, and S. Gamboa, "Implementation and Validation of an LTE D2D Model for ns-3," in *Proceedings of the Workshop on ns-3*, pp. 55–62, ACM, 2017.

[278] 3GPP, "3GPP TR 36.885: Technical Specification Group Radio Access Network; Study on LTE-based V2X Services (Release 14)," June 2016.

[279] FCC, "Memorandum Opinion and Order; In the Matter of Revision of Part 15 of the Commission's Rules to Permit Unlicensed National Information Infrastructure (U-NII) Devices in the 5 GHz Band (ET Docket No. 13-49)." Online: urlhttps://www.fcc.gov/document/unlicensed-national-information-infrastructure-order-recon, March 2016.

[280] Cisco, "RF Power Values." https://www.cisco.com/c/en/us/support/docs/wireless-mobility/wireless-lan-wlan/23231-powervalues-23231.html, March 2008 (accessed November 9, 2020).

[281] S. Lagen, L. Giupponi, S. Goyal, N. Patriciello, B. Bojovic, A. Demir, and M. Beluri, "New Radio Beam-based Access to Unlicensed Spectrum: Design Challenges and Solutions," *IEEE Communications Surveys & Tutorials*, 2019.

[282] A. Mbengue and Y. Chang, "Performance analysis of LAA/Wi-Fi coexistence: Stochastic geometry model," in *2018 IEEE Wireless Communications and Networking Conference (WCNC)*, pp. 1–6, IEEE, 2018.

[283] X. Wang, T. Q. Quek, M. Sheng, and J. Li, "Throughput and fairness analysis of Wi-Fi and LTE-U in unlicensed band," *IEEE Journal on Selected Areas in Communications*, vol. 35, no. 1, pp. 63–78, 2016.

[284] A. Bhorkar, C. Ibars, and P. Zong, "On the throughput analysis of LTE and WiFi in unlicensed band," in *2014 48th Asilomar Conference on Signals, Systems and Computers*, pp. 1309–1313, IEEE, 2014.

[285] M. Nurchis and B. Bellalta, "Target wake time: Scheduled access in IEEE 802.11 ax WLANs," *IEEE Wireless Communications*, vol. 26, no. 2, pp. 142–150, 2019.

[286] R. K. Ganti and M. Haenggi, "Spatial and temporal correlation of the interference in ALOHA ad hoc networks," *IEEE Communications Letters*, vol. 13, no. 9, pp. 631–633, 2009.

[287] Z. Gong and M. Haenggi, "Interference and outage in mobile random networks: Expectation, distribution, and correlation," *IEEE Transactions on Mobile Computing*, vol. 13, no. 2, pp. 337–349, 2012.

[288] D. Torrieri and M. C. Valenti, "The outage probability of a finite ad hoc network in Nakagami fading," *IEEE Transactions on Communications*, vol. 60, no. 11, pp. 3509–3518, 2012.

[289] J. Guo, S. Durrani, and X. Zhou, "Outage probability in arbitrarily-shaped finite wireless networks," *IEEE Transactions on Communications*, vol. 62, no. 2, pp. 699–712, 2014.

[290] J. G. Andrews, A. K. Gupta, and H. S. Dhillon, "A primer on cellular network analysis using stochastic geometry," *arXiv preprint arXiv:1604.03183*, 2016.

[291] Cisco, "Enterprise Best Practices for iOS devices and Mac computers on Cisco Wireless LAN." White Paper, Online: https://www.cisco.com/c/dam/en/us/td/docs/wireless/controller/technotes/8-6/Enterprise_Best_Practices_for_iOS_devices_and_Mac_computers_on_Cisco_Wireless_LAN.pdf, January 2018.

[292] Qualcomm Inc., "Accelerating C-V2X commercialization." Online: https://www.qualcomm.com/documents/path-5g-cellular-vehicle-everything-c-v2x, September (accessed November 9, 2020) 2017.

[293] A. Bazzi, B. M. Masini, A. Zanella, and I. Thibault, "On the Performance of IEEE 802.11p and LTE-V2V for the Cooperative Awareness of Connected Vehicles," *IEEE Transactions on Vehicular Technology*, vol. 66, no. 11, pp. 10419–10432, 2017.

[294] A. Bazzi, B. M. Masini, and A. Zanella, "How many vehicles in the LTE-V2V awareness range with half or full duplex radios?," in *ITS Telecommunications (ITST), 2017 15th International Conference on*, pp. 1–6, IEEE, 2017.

[295] R. Molina-Masegosa and J. Gozalvez, "System Level Evaluation of LTE-V2V Mode 4 Communications and its Distributed Scheduling," in *Vehicular Technology Conference (VTC 2017-Spring), 2017 IEEE 85th*, IEEE, 2017.

[296] A. Bazzi, G. Cecchini, A. Zanella, and B. M. Masini, "Study of the Impact of PHY and MAC Parameters in 3GPP C-V2V Mode 4," *IEEE Access*, vol. 6, pp. 71685–71698, 2018.

[297] M. Gonzalez-Martín, M. Sepulcre, R. Molina-Masegosa, and J. Gozalvez, "Analytical models of the performance of C-V2X mode 4 vehicular communications," *IEEE Transactions on Vehicular Technology*, vol. 68, no. 2, pp. 1155–1166, 2018.

[298] Huawei, HSilicon, "R1-160284: DMRS enhancement of V2V." 3GPP TSG RAN WG1 Meeting # 84, St. Julian's Malta, 2016.

[299] 3GPP, "3GPP TR 36.885: Study on LTE-based V2X Services (v14.0.0, Release 14)," June 2016.

[300] Qualcomm Incorporated, "R1-1611594: Congestion control for V2V." 3GPP TSG RAN WG1 Meeting # 87, Reno, USA, 2016.

[301] MarketsandMarkets, "Global Wi-Fi Market by Business (Model Indoor Wi-Fi, Outdoor Wi-Fi, Transportation Wi-Fi), Product (Access Points, WLAN Controllers, Wireless Hotspot Gateways, Others), Service, Vertical, Region- Global Forecast to 2022," August 2019 (accessed November 9, 2020).

[302] IEEE, "Status of Project IEEE 802.11ax." Online: http://www.ieee802.org/11/Reports/tgax_update.htm, 2013 (accessed November 9, 2020).

[303] O. Aboul-Magd, "IEEE 802.11-14/0165r1: 802.11 HEW SG Proposed PAR." Project Authorization Report of HEW SG, Online: https://mentor.ieee.org/802.11/dcn/14/11-14-0165-01, March 2014.

[304] R. Karmakar, S. Chattopadhyay, and S. Chakraborty, "Impact of IEEE 802.11n/ac PHY/MAC High Throughput Enhancements on Transport and Application Protocols-A Survey," *IEEE Communications Surveys Tutorials*, vol. 19, pp. 2050–2091, Fourthquarter 2017.

[305] C. Ghosh, R. Stacey, E. Perahia, S. Azizi, *et al.*, "IEEE 802.11-15/0604r0: Random Access with Trigger Frames using OFDMA." contribution to the IEEE TGax, Online: https://mentor.ieee.org/802.11/dcn/15/11-15-0604, May 2015.

[306] G. Bianchi, "Performance Analysis of the IEEE 802.11 Distributed Coordination Function," *IEEE J.Sel. A. Commun.*, vol. 18, pp. 535–547, Sept. 2006.

[307] O. Sharon and Y. Alpert, "Scheduling strategies and throughput optimization for the Downlink for IEEE 802.11 ax and IEEE 802.11 ac based networks," *arXiv preprint arXiv:1709.04818*, 2017.

[308] I. Arun and T. Venkatesh, "Adaptive backoff algorithm for ieee 802.11 dcf under mpr wireless channels," in *2013 Intl. Conf. on Computer Communications and Networks*, Citeseer, 2013.

[309] M. Laddomada, F. Mesiti, M. Mondin, and F. Daneshgaran, "On the throughput performance of multirate IEEE 802.11 networks with variable-loaded stations: analysis, modeling, and a novel proportional fairness criterion," *IEEE Transactions on Wireless Communications*, vol. 9, pp. 1594–1607, May 2010.

[310] L. B. Jiang and S. C. Liew, "Proportional fairness in wireless LANs and ad hoc networks," in *IEEE Wireless Communications and Networking Conference, 2005*, vol. 3, pp. 1551–1556 Vol. 3, March 2005.

[311] G. Tan and J. Guttag, "Time-based Fairness Improves Performance in Multi-rate WLANs," in *Proceedings of the Annual Conference on USENIX Annual Technical Conference*, ATEC '04, (Berkeley, CA, USA), pp. 23–23, USENIX Association, 2004.

[312] G. Naik, "IEEE 802.11ax MU OFDMA Simulator." https://github.com/ieee80211axsimulator/muofdma, 2017 (accessed November 9, 2020).

[313] Ericsson, "Ericsson Mobility Report—on the pulse of the networked society." http://www.kiwanja.net/media/docs/Ericsson-Mobility-Report-November-2012.pdf, November 2012 (accessed November 9, 2020).

[314] Allied Market Research, "Augmented and Virtual Reality Market Report." Online: https://www.alliedmarketresearch.com/augmented-and-virtual-reality-market, December 2018.

[315] Allied Market Research, "U.S. Augmented and Virtual Reality Market Report." Online: https://www.alliedmarketresearch.com/us-augmented-and-virtual-reality-market-A06735, August 2020.

[316] K. Meng, A. Jones, and D. Cavalcanti, "IEEE 802.11-19/0065r6: RTA report summary." contribution to the IEEE RTA TIG, Online: https://mentor.ieee.org/802.11/dcn/19/11-19-0065-06, January 2019 (accessed November 9, 2020).

[317] Qualcomm Technologies, Inc., "VR and AR pushing connectivity limits." Online: https://www.qualcomm.com/media/documents/files/vr-and-ar-pushing-connectivity-limits.pdf, October 2018.

[318] L. Cariou, "IEEE 802.11-18/0540r2: IEEE P802.11 Wireless LANs: 802.11 EHT Proposed PAR." IEEE 802.11be Project Authorization Report, January 2019 (accessed July 23, 2020).

[319] E. Perahia, C. Cordeiro, M. Park, and L. L. Yang, "IEEE 802.11 ad: Defining the next generation multi-Gbps Wi-Fi," in *2010 7th IEEE consumer communications and networking conference*, pp. 1–5, IEEE, 2010.

[320] A. Patil, G. Cherian, A. Asterjadhi, and D. Ho, "IEEE 802.11-19/0764r1: Multi-Link Aggregation: Peak Throughput Gains." contribution to the IEEE TGbe, Online: https://mentor.ieee.org/802.11/dcn/19/11-19-0764-01, May 2019 (accessed November 9, 2020).

[321] A. Patil, G. Cherian, A. Asterjadhi, and D. Ho, "IEEE 802.11-19/1081r1: Multi-Link Aggregation: Latency Gains." contribution to the IEEE TGbe, Online: https://mentor.ieee.org/802.11/dcn/19/11-19-1081-01, August 2019 (accessed November 9, 2020).

[322] Y. Seok, W. Tsao, G. Bajko, J. Yee, J. Liu, P. Cheng, and T. Pare, "IEEE 802.11-19/0979r2: EHT Multi-Link Operation Follow-up." contribution to the IEEE TGbe, Online: https://mentor.ieee.org/802.11/dcn/19/11-19-0979-02, September 2019 (accessed November 9, 2020).

[323] C. Deng, X. Fang, X. Han, X. Wang, L. Yan, R. He, Y. Long, and Y. Guo, "IEEE 802.11 be–Wi-Fi 7: New Challenges and Opportunities," *IEEE Communications Surveys & Tutorials*, 2020.

[324] E. Avdotin, D. Bankov, E. Khorov, and A. Lyakhov, "Enabling Massive Real-Time Applications in IEEE 802.11 be Networks," in *2019 IEEE 30th Annual International Symposium on Personal, Indoor and Mobile Radio Communications (PIMRC)*, pp. 1–6, IEEE, 2019.

[325] G. Yuan, X. Zhang, W. Wang, and Y. Yang, "Carrier aggregation for LTE-advanced mobile communication systems," *IEEE communications Magazine*, vol. 48, no. 2, pp. 88–93, 2010.

[326] Y. Seok, J. Yee, J. Liu, and T. Pare, "IEEE 802.11-19/1305r4: Synchronous Multi-Link Operation." contribution to the IEEE TGbe, January 2020 (accessed July 23, 2020).

[327] S. Naribole, S. Kandala, W. Lee, and A. Ranganath, "IEEE 802.11-19/1405r7: Multi-link Channel Access Discussion." contribution to the IEEE TGbe, November 2019 (accessed July 23, 2020).

[328] A. Garcia-Rodriguez, D. Lopez-Perez, L. Galati-Giordano, and G. Geraci, "IEEE 802.11 be: Wi-Fi 7 Strikes Back," *arXiv preprint arXiv:2008.02815*, 2020.

[329] D. J. Urban, "The Importance Of Wi-Fi 6 Technology For Delivery Of gbps Internet Service," *SCTE ISBE Cable-Tec Expo*, September 2019.